STUDIES ON CHROMATIN ORGANIZATION AND THE ROLE OF CURCUMIN IN CHROMATIN STABILITY IN RELEVANCE TO NEURODEGENERATION

A Thesis submitted to the

UNIVERSITY OF MYSORE

for the award of the degree of

Doctor of Philosophy

in

BIOCHEMISTRY

by

P.VASUDEVA RAJU

Under the supervision of

Dr.K.S.Jagannatha Rao

Department of Biochemistry and Nutrition

CENTRAL FOOD TECHNOLOGICAL RESEARCH INSTITUTE

Mysore - 570020, India

February 2011

Acknowledgements

It is indeed a great pleasure to express my deep sense of sincere gratitude to **Dr. *K.S. Jagannatha Rao,*** *my supervisor for his constant guidance and support throughout this work. I also thank for the tremendous freedom in work that I enjoyed in the lab. His approach of solving problem (scientific as well as technical), critical analysis of the subject have been very impressive. Working with him has been a pleasant and stimulating experience and I shall always cherish these memories.*

I am gratified to ***Dr. V. Prakash,*** *Director, CFTRI, for providing me an opportunity to work and utilize the facilities at CFTRI to carry out research. I would also like to add a word of thanks for his interesting and useful discussions, which will be evergreen in my memory.*

I would like to thank ***Dr. P.V. Salimath,*** *Head, Department of Biochemistry and Nutrition for providing the department facilities. I am also thankful to* ***Dr. S.G. Bhat*** *(retired Head), for his constant support and encouragement throughout this research work. I profusely thank* ***Dr.U.J.S. Prasada Rao****, Scientist, Biochemistry and Nutrition for all his help and suggestions in my research work.*

I am obliged to ***Dr. P. Srinivas,*** *Head, PPSFT, who extended openhanded milieu in synthesizing and characterizing organic molecules for my research work. The significant discussions and suggestions made by him during my research work are highly valuable.*

My sincere thanks ***Dr.S.K.Shankar, NIMHANS*** *for providing Brain samples for the study and helpful suggestions*

Heartfelt thanks are due to ***Dr. M.R.S.Rao, JNCASR*** *for the chromatin study and helpful suggestions.*

I wish to thank ***Dr. T.S. Sathyanarayana Rao, Dr. B.S. Keshav****,* ***Dr. S. Harsha****, and staff of pathology lab of JSS Hospital, for the biomarker study. I am obliged to* ***Dr.K.P.Raichurkar****, chief radiologist, Vikram Hospital, Mysore, who extended his untired support in conducting MRI study and analysis. I thank* ***Dr.Vikram,*** *MD, Vikram group of hospitals, Mysore for allowing me to do MRI. I wish to acknowledge* ***Dr. Shama Sundar, Dr. Basavaraj, Dr. Bharathi,*** *JSSMC, Mysore for their discussions and suggestions. I am indebted to them. I thank all the people who participated in biomarker study for their charity to society.*

I consider myself very fortunate to interact with ***Dr. Luigi Zecca,*** *Italy,* ***Dr. Rivka Ravid,*** *Amsterdam and* ***Dr. Sambamurthi****, South Carolina, for their valuable suggestions during their stay in our laboratory.*

A word of thanks to Shri. ***M.R. Radhakantha,*** *COA, CFTRI, for his constant support, encouragement during my research work. I profoundly thank Research Fellows Assessment Committee for their important suggestions.*

I thank ***Dr. G. Appu Rao*** *Head, PCT, CFTRI, Mysore, for his stimulative discussions and allowing me to use Circular Dichroism Instrument during my work.*

I am grateful to ***Mr. Govindarajulu,*** *MBU, and* ***Dr. Indi S.S,*** *MCB, Indian Institute of Science for their constant help and providing their laboratory facilities for my research work.*

I wish to acknowledge ***Ms. Parvathy,*** *PPSFT for synthesizing and characterizing the dietary components used for my research work. I thank* ***Mr. Manjunath,*** *PPSFT for his help in NMR experiments.*

I thank all the members and staff of our department for creating a conducive environment, a memorable experience. I thank ***Mr.Vishnu kumar*** *for his support.*

I record my acknowledgement to my seniors ***Dr. Muralidhar Hegde, Dr. Anitha, Dr. Mushtak Dr. Bharathi, Dr. Veer Bala Guptha and Ramesh B.N,*** *for the knowledge shared, the advice given and assistance rendered by them during my stay in the lab. I thank my friend* ***Dr.Sivaramakrishna*** *for his motivation and encouragement in my research career.*

I am thankful to ***Indira madam*** *for the help and guidance provided by her. Thanks are due and endless to* ***Mr. Jayant Rao,*** *which remains in my fond memories through out. Special thanks to* ***Mr. M.A. Sharma*** *and their family for their suggestions and support, which will remain evergreen.*

I am honored to thank my Parents, ***Mr. Chandrasekhara Raju*** *and* ***Mrs Jayamma*** *for their selfless and endless sacrifice; constant support and encouragement, which rendered me to reach the present position in my life.*

I acknowledge the financial support in the form of Junior Research Fellowship (JRF) from the ***Council of Scientific and Industrial Research (CSIR),*** *New Delhi, India.*

-P.Vasudeva Raju.

ABSTRACT OF THE THESIS

The progressive loss of structure and function of neurons is the final consequence of the all neurodegenerative diseases like Parkinson's disease (PD). Genomic integrity is essential for the proper functioning of the neuronal cell and altered genomic integrity lead to neurodegeneration. DNA in eukaryotic cell is arranged in the form of compactly condensed state known as chromatin. Chromatin organization was a dynamic process occurring in the living cells by continuously opening and reorganizing according to the cellular needs. Chromatin organization plays an important role in regulation of the gene expression. Chromatin organization was altered in Parkinson's disease. Histone H3 was acetylated in all the PD chromatin samples compared to 50% of histone acetylation levels in the control sample. DNA methylation was more in PD DNA compared to that of control. Micrococcal nuclease digestion revealed that looser chromatin loops were present in PD chromatin compared to control. The levels of 8-OHdG (Oxidative DNA damage biomarker) were increased in PD patients compared to control indicating more genotoxicity in brain cells. MRI analysis of PD patients brain showed atrophy in caudate nucleus, thalamus, hippocampus and substantia nigra regions compared to control. Trace metals like Fe and Cu were increased, while Zn levels were decreased in aging brain. Single strand breaks and double strand breaks were accumulated in frontal cortex and hippocampus of aging brain. Neuroproteins like α-synuclein, tau and neuromelanin were involved in the pathogenesis of PD. As these neuroproteins are localized in the nuclear region, they may have a role in nuclear functions. We showed that α-synuclein, Tau and neuromelanin bound to supercoiled DNA and nick the DNA like endonuclease. These neuroproteins altered the DNA integrity indicating their genotoxic role. α-synuclein and Tau bind to conformation and sequence specific oligonucleotides of both in B-DNA and biologically significant Z-form. Curcumin, a dietary polyphenol is the principle component of the rhizome (turmeric) of the herb *Curcuma longa*. Curcumin altered chromatin organization and destabilized the chromatin. Curcumin binds to DNA and altered DNA integrity. Curcumin also destabilized the Tau-DNA, α-synuclein-DNA complexes. The present investigation provides a new evidence on the pathological mechanism in PD.

TABLE OF CONTENTS

LIST OF FIGURES

LIST OF TABLES

ABBREVIATIONS

γ-GCL	Gamma-glutamyl cysteine ligase
8-OHdG	8-hydroxy -2'-deoxyguanosine
AD	Alzheimer's disease
ALS	Amyotrophic lateral sclerosis
AMD	Actinomycin D
AP-1	Activator protein-1
ATA	Aurinetricarboxylic acid
ATM	Ataxia-telangiectasia mutated
BBB	Blood brain barrier
BDMC	Bisdemethoxycurcumin
BER	Base excision repair
BM	Biomarker
CaMKII	Ca2+/calmodulin dependent protein kinase II
$CaCl_2$	Calcium chloride
CBP	CREB-binding protein
CREB	cAMP-responsive element
CSF	Cerebrospinal fluid
Cu	Copper
DA	Dopamine
DHC	Dihydrocurcumin
DLB	Dementia with LBs
DMC	Demethoxycurcumin
DMSO	Dimethylsulfoxide
DNA	Deoxyribonucleic acid
DNAse I	Deoxyribonuclease
DOPAC	3,4-dihydroxy phenyl acetic acid
DSB	Double strand breaks
dsDNA	Double stranded DNA
DTT	Dithiothreritol
EDTA	Ethylenediaminetetraacetic acid

EtBr	Ethidium bromide
Fe	Iron
FMRI	Functional Magnetic Resonance Imaging
FTD	Fronto temporal dementia
GABA	γ-Aminobutyric acid
GSH	Glutathione
GSK3B	Glycogen synthase kinase-3
H_2SO_4	Sulphuric acid
HAT	Histone acetylases
HCl	Hydrochloric acid
HDAC	Histone deacetylases
HHC	Hexahydrocurcumin
LB	Lewy Bodies
LPS	Lipopolyscaccharide
LRRK2	Leucine-rich repeat kinase 2
LTP	Long-term potentiation
MAO-B	Monoamine oxidase-B
MAPT	Microtubule-associated protein tau
Mg	Magnesium
$MgCl_2$	Magnesium chloride
MPTP	1-methyl-4-phenyl-1,2,3,6-tetrahydropiridine
MR	Magnetic Resonance
MRI	Magnetic Resonance Imaging
NAC	Non-amyloid component
NaCl	Sodium chloride
NF-kB	Nuclear factor κB
NFT	Neurofibrillary tangles
NIH	Nationsl institute of health
NM	Neuromelanin
NMR	Nuclear magnetic resonance
NOR	Nucleolar organizer region
OHC	Octahydrocurcumin

PARP	ADP-ribose polymerase
PD	Parkinson’s disaese
PMSF	Phenylmethanesulfonylfluoride
rDNA	Ribosomal DNA
REST	Repressor element-1 silencing transcription factor
ROS	Reactive oxygen species
SAM	S-adenosyl methionine
scDNA	Supercoiled DNA
SD	Standard deviation
SDS	Sodium dodyceyl sulphase
SN	Substantia nigra
SNCA	α-synuclein gene
SNpc	Substantia nigra pars compacta
SOD	Superoxide dismutase
SSB	Single-strand breaks
ssDNA	Single stranded DNA
TAMO	Trimethylamine-N-oxide
TEM	Transmission electron microscopy
THC	Tetrahydrocurcumin
TMB	3,3',5,5'-tetramethylbenzidine
TNF	Tumour necrosis factor
UPDRS	Unified Parkinson’s Disease Rating Scale
Zn	Zinc

Synopsis of the thesis submitted to the University of Mysore for the award of PhD degree under the faculty of Biochemistry

Title of the thesis: Studies on chromatin organization and the role of curcumin in chromatin stability in relevance to neurodegeneration

Candidate : P.Vasudeva Raju

Aging is a universal and inevitable phenomenon characterized by slow progressive change in structures and a decline in functions observed in an individual. Aging brain is associated with increased susceptibility to neuronal loss. Studies to interplay between aging and age related brain disorders are of great interest. Along with aging, risk factors like aggregation of modified proteins, disturbance in ion homeostasis, protein and DNA modification, oxidative stress are implicated in age related neurodegeneration. DNA is the critical molecular target primarily because it is subjected to minimal turnover in non-dividing cells and cell contains only one or two copies of DNA sequences that code for the essential genes. Genomic integrity is essential and any change or damage in DNA molecule whether in terms of sequence or handedness, affect the transcriptional fidelity and has an impact in the gene expression. There is limited information on damage or alteration of the conformation of DNA in normal aging and age related disorders. DNA is subjected to such kind of damage by both exogenous and endogenous events. The damage to DNA molecule is observed in the form of modified bases, single and double strand breaks, DNA-protein cross links and DNA topological changes. The role of DNA damage in aging process has gained importance with increasing evidence of DNA damage in aging brain and age related neurological disorders. Accumulated DNA fragmentation is observed in normal aging and neurodegenerative diseases. There are studies on DNA damage and repair mechanisms in aging brain in animal models. Transcriptional efficiency is decreased in old rats when compared to adult rats. DNA repair activity is decreased in aging process and repair defects may contribute to neurological diseases. Suram et al reported a B-Z transition in the severely affected hippocampus region of Alzheimer's disease (AD) brain. Z-DNA is further known to be

involved in the regulation of gene expression. Hedge et al reported that Aβ induces B-ψ transition in supercoiled DNA. Ψ-DNA is structurally and immunologically similar to Z-DNA. The major risk factors of AD, amyloid beta (Aβ) and tau had been reported to be localized in the nucleus and can able to bind DNA molecule. Advanced glycation end products (AGEs) are increased in the brain regions which prone to neurodegeneration. In AD, neuritic plaques and neurofibrillary tangles have been demonstrated to crosslink with AGEs causing an increased rate of free radical production. Dietary components like curcumin, a natural pigment showed neuroprotective effects depending on cell type and concentration. Curcumin is reported to inhibit the plasmid DNA and chromatin degradation. There are limited studies in understanding the role of curcumin derivatives, which can stabilize DNA. Following are aims to be studied in brain and cell culture system

Objectives:

1. To study the Chromatin organization in normal and neurodegenerative brain and the role of curcumin in chromatin stability (**chapter 2A and 2B**) .
2. To study genotoxicity brain cells and prevention by curcumin (**Chapter 3A and 3B**).
3. To understand the molecular mechanism of sequence specific oligonucleotide and DNA binding of neuropeptides, curcumin and Actinomycin D (**Chapter 4A, 4B, 4C, 4D, 4E and 2A**)

Chapter 1: General introduction

This chapter deals with Introduction on etiology and complex pathology of Parkinson disease. The chapter deals in depth with regard to Synuclein biology, aggregation and toxicity. The chapter also deals with DNA stability in PD brain and also role of metals in genomic instability. Chapter has focused discussion on neuropeptide-DNA interactions in relevance to neurodegeneration. The chapter also deals with Curcumin role in neurodegeneration. The chapter ends with objectives of the thesis.

Chapter 2: studies on the chromatin organization in parkinson's disease and the role of curcumin on chromatin organization, tau-DNA interactions and α-synuclein-DNA interactions.

Chapter 2A: chromatin organization in Parkinson's disease.

Chromatin organization in normal and neurodegenerative brain was analysed. We found the following significant findings. Chromatin was isolated from 20 PD and 20 control aged matched brain regions. DNA isolated from the chromatin is in B-form in normal brain, while it is in modified B-form in Parkinson's disease brain. Stability studies showed that chromatin is destabilized in Parkinson's disease brain. Studies also conducted to characterize chromatin from PD and normal brain. The studies include Micrococcal nuclease digestion, Histone modifications (acetylation of H3), DNA methylation. Micrococcal nuclease digestion revealed that PD chromatin was more sensitive to digestion compared to that of control. Histone H3 was acetylated in all the PD chromatin samples compared to 50% of detectable histone acetylation levels in the control sample. Restriction digestion analysis with methylation specific Msp I and HpaII endonuclease revealed the differences in the methylation status of the DNA between PD and normal subjects

Chapter 2B: Role of curcumin on chromatin organization, tau-DNA interactions and α-synuclein-DNA interactions.

Curcumin binds to chromatin as indicated by the altered absorbance and fluorescence spectrum, ethidium bromide binding of curcumin-chromatin and THC-chromatin complex. Curcumin altered the chromatin organization by altering its integrity as evidenced by decreased thermal transition of curcumin-chromatin complex. Curcumin did not alterd the secondary conformation of chromatin components, but binding of curcumin to chromatin evidenced by the small changes in the CD spectrum. Curcumin binds to scDNA as indicated by the absorption, fluorescence and EtBr binding. Curcumin altered integrity of scDNA observed by the thermal denaturation studies. Curcumin also binds to tau, α-synuclein proteins involved in neurodegeneration. Curcumin and THC could not able to prevent the tau, α-synuclein induced DNA nicking.

Chapter 3: Biomarker study on Parkinson's disease and increase of Iron and Copper and its correlation to DNA integrity in ageing human brain

Chapter 3A: Biomarker study on Parkinson's disease

This chapter deals understand the genotoxicity brain cells with an interrelation between serum genotoxic biomarkers to cell atrophy and Ferritin levels in PD brain. We have analysed 15 control and 21 PD patients serum for 8-OHDG, Ceruloplasmin, Ferritin. We found that 8-OHDG levels were elevated and Ceruloplasmin, Ferritin levels are decreased. We analyzed brain cell atrophy by MRI and significant atrophy in Thalamus, , substantia nigra, hippocampus and caudate nucleus in PD brain compared to age matched control. A correlation is established under in vivo between serum genotoxic biomarkers to cell atrophy is brain.

Chapter 3B: New evidence on increase of Iron and Copper and its correlation to DNA integrity in ageing human brain cells

Genomic stability based on the conformation of DNA play a significant role in brain function. Previous studies reported that alterations in DNA integrity exist in the brain regions of neurological disorders like Parkinson and Alzheimer's disease. In this present investigation, we assessed the levels of Copper (Cu), Iron (Fe) and Zinc (Zn) in three age groups (Group I: below 40 years), Group II: between 41-60 years) and Group III: above 60 years) in hippocampus and frontal cortex of aged human brain subjects (n=8 in each groups). Genomic DNA was isolated and its integrity was studied by nick translation study and presented as single and double strand breaks. We observed that the levels of Cu and Fe were significantly elevated while Zn significantly depleted from Group I to III. The increase in the level of metal ions was high in frontal cortex compared to hippocampus region. During the process of ageing, the amount of single strand breaks increases compared to double strand breaks. Nick translation analysis revealed that the amount of single strand breaks was high in frontal cortex compared to hippocampus region. The results indicate that genomic instability is progressive with ageing and later alter the gene expression. To the best of our knowledge, till date this is a new comprehensive database on the accumulation of Cu and Fe and induction of DNA strand

breaks in DNA in the brain regions of ageing human brain. The biological significance of these findings relevance to mental health has been further elucidated.

Chapter 4: DNA binding properties of neuropeptises, curcumin and actinomycin D

Chapter 4 deals with Tau, Neuromelanin and Synuclein interaction with DNA and also sequence and conformation specific oligonucleotide.

Chapter 4A: New evidences on Tau–DNA interactions and relevance to neurodegeneration

Tau is mainly distributed in cytoplasm and also found to be localized in the nucleus. There is limited data on DNA binding potential of Tau. We provide novel evidence on nicking of DNA by recombinant-Tau. Tau nicks the supercoiled DNA leading to open circular and linear forms. Magnesium (a cofactor for endonuclease) enhanced the Tau DNA nicking ability, while an endonuclease specific inhibitor, ATA inhibited the Tau DNA nicking. This indicates, Tau may nick DNA mimicking endonuclease?. It is hypothesized that Tau DNA nicking ability may be due to 11 histidine residues, as histidine plays a major role in endonuclease activity. Further, we also evidenced that Tau induces B-C-A mixed conformational transition in DNA and also changes in DNA stability. The relevance of these new and intriguing findings regarding Tau changing DNA conformation and stability in neuronal dysfunction is discussed.

Chapter 4B: DNA binding properties of α-synuclein and AGE-α-synuclein (glycated α-synuclein).

α-synuclein is involved in pathogenesis of PD and we studied the α-synuclein and glycated α-synuclein DNA binding ability. α-synuclein was glycated using methylglyoxal (MGO) and formation of AGE-α-synuclein was characterized using fluorescence studies, intrinsic tyrosine fluorescence and fructosamine estimation. α-synuclein and AGE-α-synuclein nick the scDNA like endonuclease. magnesium enhanced α-synuclein and AGE-α-synuclein nicking. Specific nuclease inhibitor aurinetricarboxylic acid inhibited the α-synuclein and AGE-α-synuclein nicking. α-synuclein and AGE-α-synuclein induced B-C-A mixed conformation in scDNA similar

to that of α-synuclein. Both α-synuclein and AGE α-synuclein altered DNA integrity as evidenced by the transition of biphasic melting profile to monophasic melting profile and decreased ethidium bromide binding

Chapter 4C: New evidence on Neuromelanin from the substantia nigra of Parkinson's disease altering the DNA topology

Neuromelanin (NM) is an insoluble pigment found in substantia nigra (SN) pars compacta (pc). The degeneration of neurons within substantia nigra and the presence of extra cellular neuromelanin in PD brain suggest its role in Parkinson's disease. Neuromelanin molecule is composed of melanic, aliphatic, and peptide residues. NM is formed by the oxidative polymerization of dopamine and noradrenaline with the involment of cysteinyl derivatives. NM accumulates large amount of redox active metal ions like Fe, Cu and Mn suggesting its protective role. Extracellular NM has shown to stimulate the microglial release of neurotoxic factor and proteosome inhibition, which aggravate neurodegeneration. Rao et al., (Prog Neurobiol, 2006) hypothesized that NM may have DNA interacting ability similar to amyloid β-peptides. However, there is no data available to validate this hypothesis. Here, we report new data on NM binding to Supercoiled DNA and altering its integrity. We studied NM-DNA interaction by taking supercoiled DNA (scDNA) as model system. NM isolated from the substantia nigra (NM-SN) and NM isolated from the cortex brain region (NM-C) of PD brain. NM-SN is able to convert supercoiled (SC) form to open circular (OC) form indicating NM-SN may be nicking DNA. NM-C does not alter DNA integrity. The DNA nicking of NM-SN was increased with time. Furher Magnesium (1 mM) enhanced the NM nicking property. Magnesium acts as co-factor for endonuclease. It is then significant to mention that NM-SN induced DNA nicking is prevented by nuclease inhibitor like ATA. These studies provide new evidence that NM-SN may be cleaving DNA like endonuclease. Further, NM-SN induced a B-C-A mixed conformation in scDNA, while NM-C induced only altered B-conformation in scDNA. NM-SN changed the characteristic biphasic pattern of the melting profile (Tm) of supercoiled DNA into monophasic and NM-C retained biphasic $T_{m..}$ Our findings revealed that NM-SN and NM-C alter helicity and integrity of DNA. We hypothesize that NM-SN may induce toxicity through an independent non-

apoptotic mechanism in addition to other well known mechanisms. Hence, it can be hypothesized that superhelical DNA component of chromatin may have a significant effect on nuclear– translocated NM functioning. Another probability is that NM may interact with histone-free and transcriptionally active DNA segments and thereby lead to a decreased transcriptional activity of selected genes responding to environmental stimuli.

Chapter 4D: New evidence on α-Synuclein and Tau binding to conformation and sequence specific GC* rich DNA

DNA topology has a significant role in cell integrity. Earlier studies have shown that there is a conformational change in the genomic DNA of Parkinson's disease (PD) brain (B to altered B-DNA) and Alzheimer's Disease (AD) brain (B to Z-DNA). α-Synuclein and Tau proteins are implicated in PD and AD respectively. These proteins are shown to be localized in the nucleus and there is limited data on DNA binding abilities of these proteins. There is no information, whether Tau and α-synuclein binding is sequence and conformation specific? In the present study, we have analyzed the DNA conformation specific binding ability of α-Synuclein and Tau with reference to B-DNA and Z-DNA using oligonucleotide $(CGCGCGCG)_2$ as novel model DNA system. This sequence is predominantly present in the promoter region of the genes. Normally, $(CGCGCGCG)_2$ sequence exists in B-DNA conformation, but at high sodium concentration (4 M NaCl) the oligo goes into Z-DNA form. Both α-Synuclein and Tau bind to B-DNA conformation of $(CGCGCGCG)_2$ and induce altered B-form. Further, these proteins increased the melting temperature and decreased the number of EtBr molecules bound per base pair of DNA of B-form indicating that DNA stability is favored to alter B-DNA conformation. The results confirm that α-Synuclein and Tau could induce the conformational change in the B-DNA to more stable altered B-form. But both α-Synuclein and Tau bind to Z-DNA conformation of $(CGCGCGCG)_2$ and further stabilized the Z-conformation (relevant DNA in neurodegeneration). DNA conformation is very important for the normal functions of DNA molecule and any change in conformation will lead to altered gene expressions. The biological relevance of these novel findings are discussed.

Chapter 4E: Studies on Actionomycin D induced changes in supercoiled DNA integrity

Actinomycin D (AMD) is used as a model compound to understand DNA topology and stability. AMD inhibits the transcriptional process. AMD acts as an intercalating agent blocking the site for RNA polymerase on DNA. In the present investigation, we have studied the effect of AMD on the supercoiling nature (ScDNA) of the DNA and also on single (SSC) and double strand circular (DSC) DNA. The results showed that the ScDNA undergoes a B-A conformational change as demonstrated by a red shift in the CD spectra, an alteration in melting temperature, and also a change in ethidium bromide binding in the presence of AMD. The results clearly indicated that AMD binds to ScDNA and DSC-DNA. The role of altered supercoiling of the DNA molecule in gene expression is discussed.

The thesis ends with a comprehensive Summary and Conclusions and Bibliography.

Summary and Outcome of the work:

1. We have shown that chromatin organization was altered in Parkinson's disease. Histone H3 was acetylated in all the PD chromatin samples compared to 50% of detectable histone acetylation levels in the control sample. DNA methylation was more in PD DNA compared to that of control. Micrococcal nuclease digestion revealed that looser chromatin loops were present in PD chromatin compared to control (**Chapter 2A**).

2. It has been shown that more genotoxicity was observed in PD patients compared to control. Oxidative DNA damage biomarkers 8-OHdG levels were increased in PD patients compared to control indicating more genotoxicity in brain cells. Serum ceruloplasmin and ferritin levels were decreased in PD patients. Serum total antioxidant capacity was increased in PD patients. Atrophy was observed in caudate nucleus, thalamus, hippocampus and substantia nigra regions of PD brain (**Chapter 3A**).

3. We showed that levels of Fe and Cu were increased, while Zn levels were decreased in aging brain. SSBs and DSBs were accumulated in frontal cortex and hippocampus of aging brain (**Chapter 3B**)

4. We showed that tau binds to scDNA and alters DNA integrity. Tau nicks the supercoiled DNA leading to open circular and linear forms like endonuclease (**Chapter 4A**). We also showed that α-synuclein and AGE-α-synuclein alters the scDNA integrity and nick the scDNA (**Chapter 4B**). We also found that actinomycin D alter the DNA supercoiling (**Chapter 4E**)

5. We report new data on NM binding to Supercoiled DNA and altering its integrity. Neuromelanin isolated from the substantia nigra region of the PD brain showed genotoxicity by nicking the DNA and inducing conformational change (**Chapter 4C**).

6. We showed that tau and α-synuclein bind to conformation and sequence specific oligonucleotide both in B-DNA and biologically significant Z-form (**Chapter 4D**).

7. We showed new role of curcumin in altering the chromatin organization. We also showed that curcumin interacts with neuroprotein-DNA complexes destabilizing the chromatin and neuroprotein-DNA complexes. Since several studies showed that curcumin preventing neurotoxicity through antioxidant mechanism, our finding reveals its new role in nucleus (**Chapter 2B**).

8. The present investigation provides new evidence on the pathological mechanism in PD. Our data on chromatin organization, neuroprotein-DNA interaction relevance to neurodegeneration in PD provide new targets for the therapeutic intervention.

Chapter 1

Neurodegeneration in parkinson's disease: an introduction

1. Introduction

Neurodegenerative diseases: The progressive loss of structure and function of neurons is the final consequence of the all neurodegenerative diseases. In different neurodegenerative diseases different regions of brain regions undergo neurodegeneration. Several pathways are involved in the process of neurodegeneration in different neurodegentive diseases and often the pathways overlap. As regeneration is absent in the brain, neuronal loss will lead to the permanent damage and loss of function. It is important to identify the neurodegeneration in the early stages of diseases development and stop the neurodegeneration. In this connection, it becomes vital to know all the possible mechanisms leading to the disease development. Parkinson's Disease and Alzheimer's are the two major neurodegenerative diseases which are affecting the quite large population world wide.

1.1 Pathways of neurodegeneration

Protein degradation: In neurodegenerative diseases like Parkinson's Disease (PD), Alzheimer's Disease (AD) and Huntington Disease, there is involvement of aggregation of proteins. These proteins starts aggregating due to several external and internal factors and impaired function of degradation and removal of these aggregates. Ubiquitin-proteosome is involved in the degradation and removal of non-functional proteins. In neurodegenerative diseases like PD, AD and Huntington the Ubiquitin-proteosome system was unable to remove these altered proteins. In the postmortem neurodegenerative brain and neurodegenerative models compromised proteosome function was observed. Protein misfolding plays important role in the formation of aggregates and the failure of protease system. Still, whether this aggregation of the proteins is the cause or consequence is a debatable issue (Gupta et al., 2006).

Mitochondrial Dysfunction: Mitochondrial dysfunction is the common mechanism leading to neuronal cell death in neurodegeneration (Moreira et al., 2010**).** Mitochondrial dysfunction leads to intrinsic mitochondrial apoptotic pathway. In this

pathway the relase of Cytochrome C release due to internal insult activates the capsase-9, finally lead to cell death. Reactive oxygen species (ROS) generation is more in the mitochondria due to the respiratory electron transport chain. Oxidative stress induced by ROS will lead to activation of several toxic pathways and finally to cell death (Fernández-Checa et al., 2010)

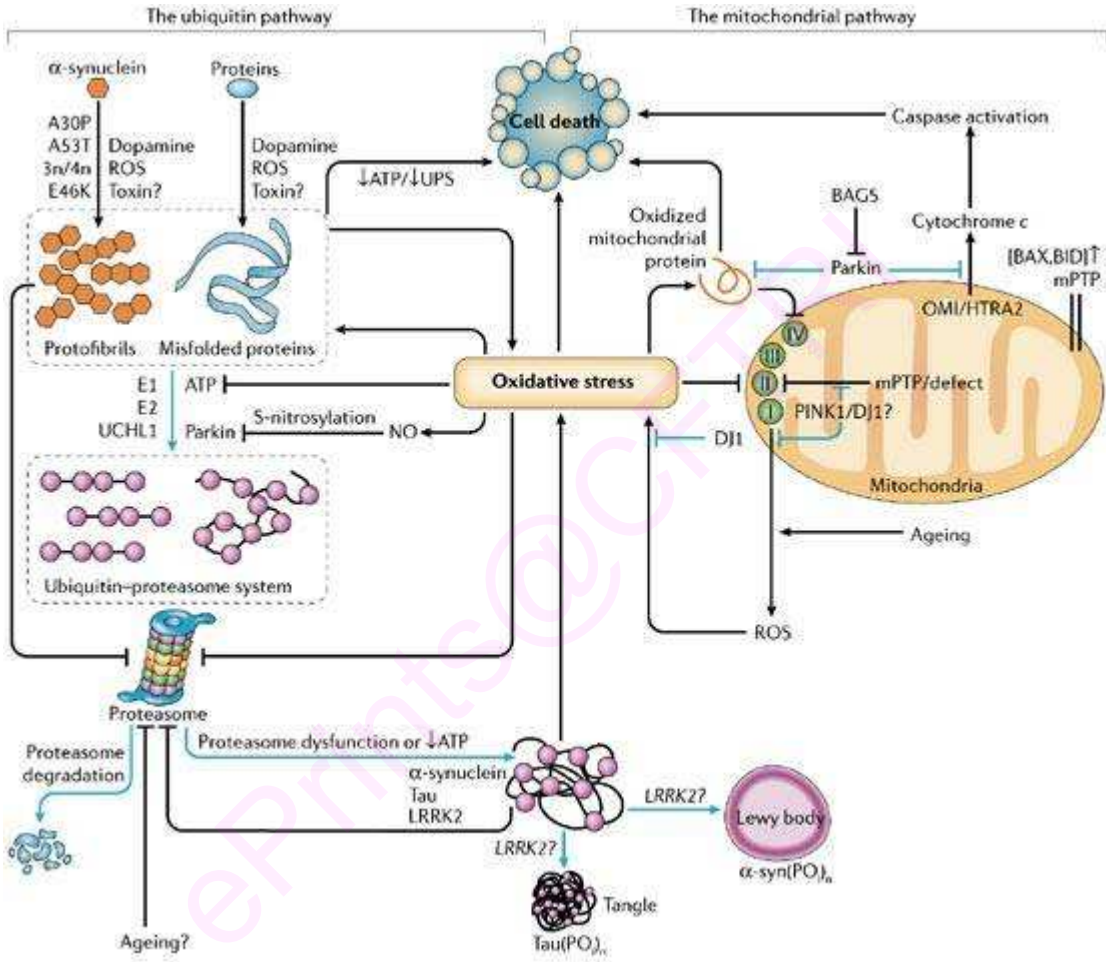

Fig 1.1: Ubiquitin-protease system and Mytochondrial Dysfunction in Parkinson's Disease (**courtesy:** www.nature.com/.../v7/n3/fig_tab/nrn1868_F3.html).

Programmed cell death: In programmed cell death, an intracellular programme directs the cell to death with characteristic cell morphology. The programmed cell death is of three types, apoptosis and autophagy.

Apoptosis: Apoptosis is one way of programmed cell death which is advantageous to cell. The cell which is undergoing the apoptosis shown characteristic changes which

include, blebbing, cell shrinkage, loss of cell membrane, nuclear fragmentation, chromatin condensation and DNA fragmentation. Apoptosis is controlled by the extracellular or intracellular signals. The extracellular signals include toxins, cytokines, growth factors, harmones, nitric oxide etc.,. The intracellular signals released due to the stress induced within the cell wich include, altered intracellular calcium homeostasis, membrane damage, mitochondrial dysfunction, activation of nuclear receptors etc. Both external and internal signals activate the signal transduction of apoptototic mechanisms either by Tumour necrosis factor (TNF) mediated or Fas-Fas ligand mediated cell death. In both mechanisms the balance between the pro-apoptotic molecules (BAX, BID, BAK or BAD) and anti-apoptotic molecues (Bcl-X, Bcl-2) decide the fate of the cell **(**Tatton et al., 2003**)**

Autophagy: Autophagy is a form of intracellular phagocytosis in which the damaged organelles or misfolded proteins are encapsulated into phagosome. The phagosome is finally fuses with lysosome and the misfolded proteins and damaged orgenelles are degraded by the enzymes of lysosome. The cell which is unable to clear the damaged proteins and organelles enter into cell death programme. It was hypothesized that in several neurodegenerative diseases, neuron unable clear the aggregates and proced for the neurodegeneration **(**Ravikumar and Rubinsztein, 2004**)**

1.2 Neurodegeneration in parkinson's disease

Parkinson's Disease (PD) was first formally described in "An Essay on the Shaking Palsy," published in 1817 by a London physician named James Parkinson (Parkinson J, 1817). It is a common progressive neurological disorder that results from degeneration of nerve cells in a region of the brain called '*substantia nigra*' (SN) that controls balance and coordinates muscle movement. These nerve cells, for reasons that are not fully understood, are especially vulnerable to damage of various sorts, including drugs, disease, and head trauma. These neurons project to the striatum and their loss leads to alterations in the activity of the neural circuits within the basal ganglia that regulate movement. This degeneration creates a shortage of dopamine, a neurotransmitter, which causes impaired movement. In the United States alone, about a million people are believed to suffer from PD, and about 50,000 new cases are reported every year (Rajput

and Birdi, 1997). Because the symptoms typically appear later in life, these figures are expected to grow as the average age of the population increases over the next several decades. There is no cure for PD to date. Available drugs suppress symptoms early in PD, but progressively fail as more nerve cells die. The emergence of drug-induced dyskinesias and motor fluctuations often limits drug benefits. Developing therapies to prevent PD, to suppress symptoms, to halt disease progression, and to repair damage are all fundamental goals in modern day research, besides early diagnosis of PD. The preclinical diagnosis of PD is critical, so that neuroprotective therapies might be administered during the early stage and efficiently slow down the diaease progression. To achieve therapeutic goals, new and innovative studies are required, from basic research advances to translating the same in to animal testing, and safety studies in human patients.

1.2.1 Lewy bodie pathology

Pathologically, PD is characterized by the loss of the pigmented dopaminergic neurons from the substantia nigra pars compacta (SNpc). These nerve cells, for reasons that are not fully understood, are especially vulnerable to damage of various sorts, including drugs, disease, and head trauma. These neurons project to the striatum and their loss leads to alterations in the activity of the neural circuits within the basal ganglia that regulate movement. Disruption of dopamine along the non-striatal pathways likely explains much of the neuropsychiatric pathology associated with PD. Excessive accumulations of iron, which are toxic to nerve cells, are also typically observed in conjunction with the protein inclusions. Other pathological events include the presence of extracellular melanin (a dark pigment), released from degenerating neurons, reactive gliosis (increase in numbers of glial or support cells), and pink-staining cellular inclusions known as *Lewy Bodies* (LBs) in the remaining SNpc neurons. The LB, which was first described by Frederick Lewy in 1913, is present in essentially all cases of PD. The major protein constituent of LBs is α-Synuclein, a natively unfolded protein having high propensity for fibrillation/aggregation. The mechanism by which the brain cells in Parkinson's are lost may consist of an abnormal accumulation of the protein α-synuclein bound to ubiquitin in the damaged cells.

1.2.2. Oxidative stress and DNA damage in PD

Substantial evidence implies that redox imbalance or oxidative stress following overproduction of reactive oxygen/nitrogen species overwhelming the protective defense mechanism of cells contributes to the pathogenesis of PD (Olanow, 2007). Nigral dopaminergic neurons in human brain are particularly exposed to oxidative stress because the metabolism of dopamine gives rise to various molecules that can act as endogenous toxins if not handled properly (Graham, 1978). In PD, nigral cells seem to be further under a heightened state of oxidative stress, as indicated by elevations in by-products of lipid, protein and DNA oxidation, and by compensatory increase in antioxidant systems (Jenner, 1998). The level of iron, which is significantly higher in the normal SN than in other regions owing to its binding affinity to neuromelanin, was further increased in the SN of PD further contributing to oxidative stress (Ben-Shachar, 1991).

One of the consequences of redox imbalance is apoptosis and/or necrosis which are associated with neurodegeneration in PD (Ziv and Melamed, 1998). Studies have also shown that the levels of the nucleoside, 8-hydroxy -2'-deoxyguanosine (8-OHdG), a product of free radical attack on DNA were generally increased and differentially distributed in PD brains with highest levels in caudate, putamen, SN and cerebral cortex (Alam et al., 1997). Features of apoptosis based on histochemical methods to mark endonuclease-induced DNA fragmentation by *in situ* terminal deoxynucleotidyl transferase-mediated dUTP nick-end labeling-TUNEL/ISEL (Gavrieli et al., 1992) or *in situ* nick translation (Gold et al., 1994) have been reported in SN in PD.

We have recently shown increased DNA fragmentation and decreased DNA stability in affected human brain regions of PD (Hegde et al., 2006). Similarly, we also showed an altered DNA conformation in hippocampus of human brains affected with Alzheimer's disease (AD) (Suram et al., 2002). Nunomora *et al.*, (2002) demonstrated using immunoreactivity to 8-hydroxyguanosine in neurons that RNA was a major site of nucleic acid oxidation in DLB. The authors suggested that normal RNA oxidation might represent one of the fundamental abnormalities in age-associated neurodegeneration including PD and AD.

1.2.3. Cross-talk of environment and genome

The precise causes of PD remain undetermined. The causes are likely to include both genetic (Parkin and α-Synuclein) and environmental factors (metals, pesticides etc). However, very few cases of PD have pure genetic or environmental etiology; while in vast majority both genetic and environmental factors are involved. Understanding this 'cross-talk' between genetic and environmental factors is important in PD research.

During the past decade, genetic approaches to the study of PD have resulted in major insights. The number of genes implicated in the pathogenesis of PD has been constantly increasing, and includes genes encoding for α-Synuclein, Parkin, DJ-1 and PINK1 (Hofer and Gasser, 2004). These genes are thought to be involved in the proteasomal protein degradation pathway, in the cell's response to oxidative stress, and in mitochondrial function, respectively (Hofer and Gasser, 2004). Over the last few years, several genes for rare, monogenically inherited forms of PD have been mapped and/or cloned. In dominant families, mutations have been identified in the gene for α-Synuclein. Although most people do not inherit PD, studying the genes responsible for the inherited cases is advancing our understanding of both common and familial PD.

Evidence has accumulated steadily to support the view that PD can originate from long-term, subclinical damage to the nervous system caused by environmental toxins (Calne et al., 1987). In fact, several studies have implicated such environmental factors as pesticides, herbicides, and heavy metals in the PD origin (Gorell et al., 1999; Le Couteur DG et al., 1999). Our lab recently showed that trace metal homeostasis is significantly affected in serum samples from PD affected human subjects and there is a direct link between disturbance of trace metal levels in serum and brain (Hegde et al., 2004), suggesting important role played by metals in PD pathology (Hegde et al., 2009; Gupta et al., 2005; Pande et al., 2005).

There is interaction between the environment and the genome; in some disorders inheritance establishes susceptibility and environment triggers pathology. Hence, the recent trend to study PD is to look at the interplay or *cross-talk* between

genetics and environmental triggers (Figure 1.2). Hence, it is important to understand/explore the complex interactions between genetic predisposition and environmental influences that probably cause most cases of PD.

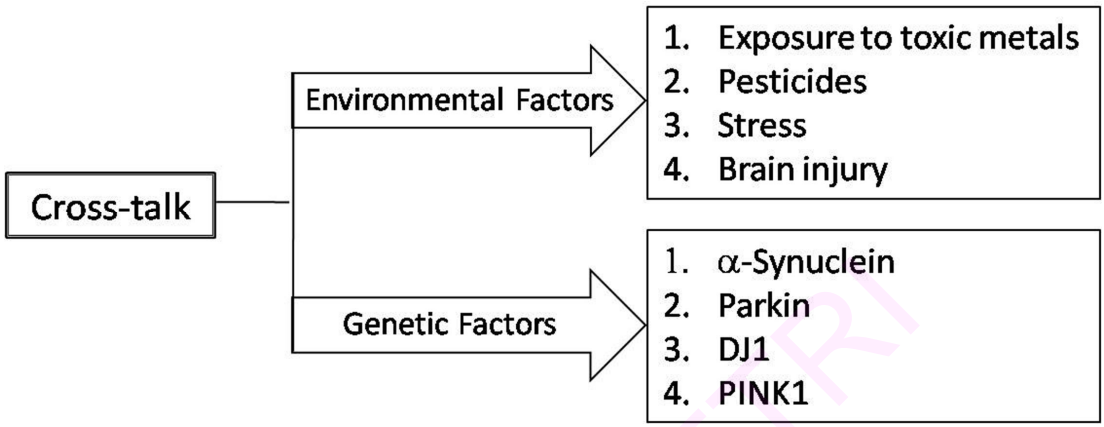

Figure 1.2: The 'Cross-Talk' or interplay of environmental and genetic causative factors for Parkinson's disease.

1.2.4. α-Synuclein and PD

The synucleins are a family of proteins whose function in normal cell is not well understood. The first of the synuclein proteins described in 1988 was α-Synuclein. The name 'synuclein' was chosen because the protein was found in both synapses and nuclear envelope (Maroteaux et al., 1988). Later, it was also named the non-amyloid component (NAC) of beta-amyloid plaque precursor protein. The NAC peptide was isolated from amyloid-rich senile plaques of brains of patients with AD. Amyloid plaques are one of the hallmarks of AD. NAC peptide was shown to be identical to a certain part of α-synuclein. The second member of the synuclein family is known as beta-synuclein. Both these proteins are found in the presynaptic terminals of neurons and many researchers believe they may be involved in synaptic function. The third member of synuclein family is gama-synuclein. All synucleins have in common a highly conserved α-helical lipid-binding motif with similarity to the class-A2 lipid–binding domains of the exchangeable apolipoproteins (George, 2002). Synuclein family members are not found outside vertebrates, although they have some conserved

structural similarity with plant 'late-embryo-abundant' proteins. The alpa and beta Synuclein proteins are found primarily in brain tissue. The gama-Synuclein is found primarily in the peripheral nervous system and retina, but its expression in breast tumors is a marker for tumor progression. While α-Synuclein has been implicated in neurodegenerative disorders mainly PD, until recently there has been no evidence to suggest a role for the other synucleins in neurodegeneration. α-Synuclein forms fibrillar aggregates known as LBs in PD brain, these insoluble protein aggregates are morphologically similar to the amyloid fibrils found in AD neuritic plaques and in protein deposits associated with other amyloidogenic diseases (Conway et al., 2000).

Three missense mutations in the alpa-Synuclein gene have been reported to be associated with families susceptible to inherited forms of PD (Polymeropoulos et al., 1997). These mutations cause alterations in the amino acid sequence of alpa Synuclein (at residues Ala30Pro or Ala53Thr or Glu46Lys) in regions predicted to influence the secondary structure of α-Synuclein. The substitutions may disrupt the structure of alpa-Synuclein, rendering the protein more prone to self- aggregation (Heintz NH, 1997).

Several lines of converging evidence directly implicate α-Synuclein in mechanisms underlying the onset/ progression of PD (Trojanowski and Lee, 2001). They are: (i) Missense mutations in the α-Synuclein gene (A53T, A30P and E46K) cause familial PD in rare kinds (Krüger et al., 1998; Zarranz et al., 2004; Polymeropoulos et al., 1997); (ii) Antibodies to α-Synuclein specifically detect LBs, (Spillantini et al., 1997); (iii) LBs purified from PD brains contain abnormally aggregated α-Synuclein and insoluble forms of α-Synuclein (Baba et al., 1998). The precise mechanism whereby such aggregates of α-Synuclein cause degeneration of dopaminergic neurons is not known. The aggregates may be merely a normal reaction by the cells as part of their effort to correct a different pathological event, as-yet unknown. This issue is dealt with in detail in the latter part of the article.

An important feature of α-Synuclein primary structure is six imperfect repeats within the first 95 residues. This brings the similarity of α-Synuclein with the amphipathic lipid-binding α-helical domains of apolipoproteins (George et al., 1995), which show variation in hydrophobicity with a strictly conserved periodicity of 11. α-

Synuclein shares the defining properties of the class A2 lipid-binding helix, distinguished by the clustered basic residues at the polar-apolar interface, positioned $\pm 100^0$ from the center of apolar face; predominance of lysines relative to arginines among these basic residues; and several glutamate residues at the polar surface (Segrest et al., 1992). In agreement with the above structural features, α-Synuclein binds specifically to synthetic vesicles containing acidic phospholipids (Perrin et al., 2000). Further, this binding was shown to be accompanied by a dramatic increase in α-helix content.

Recently, attempts have been made to analyze the structure of α-Synuclein using NMR studies (Bussell R Jr and Eliezer, 2003; Eliezer et al., 2001; Chandra et al., 2003). It was shown that the conformation of α-Synuclein consists of two α-helical regions that are interrupted by a short break (Chandra et al., 2003). NMR study of free monomeric α-Synuclein revealed that the first 100 residues in N-terminus region of free α-Synuclein have an overall preference for helical structure and there may be the presence of a transient helical structure from residues 6 to 37. In contrast, the final 40 residues of free α-Synuclein exhibited secondary shifts indicative of highly unfolded and extended form (Eliezer et al., 2001). We used the predictor of naturally disordered regions (PONDR, Molecular Kinetics, Inc.) (Li et al., 1999) software to α-Synuclein (Figure 1.3). This shows that about 40-50 residues in in α-Synuclein C-terminus is relatively disordered.

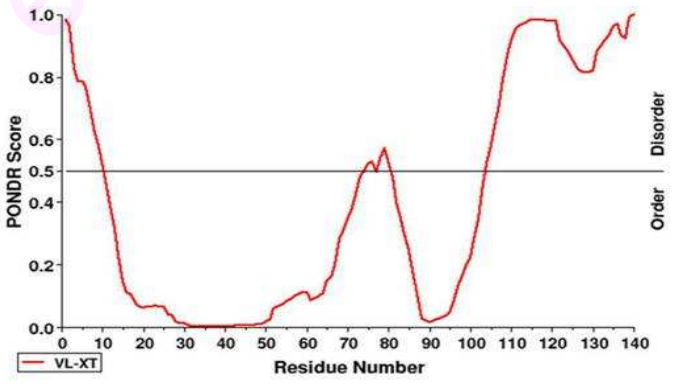

1 MDVFMKGLSK AKEGVVAAAE KTKQGVAEAA GKTKEGVLYV GSKTKEGVVH

51 GVATVAEKTK EQVTNVGGAV VTGVTAVAQK TVEGAGSIAA ATGFVKKDQL

101 GKNEEGAPQE GILEDMPVDP DNEAYEMPSE EGYQDYEPEA

Figure 1.3: PONDR plot of the predicted secondary structure of α-Synuclein.The protein sequence is obtained from NCBI database. PONDR score of 0.5 and higher indicates disordered structures (Li et al., 1999). The C-terminal ~40-50 residues in α-Synuclein are disordered. The lower panel shows α-Synuclein aminoacid sequence, the regions with disoreder propensity are underlined.

NMR data of α-Synuclein in presence of unilamellar vesicles suggested that the N-terminal region is responsible for lipid binding and the boundary for this region occurs between residues 102 and 103. The shifts in C^{α} chemical shifts clearly indicated that there is the formation of helical structure upon α-Synuclein association with unilamellar vesicles. It was noted that it is only the N-terminal region of the protein containing the amphipathic apolipoprotein helical motifs, which binds and adopts a helical conformation. The C-terminal region remains in the same conformation as in the free α-Synuclein and does not bind to the lipid vesicle surface (Eliezer et al., 2001).

α-Synuclein folding and fibrillation have been found to be promoted on binding to long chain fatty acids (Perrin et al., 2001) and also upon its interaction with lipid droplets (Cole et al., 2002). It was also shown that membrane interactions induce a large conformational change from random coil to α-helix in α-Synuclein and these interactions may be physiologically important (Jo et al., 2000). On the basis of these observations, it has been assumed that α-Synuclein may exist in two structurally different isoforms *in vivo*: a helix-rich, membrane-bound form and a disordered, cytosolic form, with the membrane-bound α-Synuclein generating nuclei that seed the aggregation of the more abundant cytosolic form. The partially folded intermediate of α-Synuclein is more prone for aggregation. The aggregation of α-Synuclein depends upon extent of folding induced by the membrane interaction but the mechanism is not clear.

It is suggested that the misfolded or partially folded α-Synuclein is more cytotoxic than the protein aggregates. The intermediate partially folded or misfolded form may be entropically rich in energy and may bind to other components in the cell and may be a cause for neurodegeneration. Transgenic animal models expressing

human α-Synuclein had shown neurodegeneration, without fibrillar α-Synuclein (Feany and Bender, 2000). In that sense, the formation of aggregates could be a protective measure adapted by the cell against the toxicity of this intermediate. However, it is still a matter of debate regarding the toxic form of the protein (monomeric or oligomeric?) in neurodegenerative disorders.

1.2.5 Potential normal functions of α-Synuclein

Dispite of strong evidence implicating α-Synuclein in the pathogenesis of several meurodegenerative diseases, its physiological function remains poorly understood. The difficulty in determining the functions of α-Synuclein is because inactivation of the α-Synuclein gene does not lead to a significant neurological phenotype. However, overexpression of α-Synuclein in rat substantia nigra was shown to cause loss of dopaminergic neurons, but is limited to the targeted region and does not mimic the broad pathology observed in the disease (Yamada et al., 2004). Furthermore, mouse models based on overexpression of α-Synuclein through genetic methods lead to a wide variety of phenotypes accompanied by non-existant, late onset, or non-specific neurodegeneration (Chesselet MF, 2008). Understanding the role of α-Synuclein in normal cell life might be critical importance since disruption of its normal function might indirectly result in neurodegeneration. The association with membrane lipids and its functional homology with 14-3-3 chaperone proteins suggested that α-Synuclein may play a role in cell signaling pathways (Ostrerova et al., 1999). It was also suggested that α-Synuclein may modulate tau function. α-Synuclein was detected in axons and developing pre-synaptic terminals after their formation in rat embryonic hippocampal cells in culture, suggesting a possible role in synaptic development and maintenance. α-Synuclein may contribute to neuronal differentiation as well (Stefanis et al., 2001). The involvement of α-Synuclein in synaptic plasticity and neuronal differentiation may be mediated by the selective inhibition of Phospholipase D2 by α-Synuclein (Jenco et al., 1998). When α-Synuclein expression was markedly reduced in cultured rat neurons (Murphy et al., 2000) or abolished in α-Synuclein knock out mice, the number of vesicles in the distal pool of the pre-synaptic terminal is reduced indicating a role for α-Synuclein in vesicular dynamics. According to Cole and Murphy (2002) α-Synuclein's involvement in lipid metabolism cannot be ruled out, given its

propensity to bind molecules with high hydrophobic content or exposed hydrophobic domains. Thus persuasive evidence of a role of α-Synuclein in any pathway or function requires multiple approaches. The structure, expression and functions of α-Synuclein have been recently reviewed by Dev *et al.*, (2003).

1.2.6 α-synuclein toxicity in diffuse Lewy body disease

Diffuse Lewy Body Disease is the second most common cause of dementia after AD. It is also commonly reffered to as Dementia with LBs (DLB). DLB usually presents with a neurobehavioral syndrome that may include hellucinations, delutions, and psychosis, eventually leading to dementia. DLB overlaps in clinical, pathological, and genetic features with AD and PD. Pathologically DLB demonstrate prominent cortical and subcortical LB formation, which differentiates it from PD (Kalra et al., 1996). Similar to PD, LBs in DLB are rich in α-Synuclein protein aggregates. Infact the neuritic α-Synuclein accumulation, density of cortical LBs and AD-type pathology (senile plaques and hippocapal neurofibrillary tangles) are more intense in DLB than PD (Tsuboi et al., 2007). Pathologically, most PD cases have minimal or no senile plaques and neurofibrillary tangles, while they are present in DLB. It is also suggested that α-Synuclein and amyloid beta interact in DLB (Pletnikova et al., 2005).

1.2.7 Expression and subcellular distribution of α-synuclein

α-Synuclein appears to be expressed ubiquitously throughout the brain (Lavedan C, 1998). In the early weeks of development, α-Synuclein redistributes from cell bodies to synaptic terminals (Galvin et al., 2001). The transcription of α-Synuclein is developmentally regulated. The levels increase during development and are sustained at fairly high levels throughout adulthood (Petersen et al., 1999). Furthermore, various cellular treatments have been shown to affect synuclein levels, including nerve growth factor (Stefanis et al., 2001), 1-methyl-4-phenyl-1,2,3,6-tetrahydropiridine (MPTP) (Vila et al., 2000), certain inflammatory cytokines, cellular stress, and during megakaryocyte differentiation. However, a clearer understanding of the transcriptional and translational regulation of synuclein expression is needed before we can understand

how any changes in these mechanisms may affect the disease process (Cole and Murphy, 2002).

Recently Zhang *et al.*, (2008) examined the subcellular localization and relative amounts in different subcellular pools in rat brain neurons. They showed that α-Synuclein was unevenly distributed in axons, presynaptic terminals, cytoplasm and nucleus in neurons. The density was more in presynaptic terminal and nucleus, compared to other subcellular compartments. Interestingly, α-Synuclein was also present in mitochondria.

1.2.8 Nuclear localization of α-Synuclein

Several studies have shown the presence of α-Synuclein in the neuronal nuclei. However, no definite nuclear functions have been attributed to α-Synuclein to date. It is not known if nuclear localization is the common property of α-Synuclein or it is cause/consequence of PD pathology. Overexpression of α-Synuclein in neuronal cell lines showed diffused nuclear staining (Schneider et al., 2007). The term α-Synuclein was first coined by Maroteaux based on its localization in the synaptic region and nucleus (Maroteaux et al., 1988). Mori *et al.*, showed localization in the nucleus of substantia nigra and pontine nucleus neurons of rat brain (Mori et al., 2002). Further, nuclear localization of α-Synuclein was shown in cultured primary neurons (Specht et al., 2005) and cell lines (Yu et al., 2004). Nuclear inclusions of neurons and oligodendroglia of multiple system atrophy contain the α-Synuclein protein (Lin et al., 2004). Yu *et al.*, showed nuclear localization of α-Synuclein in the rat brain by immunoelectron microscopy using colloidal gold probes (Yu et al., 2007). Mono and oligomeric forms of α-Synuclein were observed in the nuclear fractions of human dopaminergic neuroblastoma SH-SY5Y cells (Leng et al., 2001). Extensive nuclear localization of α-Synuclein indicates that it might play important role in the nucleus.

Although the above observations do not suggest what the function of α-Synuclein in nucleus is, Leng *et al.*, (2001) predicted that α-Synuclein may play a role in regulating processes in the PI- cycle in the nucleus and phosphatidyl inositol-linked activities may also occur in nucleus.

1.2.9 Nuclear transport of α-Synuclein

The mode of appearance of α-Synuclein into the neuronal nuclei and functions of α-Synuclein in nuclei is still obscure. According to Maroteaux *et al.*, (1988) the mode of localization of α-Synuclein in the nucleus could involve a lateral diffusion along the endoplasmic reticulum and outer nuclear membrane or more conventional transport through nuclear pores. They proposed that α-Synuclein family proteins may be involved in coordinating nuclear and synaptic events. However, under PD conditions, the nuclear localization of α-Synuclein could be enhanced due to non-specific transportation through oxidatively damaged nuclear membrane (Hegde et al., 2003). The highly oxidative cytological environment in PD brain, because of increase in paramagnetic ferrous and other free radical generating metals, are known to disrupt the biological membranes leading to translocation of α-Synuclein in to the nucleus. Sangchot *et al.*, (2002) have provided new evidences for nuclear membrane disruption by lipid peroxidation caused by increase in iron and consequent translocation of α-Synuclein aggregates in to perinuclear and endonuclear regions of human dopaminergic neuroblastoma SK-N-SH cell lines. Leng *et al.*, (2001) also observed α-Synuclein both in monomeric and oligomeric forms in nuclear fractions of human dopaminergic neuroblastoma SH-SYSY cell cultures.

1.2.10 α-Synuclein genotoxicity

With several evidences showing the presence of α-Synuclein in neuronal nuclei, as discussed above, the question arises about its function/role in the nuclein. Further, it is interesting to discuss whether nuclear α-Synuclein is an active or passive response to PD pathology. It was shown that α-Synuclein interacts with histones *in vitro* and this interaction if confirmed *in vivo*, might alter the gene transcription (Goers et al., 2003). To support this, when, transfected to cell lines, α-Synuclein changes the expression of many genes (Baptista et al., 2003). α-Synuclein alters gene expression changes of stress response genes, transcription regulators, apoptosis inducers, transcription factors, membrane bound proteins and protein involved in the dopamine synthesis. In α-Synuclein transfected dopamenergic cell lines, tyrosine hydroxylase was inhibited (Yu et al., 2004). Furthermore, α-Synuclein over expression in PC12 cells showed enhanced

proliferation and enrichment of cells with S-phase, again suggesting enhanced gene expression.

α-Synuclein nuclear targeting accelerated the neurodegenerative process in the dopaminergic neurons of flies (Kontopoulos et al., 2006). Histone deacetylase inhibitors prevented this neurodegenerative process when administrated. This may be explained assuming that α-Synuclein induces its toxicity by inhibiting the histone acetylation. α-Synuclein was also shown to associate with histone H3 and inhibit its acetylation.

Further, widespread DNA damage is observed in the brain regions affected with synucleinopathies in which neurodegeneration is observed (Hegde et al., 2006; Suram et al., 2007). These brain regions have been quite often linked to excess iron accumulation. In presence Fe (II) α-Synuclein can generate reactive oxygen species and damage DNA indirectly in the neuronal cells (Tabner et al., 2002; Martin et al., 2003). Although, this is an indirect indication, the fact that ncreased DNA damage is observed in cells transfected with wild type α-Synuclein and mutants A30P, A53T after treating with Fe (II), strengthens this hypothesis. The above observations suggest that α-Synuclein contributes to genotoxicity in various ways.

Our lab reported the ability of α-Synuclein to directly bind to DNA molecule that results in altered DNA conformation and damage which will be discussed later in this review.

1.2. 11 α-synuclein dna interactions: a new concept

We recently made an interesting observation that α-Synuclein has DNA binding property which has created a new opportunity in understanding role of α-Synuclein in PD pathology (Hegde et al., 2003; Hegde et al., 2006; Hegde et al., 2007). Previously we also showed for the first time that amyloid beta peptides implicated in AD can also bind to DNA (Hegde et al., 2004; Suram et al., 2007). The origin of the above concept and subsequent progress are discussed below.

Our hypothesis on DNA binding of α-Synuclein- genesis of model

As stated earlier, several studies showed that α-Synuclein is localized in the chromatin region of nuclei in the brain. This strongly indicated the association of α-Synuclein with chromatin in the nucleus. It was also shown previously that several cationic and anionic ligands interact with α-Synuclein such as polyamines and metals (Uversky et al., 2001, Grabenauer et al., 2008). Furthermore, a close look into the peculiar primary sequence/structure of α-Synuclein shows presence of several positively charged lysine residues at its N-terminus, suggesting a possible DNA binding property. It was recently observed that α-Synuclein interacts with histone proteins, a major component of chromatin, which modulates its conformation and aggregation properties (Gores et al., 2003). We thought it is interesting to investigate the DNA binding property of α-Synuclein and study the effect of DNA binding on α-Synuclein folding/conformation and aggregation properties. Moreover, we had previously observed DNA binding of amyloid beta peptides, which led us to examine α-Synuclein in similar lines (Hegde et al., 2004; Suram et al., 2007). We also proposed that understanding the effect of DNA binding on α-Synuclein stability, conformation and fibrillation could lead to a better understanding of PD pathogenesis and could also be exploited for DNA binding based therapeutic interventions.

1.2.12 New evidence for DNA binding property of α-Synuclein

We first time demonstrated that α-Synuclein binds to DNA *in vitro*, a new and novel property of α-Synuclein (Hegde et al., 2003; Hegde et al., 2006; Hegde et al., 2007). This was independently confirmed by other groups as well (Cherny et al., 2004). This is the first report on DNA binding property/ability of α-Synuclein and presents an interesting curiosity about the implications of this property in PD. The association of DNA with α-Synuclein is not limited to wild-type protein. Familial mutants A53T and A30P also showed DNA binding (Cherny et al., 2004). Numerous studies have demonstrated that various intracellular factors affect folding and fibrillation properties of α-Synuclein. Histones, one of the important components of chromatin was shown to specifically interact with α-Synuclein and significantly stimulate its aggregation (Gores et al., 2003). DNA being another component of chromatin, its interaction with α-

Synuclein strongly suggests an important role of α-Synuclein in the nucleus. The possible mechanisms and implications of α-Synuclein-DNA interactions are discussed below.

1.2. 13 α-Synuclein affects DNA conformation

Circular dichroism (CD) spectra of α-Synuclein-supercoiled DNA complex demonstrated a strong binding of α-Synuclein to supercoiled DNA, causing a conformational change from the B-form of DNA to an altered B-form (Hegde et al., 2003). It was further shown that α-Synuclein uncoils supercoiled DNA to open cicular form. Differential sensitivity of synuclein-supercoiled DNA complex to chloroquine induced topoisomers separation compared to DNA alone suggested destabilization of DNA by α-Synuclein (Hegde et al., 2003). The modulation of DNA conformation and stability by α-Synuclein could be important in PD pathology as it may affect DNA transactions such as replication and transcription and hasten accumulation of DNA damage. However, considering that α-Synuclein is expressed ubiquitously in the brain, the question arises, if this interaction could eventually take place in any other brain region not affected during PD? Or is there brain region selectivity?. Our recent observations show that the most pathological, misfolded form of α-Synuclein found in dopaminergic neurons exhibit significantly higher DNA binding and damage activity compared to the native monomeric form found in normal brain which suggests that the DNA interaction of α-Synuclein might be higher in PD affected brain regions (Hedge et al., 2004); Hegde *et al., unpublished observation*).

A plausible scenario for DNA binding to α-Synuclein could be as follows: It appears that initially on mixing with α-Synuclein in solution, α-Synuclein monomers interact electrostatically with DNA phosphate groups. DNA interacts possibly with the positively charged lysine side chains located predominantly in the N-terminal and partly in the central region of α-Synuclein sequence. Because it is highly unlikely to bind to the C-terminal end of α-Synuclein which is rich in negatively charged amino acid residues (Cherny et al., 2004). These electrostatic interactions may lead to (i) formation of non-sequence specific complex of α-Synuclein with DNA, and (ii) increase in the local concentration of α-Synuclein on DNA (Cherny et al., 2004). Once α-Synuclein

binds to DNA by electrostatic forces, there could be a conformational change in α-Synuclein making the protein enzymatically bind to DNA.

1.2.14 DNA induced folding of α-Synuclein

We observed that various DNAs significantly modulate conformation and fibrillation properties of α-Synuclein. Single strand circular DNA binding to native, random coiled α-Synuclein resulted in about 80% increase in α-helix content of the protein (Hegde et al.,m 2007). Although, double strand circular DNA also bound to α-Synuclein, it did not change its conformation, indicating specificity of single strand DNA binding. However, supercoiled plasmid DNA caused a biphasic conformational transition in α-Synuclein. On immediate mixing of the DNA and α-Synuclein a partial folding was induced in α-Synuclein, while α-helix conformation was formed on long term incubation (Hegde et al.,m 2007).

We also provided interesting insight on sequence specific binding affinity of DNA to α-Synuclein. Poly d(GC).d(GC) caused a partially folded conformation, where as poly d(AT).d(AT) binding to α-Synuclein did not result in any such conformational transition. It was further observed using GC- and AT-specific 8-mer oligonucleotides that only d(GCGCGCGC) induced a partial folding in α-Synuclein. Interestingly, d(GCATGCAT) also induced a partial folding in α-Synuclein,while, d(ATATATAT) did not. Closer examination of the CD data indicated that the folding induced by d(GCGCGCGC) was more in magnitude compared to d(GCATGCAT).

The effect of binding of large genomic DNA (lamda and Calf-thymus DNA) on α-Synuclein conformations showed that both these genomic DNA caused the formation of a partially folded structure in α-Synuclein. However, the amount of folding induced by lamda DNA was more when compared to calf-thymus DNA. The GC content of calf-thymus DNA is ~70%, while for lamda DNA it is ~42% which should explain the differential ability of calf-thymus and lamda DNA in inducing conformational transition in α-Synuclein.

The above studies from our lab indicated specificity of single stranded DNA and GC sequence in inducing folding in α-Synuclein. It appears that the DNA binding to α-Synuclein is mediated through electrostatic interaction between negatively charged phosphate groups of DNA and the epsilon amino group of lysine aminoacids in α-Synuclein. The DNA molecule is richly negatively charged on its surface as it is laced with phosphate groups, where as α-Synuclein has 15 basic lysine residues which are mostly clustered in the N-terminal of its sequence. The neutralization of basic charge on epsilon amino group side chain of lysine residues will reduce the repulsion between the like charges in the N-terminal end of α-Synuclein and this appears to be the driving force in inducing DNA mediated folding in the protein. Studies have shown that the N-terminal half of α-Synuclein sequence has a very high propensity to form ordered conformation (Chandra et al., 2003).

1.2.15 α-Synuclein aggregation and DNA binding

Previous studies have shown that the transformation of α-Synuclein into a partially folded conformation (induced by pH or temperature or metal ions) is strongly correlated with the enhanced formation of α-Synuclein fibrils (Uversky et al., 2001). α-Synuclein is a natively unfolded protein with little or no ordered structure under physiological conditions. At neutral pH, it is calculated to have 24 negative charges (15 of which are localized in the last third of the protein sequence), leading to a strong electrostatic repulsion, which hinders the folding of α-Synuclein (Uversky et al., 2001). As a consequence of the structural flexibility of α-Synuclein, many diverse ligands change its conformation and modulate its aggregation property (Cherny et al., 2004). Generally, transition from random coiled α-Synuclein to partially folded conformation accelerates the fibrillation reaction, while stabilizing α-Synuclein in to α-helix-rich conformation delays fibrillation. Aggregation or self-association is a characteristic property of a partially folded (denatured) proteins and most aggregating protein systems probably involve a transient partially folded intermediate as the key precursor of fibrillation. It has also been shown that in some cases the self-association induces additional structure and stability in the partially folded intermediates.

Recently it was shown that double stranded DNA promotes aggregation of α-Synuclein (Cherny et al., 2004). They showed that the morphology of the fibrils remains unchanged in the presence of linear double stranded DNA. In this context, we analyzed the aggregation propensity of α-Synuclein in the presence of different DNAs which induce partially folded conformation and also α-helix. Our studies showed that DNA induced aggregation of α-Synuclein correlated with the ability of that DNA to induce partially folded conformation in α-Synuclein (Hegde et al., 2007). DNA which induced partial folding in α-Synuclein such as GC-rich oligonucleotides resulted in a very substantial acceleration of the kinetics of aggregation indicated by a shorter lag time and a larger rate of fibril formation compared to α-Synuclein alone. However, single-strand circular DNA which formed α-helix conformation in α-Synuclein delayed the aggregation significantly by nearly ~25 hrs. The structure of α-Synuclein aggregates/ fibrils were qualitatively similar in the presence or absence of DNA.

Similar observations were made by Uversky *et al*, (2001), where they showed that trimethylamine-N-oxide (TMAO) induces a partial folding and acceleration of fibrillization in α-Synuclein at low concentrations, where as, at high concentrations causes the formation of α-helix conformation and inhibits aggregation to a considerable extent. Our results are in agreement with Uversky *et al.*, (2001). Hence, it appears that a partially folded intermediate conformation is a very critical step in α-Synuclein aggregation pathway.

The possible mechanisms of double stranded DNA promoting α-Synuclein fibrillation has been proposed recently by Cherny *et al.*, (2004). The authors observed that neuronal nuclear inclusions potentially account for a significant fraction of the total amount of α-Synuclein in a cell. Hence, minute variations in local α-Synuclein concentrations or the presence of factors enhancing its fibrillation, *e.g.*, DNA or histones, may stimulate the aggregation of α-Synuclein significantly. It was further proposed that effective mechanisms preventing occasional conversion of a soluble α-Synuclein into insoluble isoforms must exist in both cytoplasm and nucleus (Cherny *et al.*, 2004). We provided a comprehensive picture of DNA binding effect on α-Synuclein fibrillation using different DNAs such as double and single stranded DNA,

AT and GC sequence specific DNA of different sizes etc and showed that only those DNA which induce a partial folding in α-Synuclein promote its aggregation, while, single strand circular DNA forms α-helix conformation in α-Synuclein and inhibits aggregation to a considerable extent. Hence, we feel that extrapolation of *in vitro* results on DNA binding property of α-Synuclein to *in vivo* system in PD has to be more cautiously done.

We used effect of osmolytes on α-Synuclein conformation to understand the mechanism of DNA induced folding/fibrillation of α-Synuclein (Hegde et al., 2007). Osmolytes such as TMAO, Betaine, sarcosine converted natively unfolded α-Synuclein to partially folded form which accelerated the kinetics of fibrillation. The ability of DNA and osmolytes in inducing conformational transition in α-Synuclein, indicates that two factors are critical in modulating α-Synuclein folding: (i) Electrostatic interaction as in the case of DNA, and (ii) Hydrophobic interactions as in the case of osmolytes.

1.2.16 Our model on α-synuclein genotoxicity

We propose α-Synuclein-mediated genotoxicity as one of the key underlying mechanisms of disease progression in the PD. Normally α-Synuclein is in random coil conformation in aqueous solutions *in vitro.* It is suggested that free α-Synuclein in neuronal cytoplasm may also be in random coil conformation. However, in association with membranes α-Synuclein is in α-helix-rich conformation. α-Synuclein is diversly/unevenly distributed in various subcellular mileu such as cytoplasm, presynaptic terminus, nucleus, endoplasmic reticulum and mitochondria (Zhang et al., 2008). The factors that govern α-Synuclein distribution in cell are not fully understood. However it is known that oxidative stress and other cytological scenario that exists in PD such as metal toxicity may modulate α-Synuclein subcellular translocation significantly, especially the nuclear α-Synuclein, because these factors greatly affect the permeability of membranes.

Several studies have reported higher levels of iron (Fe) and other transition metals in PD brain substantia nigra, the main target of PD (Dexter et al., 1989). However, how a specific increase in the total Fe content of SN should occur in PD is not understood (Zecca et al., 2004). It has been argued that the increased Fe levels with the severity of neuropathological changes in PD are presumably due to increased transport through the BBB (Gotz et al., 2004). Furthermore, in PD the increased total Fe level in SN was not associated with a compensatory increase in ferritin; instead the brain ferritin immunoreactivity was decreased (Dexter et al., 1990). Hence the increased Fe load in PD may exceed the storage capacity of available ferritin, leading to excess reactive Fe, driving free radical generation. In the presence of these metals α-Synuclein acquires a misfolded or partially folded conformation and promote aggregation *in vitro* (Uversky et al., 2001). We hypothesized that the partially folded or misfolded α-Synuclein induced by metals may not bind to vesicle membrane lipids as it does in normal brain. In addition, it was observed that one of the familial mutant α-Synucleins, A30P completely abolished membrane-binding property of α-Synuclein. Hence, the disruption in membrane binding resulting from increase in metals and mutations in familial PD would result in the increase in free α-Synuclein (partially folded or unfolded native conformation) levels in cell. This possibly triggers the increase in precursor for α-Synuclein aggregation in PD (Hegde et al., 2003). In addition to the accumulating evidence for normal nuclear localization of α-Synuclein, the increased oxidative stress and altered permeability of nuclear membrane could ensure significant amount of α-Synuclein in the nucleus. In the nucleus it exerts toxic role by altering chromatin organization or by directly binding to DNA or by both. α-Synuclein can bind to the histone proteins and affect their normal functioning of maintaining the chromatin integrity. As histones loss their function, chromatin will open up exposing DNA to α-Synuclein and other targets. Now the transcription factors or inhibitors can bind to DNA altering the gene expression. α-Synuclein can itself bind to DNA and relax the supercoils in the DNA molecule and can induce a conformational change, which may further affect the gene expression profile. The altered gene expressions finally lead to altered neuronal cell metabolism leading to cell death. Besides, DNA induced partial folding in α-Synuclein enhances its toxicity to the cell. Several studies have shown that partially folded intermediate form of α-Synuclein is more toxic than monomers or

aggregates. Partially folded α-Synuclein has higher aggregation propensity and in PD the presence of metals and other free radicals can further stimulate the aggregation process. The aggregated protein can disrupt several processes in the nucleus including gene expression and DNA functioning. Our model on α-Synuclein Genotoxicity is represented in Figure 1.4.

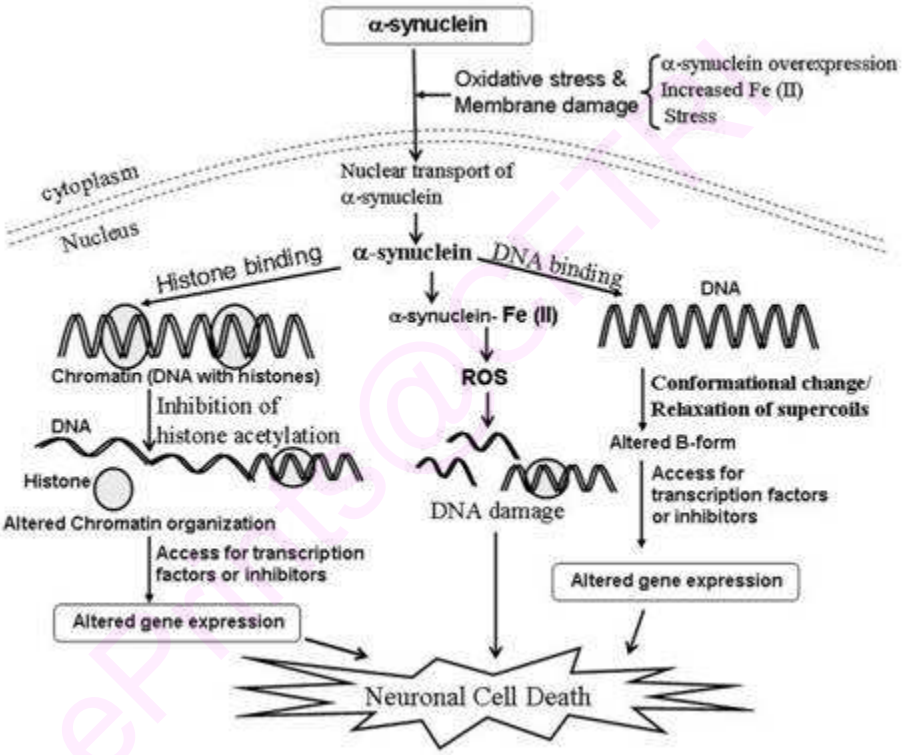

Figure 1.4: Our model on genotoxicity of α-Synuclein: During stress conditions, there is increased transportation of α-Synuclein into the nucleus. In the nucleus, α-Synuclein can directly interact with histones or inhibits histone acetylation affecting the chromatin organization. α-Synuclein can bind to DNA and alter the conformation of DNA, relax supercoiling of DNA. Change in chromatin organization, conformation of DNA and supercoil relaxation may lead to altered gene expression. α-Synuclein in the presence of Fe(II) can generate reactive oxygen species and induce DNA damage. Altered gene expression and DNA damage lead to neuronal cell death.

1.2.17 Tau proteins

Tau is a microtubule-associated protein expressed in neurons (Binder et al, 1985). It normally exists as a random coiled hydrophilic protein containing two distinct domains- the projection domain and the microtubule binding domain. Tau protein is involved in tubulin assembly by forming a bridge between two tubulin dimmers. The tau function is mainly regulated by post-translational modifications. (Johnson and Stoothoff, 2004).

The aggregation of Tau protein is observed in some neurological disease conditions which are collectively known as Tauopathies (Iqbal et al., 2009). Alzheimer's disease (AD) is a principal tauopathy where Tau is aggregated in the form of neurofibrillary tangles (NFTs) (Avila et al., 2004). The precise role of Tau in AD neurodeneration is not clearly understood (Delacourte, 2008; Brandt et al., 2005). Tau is also found in synucleinopathies in the lewy bodies like Dementia with lewy bodies. This suggests that tau function is also altered in synucleinopathies apart from tauopathies (Galpern and Lang, 2006). An Goris et al., studied the pathological hall mark genes namely, microtubule-associated protein tau (MAPT), glycogen synthase kinase-3 (GSK3B) and α-synuclein (SNCA) in 659 PD patients and 2176 control subjects. The authours are observed PD dementia and cognitive decline associated with inverse polymorphism containing MATP. They also reported that inverse polymorphism in MATP is in synergy with single nucleotide polymorphisms in SNCA gene (Goris et al., 2007).

Tau is localized in the nucleus in neuronal and non-neuronal cells (Thurston et al., 1997) and is associated with the nucleolar organizer region (NOR) in the mitotic cell. The NOR in the chromosome consists of GC rich ribosomal DNA (rDNA) near the centromeres. In mammalian chromosomes they are composed of repeated satellite DNA sequences in the form of constitutive heterochromatin. The exact role of tau in the nucleus is nit clearly understood. Tau binds directly to these satellite sequences of centromeric region (Sjoberg et al., 2006). It was shown that tau could bind to single stranded DNA (ssDNA) and double stranded DNA (dsDNA) (Hua and He, 2003; Krylova et al., 2005). The binding might be phosphorylation independent and aggregation dependent. Both phosphorylated tau and non-phosphorylated tau can bind to DNA. Phosphorylated tau binds strongly than non-phosphorylated tau as the former

binding to DNA have higher melting point than later (Hua and He, 2002). Both cytoplasmic and nuclear tau are equally phosphorylated. Phosphorylation of tau occurs in the cytoplasm and transported into the nucleus. Qu et al (2004) found that tau can induce a conformational change in the DNA molecule as a function of the mass ratio of tau to DNA. One tau molecule per 700 bp of DNA could induce a DNA conformational change. Tau also plays a role in chromatin structure, rDNA transcription and recombination, nucleo-cytoplasmic transport and ribosomal assembly (Qu et al., 2004). When Tau binds to one of the strands of DNA in a sequence specific manner, it induces the dissociation of double stranded DNA (Krylova et al., 2005). The biological significance of the tau-DNA complex still needs to be explored. Further we need to understand the mechanism of tau binding to DNA.

1.2.18. Is DNA binding, common property of many amyloidogenic proteins?

It has been widely reported by us and others, that nucleic acids interact with different amyloid peptides such as beta-amyloid, tau protein, prion peptides and α-Synuclein and modulate their folding and aggregation kinetics (Hegde et al., 2003; 2004; Suram et al., 2007; Gabus et al., 2001; Nandi et al., 2002). In many cases double stranded DNA accelerated the kinetics of fibrillation. However, an extensive study by us on α-Synuclein showed that the effect was dependent on the structure of DNA (Hegde et al., 2007). Nandi group by several well designed studies showed that nucleic acids can induce structural changes to beta-sheet rich conformation in prion peptides by forming stable complexes, which catalyzes/modulates their polymerization (Nandi et al., 2002). Association of Abeta (1-40) and Abeta (25-35) with double stranded DNA was detected (Nandi, 1998). Abeta (25-35) was shown to cause formation of open circular DNA from supercoiled DNA in presence of ferrous ions (Jang et al., 2002). We have recently observed binding of Abeta (1-42) and Abeta (1-16) peptides with supercoiled DNA and their ability to convert supercoiled DNA into open circular form (Hegde et al., 2004). Our lab showed that Abeta (1-42) can directly inflict DNA nicking which could contribute DNA damage associated in AD brain (Suram et al., 2007, Gupta et al., 2006). In similar lines latest studies from our lab shows DNA single-strand

breaks directly induced by α-Synuclein in its partially folded form (Hegde et al., 2007); Hegde *et al.*, unpublished observation).

The above scenario suggests that DNA binding could be a normal property of many amyloid-forming proteins associated with diverse neurodegenerative disorders. However, at this stage it is hard to pin down whether DNA binding contributes to PD pathology as a major causative phenomenon or if it is just a consequence of the disease process where non specific nuclear transportaion of amyloid proteins result in DNA binding. We feel that a parallel approach to DNA binding of these amyloid proteins in several neurodegenerative diseases may yield better results. In addition, the finding of insoluble protein-containing materials in different neuronal and glial cell populations in a broad range of syndromes suggests that many of these disorders have something in common (Rao et al., 2006). Even though these syndromes express different symptoms and lesions, the mechanisms underlying filament formation may be similar. The assembly of normally soluble protein subunits into insoluble filaments in these diseases does not normally occur in healthy brain. Hence, another way to approach these disorders is to consider the disease state as one of an abnormality in protein metabolism. Future research efforts will pursue molecular analyses of shared protein abnormalities across several disorders. This approach should provide insights into disease mechanisms underlying one or more degenerative disorders characterized by abundant filamentous lesions.

1.2.19 Biological significance of DNA binding of α-synuclein

Structurally, purified α-Synuclein is a natively unfolded protein (Hegde et al., 2003; Uversky et al., 2001). This lack of folding has been shown to correlate with the specific combinations of low overall hydrophobicity and large net charge (Uversky et al., 2000; 2002). *In vitro,* α-Synuclein readily assembles in to fibrils, with morphologies and staining characteristics similar to those of fibrils extracted from PD affected brain (Uversky et al., 2001; Giasson et al., 1999).

The physiological significance of DNA induced α-Synuclein conformation and modulation of its assembly/ fibrillation is unclear at the present time. However, emerging lucid evidences for the presence of α-Synuclein in neuronal nuclei indicates that the DNA binding activity of α-Synuclein may not be a mere non-specific phenomenon and may have very significant role to play in neuronal cell death in PD through DNA instability. It will be evocative to speculate the potential implications of the *in vitro* findings on DNA binding of amyloid proteins to neurodegenerative changes associated with PD. Goers *et al.,* (2003) provided evidence for the co-localization of α-Synuclein with histones in the nuclei of nigral neurons from mice exposed to a toxic insult. The authors observed that histones stimulate α-Synuclein fibrillation *in vitro*. These studies further strongly suggested association of α-Synuclein with chromatin.

Cherny *et al.*, (2004) proposed that α-Synuclein may interact with histone-free, transcriptionally active DNA segments and hence may lead to a decreased transcriptional activity of some genes responding to environmental stimuli . It is suggested that the interactions of α-Synuclein with DNA and histones may function to regulate gene expressions.

Interestingly, a recent study involving semi-quantitaive analysis of α-Synuclein in subcellular pools of rat brain neurons showed that there is a significant fraction of α-Synuclein in the nuclear compartment (Zhang et al., 2008). They used immunogold electron microscopic technique with a C-terminal specific antibody. It was shown that α-Synuclein-positive gold particles were unevenly distributed in different subcellular compartnets. The density was relatively greater in presynaptic terminals and nucleus. In this perspective, association of α-Synuclein with chromatin attains significance. α-Synuclein-induced changes in DNA conformation may affect gene expression pattern in affected neurons. In addition, DNA induced folding and modulation of fibrillation property may have special pathophysiological significance and contribute enormously to the accumulation DNA damage in degenerative neurons and lead to cell death.

1.2.20 Alternative view: α-synuclein and neuroprotection

Several lines of evidences suggest α-Synuclein toxicity in PD, however, an alternative debate for the neuroprotective role of α-Synuclein in PD is emerging (Lee et al., 2006). Although, α-Synuclein accumulation in the form of aggregates in dopaminergic neurons is a common pathological feature in PD, the precise mechanism of how this aggregation process is triggered? Or how the protein aggregates cause neuronal degeneration is still obscure. Furthermore, some studies have failed to show consistant results for neurotoxicity of α-Synuclein (Hashimoto et ., 2002; Matsuoka et al., 2001) and few studies also suggested that α-Synuclein may play a neuroprotective role (Hashimoto et ., 2002; Manning-Bog et al., 2003).

In other words, there is a school of thoughts which argues that α-Synuclein has a normal function in normal brain, but in response to environmental or endogenous stimulus it aggregates as a neuroprotective response or as a passive response to pathological events. For instance, oxidative stress caused by the herbicide paraquat results in α-Synuclein aggregation in the brains of experimental animals and this increased expression and aggregation of α-Synuclein was neuroprotective (Manning-Bog et al., 2003). Studies showed that various neurotoxins including MPTP and rotenone increase α-Synuclein expression in brain (Hasegawa et al., 2004; Matsuzaki et al., 2004). These observations lead a group of researchers to suggest that the increased α-Synuclein expression may represent an adaptive homeostatic regulatory response to toxic stimuli (Lee et al., 2006). In support of this, overexpression of α-Synuclein in transgenic mice does not consistantly result in neuronal damage (Matsuoka et al., 2001), nor does it mimic MPTP induced neurodegeneration completely (Rathke-Hartlieb et al., 2001).

Similarly, other amyloidogenic proteins involved in neurodegenerative pathologies, such as, amyloid beta peptides in AD and prion proteins in prion diseases could have neuroprotective properties. These observations need to be considered when

developing therapies to PD and other neurodegenerative diseases. In other words, therapy should be targetted at the cause of the disease rather than the end result (protein aggregates), unless it is conclusively proved that dissolving/eradicating protein aggregation improves the disease symptoms.

As discussed elsewhere in this article, it is not clear whether the recently discovered DNA binding property of α-Synuclein contributes to the cause of PD pathology or it is a passive secondary response of neurons affected by PD. These studies have to be addressed as toxic vs. protective responses in PD.

1.3 Chromatin organization in neurodegeneration

DNA in eukaryotic cell is arranged in the form of compactly condensed state known as chromatin. The sequence of the DNA forms the primiary information for the gene expression and chromatin organizations forms the secondary information. The regulation of chromatin organization also contributes to the regulation of gene expression. This kind of regulation is known as epigenetic control of regulation and chromatin organization is conserved throughout cell lineage (Kornberg, 1977). The unit of chromatin is nucleosome, which consists of 146bp of DNA wrapped around the octomer of histone proteins. Histone octomer consists two tetramers of H3, H4 and H2A, H2B. The nucleosome core particles are linked by linker DNA stabilized by H1 histone proteins. The regulation at chromatin level depends on modifications of DNA (especiaaly methylation at cytosine residues), incorporations of histone varients, post-translational histone modifications and other molecules which can interact with nucleosome core particles (Kouzarides, 2007; Polo and Almouzni, 2007). The different molecules like ATP-dependent remodeling complexes, histone chaperones and histone modifying enzymes involved in maintaining and regulating the chromatin organization (Polo and Almouzni, 2007). Thus chromatin organization plays an important role in the cellular events. Several studies and models has shown that in neuron also chromatin organization is tightly regulated and alteration in chromatin organization observed in neurodegeneration. This provides strong suggestions that in neurodegenerative diseases like PD and AD chromatin organization might be playing a significant role in the

neuronal cell death. Here we discussing about the importance and some of the evidences of alterd chromatin organization in neuronal cell death.

α-synuclein localization in the nucleus and its histone binding property implicate that α-synuclein may play a role in the chromatin function. The study by the Kontopoulos et al (2006) showed that αsynuclein induces neurotoxicity when targeted to the nucleus. α-synuclein sequestration to cytoplasm prevented the neurotoxicity. The authous has shown that α-synuclein binds to histone and hamper the acetylation, which finally leads to neurotoxicity. The neurotoxicity is rescued by the administration of histone deacetylase inhibitors, which clearly demonstrated that α-synuclein-histone interactions are the responsible for the neuronal cell death. Based on the above literature we are focusing on the chromatin organization in parkinson's disease brain.

It has been observed that proliferating cell nuclear antigen and transcription factor E2F-1 are expressed in the PD brain. The above two transcription factors are involved in the cell cycle events (Holinger, 2007) . DNA damage is observed in the PD brain in the form of Double strand breaks (DSB) and Single strand breaks (SSB) (Hegde et al., 2006). The expression of cell cycle protein and DNA damage has been reported in neurodegenerative brain. These two events in the neuron may trigger the neuronal cell death through programmed cell death (Kim etal., 2009). As DNA repair mechanism is weak in neurons compared to other cell it will be better to prevent the accumulation of DNA damage rather depending on the repair mechanisms. In this contex it is important to maintain the chromatin integrity, as loss of chromatin integrity lead to the DNA damage and abberent gene expressions. The protein which serve as DNA damage check points activate the DNA repair mechanisms and the loss of their function may lead to the neurodegeneration. As α-synuclein has possibility to alter the chromatin integrity may alter the expression of these protein, which lead to the accumulation of DNA damage and finally neurodegeneration. Similar kind of activity observed in ataxia telangiectasia where the loss of function of protein ATM leads to progressive neurodegeneration (Rolig and McKinnon, 2000). DSB can activate the nuclear protein kinase ATM and induses chromatin relaxation (Ziv et al., 2006) .

α-synuclein which has shown to has binding properties with histones and altering its states of acetylation affteting histone affinity towards DNA resulting chromatin either in open or closed state. This will alter the genomic expression and probably leading to neurodegeneration.

1.3.1 DNA methylation

DNA methylation is one of the regulating force in gene expression and also a biomarkers for the genetic damage. DNA methylation at the sites of CpG in the promoter region is an important epigenetic regulation of the gene expression. Loss of regulation on DNA methylation leading to altered gene expression has been observed in AD (Scarpa et al, 2003). Presinilin-1 gene expression is shown to be modulated depending on the state methylation in cell culture and mice Alzheimer's Disease mice model. Fuso et al (2010)., analyzed the regulation of Presinilin-1 by supplementing nutritionally with hypomethylating and hypermethylating suppliments. Hypomethylation is achieved by creating Vitamin B defiency and hypermethylation was achieved by supplementing S-adenosyl methionine (SAM). DNA methylases and demethylase are modulated according to the supplementation and finally affected the presinilin-1 expression. Amyloid (1-40) peptide is involved in AD and it altered global DNA methylation in cell model implicating the new mechanism of toxicity induced by amyloid peptides (Chen et al., 2009). α-synuclein is implicated in PD and an altered expressions are observed in PD. Jowaed et al., (2010) showed that methylation in the *SNCA* intron 1 of α-synuclein is reduced in the PD brain samples. The data indicated that methylation status of α-synuclein altered the gene expression and involoved in the disease development. Hypomethylation of DNA in Tumor necrosis factor (TNFα) promoter region is observed in the promoter regions in PD patients. TNFα is implicated in PD by activating the inflammatory responses leading to neurodegeneration (Pieper et al., 2008).

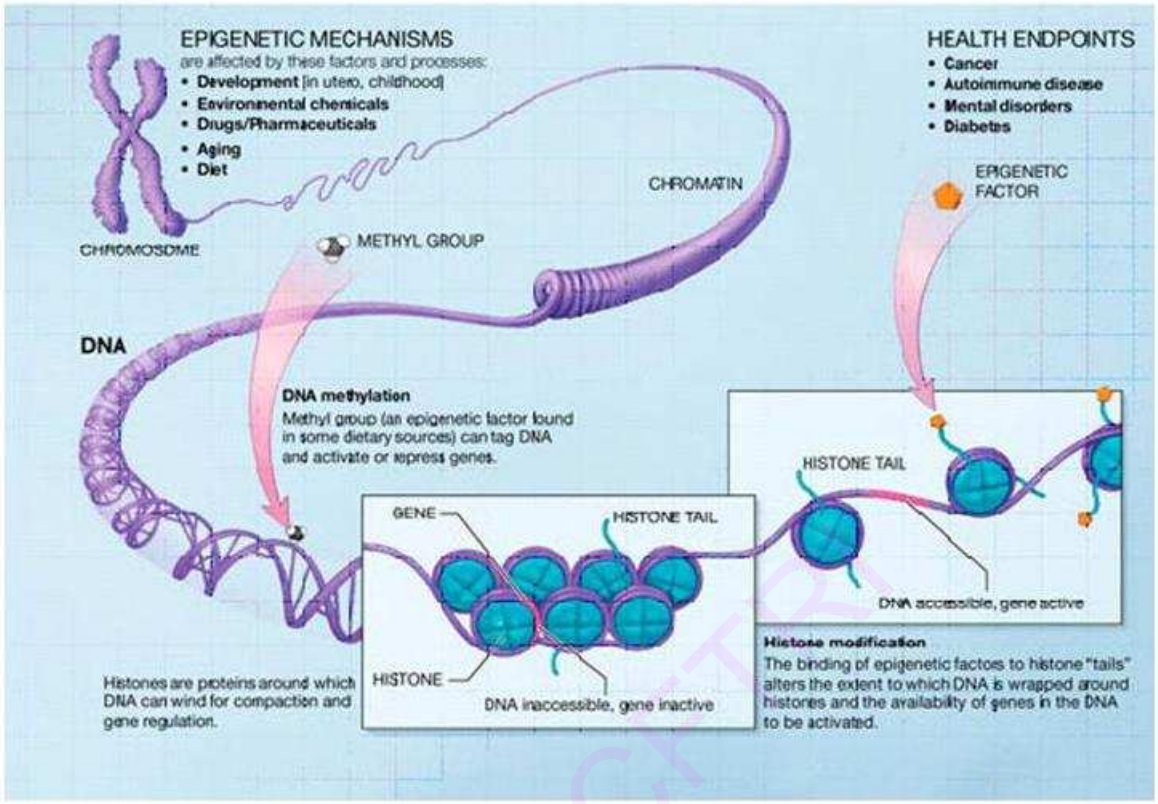

Figure 1.5: Chromatin organization and its regulation in the process of gene expression (**courtesy:** blog.targethealth.com/?p=11438)

1.3.2 Histone acetylation

Histone acetylation homeostasis in the nucleus is maintained by the combined action of Histone acetylases (HAT) and Histone deacetylases (HDAC). Histone acetylation balace is altered in neurodegenerative conditions (Saha and pahan, 2006). Histone deacetylases limit the access to DNA interacting molecues by inducing chromatin condensation. The chromatin condensation occurs as an effect of remov al of the acetyl gropus from histone proteins by histone deacetylases. Histone deacetylase inhibitors has been shown to improve the learning and memory (Fontán-Lozano et al., 2008). Kim et al, showed that p25/Cdk5 induced deregulation of Histone deacetylase 1 (HDAC1) lead to the aberrant cell cycle reentry and double strand breaks and finally neuronal death (kim et al., 2008). Alvira et al (2008) showed the activation of the

p25/Cdk5 pathway in PD patients indicating the cell cycle reentry and neuronal loss in PD. The gene expression profile of MPTP induced monkey model of PD has shown the role of Neuronal repressor element-1 silencing transcription factor (REST). REST is involved in the epigenetic regulation by recructing the histone and chromatin modifying molecules to REST targeted genes (Buckley et al., 2010). Histone acetyltransferases (HAT) are involved in the neurodegeneration. CREB-binding protein (CBP) is a HAT protein and regulates the transcription by acting as co-activator of CREB. Loss of function of CBP activity was observed in apoptotic neuronal cell death (Rouaux et al., 2003). In AD, an alteration of cAMP-responsive element (CREB) dependent genes has been observed indicating role of histone and chromatin complexes in AD (Ikezu et al., 1996). Rossi et al., (2008) showed that chromatid breaks and chromatid bridges in the lymphocytes of the Fronto temporal dementia (FTD) patients carrying P301L mutated Tau protein. Tau protein is mainly involved in the polymerization and stabilization of the microtubules in the neurons may also involved in the chromatin maintanence. As Tau protein implicated in both PD and AD, the role of Tau protein in altering chromatin structure was reasonable in neurodegeneration. Sirtuin 2, a member of histone deacetylase family has shown to be involved in the α-synuclein mediated toxicity. α-synuclein mediated cytotoxicity has been rescued by using the inhibitors of Sirtuin 2 by using small interfering RNA silencing (Outeiro et al., 2007). In PD, pestiside exposed has been implicated in the process of neuronal cell death. Song et al., (2010) showed that dieldrin treatment induced neuronal cell death by the hyperacetylation of histone molecules (Song et al., 2010). Almeda et al., (2010) showed that 3-Nitropropionic acid treatment decreased the HDAC activity and affected the histone acetylation in neuronal cell culture. 3-Nitropropinoic acid inhibits the mitochondrial complex II and leads neuronal cell death. Histone deacetylase inhibitors showed neuroprotection in Huntington disease and Amyotrophic lateral sclerosis (ALS) (Petri et al., 2006; Pallos et al., 2008). These inhibitors mainly act on the CREB binding protein (CBP) regulation of the gene expression.

1.4. Role of curcumin in neurodegenerative diseases

Curcumin is a hydrophobic polyphenol derived from the rhizome (turmeric) of the herb Curcuma longa. Turmeric is commonly used spice in india and curcumin is the principle component of turmeric. Curcumin is also used widely as pharmacological active compound because of its wide spectrum of biological activities. Curcumin has been reported to have the antioxidant, antimicrobial, anti-inflamatory and anti-carcinogeneic activities. The antioxidant property of curcumin is due its scavenging activity of free radicals such as hydroxyl radicals, singlet oxygen, superoxide radicals and peroxyl radicals. Curcumin has prevented the DNA damage in plasmid pBR322 plasmid by singlet oxygen species (Subramanian et al., 1994)

1.4.1 Curcumin metabolism

Curcumin belongs to the diarylheptanoid class of natural products in which a cental seven carbon chain links the two oxy substituted aryl moieties. In the C_7 linker unit the unsaturation has trans C=C bonds. The aryl rings may be symmetrically or unsymmetrically substituted. Natural turmeric has three analogs of curcumin collectively known as curcuminoids namely Curcumin, demethoxycurcumin (DMC) and bisdemethoxycurcumin (BDMC). curcumin has two symmetric o-methoxy phenols linked through the α, β-unsaturated β-diketone moiety. Commercially available turmeric contain mixture of 77% curcumin, 17% DMC, and 3% BDMC. Curcumin is metabolized in the body and gives various metabolites, namely dihydrocurcumin (DHC), tetrahydrocurcumin (THC), hexahydrocurcumin (HHC), octahydrocurcumin (OHC), curcumin glucuronide, and curcumin sulfate.

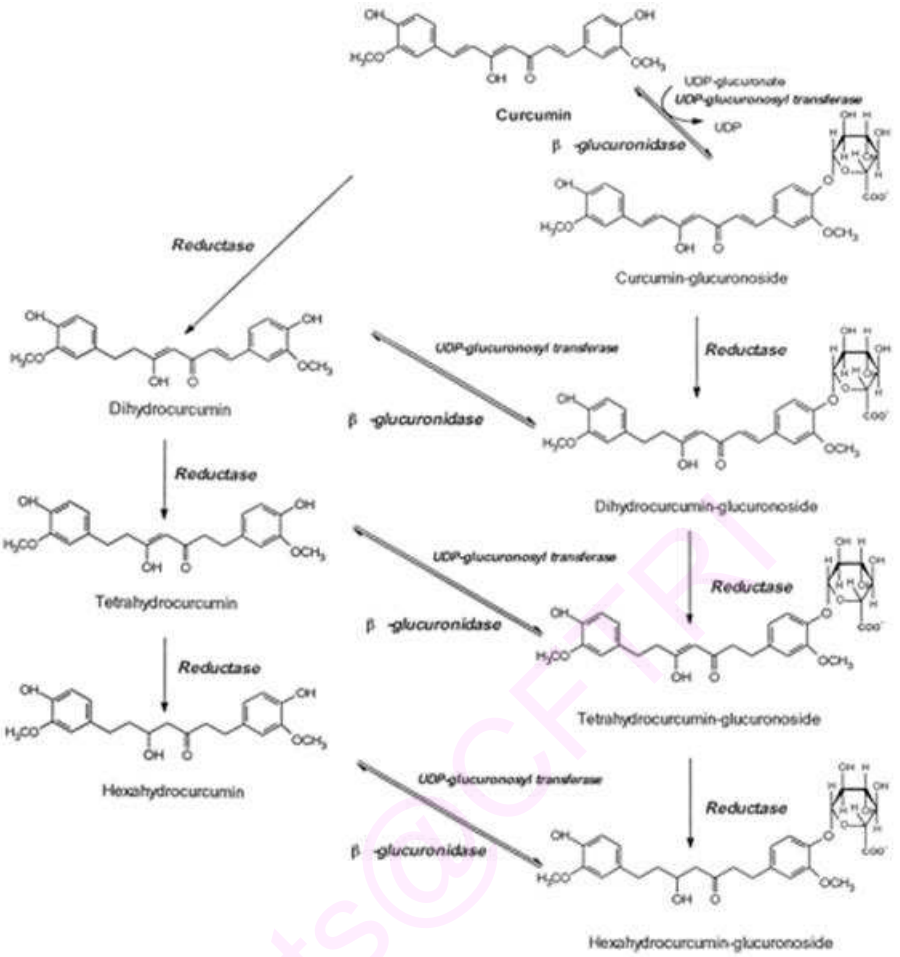

Figure 1.6: Curcumin metabolism and the metabolites formed in the body (dmd.aspetjournals.org/.../27/4/486/F8.expansion)

1.4.2 Curcumin neuroprotection

Curcumin has shown protective effects against intracerebroventricular–streptozotocin (ICV–STZ) induced cognitive deficits and oxidative damage in rats (Ishrat et al., 2009). Recently, it is reported the a pyrazole derivative of curcumin enhances memory by activating Ca2+/calmodulin dependent protein kinase II (CaMKII). CaMKII plays a important role in long-term potentiation (LTP) and memory (Maher et al., 2010). Curcumin has shown the ameliorating effect against lipopolyscaccharide induced (LPS) neurotoxicity. LPS induced neurotoxicity by activating transcription factors, nuclear

factors κB (NF-κB) and activator protein-1 (AP-1) which lead to inflammation (Yang et al., 2008). Curcumin has shown protective role against neuroinflamation and neuroinflamation was seen in AD and PD (McGeer et al., 2005). Curcumin has shown to induce the glutathione (GSH) synthesis in the experimental models of PD and protected against oxidative stress. Depletion in the glutathione is observed in the PD wich results in the oxidative stress. The authours postulated that this property of curcumin may be due to its action on transcription of gamma-glutamyl cysteine ligase (γ-GCL). γ-GCL may bind to transcription factor complexes and regulate the expression (Harish et al., 2010). Ortiz-Ortiz et al., (2010) reported that exposure of rat mesencephalic cells to curcumin induces the expression of leucine-rich repeat kinase 2 (LRRK2). LRRK2 gene is genetically linked to PD and mutations in this gene lead neurodegeneration similar to PD. Curcumin neuroprotective activity is analyzed in the 1-methyl-4-phenyl-1,2,3,6-tetrahydropyridine (MPTP) model of PD. MPTP is a neurotoxin that causes pathology similar to PD by degenerating dopaminergic neurons in the substantia nigra of the brain. MPTP is converted to MPP+ by the action of monoamine oxidase, the resultant MPP+ is toxic to cell. MPP+ interferes with complex I of the electron transport chain in mitochondria leading to cell death. MPTP triggers the generation of free radicals which contribute to cell destruction (Smeyne and Jackson-Lewis, 2005). MPTP administration to mice resulted in the loss of dopamine(DA) and DOPAC (3,4-dihydroxy phenyl acetic acid) with increased monoamine oxidase (MAO-B) activity. Curcumin and Tetrahydrocurcumin prevented the MPTP induced depletion of DA and DOPAC by the inhibition of MAO-B activity (Rajeswari and Sabesan, 2008).

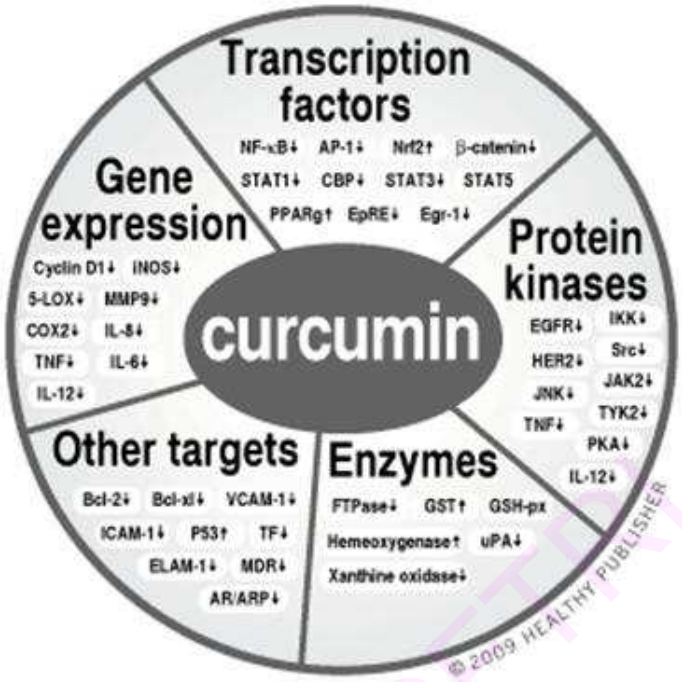

Figure 1.7: Curcumin molecular targets in the process of protection. (**courtesy:** curcumin-turmeric.net/)

Curcumin has shown to associate with fibrillar aggregates of Tau and amyloid peptides (Mohorko et al., 2010; Yang et al., 2005). Curcumin has shown to inhibit the aggregation of the amyloid peptide and even disaggregates the preformed aggregates of amyloid peptides (Yang et al., 2005). The *in vivo* studies showed that curcumin can cross the blood-brain barrier (BBB) in the mice model (Yang et al., 2005). α-Synuclein plays a central role in PD pathogenisis and found in the form of aggregates in PD brain. Wang et al., (2010) reported that extracellular addition of oligomeric α-Synuclein induces cytotoxic effects and curcumin protected the toxic effect induced by oligomeric α-Synuclein. Curcumin has improved the memory in aluminium induced AD mice model (Pan et al., 2008). Pandey et al., (2008) showed that curcumin inhibits the oligomerization of α-synuclein and therby inhibiting the aggregation in in vitro model of aggregation assay. They also showed that aggregatiuon of mutant α-synuclein was inhibited by the curcumin in SH-SY5Y cell line model.

1.5 Biomarkers for neurodegeneration

Biomarker is a ' a characteristic that is objectively measured and evaluated as an indicator of normal biological processes, pathogenic process or pharmacological response to a therapeutic intervention. The availability of BMs for early disease diagnosis will impact the management of PD in several dimensions. 1) BMs help to identify the high risk individuals before symptoms develop. 2) BMs help to discriminate between true PD and other causes of a similar clinical syndrome. 3) BM may help determination of the clinical efficacy of newer neuroprotective therapies. 4) BMs must therefore gain insight into processes underlying the pathological changes, associated with PD (Scherzer, 2009; Halperin et al., 2009).

Body fluids, which can easily drawn like blood, urine and cerebrospinal fluid will be used to identify biomarkers. Several molecules like trace metals, protein profile, oxidative stress markers etc can act as biomarkers which can be estimated biochemically in these body fluids. Trace metals like copper and iron, metal transport protein levels in blood like ceruloplasmin, ferritin, oxidative stress markers like 8-OHdG are estimated in the sample fluids (Bharucha et al., 2008; Gmitterová et al., 2009; Bartzokis et al., 2007). Specic proteins involved in different neurodegenerative disorders like amyloid proteins, Tau in AD, α-synuclein PD and their detection in the body fluids become import in early detection of these diseases. Primarily the detection of nearly every neurodegenerative disorder in the clinics now rely on the symptons and no biochemical markers has been established so far. Now the reaserch is focusing on the identification of biomarkers for every neurodegenerative disorders. Some studies are focused on identifying biomarker by targeting the certain established molecules in the blood and CSF.

Neuroimaging is used as non invasive technique to diagnose the brain structural and functional changes. In neuroimaging several techniques like Positron Emission Tomography (PET), Magnetic Resonance Imaging (MRI), Functional Magnetic Resonance Imaging (FMRI), Magnetic Resonance (MR) specytroscopy are applied in these studies. Among the above mentioned methos of neuroimaging, MRI is the simple

and cost effective technique in analyzing the brain structural changes. MRI measures the change in whole brain atrophy and different regional atrophy of the brain (Jack Jr *et al.,* 2005). Jokinen et al., (2009) performed the MRI of PD and healthy elderly volunteers. The patient sample consisted of 19 patients (age 64.4) with idiopathic PD. PD patients showed atrophy in the hippocampus and prefrontal cortex. Hippocampal atrophy correlated with impaired memory. Striatal dopaminergic neuronal loss and global brain volume loss contribute to cognitive impairment in non-demented PD patients.. Studies involving AD patients have shown early involvement of medial temporal lobe structures such as entorhinal cortex and hippocampus in the disease initiation (Barnes *et al*., 2004; Lerch *et al*., 2005). The decrease in the hippocampal volume is associated to severity of the AD. The study of Archer et al. (2006) reported that there is a positive correlation between amyloid load and cerebral atrophy in AD.

1.6 Research lacunae

There are limited studies in the area of genomic biology of brain and brain disorders. Still the mechanisms for neuronal cell death in brain disorders are not clear. It can be possibly by both apoptotic and necrotic cell death events. Further, the functional role of genomic stability in augmenting gene expression is still not clear. The DNA repair mechanisms are much more complex and the secrets of repair enzymes need to be further explored. The clinical and biological link between neuropsychiatry to neurodegeneration is overlapping, making it difficult for Scientists, Clinicians for diagnosis and drug discovery. There is lot of debate on translational research and neurochemistry in overlapping clinical conditions in neuropsychiatry-neurodegenerative diseases. **The major questions are**, i) will MRI help to design end points to map cross-talk between neuropsychiatry to neurodegeneration?, ii) Does neurochemistry mapping help to interlink Clinics and neurochemistry?, iii) will depression be an early event and risk factor for neurodegeneration?. **There are three major challenges**, i) can neuropsychiatry illness be risk factor for neurodegeneration?, ii) to map neurochemical and clinical complexicities to classify neuropsychiatry versus neurodegeneration, iii) to develop biomarker end points to classify neuropsychiatry and neurodegenerative disorders in independent and over-lapping situations. Lot of debate in understanding the translational parameters related to diagnosis and drug discovery and also understanding

complex biology in overlapping clinical conditions like neuropsychiatry-neurodegenerative features is still under hot topic. We propose that failure in DNA repair due to altered DNA topology may be the early onset for pathophysiology of brain disorders. Still this topic needs to be investigated.

1.7 Aim and Scope of the study : Neurodegeneration is the main consequence of the all neurodegenerative diseases. The intiation and exact pathwy due to which the neuron undergoes cell death is not clear. In most of the diseases the alteration in the function of certain neuroprotein has been assigned the cause of the neurodegeneration. In PD, α-synuclein, Tau, neuromelanin protein functions are altered. As α-synuclein and Tau are found in in the aggregates which are found in brains of PD patients, the aggregation was believed to be the culprit. Still it is a debatable conclusion whether the aggregation and is the cause or consequence of disease pathology. In light of this, the alternative toxic role of these proteins gained the importance. One of such alternative toxic pathway is the role of these neuropeptide in the nucleus as these neuropeptides are localized in the nucleus. Recent studies has shown binding parterns in the nucleus, having ability to interact with DNA and histone proteins. However the studies are not focused on mechanism of their interaction and their relevance to neurodegeneration. Therefore, the following objectives have been proposed to study in the thesis

Objectives:

1. To study the chromatin organization in normal and neurodegenerative brain and the role of curcumin in chromatin stability
2. To study the genotoxicity in brain cells and prevention by curcumin
3. To understand the molecular mechanism of sequence specific oligonucleotide and DNA binding of neuropeptides, curcumin and Actinomycin D

Chapter 2A

Chromatin organization in Parkinson's disease

2A.1 Introduction

Chromatin organization plays an important role in the cellular events including gene expression. The alteration in the chromatin organization may lead to the neuronal cell death and disease. The regulation of gene expression at chromatin levels depends upon the state of DNA methylation and histone binding to DNA. Any alteration in the mathylation of DNA and histone modification affect its organization and alters gene expression. Loss of regulation on DNA methylation leading to altered gene expression has been observed in AD (Scarpa et al, 2003). Presinilin-1 gene expression is shown to be modulated depending on the state of DNA methylation. Jowaed et al., (2010) showed that methylation in the *SNCA* intron 1 of alpha synuclein is reduced in the PD brain samples. Histone acetylation homeostasis in the nucleus is maintained by the combined action of Histone acetylases (HAT) and histone deacetylases (HDAC). Histone acetylation balace is altered in neurodegenerative conditions (Saha and pahan, 2006). Kim et al, (2008) showed that p25/Cdk5 induced deregulation of Histone deacetylase 1 (HDAC1) lead to the aberrant cell cycle reentry and double strand breaks and finally neuronal death. Alvira et al (2008) showed the activation of the p25/Cdk5 pathway in PD patients indicating the cell cycle re-entry and neuronal loss in PD. In PD, pesticide exposure has been implicated in the process of neuronal cell death. Song et al., (2010) showed that dieldrin treatment induced neuronal cell death by the hyperacetylation of histone molecules (Song et al., 2010).

Kontopoulos et al (2006) showed that alpha synuclein induces neurotoxicity when targeted to the nucleus. Alpha synuclein sequestration to cytoplasm prevented the neurotoxicity. These authors have shown that alpha synuclein binds to histone and hamper the acetylation, which finally leads to neurotoxicity. The neurotoxicity is rescued by the administration of histone deacetylase inhibitors, which clearly

demonstrated that alpha synuclein-histone interactions are the responsible for the neuronal cell death.

In the present study, the chromatin organization in Parkinson's disease brain samples was analyzed.

2A.2 Materials

Anti-Histone H3 antibody, PMSF, Msp I, Hpa II, micrococcal nuclease and nitrocellulose membrane were purchased from sigma (USA). HRP-cojugated IgG, TMB/H_2O_2, Ribonuclease A (RNAse A), Proteinase K, 1kb DNA ladder, Tris saturated phenol were purchased from Genei, India. Phenol, chloroform, isoamyl alcohol, sodium chloride, SDS, Tris, HEPES, EDTA sodium salt, glacial acetic acid, ethanol, sodium hydroxide, bromocresol green, and ethidium bromide were purchased from SRL Pvt. Ltd. All other chemicals were of analytical grade and were purchased from Sisco Research Labs, Mumbai, India.

2A. 3 Methodology

2A. 3.1 Brain samples

Five normal and five PD-affected human brain samples were obtained from the National Institute of Mental Health and Neurosciences (NIMHANS), India. Autopsies were performed on donors from whom written informed consent has been obtained either from the donor or direct next of kin. The control human brains (age 45-65 years) were collected from accident victims, who had no history of long-term illness, movement disorders, dementia, or neurological disease prior to death. The PD-affected (48–68 years) brains were postmortem specimens from clinically well documented and neuropathologically confirmed cases who were under long-term follow up at the Neurological services at National Institute of Mental Health and Neurosciences, Bangalore, India. The average postmortem interval between the time of death and collection of brain and freezing was 6-15 h. Within one hour after death the body was kept in refrigerator maintained at 4°C. Dissected brain tissue was stored frozen at -70°C till the analysis.

Number	Age (yr)	PMI (hr)	Tissue (pH)	Sex	Cause of Death
Control group					
C-1	45	7	6.76	F	Head injury
C-2	51	12	6.61	M	Head injury
C-3	55	7	6.71	M	Head injury
C-4	48	15	6.45	M	Spinal cord injury
C-5	65	13	6.68	M	Head injury
Group II 41-60 yrs					
PD-1	56	1	6.15	M	PD
PD-2	62	14	6.38	M	PD
PD-3	68	15	6.87	M	PD
PD-4	65	6	6.67	F	PD
PD-5	48	1	6.23	F	PD

Table 2A.1: Demographic data of PD and control brains

2A.3.2 Isolation of the nuclei from the brain samples

Nuclei were isolated from the brain regions namely hippocampus, thalamus, midbrain and caudate nucleus according to the method described by Rao et al., (1983). Briefly, brain tissue was weighed (5 grams) and perfused with normal saline to remove the any blood in the tissue. Brain tissue was cut into small pieces and minced thoroughly. The minced brain tissue was homogenized in 0.34M sucrose in buffer A (50 mM Tris –HCl, pH 7.5, 25 mM KCl, 5 mM $MgCl_2$, 0.5 mM PMSF) using motor duer homogenizer. The homogenate was filtered through 2 layers of cheese cloth and the filtrate was centrifuged at 1000g (3500 rpm) for 10 min at 4°C. The supernatant was decanted carefully and the pellet was resuspended in 1M sucrose in buffer A. the suspended pellet was homogenized using hand held homogenizer and centrifuged at 100,000g (42,000 rpm) in ultracentrifuge for 1 h. The pellet obtained was washed with 1M sucrose in buffer A and then washed again with 0.34 M sucrose with 0.1% Triton X 100. The pellet is dissolved in Tris-HCl buffer. The concentration of the nuclear suspension was determined by taking absorbance at A_{260} in 1 ml of 2M NaCl/5M urea.

2A.3.3 DNA isolation from the brain tissue

DNA was isolated from the brain regions by phenol-chloroform extraction. Brain tissue was cut into small pieces and was transferred into an autoclaved porcelain mortar and pestle. All glasswares, mortar, pestle, etc., were autoclaved to avoid bacterial

contamination. Liquid nitrogen was poured into the mortar and the tissue was allowed to freeze. Tissue was ground thoroughly with pestle with frequent additions of liquid nitrogen. Tissue homogenate was transferred into a sterile tube and the liquid N2 was allowed to evaporate (a sterile spatula was used to transfer the powdered tissue into a graduated tube). The tissue homogenate was incubated with lysis buffer (50 mM Tris–HCl (pH 8.0), 10 mM EDTA (pH 8.0), 100 mM NaCl) and was added with 15 mg/mL of proteinase K and 2% SDS in the final volume. One milliliter of lysis buffer was used for every 500 mg of tissue (Note 1: Lysis buffer should be pre-warmed, Note 2: Add proteinase K after first 2 h, optimum: 3 h.). The homogenate was incubated at 37 ^{0}C in a water bath for 12–16h or overnight. After the completion of incubation, the incubated lysate was transferred to an autoclaved 50 mL conical flask. Then, equal volume of tris-saturated phenol (pH 8.0) was added and mixed thoroughly, either manually or mechanically for 10 min. The lysate was centrifuged for 10 min at 10,000 rpm at 13 ^{0}C. The supernatant was collected into a fresh autoclaved 50 mL conical flasks and 1/2 volume of Tris-saturated phenol and chloroform: isoamyl alcohol was added and mixed thoroughly. One part phenol: one part chloroform (C) and iso-amyl alcohol (IA) mixture (C: IA = 23:1) (Note: Tris saturated phenol was stored in amber colored bottles at low temperature to avoid oxidation of phenol.). The supernatant and Tris-saturated phenol–chloroform mixture was centrifuged at 5000 rpm at 4°C. The upper aqueous layer was collected into a fresh tube and 1/30th volume of sodium acetate (pH 5.5) and equal volume of chilled absolute ethanol was added. DNA was precipitated by slowly swirling the tube manually. (Note: Pre-cooled tubes were used and DNA was transferred into another tube containing 70% alcohol for washing). DNA was washed twice with 70% alcohol and once with absolute alcohol to remove excess salt and vacuum dried and stored at –20°C. The vacuum dried DNA was dissolved in 1 mL of TE buffer (10 mM Tris–HCL, 1 mM EDTA, pH 8.0). The DNA isolated from cells also contains RNA, which was removed by digesting the preparation with RNase enzyme. RNase solution was kept in boiling water for 10 min before use so as to inactivate DNase I. The method provides high quality genomic DNA with good yield. It is important to mention that the genomic DNA was isolated from total brain tissue of different brain regions (i.e., containing both neurons and glia).

2A.3.4 Preparation of soluble chromatin

Soluble chromatin was prepared from the isolated nuclei by limited digestion of nuclei with micrococcal nuclease (Korenberg et al., 1989). Nuclear suspension (100 µL) was mixed with 0.1M $CaCl_2$ and incubated at 37°C for 2 min. After incubation, the nuclear suspension was digested with micrococcal nuclease (50 units) by incubating at 37°C for 1 min. The reaction was stopped by 0.25 M EDTA and centrifuged at 5000 rpm for 5 min. The pellet obtained was suspended in 10mM $NaHSO_3$, pH 7.5, 1mM EDTA. The soluble chromatin obtained by the limited digestion was used for the thermal denaturation and circular dichroism studies.

2A.3.5 Histone protein extraction

The nuclear pellets were resuspended in 500 µL of 0.4 N H_2SO_4 , incubated on ice for 30 min and then centrifuged at 4°C for 10 min at 14 000g. The supernatant was transferred to fresh tube and the proteins were precipitated trichloroacetic acid containing 4 mg/mL deoxycholic acid on ice for 30 min. The supernatant was discarded, and the pellet was washed with ice-cold acidified acetone(0.1% HCl) and then with ice-cold acetone for 5 min each. The protein precipitates were collected between the washes by centrifugation at 14 000g. The purified proteins were resuspended in 10 mM Tris-HCl (pH 8.0) and stored at -80°C (Nicholas et al., 2008). Protein concentration in the histone extraction sample was estimated by the method of Lowry method (Lowry et al., 1951).

2A.3.6 Thermal denaturation studies

Thermal melting of the whole chromatin samples was done on Spectrophotometer equipped with a thermostat programmer and data processor (Amarsham Biosciences, HongKong). All the chromatin samples, at OD_{260} = 0.6 were used for the melting temperature studies in HEPES buffer (10mM, pH 7.4). The melting profiles were recorded with increase of 1°C/min in the temperature range of 25-95°C.

2A.3.7 Circular Dichroism (CD) studies

Circular dichroism spectra of the whole chromatin samples were obtained by using JASCO J700 spectropolarimeter at 25°C, with 2mm cell length in the wavelength range

between 200-320 nm in Tris-HCl buffer (5 mM, pH 7.4)/0.2 mM EDTA. Each CD spectrum was the average of four scans.

2A.3.8 Dot blot assay

Histone protein samples were applied to nitrocellulose membrane in a Bio-Dot apparatus (Bio-Rad). The membrane is blocked with 10% non-fat milk in Tris buffer saline-Tween (TBS-T) at room temperature for 1h, washed with TBS-T and probed with anti-α-synuclein antibody (Sigma, USA, raised in rabbit) solution (dilution ratio) in 3% BSA-TBS-T overnight at 4°C. After washing it is probed with secondary antibody (anti-goat) coupled with horse raddish peroxidase antibody (dilution) for 1h at room temperature. The blot is developed using substrate TMB/H_2O_2. The presence of acetylated histone H3 was detected using anti-histone H3 of mouse as primary antibody and peroxidase conjugated anti-rabbit-goat antibody as secondary antibody. BSA is used as control where no immunoreactivity is observed.

2A.3.9 Micrococal nuclease digestion

The nuclear pellet was washed with 0.1% Triton X-100 to create the pores in the nuclear pellet which allow MNAse to enter into the nuclei and digest chromatin. Then nuclear pellet was suspended in MNAse digestion buffer (50 mM Tris –HCl, pH 7.5, 25 mM KCl, 5 mM $MgCl_2$, 1mM $CaCl_2$, 0.1 mM PMSF) and equilibrated at 37°C for 10 min. the equilibrated nuclear suspension was treated with 80 units of the enzyme (Worthington) MNAse and incubated for 15 min. Reaction was stopped by adding 100 mM EDTA. The digested nuclear suspension was mixed with nuclear lysis buffer (50 mM Tris –HCL, pH 8.0, 10 mM EDTA, 0.2% SDS) and proteinase K added to the final concentration of 0.5 mg/mL and incubated for 12 h. After the incubation DNA was isolated by phenol-chliroform extraction. The DNA was analyzed on 1.2 % agrose gel electrophoresis and stained the gel with ethidium bromide.

2A.3.10. Restriction digestion analysis for the methylation of DNA

Digestion of genomic DNA was performed with methylation specific Msp I and Hpa II restriction endonucleases to know the methylation status of the DNA. MSP I/ HpaII isoschizomers were used for the detection of methylated cytosines. Both the enzymes

digest CpCpGpG motif in dsDNA, but they recognize different state of the cytosine residue. Msp I cleaves both methylated and unmethylated DNA, while Hpa II cleaves unmethylated CpCpGpG motif. About 10 μg of DNA was digested with Msp I and HpaII in the restriction digestion buffer (10 mM Tris-HCl, pH 7.5, 50 mM NaCl, 10 mM $MgCl_2$) for 2 h. The reaction was stopped by heating the reaction mixture for 5 min at 60°C. The digested DNA was analyzed on 1.2% agarose gel electrophoresis.

2A.4 Results

2A.4.1 Thermal denaturation of chromatin

Thermal denaturation of control and PD chromatin samples were analyzed for the structural integrity of chromatin. A mean thermal transition around 80.3 ± 1.3°C, 78.4 ± 0.9°C, 77.8 ± 1.1°C and 79.9 ± 1.4°C for thalamus, midbrain, hippocampus and caudate nucleus, respectively for the control chromatin samples was observed. The mean thermal transition values for the PD samples were 78.7 ± 1.2°C, 76.5 ± 1.1°C, 77.2 ± 0.7°C and 77.8 ± 0.8°C for thalamus, midbrain, hippocampus and caudate nucleus, respectively. It was also observed one more minor transition for all the samples. The minor transition for the thalamus, midbrain, hippocampus and caudate nucleus for control chromatin samples were 66°C, 67°C, 67°C and 65°C, respectively. The minor transition for the thalamus, midbrain, hippocampus and caudate nucleus for PD chromatin samples were 63°C, 63°C, 64°C and 65°C, respectively. Compared to the control, melting profile of chromatin samples, melting transition points of PD samples were decreased. This suggested that chromatin organization was altered in PD compared to age matched control samples.

Brain region	**Melting temperature**	
	Control	**PD**
Thalamus	**80.3 ± 1.3°C**	**78.7 ± 1.2°C**
Midbrain	**78.4 ± 0.9°C**	**76.5 ± 1.1°C**
Hippocampus	**77.8 ± 1.1°C**	**77.2 ± 0.7°C**
Caudate nucleus	**79.9 ± 1.4°C**	**77.8 ± 0.8°C**

Table 2A.2: Thermal melting profile of the control and PD chromatin samples of thalamus, midbrain, hippocampus and caudate nucleus.

2A.4.2 Circular dichroism analysis of chromatin samples

Control and PD chromatin samples were analyzed by circular dichroism spectroscopy by taking all samples equivalent to DNA concentration from the thalamus, midbrain, hippocampus and caudate nucleus regions (Fig 2A.1). CD spectra of hippocampus region of PD brain samples showed decrease in the 220 nm negative peak and increase in 275 nm positive peak compared to control brain region. PD Thalamus region showed decrease in the 225 nm negative peak in CD spectra compared to control hippocampus region. The CD spectra of midbrain region showed decrease and a red shift in the 225 nm negative peak to 230 nm peak in PD chromatin sample compared to control chromatin sample. CD spectrum of caudate nucleus showed decrease both in the 225 nm negative peak and 280 positive peak and a shift in the positive peak from 280 nm to 275 nm in PD chromatin sample compared to control chromatin samples. The differences in the CD spectra may be due to the different protein/DNA ratio from the control and PD samples. The data suggest that the chromatin organization in terms of histone-DNA concentration and modifications of either histone or DNA and their interactions were different in PD brains compared to age matched control brains.

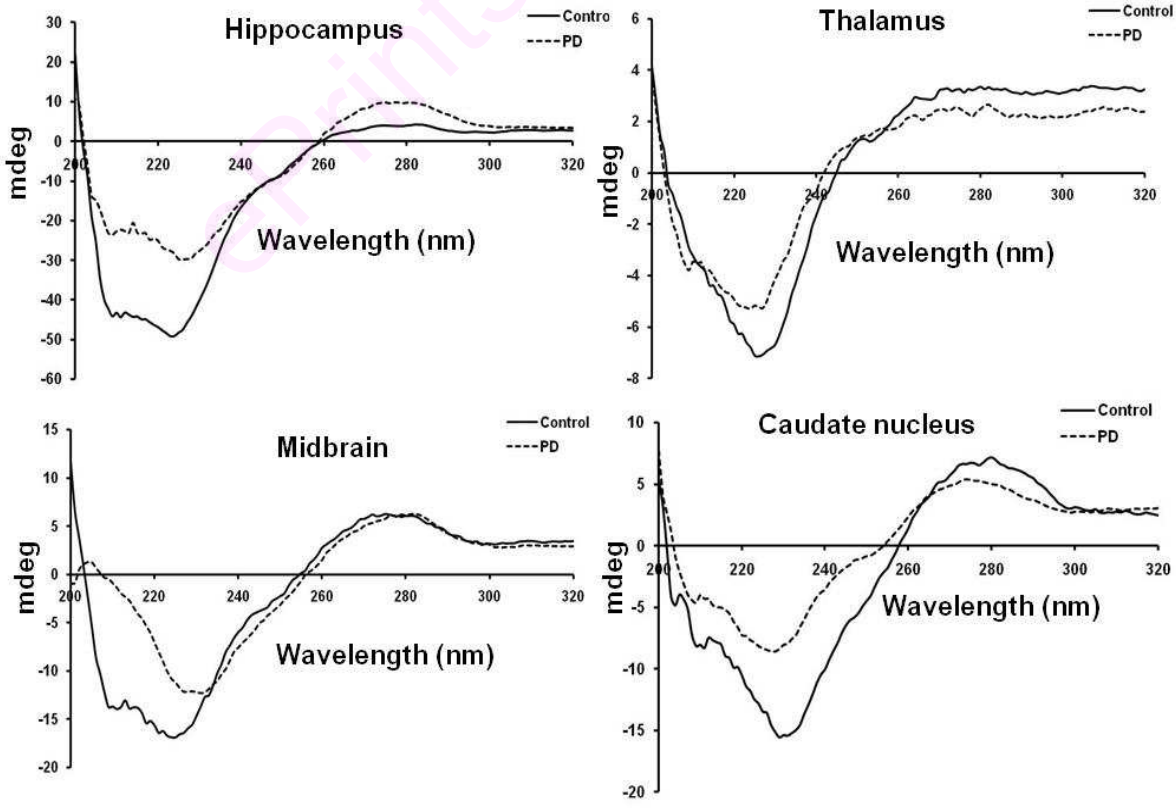

Figure 2A.1: CD spectra of the chromatin samples isolated from the hippocampus, thalamus, midbrain and caudate nucleus regions of the Parkinson's disease and age matched control brains.

2A.4.3 Dot blot assay for the Histone acetylation

Acetylation of the histone H3 protein was analyzed using dot blot assay to know the histone acetylation status of the thalamus, hippocampus, midbrain and caudate nucleus of 5 PD brain regions and 5 age matched control brains (Fig 2A.2). Dot blot assay of histones from the hippocampus regions of control brain showed immunoreactivity for the 3 samples (C1, C3, C5) out of 5 samples probed with anti-histone H3 antibody while all the 5 PD histone samples showed immunoreactivity. In the thalamus region also 3 control samples (C2, C3, C4) showed immunoreactivity and all 5 PD brain samples showed immunoreactivity. In midbrain region only one sample (C5) showed immunoreactivity in control group and all 5 samples in the PD group showed immunoreactivity. In the caudate nucleus group 3 samples (C2, C3, C5) showed immunoreactivity in control group and 4 samples (PD1-PD3, PD5) showed immunoreactivity in PD group. The differences in the immunoreactivty may due to the differences in the levels of acetylated histone H3 in the samples. The differences in the acetylated histone H3 immunoreactivity reflect the degree of histone acetylation in the brain samples. In conclusion the data suggest that acetylation of histone H3 more common in PD conditions compared to age matched control brains.

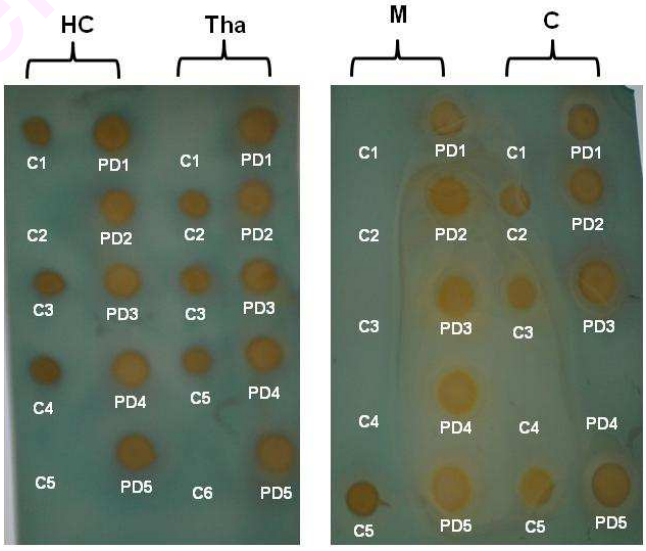

Figure 2A.2 : Dot blot assay of histone acetylation: histone samples were probed with anti-histone H3 primary antibody, peroxidase conjugated secondary antibody and developed using TMB/H_2O_2.

2A.4.4 Micrococcal nuclease digestion of nuclei

Nucleosomal structure in the chromatin was analyzed by the micrococcal nuclease digestion. Micrococcal nuclease digestion of the control (Fig 2A.3, lane 1) and PD (Fig 3, lane 2) chromatin samples from the hippocampus regions showed more digestion of the control chromatin sample compared to that of PD. PD chromatin samples showed a DNA band greater than 10 kb (Fig 2A.3, lane 2) indicating the difference in the nucleosomal structure between the control and PD chromatin. Similarly, chromatin from the thalamus region showed difference in the digestion pattern between the control and PD sample (Fig 2A.3, lane 3 and 4). Chromatin sample from the PD thalamus was less digested compared to control region. Chromatin isolated from the midbrain and caudate nucleus showed no difference the digestion pattern between the control and PD groups (Fig 2A.3, lane 5, 6, 7 and 8).

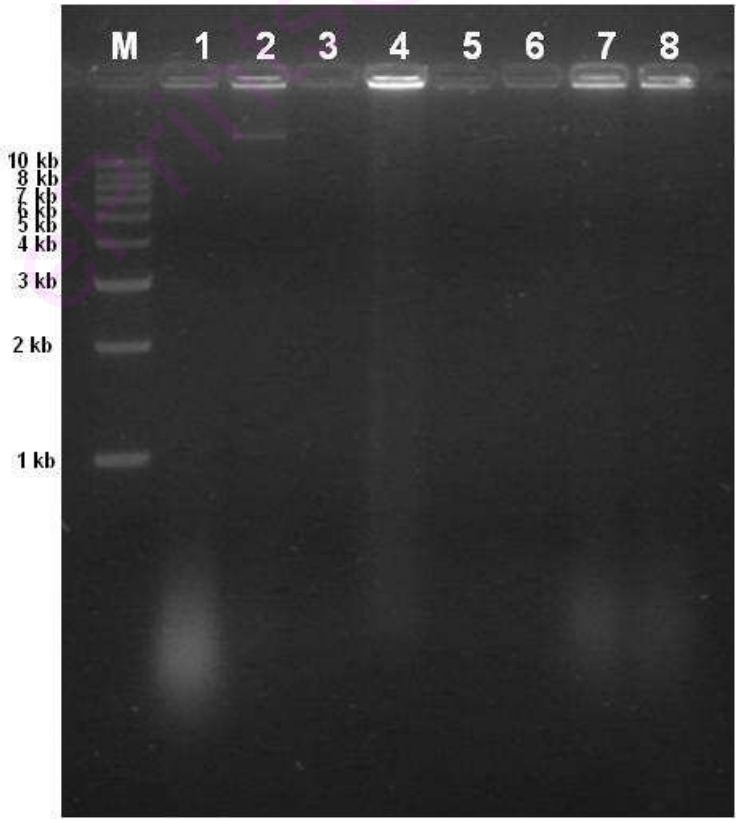

Figure 2A.3: Micrococcal nuclease digestion of nuclei. M. Marker, 1. Control hippocampus, 2. PD hippocampus, 3. Control thalamus, 4. PD thalamus, 5. Control midbrain, 6. PD midbrain, 7. Control caudate nucleus and 8. PD caudate nucleus.

2A.4.5 DNA methylation analysis using endonucleases Msp I and Hpa II

DNA methylation status of the DNA from the control and PD samples were analyzed by the methylation specific combination of the Msp I/Hpa II restriction digestion. Restriction digestion of hippocampus DNA with Msp I/Hpa II showed no differences among control group, but compared to control DNA, PD DNA digested more with Msp I/Hpa II. This indicates that compared control DNA, PD DNA from hippocampus region was more methylated in cytosine (Fig 2A.4). DNA isolated from the thalamus region of the PD showed more digestion compared to control DNA, indicating alteration in the DNA methylation status of the control and PD group (Fig 2A.5). DNA isolated from the midbrain and caudate nucleus regions of the PD brain also showed more digestion compared to control DNA, indicating alteration in the DNA methylation status of the control and PD group (Fig 2A.6 and 2A.7).

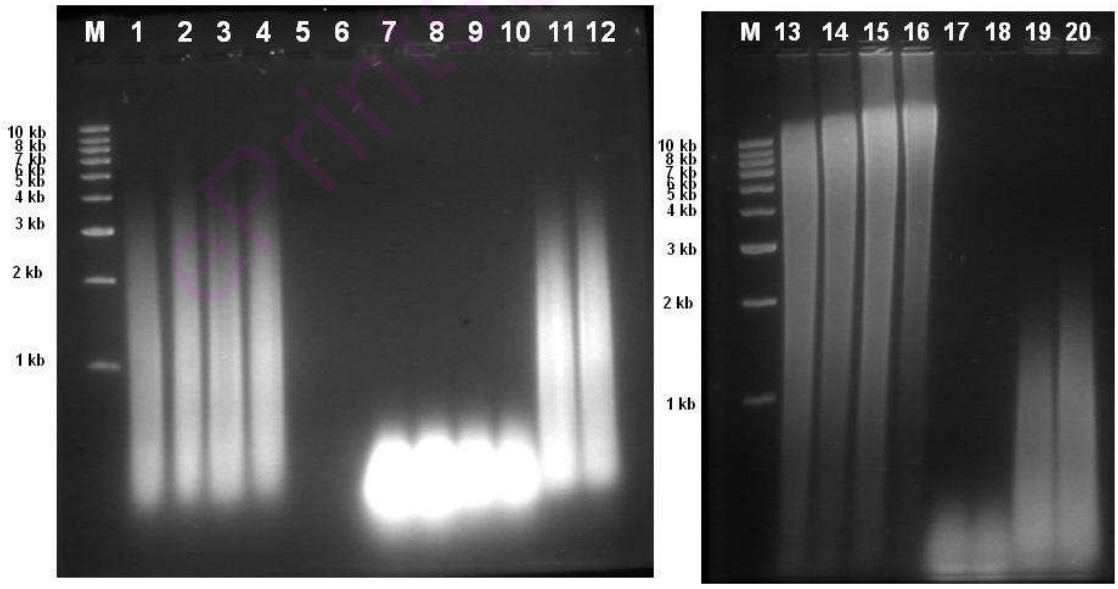

Figure 2A.4: Restriction digestion of DNA isolated from hippocampus of control and PD brain samples with Msp I/Hpa II M. Marker, lanes 1, 3, 5, 13, 15 were control hippocampus DNA digested with Msp I from C1, C2, C3, C4 and C5 respectively. lanes 2, 4, 6, 14, 16 were control hippocampus DNA digested with Hpa II from C1, C2, C3, C4 and C5 respectively. , lanes 7, 9, 11, 17, 19 were PD hippocampus DNA

digested with Msp I from C1, C2, C3, C4 and C5 respectively. lanes 8, 10, 12, 18, 20 were PD hippocampus DNA digested with Hpa II I from C1, C2, C3, C4 and C5 respectively.

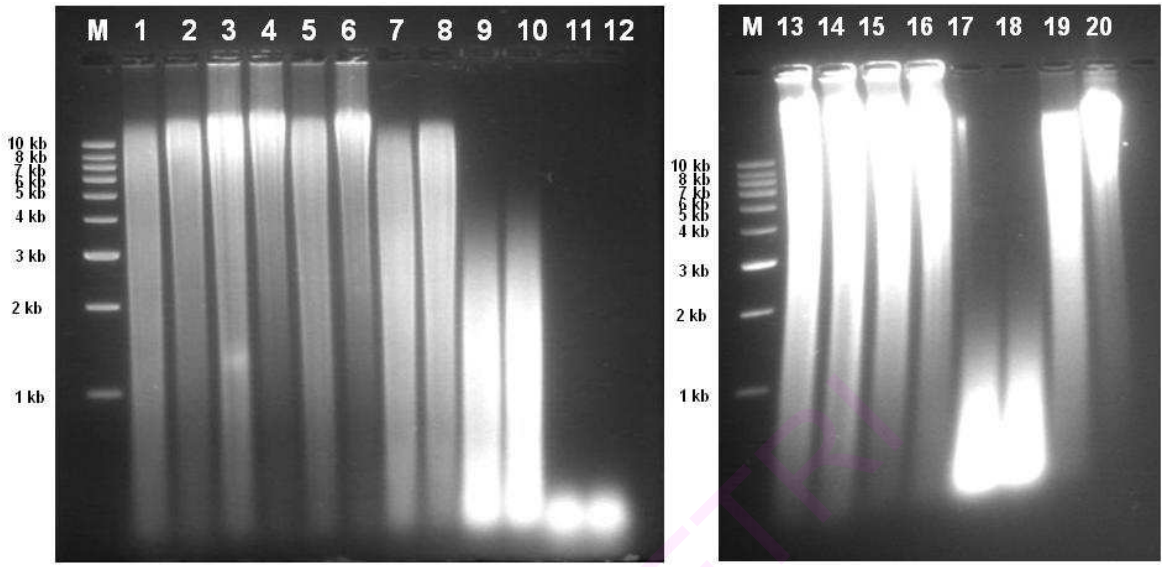

Figure 2A.5: Restriction digestion of DNA isolated from thalamus of control and PD brain samples with Msp I/Hpa II M. Marker, lanes 1, 3, 5, 13, 15 were control thalamus DNA digested with Msp I from C1, C2, C3, C4 and C5 respectively. lanes 2, 4, 6, 14, 16 were control thalamus DNA digested with Hpa II from C1, C2, C3, C4 and C5 respectively. , lanes 7, 9, 11, 17, 19 were PD thalamus DNA digested with Msp I from C1, C2, C3, C4 and C5 respectively. lanes 8, 10, 12, 18, 20 were PD thalamus DNA digested with Hpa II I from C1, C2, C3, C4 and C5 respectively.

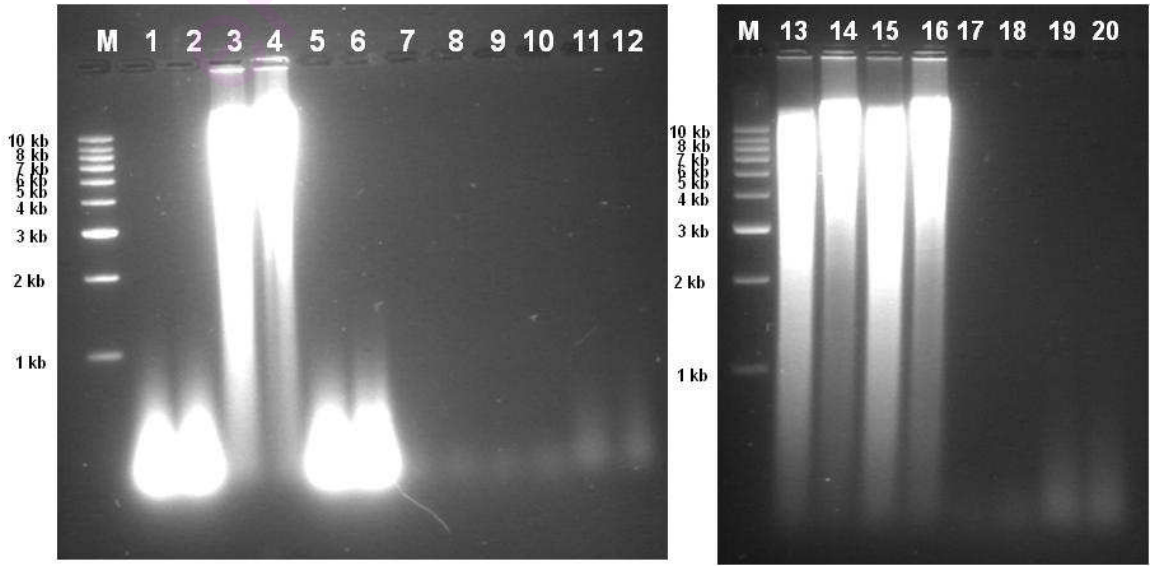

Figure 2A.6: Restriction digestion of DNA isolated from midbrain of control and PD brain samples with Msp I/Hpa II M. Marker, lanes 1, 3, 5, 13, 15 were control midbrain DNA digested with Msp I from C1, C2, C3, C4 and C5 respectively. lanes 2, 4, 6, 14, 16 were control midbrain DNA digested with Hpa II from C1, C2, C3, C4 and C5 respectively. , lanes 7, 9, 11, 17, 19 were PD midbrain DNA digested with Msp I from C1, C2, C3, C4 and C5 respectively. lanes 8, 10, 12, 18, 20 were PD midbrain DNA digested with Hpa II I from C1, C2, C3, C4 and C5 respectively.

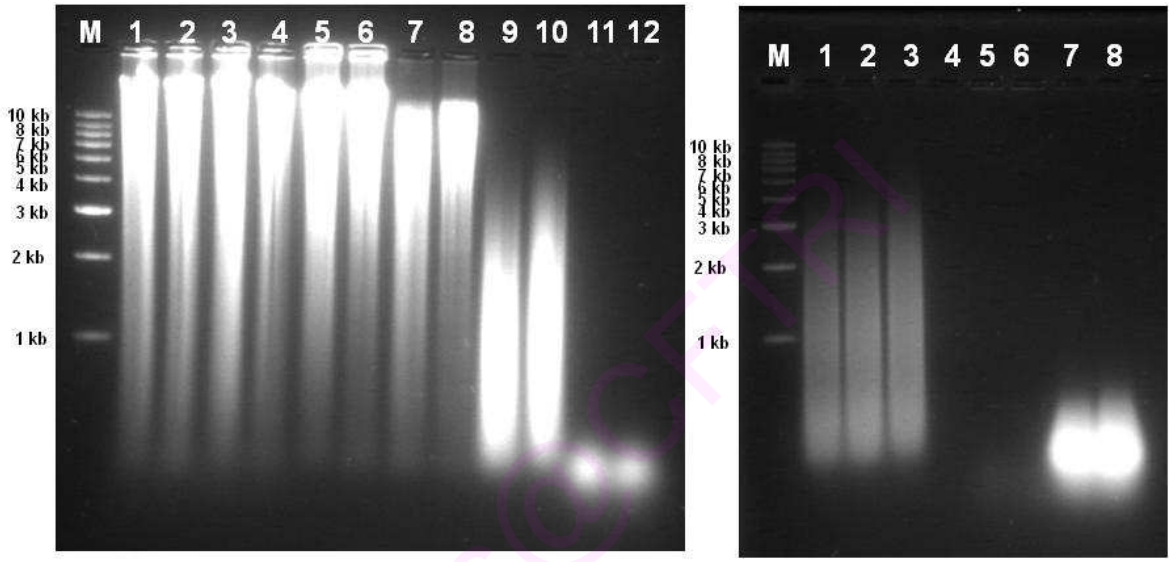

Figure 2A.7: Restriction digestion of DNA isolated from caudate nucleus of control and PD brain samples with Msp I/Hpa II M. Marker, lanes 1, 3, 5, 13, 15 were control caudate nucleus DNA digested with Msp I from C1, C2, C3, C4 and C5 respectively. lanes 2, 4, 6, 14, 16 were control caudate nucleus DNA digested with Hpa II from C1, C2, C3, C4 and C5 respectively. , lanes 7, 9, 11, 17, 19 were PD caudate nucleus DNA digested with Msp I from C1, C2, C3, C4 and C5 respectively. lanes 8, 10, 12, 18, 20 were PD caudate nucleus DNA digested with Hpa II I from C1, C2, C3, C4 and C5 respectively.

2A.5 Discussion

The DNA was organized in the form of compact condensed structure in the nucleus. This higher order of organization known as chromatin organization was responsible for the higher order regulation in gene expression etc (Joffe et al., 2010; Postberg et al., 2010). Chromatin organization was a dynamic process occurring in the living cells by continuously opening and reorganizing according to cellular needs (Mazloom et al, 2010; Jasencakova et al., 2010; Rippe, 2007). Defects in the chromatin organization are

responsible for the physiological and pathological process. Chromatin conformation signatures may even represent ideal biomarkers for the human diseases (Misteli, 2010; Crutchley et al., 2010). Chromatin organization at a particular time depends on the state of DNA, composition of DNA binding histone proteins and their modification (Chen et al., 2010; Fukuda et al., 2006). The genomic function also depends on the nucleosomal positiong on the length of the DNA (Bai et al., 2010). Epigenetic signature of the cell inherited and accounts for some of the inherited diseases.

Neurodegenerative diseases like Parkinson's disease (PD) and Alzheimer's disease (AD) affects elderly and these diseases create social and economic problems to the society. Several factors are responsible for the development of these diseases. Environmental factors may induce epigenetic modifications leading to the neurodegeneration (Marques et al., 2010). Recent study showed that in models of levedopa induced dyskinesia, deacetylation of histone H4, hyperacetylation and dephosphorylation of histone H3 (Nicholas et al., 2008). Chromatin modifying enzymes plays an important role in the memory formation indicating the importance of chromatin organization in neuronal functioning (Barrett et al., 2008). In genetically modified mice showing memory defects, memory enhancement was achieved by administrating the histone deacetylase inhibitors (HDAC) indicating the role of histone acetylation acetylation in memory formation (Roth et al., 2010). Histone deacetylase inhibitors are shown to improve defects in synaptic plasticity, cognition psychiatric diseases (Abel et al., 2008). Role of α-synuclein (protein widely implicated in PD) and epigenetic involvement in the development PD came from the study of Kontopoulos et al., (2006). In this study the authors showed that targeting α-synuclein to nucleus induced neurodegeneration and sequestering it to cytoplasm prevented neurodegeneration. Histone deacetylase inhibitors (HDAC) rescued the α-synuclein induced neurotoxicity indicating α-synuclein may be involved in modifying the histone acetylation status. α-synuclein also showed to have binding affinity to histone H1 proteins indicating it may alter the chromatin organization (Gores et al., 2003; Duce et al., 2006). Histone H1 protein is a linker protein which maintains the internucleosomal positioning in the chromatin structure. Recent study showed that MPP(+) induced misfolded α-synuclein aggregates were degraded by ubiquitin-binding histone

deacetylase-6 (HDAC-6) indicating the role of chromatin modifying enzymes in PD (Su et al., 2010). Poly (ADP-ribose) polymerase (PARP) and ADP ribosylation plays an important role in chromatin function, genomic integrity and DNA repair (Herceg et al., 2001). All the above data indicated the role of chromatin organization in parkinson's disease and neuronal cell death. In the present study the chromatin organization in parkinson's disease and control brain samples was analyzed.

Thermal denaturation analysis of the chromatin samples showed decrease in the melting transition temperature in PD chromatin compared to that of age matched control brains. The decrease in the transition temperature may be due to the altered chromatin organization compared to that of controls. The decrease may be accounted for the hyperacetylated PD chromatin compared to control. Since hyperacetylation weakens the histone-DNA interactions, this weak interaction resulted in lowering the melting temperature. Similar kind of decreased melting temperature was observed with hyperacetylated chromatin compared to normal chromatin (Riehm et al., 1987; Siino et al., 2003; Wallace et al., 1997).

CD studies with chromatin samples showed differences between the PD chromatin and control chromatin. The difference in the CD spectra may be due to different histone composition in PD chromatin compared to normal chromatin. The decrease in the 275 nm positive peak in hippocampus indicated that unfolding of chromatin, opposite to that of observed by Tikoo et al., (1997) where decrease in 275 nm peak attributed for the chromatin condensation. The hyperacetylated chromatin also showed similar kind of increase in the 275 nm peak observed by Riehm et al., (1987). This may indicate that CD spectral changes observed in PD hippocampal region may be due to differences in their histone acetylation status.

The histone acetylation status of chromatin samples by detecting histone H3 acetylation by dot blot assay was analyzed. We observed Histone H3 acetylation in all the PD chromatin samples compared to 50% of detectable histone acetylation levels in the control sample was observed. This support the thermal and CD data, indicating the hyperacetylation of histone proteins in PD subjects.

Micrococcal nuclease digestion revealed that PD chromatin was more sensitive to digestion compared to that of control. This showed that more loose chromatin loops were present in PD chromatin compared to control and nucleosomal positioning altered in PD conditions. MspI/Hpa II restriction digestion analysis indicated the PD chromatin was more sensitive than that of control subjects. Methylation specific Msp I digestion analysis indicated that PD DNA methylation was more compared to that of control DNA. Non-specific Hpa II digestion also showed higher digestion of PD DNA compared to that of control. This may be due to already damaged PD DNA which was more sensitive to restriction digestion. DNA damage was observed as single stranded breaks and double strand breaks in PD DNA compared to control in hippocampus, thalamus, caudate nucleus, midbrain (Hegde et al., 2003).

In conclusion, the present study provided initial analysis of the chromatin alteration in Parkinson's disease brain. In PD hyperacetylation of the histone was observed, especially histone H3. Hyperacetylated PD chromatin may be loosely arranged as evidenced by the CD studies, thermal denaturation analysis and micrococcal nuclease digestion analysis. Restriction digestion analysis with methylation specific Msp I and HpaII endonuclease revealed the differences in the methylation status of the DNA between PD and normal subjects. The alteration in the chromatin organization in PD brain may lead to altered gene expression and neuronal cell death observed in Parkinson's disease.

Chapter 2B

Curcumin interactions with chromatin and its role in protein-DNA interactions

2B.1 Introduction

Curcumin is a hydrophobic polyphenol derived from the rhizome (turmeric) of the herb *Curcuma longa*. Turmeric is commonly used spice in india and curcumin is the principle component of turmeric. Curcumin is also used widely as pharmacological active compound because of its wide spectrum of biological activities. Curcumin has been reported to have the antioxidant, antimicrobial, anti-inflamatory and anti-carcinogeneic activities (Epstein et al., 2010; Manjunatha and Srinivasan, 2007,2006; Joe et al., 2004). Several studies reported that curcumin shows neuroprotective properties. Curcumin has shown protective effects against intracerebroventricular–streptozotocin (ICV–STZ) induced cognitive deficits and oxidative damage in rats (Ishrat et al., 2009). Recently, it is reported a pyrazole derivative of curcumin enhances memory by activating Ca2+/calmodulin dependent protein kinase II (CaMKII). CaMKII plays a important role in long-term potentiation (LTP) and memory (Maher et al., 2010). Curcumin has shown the ameliorating effect against lipopolyscaccharide induced (LPS) neurotoxicity. LPS induced neurotoxicity by activating transcription factors, nuclear factors κB (NF-κB) and activator protein-1 (AP-1) which leads to inflammation (Yang et al., 2008).

Some of the studies showed that curcumin has potential to have the therapeutic potential for Parkinson's disease. Liu et al., (2011) showed that curcumin protected the mutant α-synuclein induced cell death in PC12 cells via inhibition of oxidative stress and mitochondrial cell death pathway. Several studies showed that curcumin prevents the α-synuclein induced toxicity through its antioxidant properties (Wang et al., 2010). Curcumin was shown to chelate the metals like iron and thereby inhibiting the iron repressed DNA base excision repair pathway (Hegde et al., 2010). Curcumin exposure to mesencephalic cells induced leucine-rich repeat kinase 2 (LRRK2) indicating that curcumin alters gene expression (Ortiz-Ortiz et al., 2010). Curcumin has shown to

regulate the expression of cytokines, adhesion proteins, cell survival proteins and inflammatory enzymes by activating transcription factors. It has been reported to have up regulate and down regulate several genes indicating its potential affecting the gene expression (Goel et al., 2008). Curcumin also reported to have the anti-aggregating properties by inhibiting the aggregation of α-synuclein and disaggregating preformed fibrils (Ono et al., 2008; Pandey et al., 2008). In MPTP(+) model of PD, monoamine oxidase-B activity was inhibited by curcumin and dopamine depletion was prevented providing the protection against MPTP(+) induced neurotoxicity (Rajeswari A and Sabesan, 2008).

In the present study the i) interaction of curcumin with chromatin and ii) its role in neuroprotein-DNA interaction was analyzed, by *in vitro* methods to understand its potential to prevent the toxicity induced by these neuroproteins.

2B.2 Materials

The curcumin powder (60 % of curcumin) was procured from Spicex Pvt. Ltd., Mysore, India. Supercoiled pUC18 DNA (cesium chloride purified, 90% supercoiled structure, scDNA), was purchased from Banglore Genei, India. Tau protein was purchased from r-peptide (USA) Agarose, HEPES, Tris and EDTA were purchased from SISCO Research laboratories. Ethidium bromide and micrococcal nuclease were from Sigma (USA) chemicals.

2B.3 Methodology

2B.3.1 Purification of curcumin

The enrichment of the curcumin to the high purity was done by silica column chromatography. Curcumin powder dissolved in chloroform and applied on silica gel (100-200 mesh) with chloroform as the eluant. The purity was checked with TLC initially and then confirmed by HPLC and NMR(^{1}H and ^{13}C NMR).

2B.3.2 Tetrahydrocurcumin preparation

Tetrahydrocurcumin was prepared by selective hydrogenation of α, β-unsaturated double bonds in curcumin according to the following flow chart.

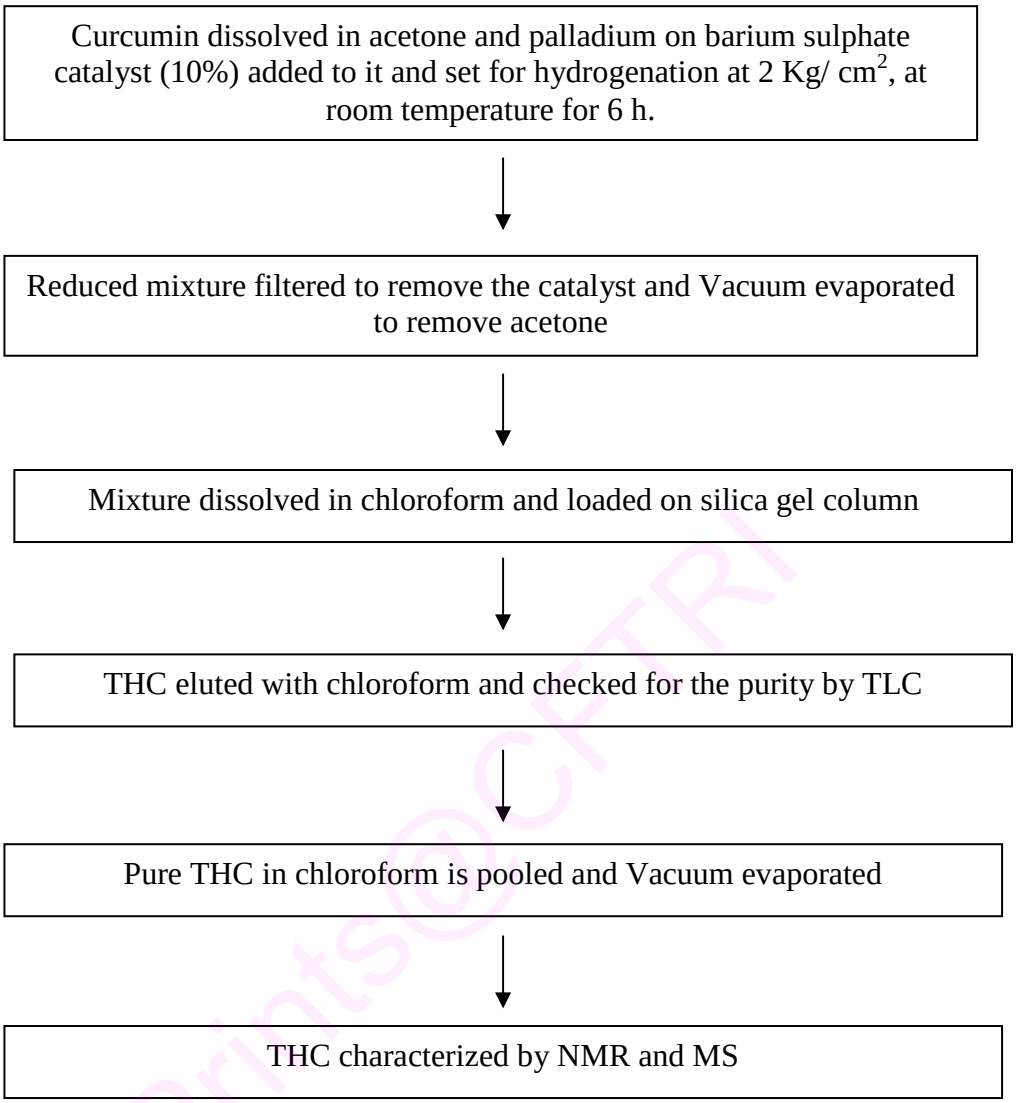

Curcumin (10g) was dissolved in acetone (30mL) and then set for hydrogenation in presence of 10% palladium on barium sulphate catalyst under 2 Kg/ cm^2 hydrogen pressure. The reaction was standardized on 10 g scale. Filtering of the catalyst and distillation of the solvent from the filtrate afforded crude product. The crude product was purified by silica gel column chromatography to afford pure tetrahydrocurcumin in over 70% yield.

2B.3.3 Preparation of nuclei and soluble chromatin

Nuclei from the control brain were isolated according to the method explained in the chapter 2A. Soluble chromatin was prepared from the isolated nuclei by limited digestion of nuclei with micrococcal nuclease (Korenberg et al., 1989). Nuclear suspension (100 µL) was mixed with 0.1M $CaCl_2$ and incubated at 37°C for 2 min.

After incubation, the nuclear suspension was digested with micrococcal nuclease (50 units) by incubating at 37°C for 1 min. The reaction was stopped by 0.25 M EDTA and centrifuged at 5000 rpm for 5 min. The pellet obtained was suspended in 10mM $NaHSO_3$, pH 7.5, 1mM EDTA. The soluble chromatin used for the curcumin interaction studies.

2B.3.4 Agarose gel electrophoresis

The effect of curcumin on Tau-DNA and α-synuclein interactions was carried out using supercoiled plasmid DNA pUC18 as model system. Tau and α-synuclein was incubated with scDNA (2686bp) (DNA/protein mass ratios 1:2 in Tris-Cl (10 mM, pH 7.4) in the presence of 100 μM curcumin and tetrahydrocurmin separately at 37°C for 24 hr. Tau and α-synuclein was also incubated with scDNA in DNA/protein mass ratio 1:2 without curcumin and tetrahydrocurcumin. After the incubation time the samples were electrophoresed along with the control scDNA in 1% agarose gel at 50 V at room temperature. Gel was stained with ethidium bromide (EtBr) and scanned using gel documentation system. Curcumin stock solution was prepared in DMSO and in all curcumin interactions the DMSO percentage was around 5%.

2B.3.5 Absorbance measurements

Absorbance spectra of curcumin interaction with chromatin, scDNA, scDNA-α-synuclein and scDNA-Tau were measured using Spectrophotometer (Amarsham Biosciences, HongKong) in the range of 300-600 nm characteristic to that of curcumin. Curcumin (100 μM) was incubated with chromatin (OD_{260} = 0.6) in 10 mM Tris-HCl (pH 7.4) for 24 h and its absorbance was recorded. Curcumin was also incubated with scDNA, scDNA-α-synuclein (DNA/protein ratio= 1: 2) complex and scDNA-Tau (DNA/protein ratio= 1: 2) complex in 10 mM Tris-HCl (pH 7.4) for 24 h and its absorbance was recorded. scDNA-α-synuclein and scDNA-Tau complexes were prepared by incubating scDNA-protein for 12 h, prior to incubating with curcumin. Similarly, the absorbance of THC interaction with chromatin, scDNA, scDNA-α-synuclein and scDNA-Tau were measured in the range of 250-350 nm characteristic to THC. Curcumin stock solution was prepared in DMSO and in all curcumin interactions the DMSO percentage was around 5%.

2B.3.6 Fluorescence measurements

Fluorescence spectra of curcumin interaction with chromatin, scDNA, scDNA-α-synuclein and scDNA-Tau were measured using Spectrofluorimeter (HITACHI) with excitation at 420 nm and emission in the range of 450-700 nm characteristic to that of curcumin. Curcumin (100 μM) was incubated with chromatin (OD_{260} = 0.6) in 10 mM Tris-HCl (pH 7.4) for 24 h and its fluorescence was recorded. Curcumin was also incubated with scDNA, scDNA-α-synuclein (DNA/protein ratio= 1: 2) complex and scDNA-Tau (DNA/protein ratio= 1: 2) complex in 10 mM Tris-HCl (pH 7.4) for 24 h and its fluorescence was recorded. scDNA-α-synuclein and scDNA-Tau complexes were prepared by incubating scDNA-protein for 12 h, prior to incubating with curcumin. Similarly, the fluorescence of THC interaction with chromatin, scDNA, scDNA-α-synuclein and scDNA-Tau were measured with excitation at 450 nm and emission in the range of 500-700 nm characteristic to that of curcumin. Curcumin stock solution was prepared in DMSO and in all curcumin interactions the DMSO percentage was around 5%.

2B.3.7 Ethidim bromide fluorescence

Curcumin interaction with chromatin, scDNA, scDNA-α-synuclein and scDNA-Tau was indirectly analyzed by ethidium bromide binding studies to these complexes. Curcumin (100 μM) was incubated with chromatin (OD_{260} = 0.6) in 10 mM Tris-HCl (pH 7.4) for 24 h and then mixed with EtBr (2 μg/mL) and the EtBr fluorescence was measured with excitation at 535 nm and emission in the range of 560-660 nm. Curcumin was also incubated with scDNA, scDNA-α-synuclein (DNA/protein ratio= 1: 2) complex and scDNA-Tau (DNA/protein ratio= 1: 2) complex in 10 mM Tris-HCl (pH 7.4) for 24 h and then mixed with EtBr (2 μg/mL) and the EtBr fluorescence was measured. scDNA-α-synuclein and scDNA-Tau complexes were prepared by incubating scDNA-protein for 12 h, prior to incubating with curcumin. Curcumin stock solution was prepared in DMSO and in all curcumin interactions the DMSO percentage was around 5%.

2B.3.8 Thermal denaturation studies

Thermal melting of the whole chromatin, curcumin-chromatin complex was done on Spectrophotometer equipped with a thermostat programmer and data processor (Amarsham Biosciences, HongKong). Curcumin (100 μM) was incubated with chromatin (OD_{260} = 0.6) in 10 mM HEPES (pH 7.4) buffer for 24 h and melting temeperature profile was recorded in the range of 25-95°C with an increase of 1°C raise in temperature. Curcumin was also incubated with scDNA, scDNA-α-synuclein (DNA/protein ratio= 1: 2) complex and scDNA-Tau (DNA/protein ratio= 1: 2) complex in 10 mM Tris-HCl (pH 7.4) for 24 h and its melting temperature profile was recorded. scDNA-α-synuclein and scDNA-Tau complexes were prepared by incubating scDNA-protein for 12 h, prior to incubating with curcumin.

2B.3.9 Circular dichroism studies

The secondary conformation of chromatin, chromatin- curcumin complexes were recorded on JASCO J700 spectropolarimeter at 25°C, with 2mm cell length in the wavelength range between 250-320 nm in Tris-Cl buffer (5 mM, pH 7.4). Curcumin was also incubated with scDNA, scDNA-α-synuclein (DNA/protein ratio= 1: 2) complex and scDNA-Tau (DNA/protein ratio= 1: 2) complex in 10 mM Tris-HCl (pH 7.4) for 24 h and CD measurements was recorded between 250-320 nm. Curcumin stock solution was prepared in DMSO and in all curcumin interactions the DMSO percentage was around 5%. The secondary conformation for the each spectrum was the average of four scans.

2B.3.10 NMR Studies of curcumin interaction with nucleosides of DNA

NMR studies were carried out to understand the mode of binding of curcumin to nucleosides, guanosine, adenosine, cytidine, thymidine and modified nitrogen base 5-methyl cytosine. All NMR experiments are performed on a Bruker 500 MHz spectrometer. Since curcumin has shown to bind DNA, we attempted to know the its binding mode to DNA. Nucleosides were taken in deuterated DMSO and were interacted with curcumin in the ratio of 2:1 respectively and then subjected to a ^{1}H, ^{13}C. Two dimensional correlation spectroscopy HSQC, and HMBC were acquired. All

spectras are recorded at 25^0C. The curcumin alone and nucleosides alone set as controls. The NMR spectra are acquired with typical mixing at 100 and 500 ms, with 500 scans.

2B.4 Results

2B.4.1 Preparation of tetrahydrocurcumin and its characterization

The purity of the curcumin and THC was confirmed by HPLC. The molecular weight was analyzed and confirmed by Mass spectrometry [MS Waters Q-Tof Ultima) in the ES positive mode] and Nuclear Magnetic Resonance spectroscopic techniques [^{1}H NMR, ^{13}C NMR, Spin Echo Fourier Transformation experiment(SEFT), Heteronuclear Single Quantum Correlation (HSQC), Heteronuclear Multiple-Bond Correlation (HMBC) experiments were done on Bruker 500MHz, Avance AQS NMR Spectrometer]. The mass spectrum and NMR spectral diagrams for tetrahydrocurcumin are enclosed (Fig. 2B.1 and 2B.2)

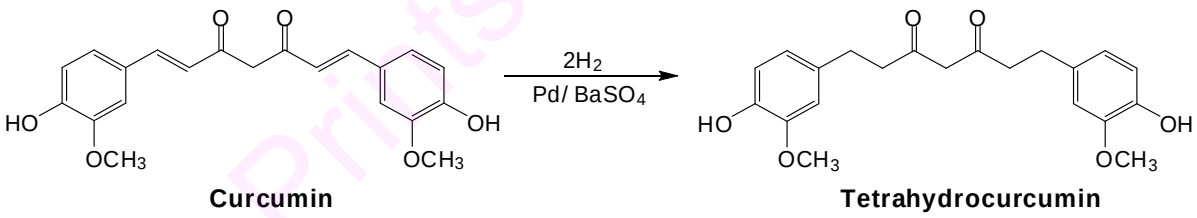

Figure 2B.1: Preparation of tetrahydrocurcumin (THC).

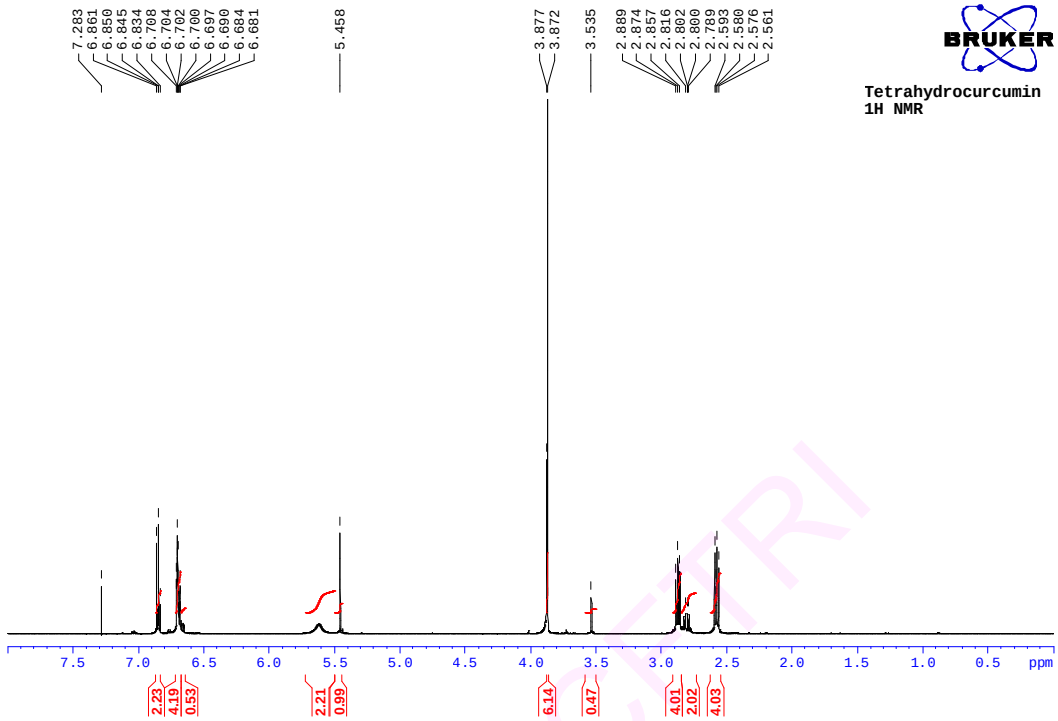

Figure 2B.2: ^{1}H NMR spectrum for tetrahydrocurcumin.

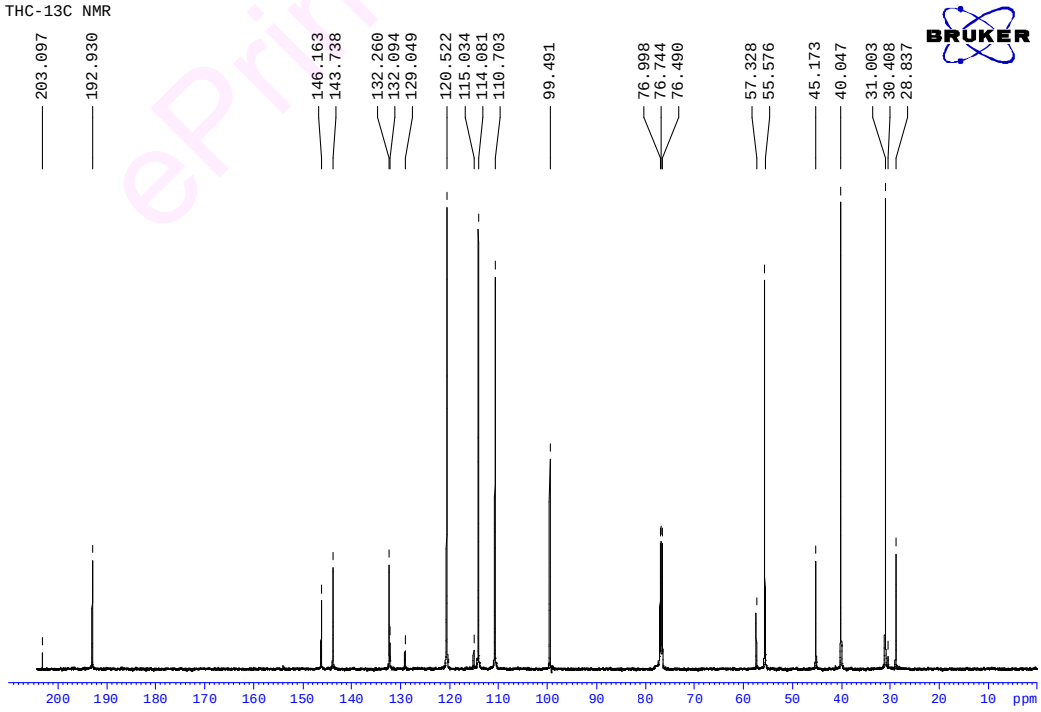

Figure 2B.3: ^{13}C NMR spectrum for tetrahydrocurcumin

2B.4.2 Agarose gel electrophoresis

scDNA gave two bands on 1% agrose gel, supercoiled DNA was found to be around 85% and open circular form was around 15% (Fig 2B.4). α-synuclein at DNA/protein ratio 1:2 converted scDNA to open circular form and linear forms (Fig 2B.4A, lane 3). Curcumin and THC could not prevented the α-synuclein nicking activity as evidenced by the conversion of scDNA to open circular form and linear forms in the presence of curcumin and THC respectively (Fig 2B.4A, lane 4 and 5). Tau at DNA/protein ratio 1:2 converted scDNA to open circular form and linear forms (Fig 2B.4B, lane 3). Curcumin and THC could not prevented the α-synuclein nicking activity as evidenced by the conversion of scDNA to open circular form and linear forms in the presence of curcumin and THC respectively (Fig 2B.4B, lane 4 and 5).

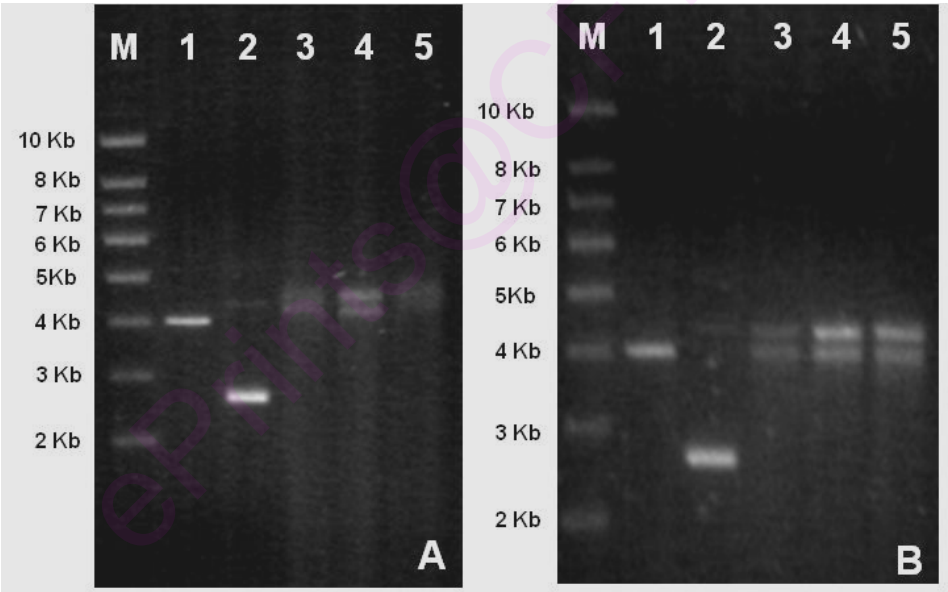

Figure 2B.4: DNA nicking activity of α-Synuclein and Tau in the presence of curcumin. A) Lanes: M. Marker, 1. Linear DNA, 2. scDNA 3. scDNA + α-Synuclein, 4. scDNA + α-Synuclein + Curcumin, 5. scDNA + α-Synuclein + THC. B) Lanes: M. Marker, 1. Linear DNA, 2. scDNA 3. scDNA + Tau, 4. scDNA + Tau + Curcumin, 5. scDNA + Tau + THC.

2B.4.3 Curcumin and THC interaction to chromatin and DNA analyzed by absorbance spectroscopy

Curcumin absorption spectra showed an absorption maxima at 440 nm (Fig 2B.5). Curcumin interaction with chromatin showed altered absorption spectrum showing

increase in 440 nm peak intensity and another peak at 360 nm. Since chromatin was not having any absorption spectra beyond 300 nm, the spectra obtained was the result of curcumin interaction with chromatin components. The altered curcumin spectra with chromatin indicated that curcumin binds to chromatin. We analyzed the curcumin interaction with tau, α-synuclein involved in the neurodegeneration and scDNA, scDNA-α-synuclein complex, scDNA-Tau complex (Fig 2B.6). Curcumin peak intensity was significantly decreased with scDNA interaction indicating the curcumin binding to scDNA. Curcumin also showed binding to tau, α-synuclein proteins as indicated by altered absorption spectra of tau-curcumin, α-synuclein-curcumin complexes. The absorption peak intensity of α-synuclein-curcumin complex was increased and tau-curcumin complex was decreased indicating the different mode of binding to these proteins. The absorption peak intensity of α-synuclein-curcumin-scDNA complex was also increased and tau-curcumin complex was also decreased indicating the binding of curcumin to protein-DNA complexes similar to that of protein binding. Similarly the tetrahydrocurcumin interaction with chromatin, tau, α-synuclein, scDNA, α-synuclein-scDNA complex, tau-scDNA complex was analyzed. The absorption spectra indicated that THC also showed binding of curcumin with chromatin, tau, α-synuclein, scDNA, α-synuclein-scDNA complex, tau-scDNA complex (Fig 2B.7;8)

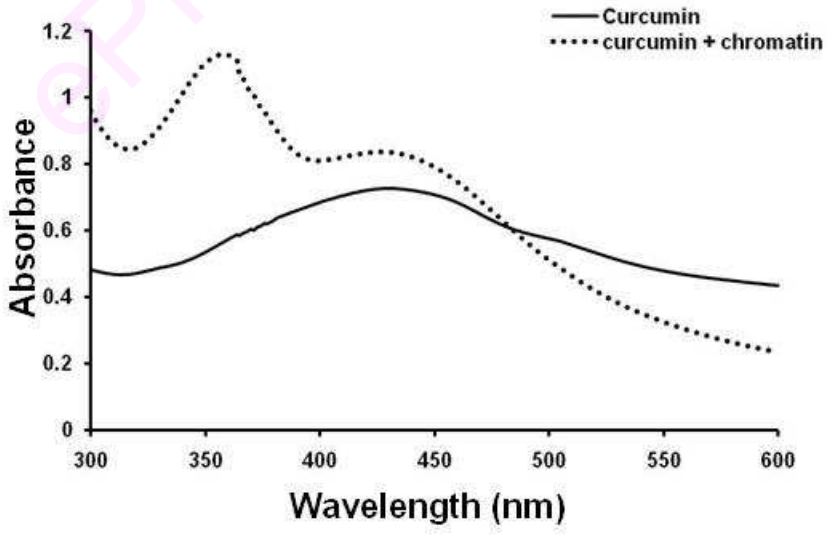

Figure 2B.5: Absorption spectra of curcumin and curcumin-chromatin complex

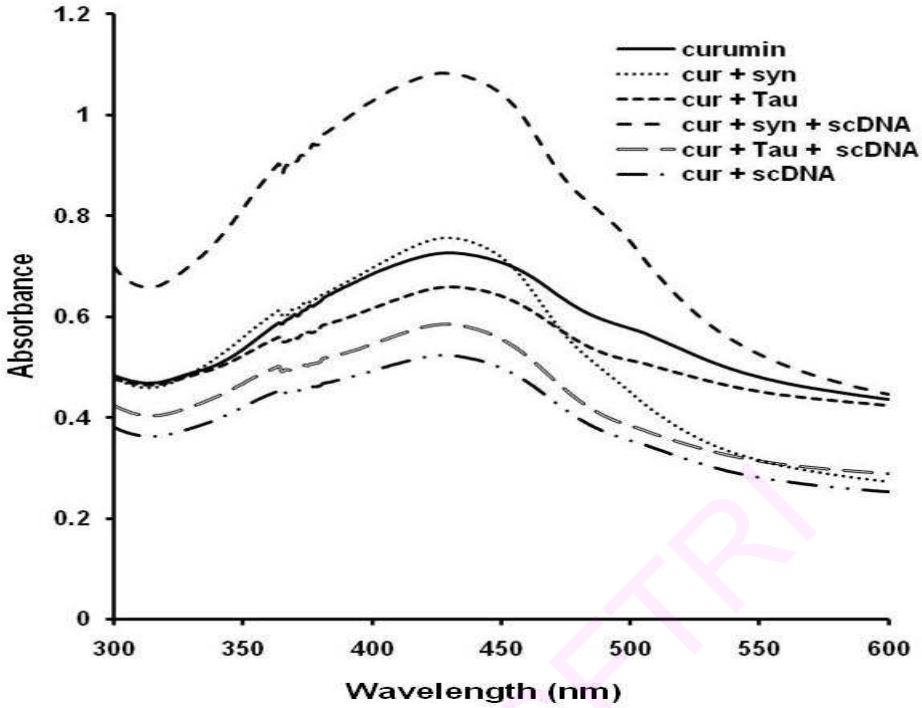

Figure 2B.6: Absorption spectra of curcumin interactions. curcumin + syn, curcumin + Tau, curcumin + syn +scDNA, curcumin + Tau + scDNA and curcumin + scDNA.

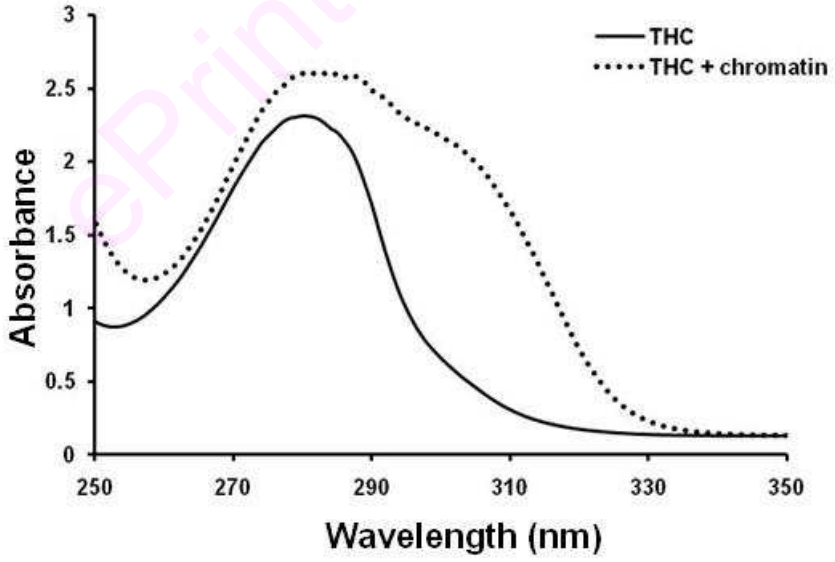

Figure 2B.7: Absorption spectra of THC and THC-chromatin complex

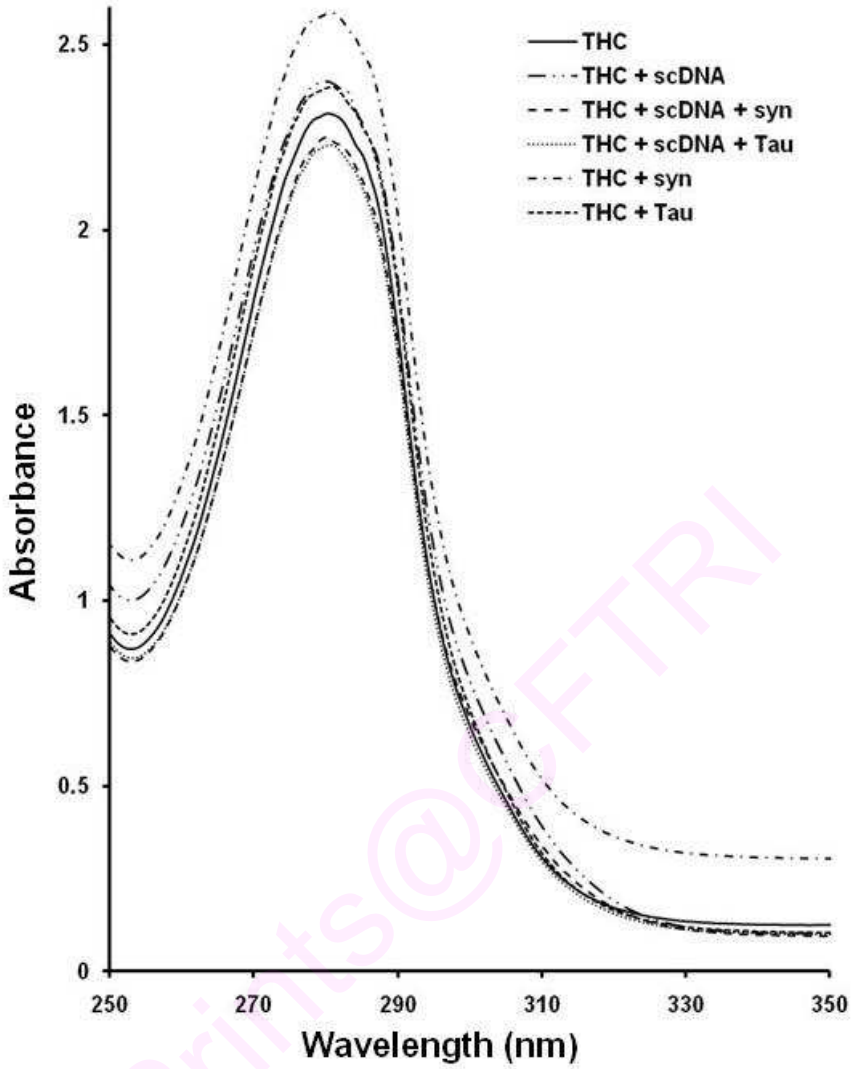

Figure 2B.8: Absorption spectra of THC interactions. THC + syn, THC + Tau, THC + syn +scDNA, THC + Tau + scDNA and THC + scDNA.

2B.4.4 Fluorescence spectroscopy of curcumin and THC interaction with chromatin and DNA

Curcumin fluorescence spectra showed a peak at 575 nm characteristic to curcumin. Curcumin incubated with chromatin decreased the fluorescence peak significantly and even the peak has shifted from 575 nm to 525 nm (Fig 2B.9). The data indicated that curcumin bind to chromatin components thereby decreasing the fluorescence of the curcumin. The curcumin binding to tau, α-synuclein, scDNA, scDNA-α-synuclein complex, scDNA-Tau complex was analyzed. Curcumin interaction with tau, α-

synuclein, scDNA, scDNA-α-synuclein complex, scDNA-Tau complex showed decrease in the fluorescence intensity indicating the curcumin binding to the scDNA and tau, α-synuclein proteins (Fig2B.10). Similarly, the THC binding to the chromatin by fluorescence spectroscopy was analyzed. THC was also showed a characteristic fluorescence peak at 525 nm and THC interacted with chromatin showed increase in the fluorescence intensity. The data indicated THC binding to chromatin. THC interaction with tau, α-synuclein, scDNA, scDNA-α-synuclein complex, scDNA-Tau complex also showed increase in the fluorescence indicating THC binding to scDNA, tau and α-synuclein (Fig 2B.12).

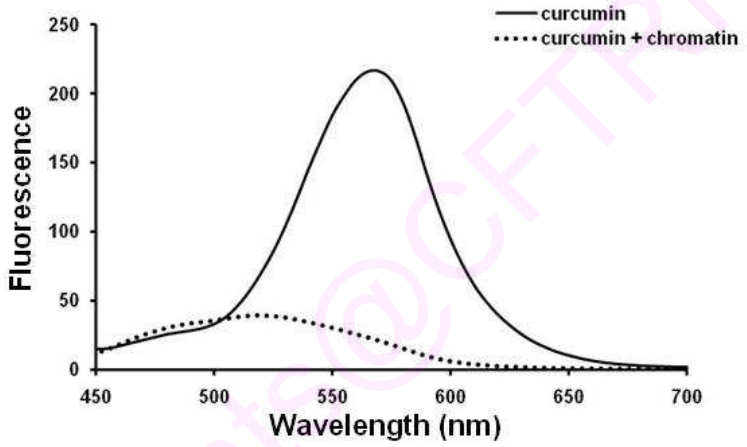

Figure 2B.9: Fluorescence spectra of curcumin and curcumin-chromatin complex

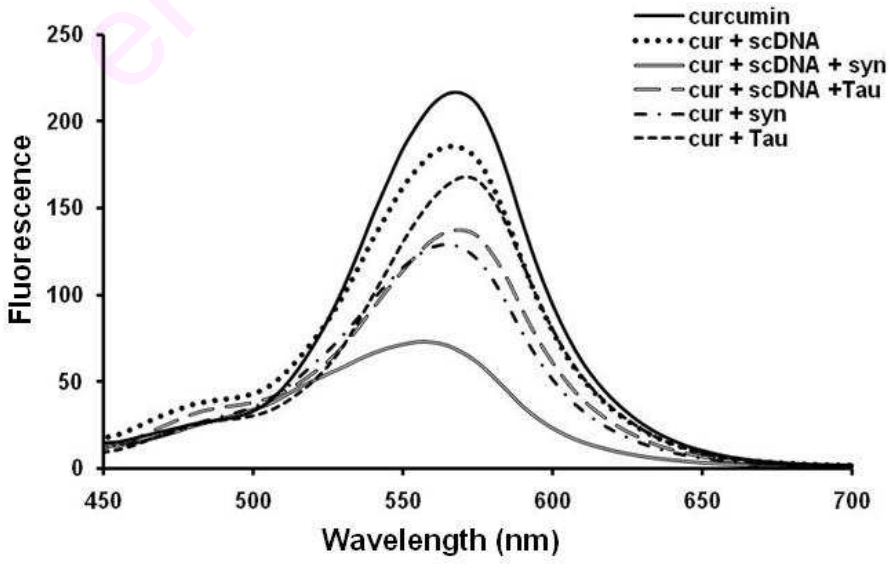

Figure 2B.10: Fluorescence spectra of curcumin interactions, 100 µM, curcumin + syn, curcumin + Tau, curcumin + syn +scDNA, curcumin + Tau + scDNA and curcumin + scDNA.

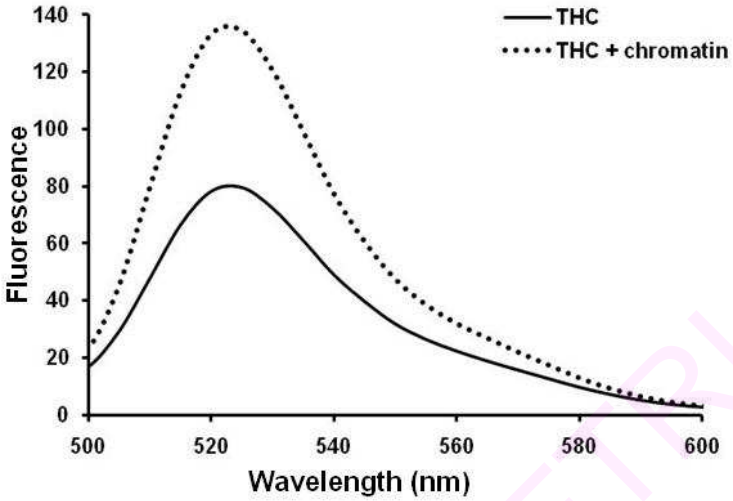

Figure 2B.11: Fluorescence spectra of THC and THC-chromatin complex

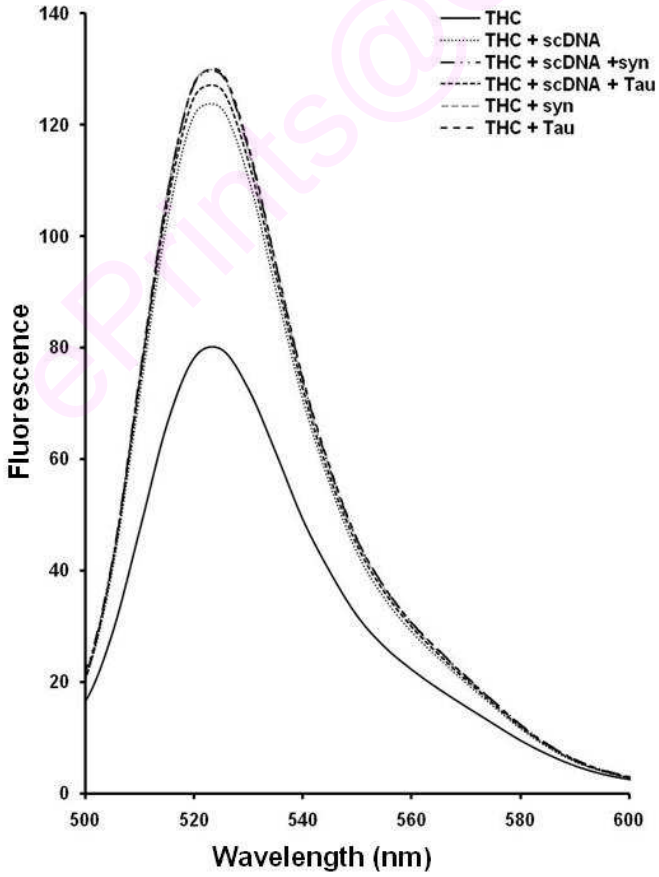

Figure 2B.12: Fluorescence spectra of THC interactions, THC + syn, THC + Tau, THC + syn +scDNA, THC + Tau + scDNA and THC + scDNA.

2B.4.5 Ethidim bromide binding studies

Curcumin interaction with chromatin and tau, α-synuclein, scDNA, scDNA-α-synuclein complex, scDNA-Tau complex was analyzed by ethidium bromide binding studies. Ethidium bromide binding to chromatin-curcumin complex was decresed compared to that of chromatin alone indicating the curcumin binding to chromatin. Ethidium bromide binding to scDNA-α-synuclein complex and scDNA-Tau complex decreased compared to scDNA indicating the curcumin binding to scDNA, scDNA-α-synuclein complex and scDNA-Tau complex (Fig 2B.13).

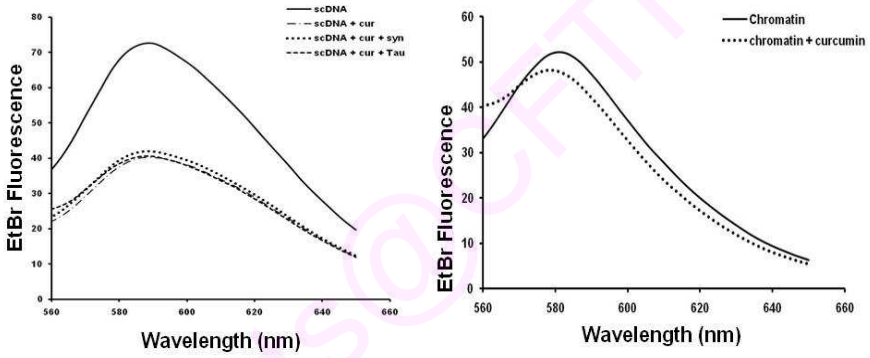

Figure 2B.13: EtBr fluorescence of chromatin, chromatin-curcumin, scDNA, scDNA-curcumin, scDNA-α-synuclein complex and scDNA-Tau complex.

2B.4.6 Thermal denaturation studies

Thermal denaturation of chromatin, curcumin-chromatin complex was analyzed for the structural integrity of chromatin. Thermal transition of the chromatin sample was around 80.3 ± 1.2°C and chromatin-curcumin complex was 76.3 ± 0.8°C indicating that curcumin altered the chromatin integrity (Table 2B.1). scDNA has biphasic melting temperature having T_{m1} = 54.2 ± 1.04°C and T_{m2} = 86.3 ± 0.9°C respectively. The melting temperature of scDNA-curcumin complex was 79.4 ± 1.3°C. The melting temperature of scDNA-synuclein-curcumin complex and scDNA-synuclein were 77.2 ± 0.8°C and 76.8 ± 1.2°C respectively. The melting temperature of scDNA-Tau-curcumin complex and scDNA-Tau were 72.3 ± 1.1°C and 81.3± 0.7°C, respectively. The data

indicated that curcumin altered the chromatin and scDNA integrity as evident by the decrease in meting temperature with curcumin interaction.

	Melting temperature
Chromatin	80.3 ± 1.2°C
Chromatin-curcumin	76.3 ± 0.8°C
scDNA	T_{m1} =54.2 ± 1.04°C T_{m2} = 86.3 ± 0.9°C
scDNA-curcumin	79.4 ± 1.3°C
scDNA-synuclein-curcumin	77.2 ± 0.8°C
scDNA-synuclein	76.8 ± 1.2°C
scDNA-Tau-curcumin	72.3 ± 1.1°C
scDNA-Tau	81.3± 0.7°C

Table 2B.1: Melting temperature profile of the curcumin interaction studies.

2B.4.7 Circular dichroism studies

Circular dichroism studies showed that curcumin interaction did not altered the secondary conformation chromatin. Small intensity changes were observed at 275 nm peak corresponding to the B-form of the DNA indicating that curcumin binding to DNA component of the chromatin samples. Similarly, curcumin interaction with scDNA, scDNA-α-synuclein complex and scDNA-Tau complex also did not show any conformational change in the secondary conformation of scDNA (Fig 2B.14).

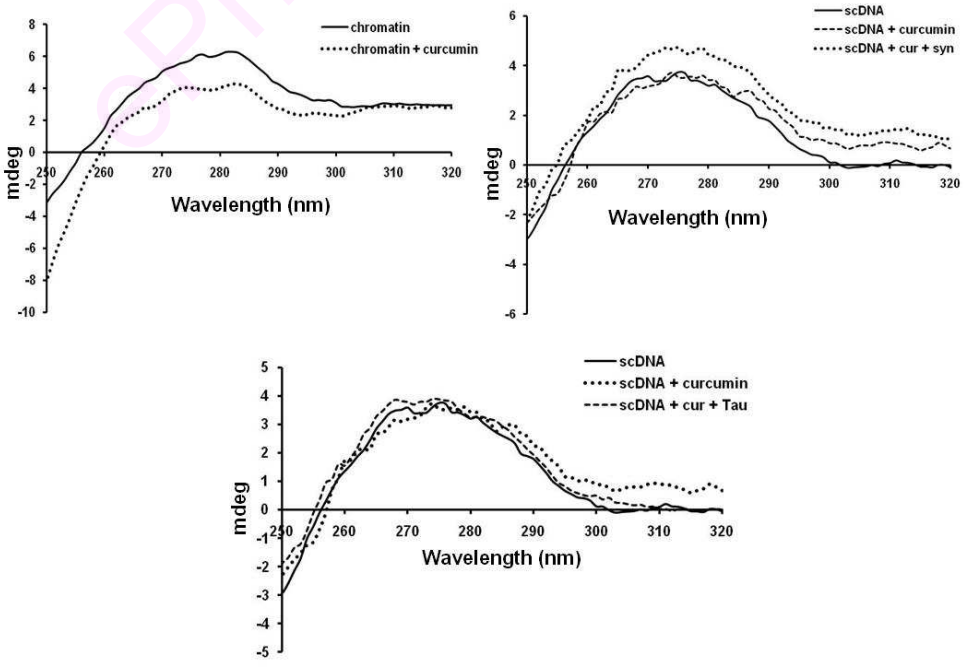

Figure 2B.14: CD spectra of chromatin, chromatin-curcumin, scDNA, scDNA-curcumin, scDNA-α-synuclein complex and scDNA-Tau complex.

2B.4.8 NMR Studies of curcumin interaction with nucleosides of DNA

Proton NMR: The 5mg sample was dissolved in 500µl DMSO-D6. The proton NMR spectrum was recorded using 5 mm BBO probe at 500MHz on BRUKER nmr spectrometer. Spectrum was collected using ***zg30*** pulse program. The experimental parameters are as follows Number of data points-65K, number of scans 32, spectral width 10330.578 Hz FID resolution 0.157632 Hz, acquisition time 3.1720407 sec, receiver gain 362, dwell time 48.400 µsec, pre scan delay 6.00 µsec, temperature at which experiment was carried out 300.0K. Relaxation delay 1.00sec

CHANNEL f1 parameters: P1 10.50 µsec, PL1 0.00 dB, SFO1 500.1830888 MHz

F2 - Processing parameters SI 32768 SF 500.1800000 MHz WDW EM, SSB 0, LB 0.30 Hz, GB 0, PC 1.00

13C NMR: The 13C NMR was collected at 125MHz with ***zgdc*** pulse program, number of data points 16K, number of scans 2K, spectral width 26455.027 Hz, FID resolution 1.614687 Hz, acquisition time 0.3097265 sec, receiver gain 16384, dwell time18.900 µsec, pre scan delay 6.00 µsec, relaxation delay 2.00 sec,

CHANNEL f1 parameters- F1 channel high power pulse width 8.50 µsec, power level 0.00 dB, frequency of observe channel 125.7828664 MHz., broadband proton decoupling pulse program employed is waltz16. 90 degree pulse for decoupling sequence 80.00 µsec

Spin echo Fourier Transformation: Attached proton test was carried out with the pulse program ***jmod***, the data points used in the experiment is 16K, number of scans collected is 5K with spectral width of 26455.027 Hz, FID resolution is 1.614687 Hz, acquisition time is 0.3097265 sec, receiver gain is 16K, dwell time is18.900 usec, pre scan delay 6.00 µsec, relaxation delay 2.00 sec,

CHANNEL f1 parameters- F1 channel high power pulse width 8.50 µsec, power level 0.00 dB, frequency of observe channel 125.7828664 MHz, broadband proton decoupling pulse program employed is waltz16. 90 degree pulse for decoupling sequence 80.00 µsec.

HSQC: Hetero nuclear single quantum correlation experiment was carried out with ***hsqcetgp*** pulse program. The experimental parameters are given below. Number of data points 16K, size of fid f2 channel 2K, f1 channel 256, number of scans 16, spectral width 10330.578 Hz. FID resolution 5.044228 Hz, acquisition time 0.0992216 sec, receiver gain 64, dwell time 48.400 μsec, pre scan delay 6.00 μsec, relaxation delay 2.00 sec.

CHANNEL f1 parameters: High power pulse width 10.50 μsec. power level 0.00 dB, frequency of observe channel 500.1830888 MHz.

CHANNEL f2 parameters: CHANNEL f2 parameters: Second nucleus 13C, F2 channel high power pulse width 8.50 μsec, power level 0.00 dB, frequency of observe channel 125.7828664 MHz

GRADIENT CHANNEL parameters: GPNAM1 SINE.100, GPNAM2 SINE.100, GPZ1 80.00 %, GPZ2 20.10 %, P16 1000.00 μsec.

HMBC: Multiple bond correlation via hetero-nuclear zero and double quantum coherence experiment was carried out by applying ***hmbcgplpndqf*** pulse program, dtat points collected is 2K, number of scans 16, size of fid f2 channel 2K, f1 channel 256, spectral width 7507.507 Hz, FID resolution 3.665775 Hz, acquisition time 0.1365134 sec, receiver gain 16K, dwell time 66.60 μsec, pre scan delay 6.00 μsec, temperature at which the experiment was carried out 300.0K, relaxation delay 2.00 sec,

CHANNEL f1 parameters: F1 channel high power pulse width 10.50 μsec, power level 0.00 dB, frequency of observe channel 500.1830888 MHz.

CHANNEL f2 parameters: Second nucleus 13C, F2 channel high power pulse width 8.50 μsec, power level 0.00 dB, frequency of observe channel 125.7828664 MHz

GRADIENT CHANNEL parameters: GPNAM1 SINE.100, GPNAM2 SINE.100, GPNAM3 SINE.100, GPZ1 50.00 %, GPZ2 30.00 %, GPZ3 40.10 %, P16 1000.00 usec

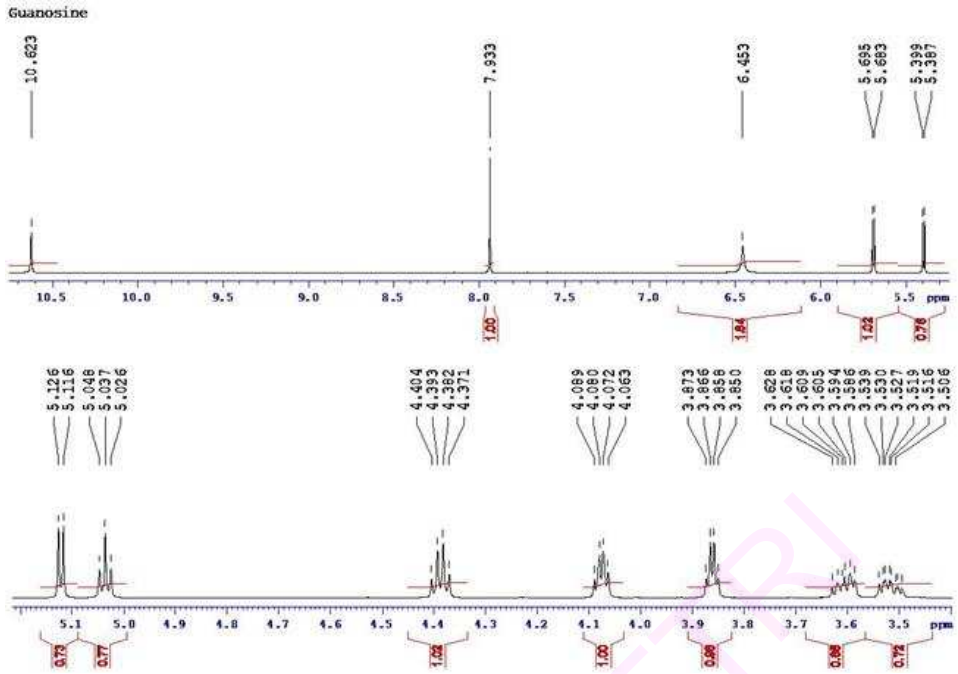

Figure 2B.15: ^{1}H NMR spectra of Guanosine

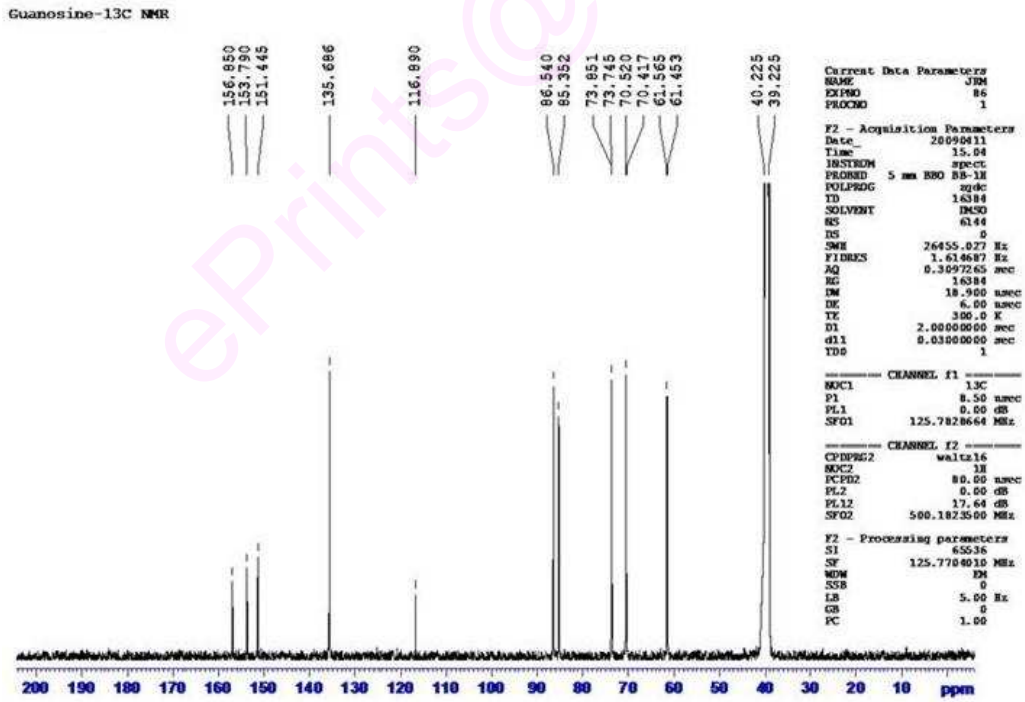

Figure 2B.16: ^{13}C NMR spectra of guanosine

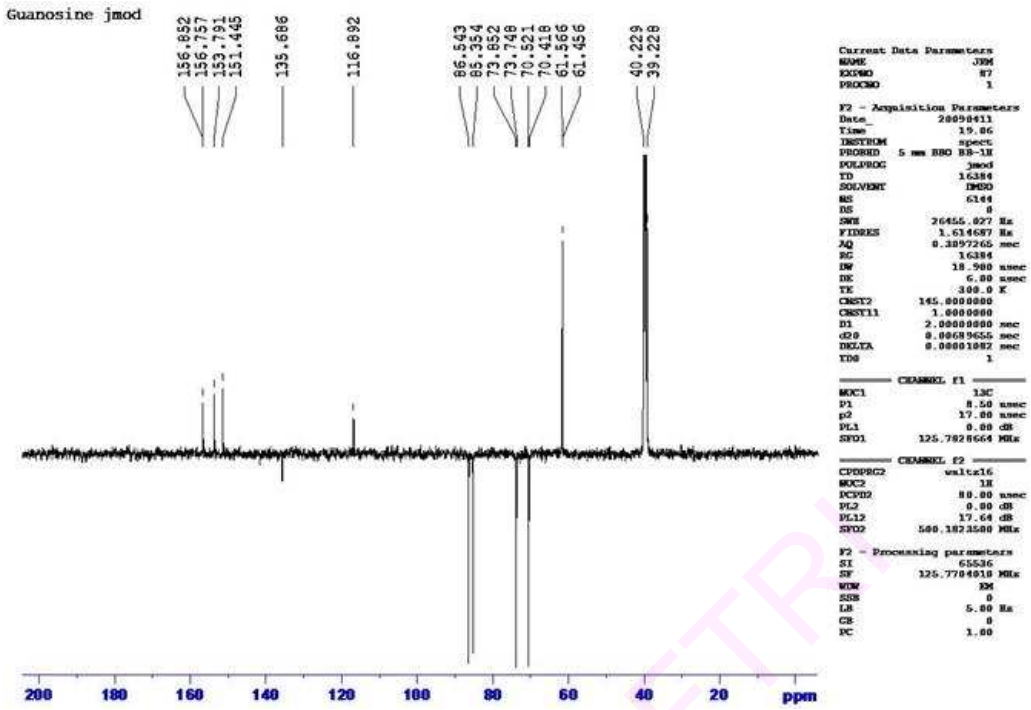

Figure 2B.17: Spin echo Fourier Transformation spectra (SEFT) of guanosine using JMOD

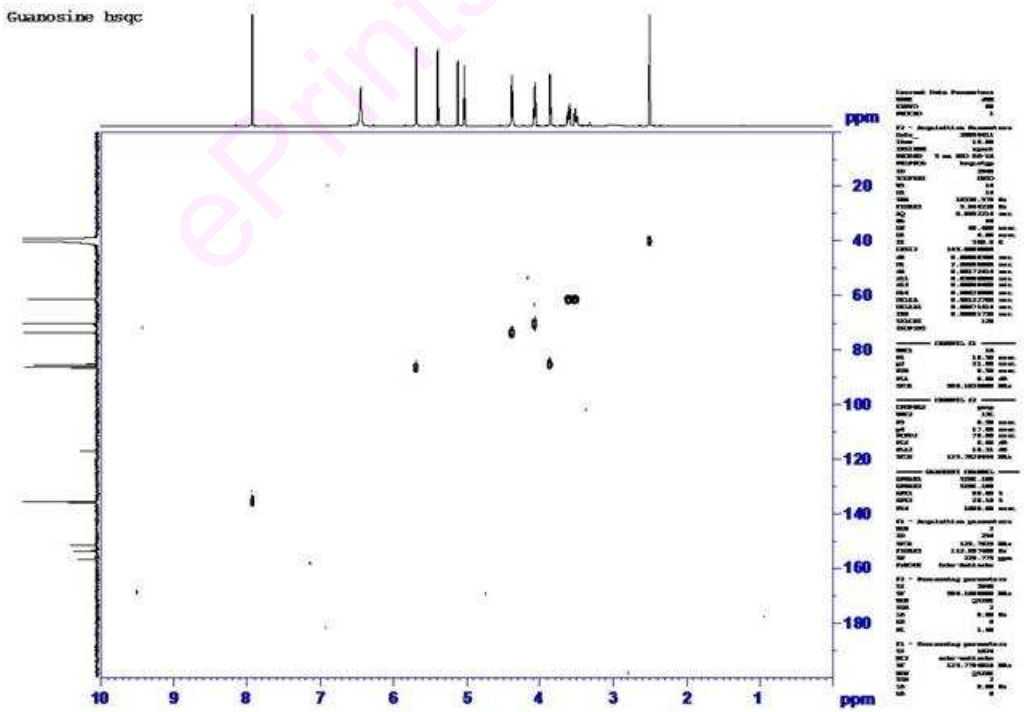

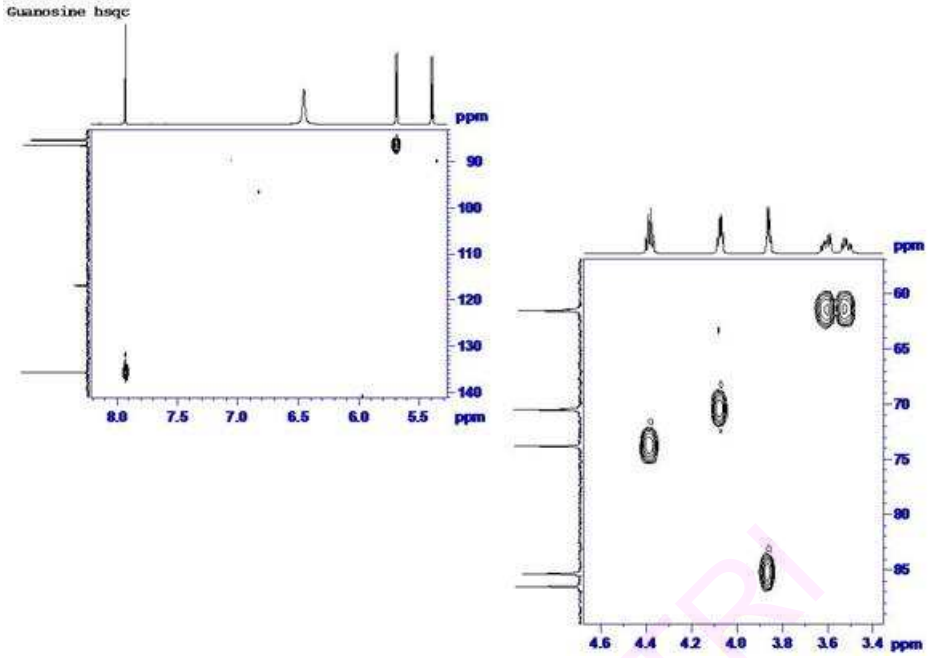

Figure 2B.18: HSQC spectra of guanosine

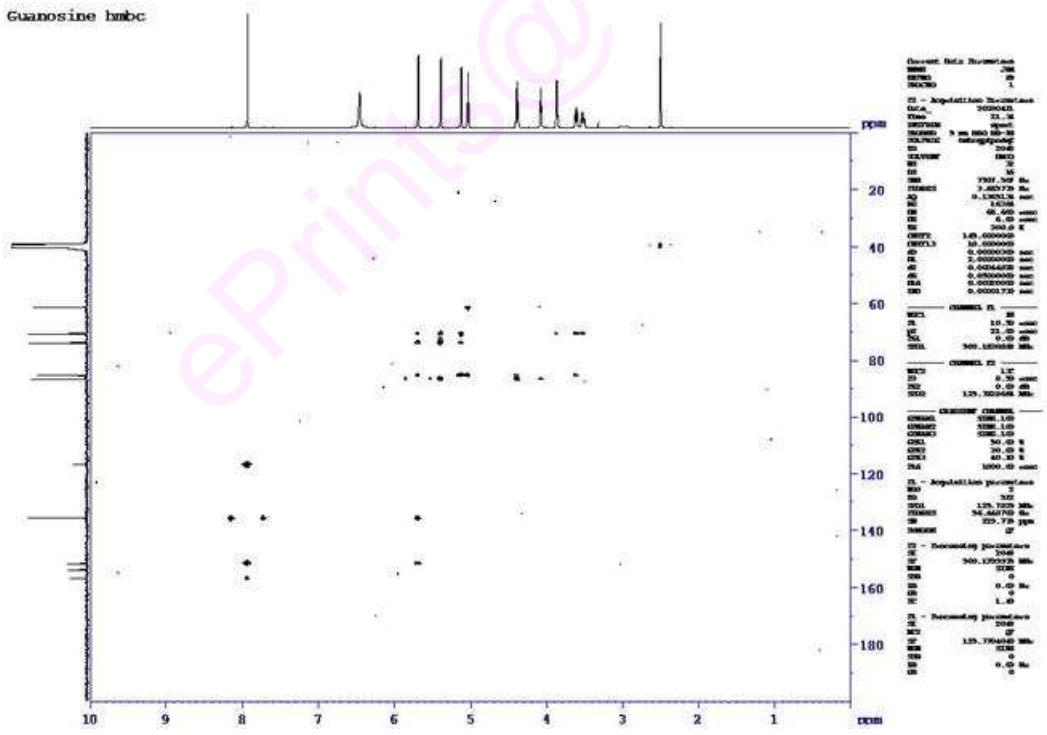

Figure 2B. 19: HMBC spectra of guanosine.

The NMR data analysis showed no interaction between the nucleosides of DNA and curcumin. This may be due to seconday conformation of DNA is important for the binding. Thus the studies have showed that curcumin binds to minor groove of the DNA.

2B.5 Discussion

Curcumin, a polyphenol showed neuroprotective activities and anti-Parkinsonian effects and has a great thereupetic potential for neurodegenerative diseases. In most of the neuroprotective studies, curcumin was shown to excert its action through anti-oxidant mechanism. Demethylated derivative of curcumin showed neuroprotective and antiinflamatory properties by increasing glutathione levels (Khanna et al., 2009). Curcumin was also shown to have epigenetic regulating properties in gene expression (Yun et al., 2010). Curcumin treatment in mouse cardiac myocytes showed decreased histone acetyltransferase (HAT) activities and reduced whole histone H3 acetylation. Reduced acetylation of H3 resulted in reduced binding to gene promoter regions and down-regulating the cardiac specific gene expression (Sun et al., 2010). Curcumin activated the sirtuin 1 (SIRT 1) which deacetylate histone protein and non-histone proteins including transcription factors, stress resistance proteins, cellular aging proteins, proteins involved in inflamation (Chung et al., 2010). Nicotine induced genotoxicity was protected by curcumin treatment in protein restricted dietary condition (Bandyopadhyaya et al., 2008; Chen et al., 2007; Rahman, 2008). Curcumin also acts as deacetylase inhibitor and resulted in histone acetylation and enhanced gene expression (Liu et al., 2005). Curcumin inhibited the p300/CREB-binding protein HAT activity dependent transcriptional activation from chromatin (Balasubramanyam et al., 2004). The biological activities of curcumin in regulating gene expression occur by the direct interaction with targeted proteins or epigenetic modulation (Fu and Kurzrock, 2010).

Curcumin also reported to have the DNA binding properties (Huang et al., 2010; Wang et al., 2007; Zsila et al., 2004). Kunwar et al., (2011) showed that synthetic analogue of curcumin dimethoxycurcumin bind to calfthymus DNA at minor groove. They also showed that dimethyoxycurcumin incubated MCF-7 cells showed curcumin nuclear localization indicating that curcumin may affect chromatin organization. Curcumin was shown to bind to the major and minor grooves of DNA and at high curcumin

concentration, DNA aggregation was reported (Nafisi et al., 2009). Liu et al., (2009) reported the possible role of curcumin as hypomethylation agent by molecular docking studies. Curcumin has shown to cross the blood brain barrier and labels senile plaques in Alzheimer's disease animal model (Garcia-Alloza et al., 2007).

In the present study, the role of curcumin and its metabolite tetrahydrocurcumin in chromatin organization by invitro methods were analyzed. The absorbance, fluorescence and EtBr binding studies showed that curcumin bound to chromatin components. It was shown that curcumin can cross the blood brain barrier (Garcia-Alloza et al., 2007) and enters into the nucleus of the cell (Kunwar et al., 2011). This shows that curcumin may interact with chromatin components and alter the gene expression. Curcumin either interact with DNA or histone proteins in the nucleus and affects chromatin structure. In the present study, it was found that curcumin bound to chromatin but did not alter the DNA conformation in chromatin. Curcumin binding to histone may block the time dependent histone modification like acetylation and deacetylation. Acetylation status of histone was important for the proper expressions of the genes. Thermal denaturation studies showed that curcumin decreased the melting transition from 80.3 ± 1.2°C to 76.3 ± 0.8°C indicating altered chromatin integrity upon curcumin binding. The stability of the chromatin was decreased upon curcumin binding. Curcumin metabolite tetrahydrocurcumin also found to bind chromatin. The studies showed that epigenetic regulation by curcumin mainly involved by the inhibition of the histone deacetylase activity and affecting the acetylation of transcription factors. The significance of curcumin binding to chromatin components must be evaluated by the *in vivo* studies to know the role of curcumin in epigenetic control. Curcumin may exert its neuroprotective role by blocking the action of different chromatin modifiers.

The role of curcumin on the DNA binding activities of α-synuclein and Tau which are involved in the neurodegeneration, especially, Parkinson's disease were studied. It was found that α-synuclein and Tau nick the DNA like endonuclease and damage the DNA. Curcumin role on the DNA nicking activity of α-synuclein and Tau was studied. Curcumin could not able to prevent the α-synuclein and Tau nicking. Then it was

further studied whether curcumin binds to DNA, α-synuclein and Tau by absorption, fluorescence studies. It was found that curcumin bound to scDNA and altered the scDNA integrity by altering its supercoiling nature as evident by the conversion of biphasic melting temperature to monophasic melting temperature in thermal denaturation studies. curcumin did not alter the secondary conformation of scDNA and even in the presence of α-synuclein and Tau. Further it was studied the curcumin binding to nucleosides to know its binding groups in curcumin-DNA interaction. However, no interaction between nucleosides and curcumin was found. Therefore, it can be assumed that curcumin binds to DNA in its double stranded structure. Curcumin metabolite tetrahydrocurcumin also bind to scDNA indicating it may alter DNA properties in *in vivo* conditions.

In conclusion, the present study showed that curcumin binds to chromatin components and alters its integrity. Curcumin also binds to scDNA and alters its integrity. Curcumin binds to α-synuclein and Tau proteins which are involved in Parkinson's disease. Curcumin could not able to prevent the α-synuclein and Tau induced DNA nicking activity. Further *in vivo* studies are needed to know the significance of curcumin binding to chromatin, α-synuclein and Tau either toxic or protective.

Chapter 3A

Biomarker study on Parkinson's Disease

3A.1 Introduction

The diagnosis of Parkinson's disease in the early stages of disease development helps in better management of the disease. Identifying a good specific biomarker for PD helps in early diagnosis (Wu et al., 2011; Prakash and Tan, 2010). Biomarker (BM) is "a characteristic that is objectively measured and evaluated as an indicator of normal biological processes, pathogenic process or pharmacological response to a therapeutic intervention". The availability of BMs for early disease diagnosis will impact the management of PD in several dimensions. 1) BMs help to identify the high risk individuals before symptoms develop. 2) BMs help to discriminate between true PD and other causes of a similar clinical syndrome. 3) BM may help determination of the clinical efficacy of newer neuroprotective therapies. 4) BMs must, therefore, gain insight into processes underlying the pathological changes, associated with PD (Scherzer, 2009; Halperin et al., 2009). Body fluids, which can be easily drawn like blood, urine and cerebrospinal fluid, will be used to identify biomarkers. Several molecules like trace metals, proteins, oxidative stress markers etc can act as biomarkers which can be estimated biochemically in these body fluids for PD (Waragai etal., 2010; Grünblatt et al., 2010). Trace metals like copper and Iron, metal transport proteins like ceruloplasmin, ferritin and oxidative stress markers like 8-OHdG are estimated in the sample fluids (Bharucha et al., 2008; Gmitterová et al., 2009; Bartzokis et al., 2007). Previously it was reported that trace metal homeostasis was altered in PD. Copper and iron levels were elevated in PD patients (Hegde et al., 2004; Pande et al., 2005). Earlier our study showed altered genomic integrity in PD brain samples. Single stranded breaks (SSB) and double stranded breaks (DSB) were accumulated in the DNA of PD brain samples (Hegde et al, 2006). Ceruloplasmin oxidative activity and serum ceruloplasmin were found to be low in Pakinkinson's disease (PD) patients (Torsdottir et al., 1999; Torsdottir et al., 2006;). Ceruloplamin immunoreactivity increased in the brain of PD patients, and attributed to an acute phase response to oxidative stress (Loeffler et al., 1996). In treated and untreated PD patients reduced levels of

ceruloplamin levels are found in spinal fluid (Boll et al., 1999). Increased 8OHdG levels were observed in the substantia nigra of Parkinson's disease patients. (Alam et al., 1997). Ferritin levels were decreased in the substantia nigra of PD patients. L-ferritin levels are lower in the SN region of the PD brain (Conner, 1995). Faucheux et al., (2002) reported iron accumulation with no up-regulation of the iron-storage protein ferritin in the substantia nigra of PD patients.

Neuroimaging is used as non invasive technique to diagnose the brain structural and functional changes. Magnetic resonance imaging (MRI) used to know the changes in brain of Parkinson's disease (Longoni et al., 2010; Menke et al., 2010; Roselli et al., 2010). MRI can be used for the early detection of the disease based on specific changes to the disease. Atrophy was observed in the brains of Parkinson's disease. Jokinen et al., (2009) performed the MRI of PD and healthy elderly volunteers and reported atrophy changes.

In the present study the serum biomarkers like ceruloplasmin, ferritin, 8-OHdG in the serum samples and MRI imaging of Indian patients were analyzed.

3A.2 Materials

8-OHdG ELISA kit and PAO kit was purchased from Japan aging institute. The syringes and blood collection containers were purchased locally with clinical standard. All other chemicals used were of analytical grade.

3A.3 Methodology

3A.3.1 PD Patients

The patients who come to JSS Medical Hospital were clinically identified for PD by the neurologist and patients who met the commonly accepted diagnostic criteria for PD were selected. The diagnosis was done using Unified Parkinson's Disease Rating Scale (UPDRS) and the Hoehn and Yahr staging in the clinic. The patients were explained about the study and consent was taken from them to participate in the study. Patients who were having other major illness like diabetes etc., were excluded. The study protocol was approved by JSS Medical College Ethical Committee.

3A.3.2 Blood collection and serum separation

10 ml of venous blood was collected from each PD and control patient and serum was separated by centrifugation. The serum was frozen at -20°C and protected from exposure to light until analysis. Blood collection and serum separation were carried out in dust free environments. The serum samples collected were aliquoted for different experiments and each sample was given a specific identification number. All the ethical guide lines were followed during the blood collection and MRI analysis.

3A.3.3 Serum 8-OHdG (8-Hydroxy Guanosine) detection

Serum 8-OHdG estimation was carried out using the 8-OHdG ELISA kit. The kit was based on the competitive *in vitro* enzyme-linked immunosorbent assay for the quantitative measurement of oxidative DNA adduct of 8-hydroxy-2'-deoxy guanosine. 50 µl of the serum sample was used for the estimation of 8-OHdG and quantified using the standard cure.

3A.3.4 Estimation of total antioxidant capacity of the serum

Total antioxidant capacity of the serum samples was estimated using PAO (Potential Anti oxidant) kit. PAO kits detect both hydrophilic and hydrophobic antioxidants in the serum samples. The principle behind the kit was reduction of Cu^{2+} to Cu^{+} by the antioxidants present in the serum samples. Reduced Cu^{+} was then reacted with bathocuproine and bathocuproine-Cu^{+} complex was measured by taking the absorbance at 490 nm. Uric acid was used as standard antioxidant and the results expressed as uric acid equivalents.

3A.3.5 Measurement of serum ceruloplasmin and ferritin

Serum ceruloplasmin and ferritin levels were estimated in Anand diagnostic labs, Bangalore. The serum samples are transported in frozen condition to Anand labs. Serum ceruloplamin was estimated using nephalometry and ferritin levels were estimated by chemiilluminiscence.

3A.3.6 Magnetic Resonance Imaging (MRI) of control and PD brains

15 normal and 22 PD patients were selected for the present investigation. The PD patients were diagnosed by NIH protocol by Psychiatry Professor of JSS Medical College, Mysore. MRI was done on all the above persons.

Multiplanar, multisequence MRI was done on Siemens Avanto 1.5T system using following protocol. Axial –T1, T2 and FLAIR (Fluid Attenuated inversion recovery). Sagittal –T1, Coronal –T2, 3D -gradient echo. Susceptibility weighted imaging –in axial plane, for T1- TR 550 ms and TE of 8.7 ms was used for T2 –TR of 5000 ms and TE of 118 ms was used for FLAIR sequence-TR was 9000 and TE was102 ms FOV for all sequence was 230mm. 5mm slice thickness was employed for all sequences, other than gradient sequence. 3D Gradient sequence was done in all patients in coronal plane with slice thickness of 1mm. All patients were co-operative and did not need any sedation. Typical total scan time for entire study was about 20 minutes.

3A.4 Results

3A.4.1 Serum 8-OHdG detection

Serum 8-OHdG levels were estimated using the 8-OHdG ELISA kit and the levels in the serum samples were expressed in ng/ml. The individual values of the 8-OHdG levels were tabulated along with their ID numbers (Table 3A.1). The average level of 8-OHdG were 2.4 ± 0.29 ng/ml and 4.6 ± 1.4 ng/ml for the control and Parkinson's disease patients, respectively. From the estimations it was clear that 8-OHdG levels were higher in the Parkinson's disease patients compared with that of the age matched control samples.

Table 3A.1: Serum 8-OHdG levels of PD and control

Sample	8-OHdG (ng/ml)	Sample	8-OHdG (ng/ml)
C1	2.3	PD1	4.2
C2	2.5	PD2	3.75
C3	2.55	PD3	5
C4	2.65	PD4	4.2
C5	2.75	PD5	6.75
C6	2.35	PD6	5.2
C7	2.1	PD7	5.45
C8	2.7	PD 8	5.1

C9	2.8	PD9	3.3
C10	2.3	PD10	3.45
C11	2.4	PD11	5
C12	3.1	PD12	4.3
C13	2.15	PD13	3.6
C14	2.6	PD14	10
C15	2	PD15	3.3
		PD16	3.75
		PD17	4.5
		PD18	4.2
		PD19	3.75
		PD20	4.1
		PD21	3.75
		PD22	5.2
Average levels of 8-OHdG levels in ng/ml			
Control	**2.4 ± 0.29**	**PD**	**4.6 ± 1.4**

Table 3A.1: Serum 8-OHdG levels of PD and control. Individual and average levels (with SD) of the serum 8-OHdG levels of the Control and Parkinson's disease (PD) samples. The average 8-OHdG levels of Control and PD were significant at $P<0.05$.

3A.4.2 Total antioxidant capacity of the serum

Total antioxidant capacities of serum indicate the oxidative stress implicated in PD compared to control subjects. Total antioxidant capacity was estimated using ELISA Kit (Japan Aging Institute) and expressed as uric acid equivalents (Table 3A.2). Uric acid (1mM) was equivalent to 2189 μmol/L of copper reducing power. The average level of total antioxidant capacity of control and parkinson's disease serum samples were 1472.467 ± 312 and 1662.645 ± 303 respectively. The increase in the total antioxidant capacity in serum samples of PD compared to control indicated that oxidative stress was more in PD patients compared to control.

Table 3A.2: Total antioxidant capacity of PD and control serum

Sample	Anti-oxidant potential (μmol/L)	Sample	Anti-oxidant potential (μmol/L)
C1	1357.18	PD1	1576.08
C2	1335.29	PD2	1882.54

C3	1138.28	PD3	1816.87
C4	1729.31	PD4	1379.07
C5	1532.3	PD5	1904.43
C6	1904.43	PD6	1597.97
C7	2167.11	PD7	2692.47
C8	1729.31	PD 8	1729.31
C9	1729.31	PD9	1510.41
C10	1335.29	PD10	1641.75
C11	1138.28	PD11	1641.75
C12	1335.29	PD12	1729.31
C13	1313.4	PD13	1729.31
C14	1182.06	PD14	1816.87
C15	1160.17	PD15	1335.29
		PD16	1619.86
		PD17	1532.3
		PD18	1970.1
		PD19	1291.51
		PD20	1444.74
		PD21	1444.74
		PD22	1291.51
Average values of total antioxidant potential serum samples			
Control	**1472.467 ± 312**	**PD**	**1662.645 ± 303**

Table 3A.2: Individual and average levels (with SD) of the serum total antioxidant capcity of the Control and Parkinson 's disease (PD) samples. The average serum total antioxidant capcity of Control and PD were significant at $P<0.05$.

3A.4.3 Serum ceruloplasmin and ferritin

Serum ceruloplasmin levels of Parkinson's disease and control samples were estimated using nephalometry (Table 3A. 3). The average level of ceruloplasmin of control and parkinson's disease serum samples were 0.39 ± 0.06 g/L and 0.22 ± 0.03 g/L respectively. Serum ferritin levels of Parkinson's disease and control samples were estimated using chemiilluminiscence. The average level of ferritin in control and parkinson's disease serum samples were 78 ± 26 μg/L and 61 ± 53 μg/L respectively.

Table 3A.3 : Ceruloplasmin and ferritin levels of PD and control

Sample	Ceruloplasmin g/L	Sample	Ceruloplasmin g/L	Sample	Ferritin µg/L	Sample	Ferritin µg/L
C1	0.482	PD1	0.297	C1	103	PD1	138
C2	0.344	PD2	0.266	C2	102.8	PD2	22.63
C3	0.308	PD3	0.248	C3	32.41	PD3	82.57
C4	0.31	PD4	0.211	C4	37.81	PD4	34.59
C5	0.439	PD5	0.239	C5	88.16	PD5	47.27
C6	0.336	PD6	0.262	C6	105.1	PD6	33.6
C7	0.367	PD7	0.249	C7	83.71	PD7	20.68
C8	0.363	PD 8	0.251	C8	87.32	PD 8	107.8
C9	0.442	PD9	0.273	C9	70.5	PD9	57.11
C10	0.441	PD10	0.272	C10	60.46	PD10	124
C11	0.395	PD11	0.156	C11	68.37	PD11	67.86
C12	0.47	PD12	0.214	C12	40.31	PD12	55.53
C13	0.52	PD13	0.164	C13	115.8	PD13	58.33
C14	0.313	PD14	0.24	C14	63.61	PD14	19.82
C15	0.335	PD15	0.247	C15	72.25	PD15	36.99
		PD16	0.208			PD16	24.59
		PD17	0.216			PD17	33.16
		PD18	0.208			PD18	24.42
		PD19	0.184			PD19	2.48
		PD20	0.18			PD20	103.1
		PD21	0.203			PD21	30.2
		PD22	0.189			PD22	234.1
Average values of Ceruloplasmin levels				**Average values of ferritin levels**			
Control	**0.39 ± 0.06**	**PD**	**0.22 ± 0.03**	**Control**	**78 ± 26**	**PD**	**61 ± 53**

Table 3A.3: Individual and average levels (with SD) of the serum ceruloplasmin and ferritin in control and Parkinson's disease (PD) samples. The average serum total antioxidant capacity of control and PD were significant at $P<0.05$.

3A.4.4 Magnetic Resonance Imaging (MRI) of control and PD brains

MRI imaging of brains of PD and control subjects was carried out at Vikram Hospital under the supervision of chief radiologist. The imaging procedure was explained to the patients and control subjects before the imaging. The thickness of the hippocampus, frontal lobe, temporal lobe, thalamus, cerebellum, caudate nucleus, substantia nigra and midbrain was analyzed using the inbuilt software in the MRI machine.

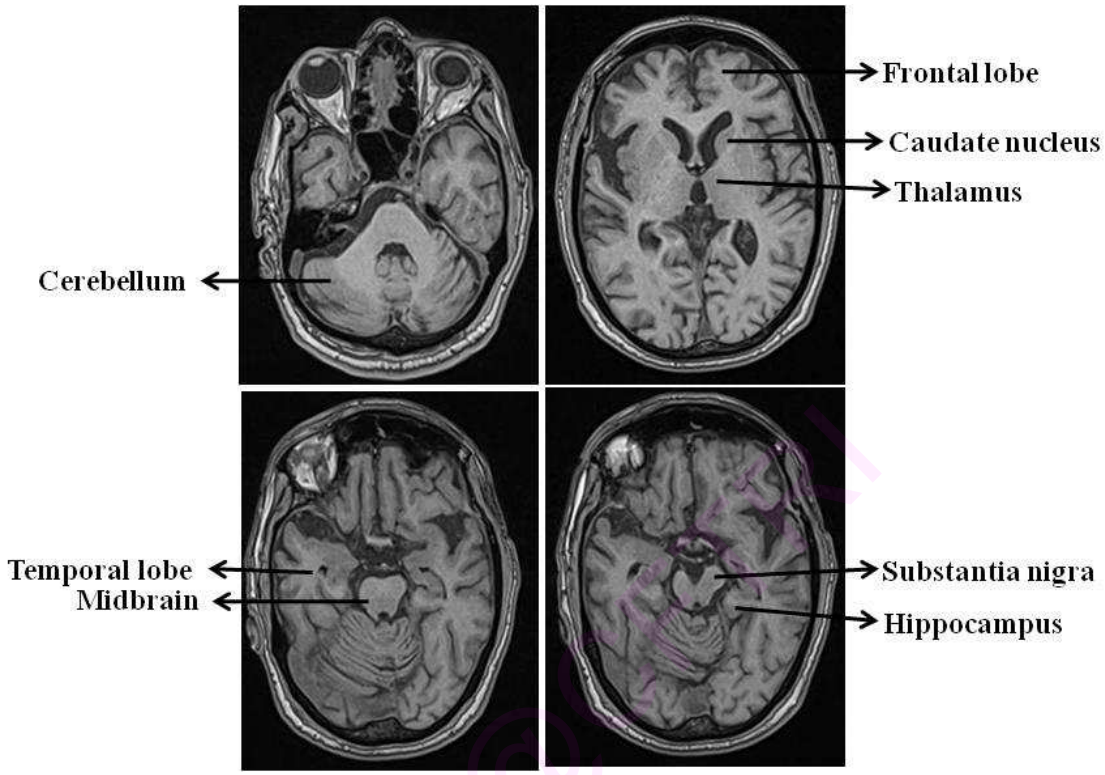

Figure 3A.1: Brain MRI images showing different regions

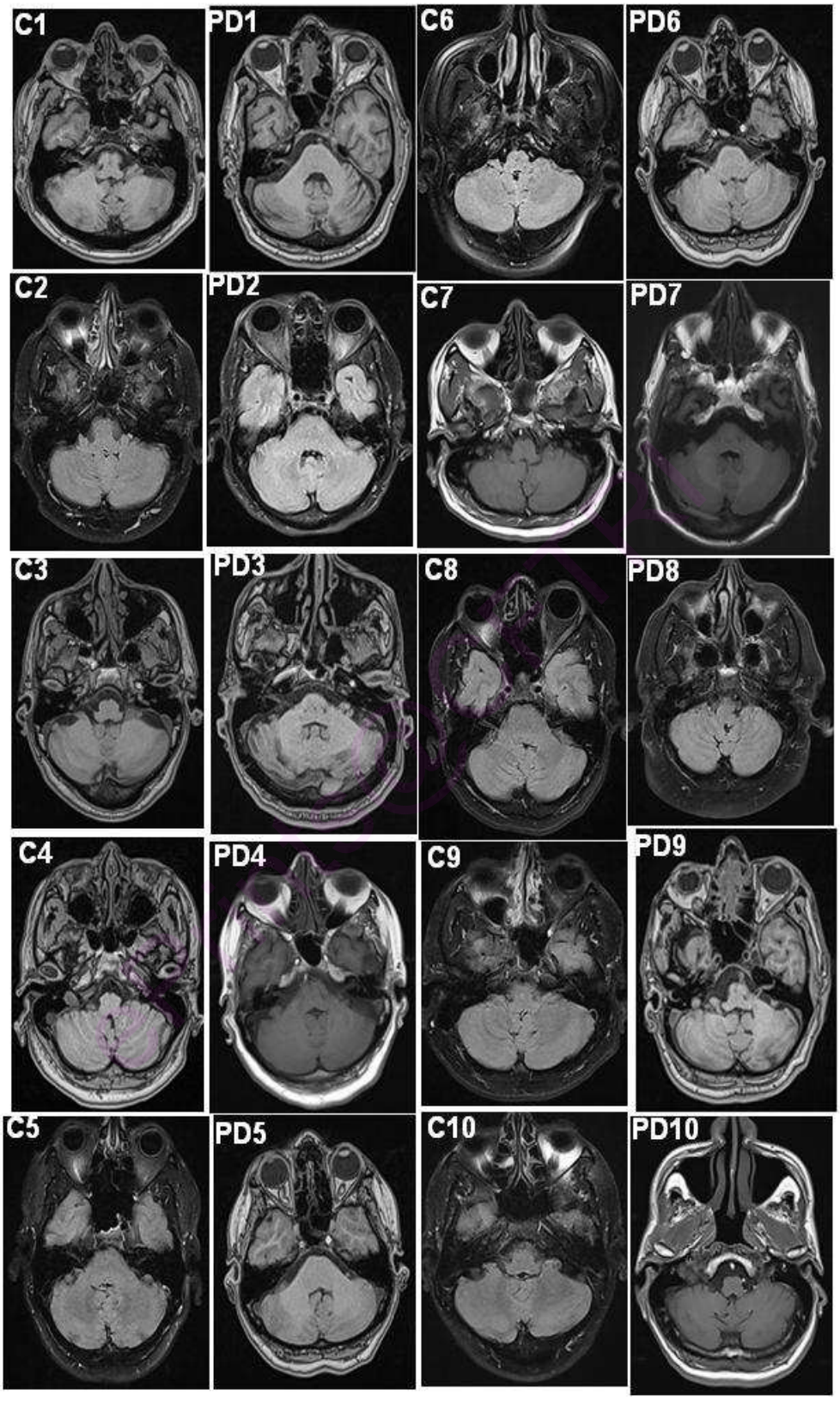

Figure 3A.2: MRI images of control and PD brains showing cerebellum

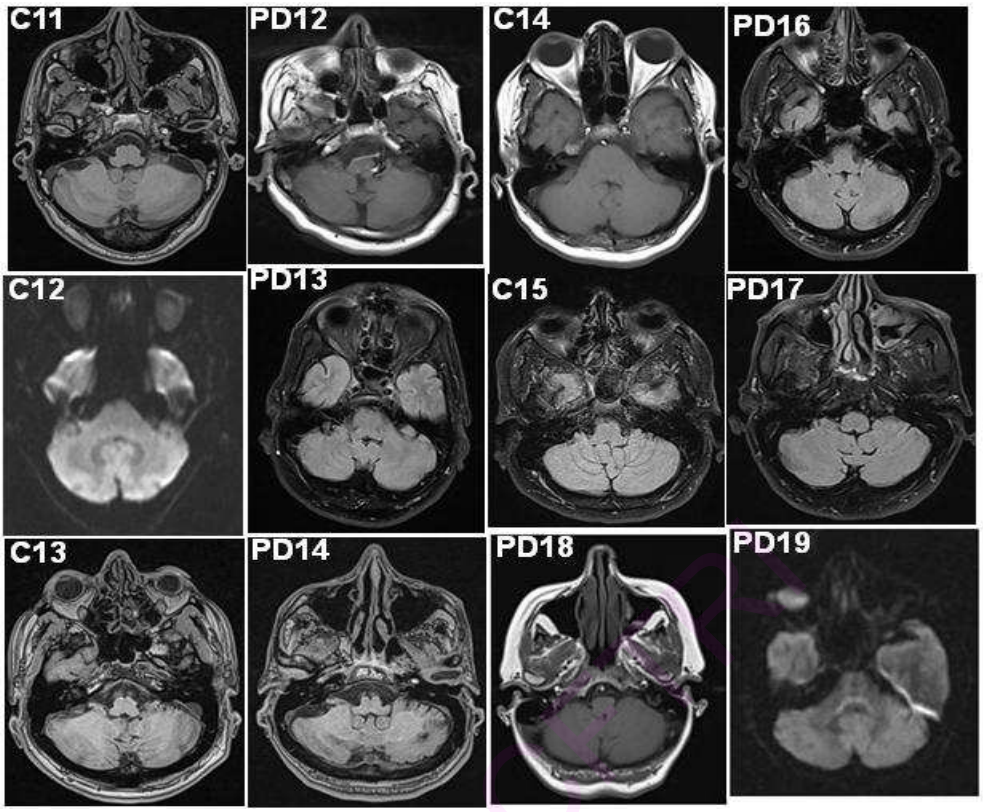

Figure 3A.2: continued

Table 3A.4: The thickness of the cerebellum and caudate nucleus.

Cerebellum (thickness in mm)						Caudate nucleus(thickness in mm)					
Control			Parkinson's disease			Control			Parkinson's disease		
ID	R	L	ID	R	L	ID	R	L	ID	R	L
C1	46.3	41.5	PD1	43.0	36.6	C1	8.3	8.1	PD1	9.1	9.4
C2	41.0	42.0	PD2	43.5	40.07	C2	8.9	10.3	PD2	6.6	6.4
C3	44.5	42.1	PD3	45.2	42.9	C3	8.3	9.0	PD3	6.7	6.3
C4	41.7	41.1	PD4	41.7	41.2	C4	8.6	8.7	PD4	9.8	10.1
C5	44.6	42.8	PD5	43.7	42.9	C5	10.7	9.2	PD5	7.3	6.8
C6	46.1	49.6	PD6	41.9	39.3	C6	9.9	9.0	PD6	8.5	8.4
C7	38.8	42.2	PD7	51.0	50.0	C7	11.1	10.3	PD7	7.5	8.2
C8	45.6	43.6	PD 8	52.0	43.0	C8	10.3	10.3	PD 8	7.0	7.4
C9	43.0	42.0	PD9	45.4	44.5	C9	7.4	8.9	PD9	6.6	6.4
C10	46.4	45.7	PD10	42.5	41.9	C10	8.6	9.1	PD10	7.1	6.3
C11	45.8	44.3	PD12	38.5	46.0	C11	9.3	8.7	PD12	8.3	8.0
C12	43.4	43.1	PD13	48.3	49.6	C12	8.5	9.4	PD13	7.0	8.2
C13	45.6	45.2	PD14	46.0	47.5	C13	8.7	9.2	PD14	8.1	7.5
C14	46.7	45.8	PD16	41.2	36.7	C14	9.4	8.6	PD16	7.5	7.7
C15	48.5	47.3	PD17	44.4	42.0	C15	9.5	10.2	PD17	7.2	6.9
			PD18	43.8	42.3				PD18	8.0	7.3

			PD19	43.4	42.1				PD19	6.9	6.2
Average thickness (mm)						**Average thickness (mm)**					
Control	**44.5± 2.5**	**43.8± 2.4**	**PD**	**44.4± 3.4**	**42.8± 3.8**	**Control**	**9.1± 1.0**	**9.2± 0.6***		**7.6± 0.9**	**7.5± 1.1***

***p<0.05**

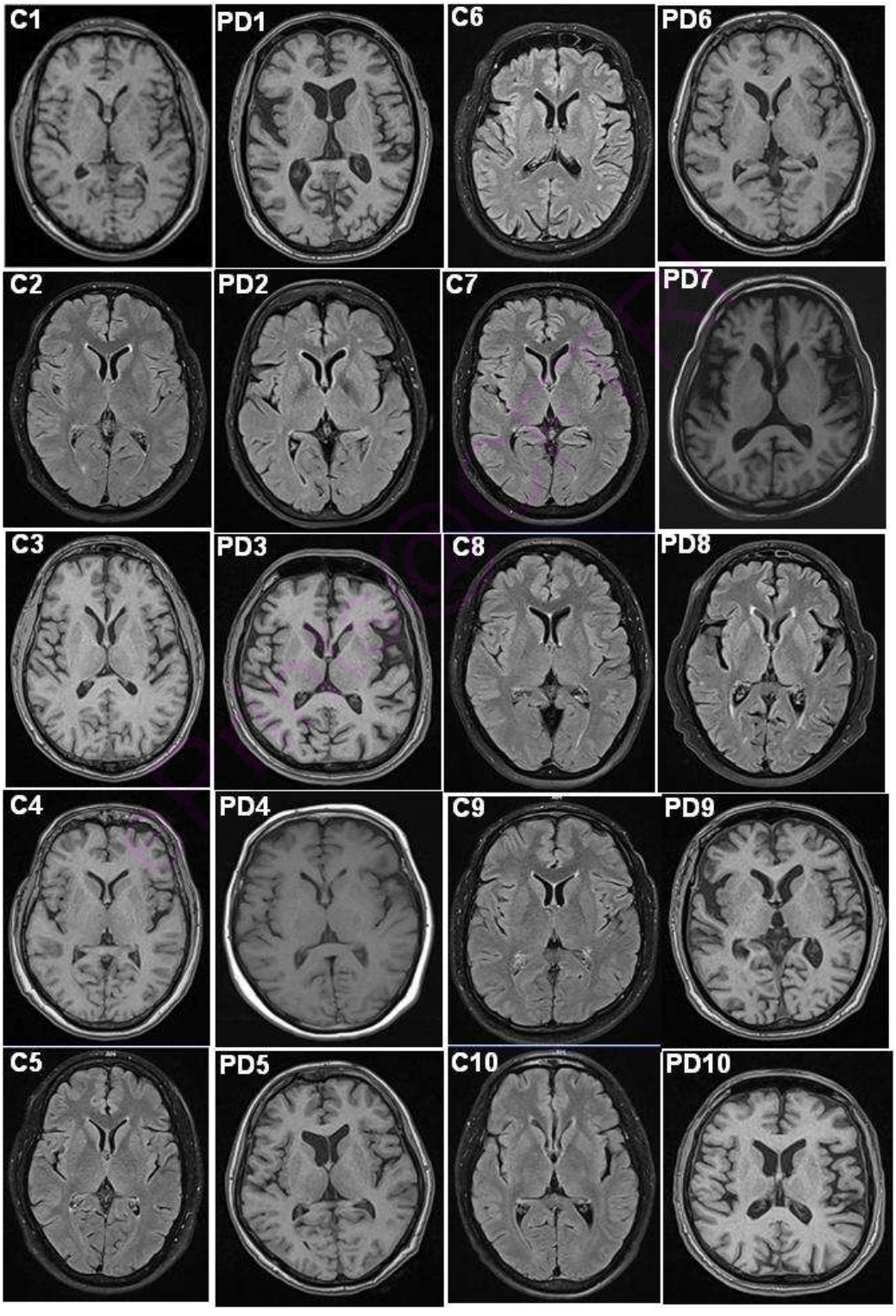

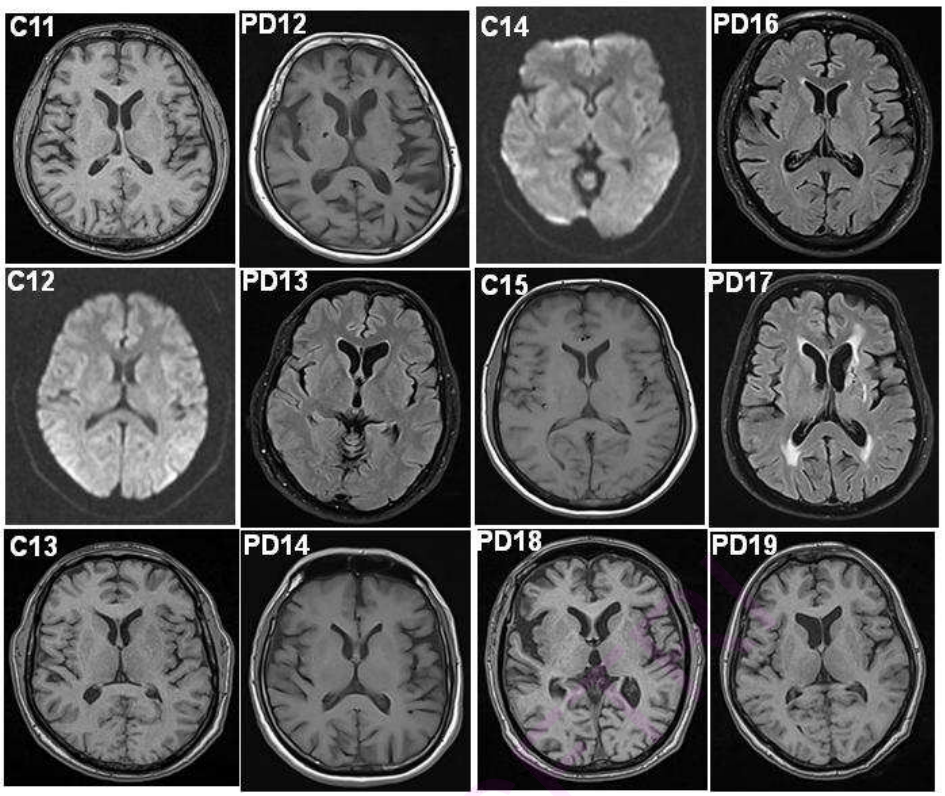

Figure 3A.3: MRI images of control and PD brains showing caudate nucleus, thalamus and frontal lobe.

Table 3A.5: The thickness of the frontal lobe and thalamus.

Frontal lobe						**Thalamus**					
Control			**Parkinson's disease**			**Control**			**Parkinson's disease**		
ID	R	L	ID	R	L	ID	R	L	ID	R	L
C1	39.6	36.7	PD1	34.2	35.7	C1	18.0	16.4	PD1	18.0	16.7
C2	38.0	38.0	PD2	37.0	37.8	C2	21.7	19.6	PD2	14.6	14.1
C3	42.7	40.4	PD3	34.6	35.2	C3	19.4	17.3	PD3	15.3	15.2
C4	39.1	39.3	PD4	39.9	41.4	C4	18.3	17.6	PD4	20.8	18.2
C5	39.1	39.8	PD5	35.6	34.3	C5	16.1	16.9	PD5	14.8	14.3
C6	37.1	34.8	PD6	33.9	35.0	C6	15.0	15.5	PD6	13.8	13.8
C7	38.8	42.2	PD7	32.8	36.5	C7	20.2	19.1	PD7	23.2	19.1
C8	40.2	40.9	PD 8	37.3	37.5	C8	18.2	16.7	PD 8	15.8	15.8
C9	46.4	43.3	PD9	36.2	36.3	C9	16.3	15.8	PD9	13.9	14.1
C10	39.4	39.9	PD10	33.7	33.9	C10	18.5	16.9	PD10	14.2	13.9
C11	41.6	41.5	PD12	32.0	31.0	C11	17.8	17.1	PD12	17.5	14.4
C12	40.5	40.8	PD13	39.4	39.3	C12	19.4	18.8	PD13	17.3	17.0
C13	42.3	41.8	PD14	36.5	36.2	C13	18.5	17.5	PD14	16.7	16.7
C14	39.7	39.9	PD16	35.9	36.5	C14	18.8	17.3	PD16	14.3	14.7
C15	38.5	40.3	PD17	41.2	39.5	C15	19.2	17.9	PD17	16.5	16.3
			PD18	35.3	35.7				PD18	15.3	14.2
			PD19	33.2	33.8				PD19	13.8	13.4

Average value						Average value					
Control	**40.2± 2.3**	**39.9± 2.1**	**PD**	**35.8± 2.5**	**36.2± 2.4**	**Control**	**18.4± 1.6***	**17.4± 1.1***	**PD**	**16.2± 2.5***	**15.4± 1.6***

***p<0.05**

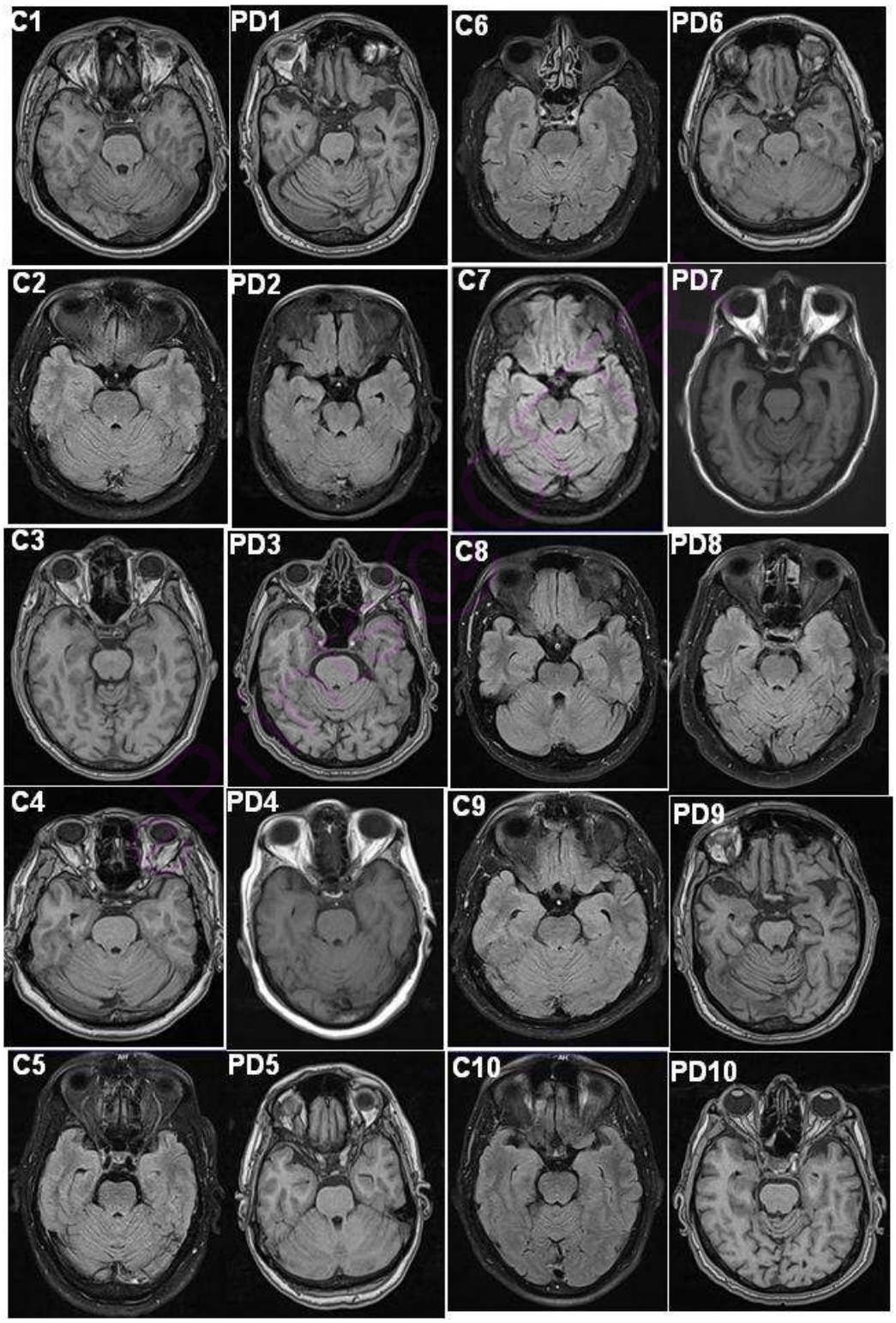

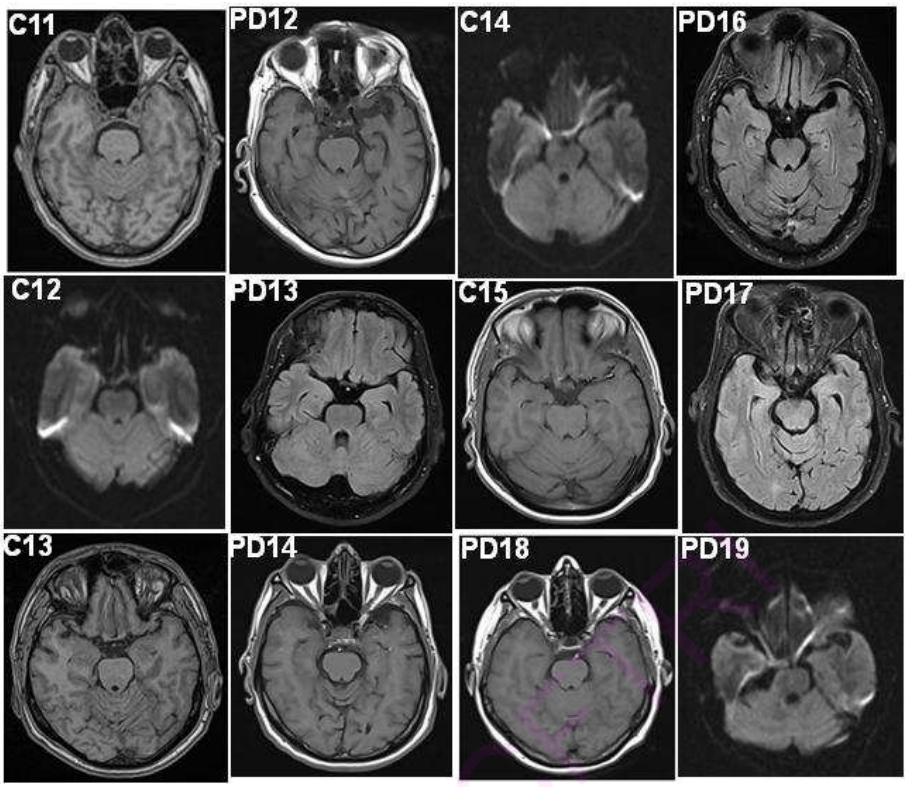

Figure 3A.4: MRI images of control and PD brains showing midbrain and temporal lobe.

Table 3A.6: The thickness of the temporal lobe and midbrain.

Temporal lobe						**Midbrain**			
Control			**Parkinson's Disease**			**Control**		**Parkinson's Disease**	
ID	R	L	ID	R	L	ID	R	ID	R
C1	44.6	44.0	PD1	46.4	46.7	C1	21.4	PD1	26.1
C2	45.4	44.2	PD2	46.5	48.2	C2	20.7	PD2	25.2
C3	48.3	49.6	PD3	44.3	45.2	C3	23.2	PD3	23.4
C4	46.3	47.8	PD4	46.4	43.5	C4	21.2	PD4	26.8
C5	48.2	48.2	PD5	45.6	45.8	C5	21.6	PD5	19.9
C6	45.7	44.7	PD6	47.2	44.9	C6	23.5	PD6	19.6
C7	44.7	44.5	PD7	49.3	47.5	C7	24.6	PD7	22.5
C8	53.9	55.7	PD 8	42.1	38.0	C8	23.4	PD 8	20.7
C9	51.1	48.0	PD9	45.3	45.3	C9	22.0	PD9	21.3
C10	45.8	46.7	PD10	44.8	45.1	C10	23.4	PD10	20.8
C11	47.6	49.3	PD12	43.7	39.5	C11	24.5	PD12	18.1
C12	48.3	48.8	PD13	43.7	43.1	C12	23.8	PD13	20.6
C13	47.9	58.7	PD14	51.1	48.0	C13	21.9	PD14	18.4
C14	49.2	51.4	PD16	47.3	48.0	C14	22.6	PD16	18.9
C15	48.5	49.4	PD17	43.6	41.9	C15	23.6	PD17	19.1

			PD18	46.3	46.4			PD18	18.7
			PD19	44.8	45.3			PD19	19.2
Average thickness (mm)					**Average thickness (mm)**				
Control	**47.7± 2.4**	**48.7± 4.1**	**PD**	**45.7± 2.2**	**44.8± 2.8**	**Control**	**22.7± 1.2**	**PD**	**21.1± 2.7**

***p<0.05**

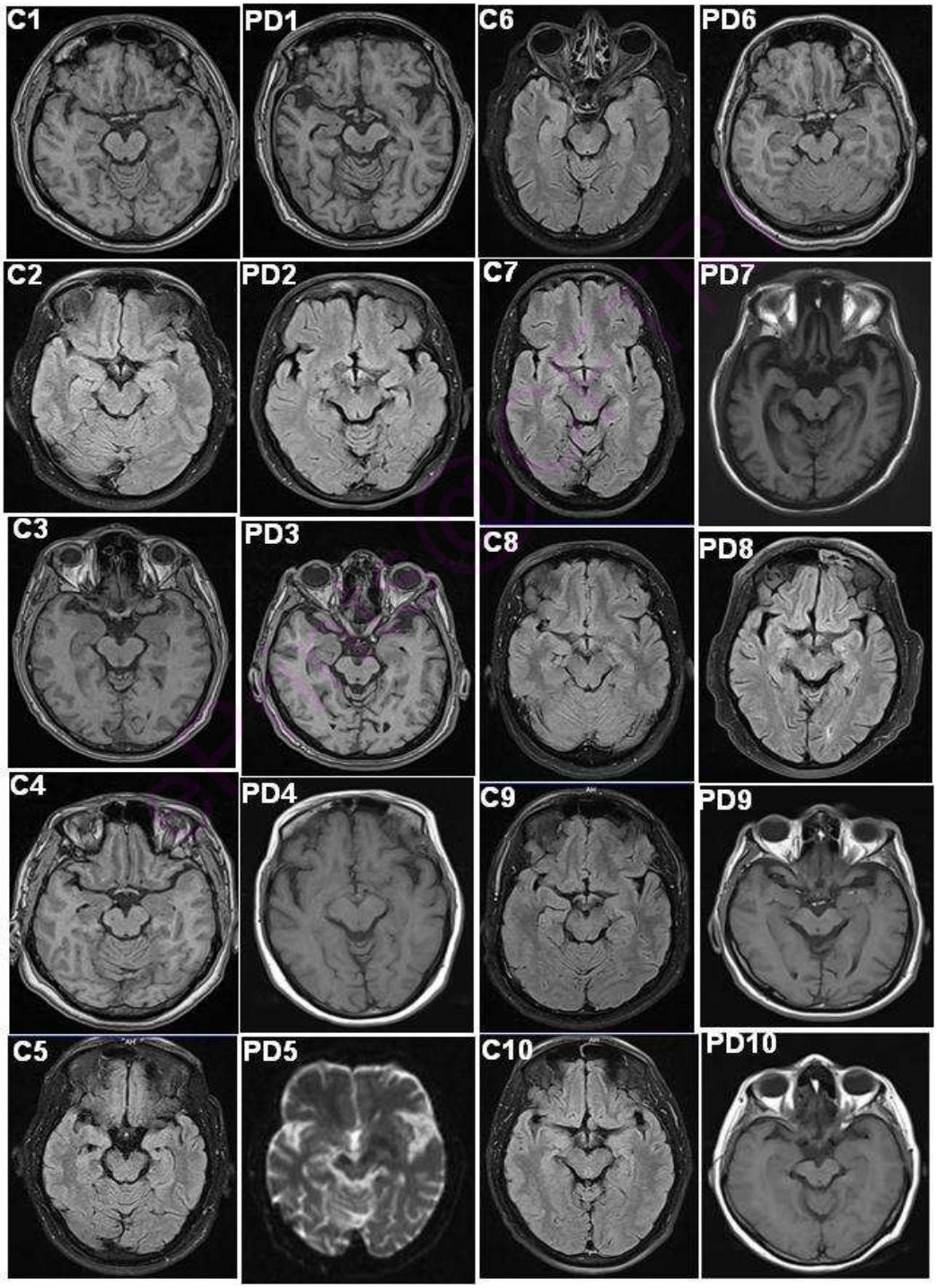

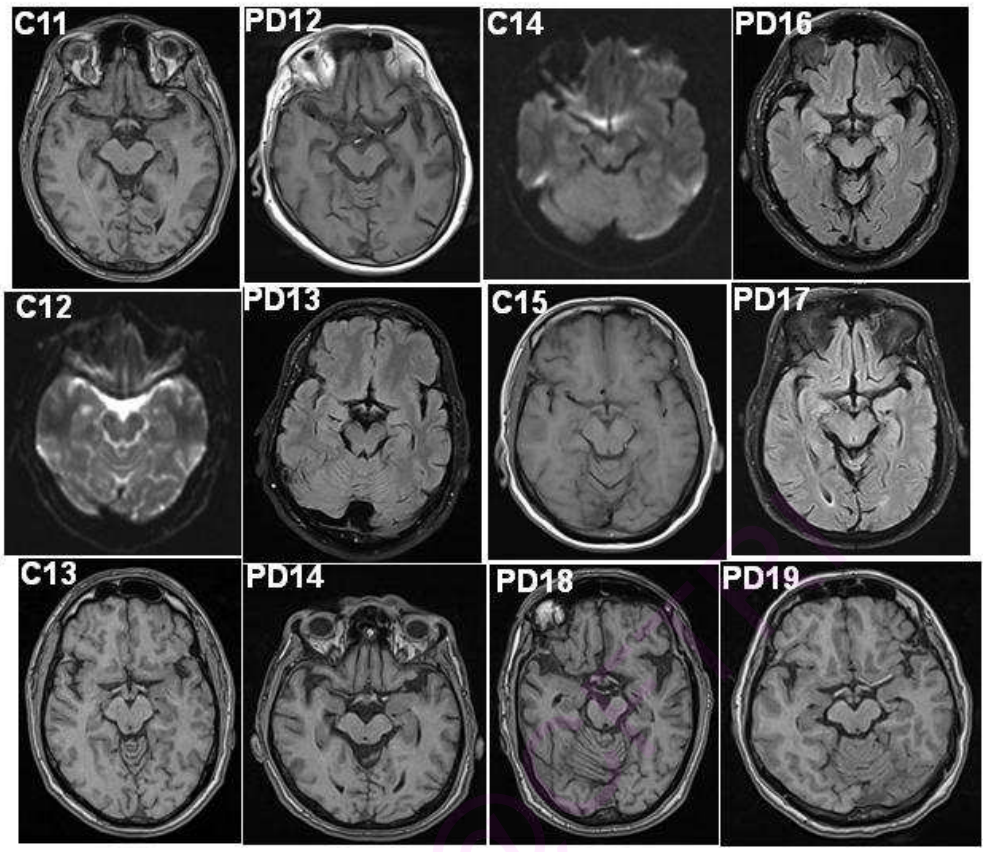

Figure 3A.5: MRI images of control and PD brains showing Hippocampus and substantia nigra.

Table 3A.7: The thickness of the Hippocampus and substantia nigra.

Hippocampus						**Substantia nigra**					
Control			**Parkinson's disease**			**Control**			**Parkinson's diseae**		
ID	R	L	ID	R	L	ID	R	L	ID	R	L
C1	16.7	20.2	PD1	14.6	18.2	C1	11.2	10.1	PD1	6.3	6.4
C2	18.2	19.9	PD2	15.4	16.7	C2	10.0	10.6	PD2	9.4	8.6
C3	19.4	17.9	PD3	14.5	15.2	C3	11.1	10.9	PD3	6.1	6.0
C4	18.2	17.3	PD4	14.6	16.7	C4	10.1	10.4	PD4	7.2	5.2
C5	20.1	18.5	PD5	12.4	13.6	C5	11.4	10.4	PD5	6.3	6.4
C6	19.4	19.4	PD6	13.8	16.6	C6	11.1	10.5	PD6	7.2	6.7
C7	19.4	19.1	PD7	15.9	15.4	C7	12.0	11.7	PD7	8.3	6.4
C8	19.5	19.1	PD 8	17.3	18.1	C8	11.0	11.3	PD 8	8.6	7.5
C9	20.4	19.6	PD9	15.2	15.8	C9	10.7	10.9	PD9	7.2	6.9
C10	18.9	19.5	PD10	16.7	15.8	C10	11.5	10.7	PD10	7.1	6.8
C11	19.2	19.3	PD12	14.7	13.7	C11	11.1	11.2	PD12	7.6	7.1
C12	20.1	20.1	PD13	20.5	17.8	C12	10.9	10.8	PD13	7.0	6.7
C13	19.5	19.6	PD14	19.1	18.0	C13	11.6	10.9	PD14	8.1	7.0
C14	19.6	19.3	PD16	11.9	16.0	C14	10.8	11.4	PD16	7.6	7.7
C15	19.9	19.8	PD17	12.3	12.5	C15	10.5	11.3	PD17	7.4	7.6
			PD18	14.5	14.7				PD18	7.4	7.1

			PD19	13.9	14.2				PD19	6.9	6.7
Average thickness (mm)						**Average thickness (mm)**					
Control	**19.2± 0.9***	**19.2± 0.7***	**PD**	**15.1± 2.2***	**15.8± 1.7***	**Control**	**11 ± 0.5***	**10.8± 0.4***	**PD**	**7.3± 0.8***	**6.8± 0.7***

***p<0.05**

The average thickness of the all the regions were calculated and compared with that of control brain thickness. Significant atrophy in terms of reduction in the thickness of the brain regions in caudate nucleus, thalamus, hippocampus and substantia nigra regions in PD brain compared to control brain regions was observed. The reduction in the thickness of these regions in PD brains were significant at $p<0.05$ compared to control brains**.** It was also observed that reduction in the in the frontal lobe, temporal lobe and midbrain regions, but not significant at $p<0.05$. There were no changes in the thickness of the cerebellum regions of control and PD brains.

3A.5 Discussion

Parkinson's disease affects millions of people around the world and patients suffers with involuntary shaking in the body and lead life with difficulty. The diagnoses of PD in early stages compromised as symptoms appear after severe neuronal loss. The patients visit the clinic after they experience difficulty in moving and handling the utensils etc. At this time, the disease will be in severe condition and neurons controlling the movements will be significantly dead. Until now the diagnosis of PD dependent on the physical evaluation and no established clinical diagnosis was established. In this context it became important to identify a good diagnostic criteria to identify the disease in the early stages of the disease development. Identifying a good biomarker for PD becomes vital and helps better treatment for Parkinson's disease. Here we attempted to identify biomarker and diagnostic criteria for Parkinson's disease by analyzing the serum and MRI analysis of PD patients and comparing to age matched controls.

In the present study, the serum 8-OHdG (oxidative DNA damage biomarker), total antioxidant potential was analyzed to know the oxidative stress status in the PD patients. As oxidative stress exists in several conditions we selected the patients having PD alone and not having any other major illness. Several studies reported oxidative

stress condition in PD brain and other neurodegenerative diseases (Jenner, 2003; Koutsilieri et al., 2003; Abe et al., 2002). Oxidative stress leads to neurotoxicity and neuronal cell death (Sayre et al., 2008). 8-OHdG was reliable biomarker for the oxidative damage (Olinski et al., 2007; Valavanidis et al., 2009). We found that 8-OHdG levels are significantly increased in the serum samples of PD patients compared to age matched controls. Oxidative modification of guanosine to 8-OHdG may lead to double strand breaks and single strand breaks in DNA and lead to DNA damage and cell death. Base excision repair (BER) system counter check the oxidative modified bases and it was reported that BER was compromised during aging. This may be the major factor responsible for the oxidative damage in age related neurological disorders (Rao, 2009). Hedge et al., (2006) reported that SSB and DSB were present in PD brain regions, supporting the oxidative damage to DNA. The oxidative stress was the result of imbalance between the reactive oxygen species (ROS) and antioxidant defence system. We analyzed the total antioxidant capacity of the serum samples using the ELISA kit which detect hydrophilic antioxidants like vitamin C, glutathione etc and hydrophobic antioxidants like vitamins E etc., giving total antioxidant capacity of the serum. Total antioxidant capacity of the serum in PD samples increased compared to age matched control samples. The data indirectly showed that oxidative stress had increased in PD patients and in response to this oxidative stress antioxidant levels were increased.

Ceruloplasmin is an acute phase reactant protein which acts as an extracellular antioxidant by ferroxidase activity. Ceruloplasmin was the major copper carrying glycoprotein in the blood carrying 6 copper atoms per molecule (Healy and Tipton, 2007). Ceruloplasmin regulates the copper and iron homeostasis in the body and defect in biosynthesis and reduction in ceruloplasmin levels results in the accumulation of iron in different organs (Mzhel'skaya, 2000; Patel et al., 2002). We analyzed the serum ceruloplasmin levels in PD and control samples and found that ceruloplasmin levels were decreased in PD patients compared to age matched control samples. Our results are in consistent with that of Torsdottir et al., (2006) where they reported low ceruloplasmin levels in PD serum samples. The reduced ceruloplasmin levels may lead to the iron deposition in the brain of PD patients. Serum ferritin levels also decreased in PD samples compared to age matched control samples. Ferritin was the major iron

storage protein responsible iron homeostasis and acts as serum biomarker for the total body iron stores (Knovich et al., 2009). The reduction of both ceruloplasmin and ferritin levels may result in the accumulation of the iron in brain.

Recently, several studies focused on the MRI changes in Parkinson's disease to establish imaging biomarker for PD (Aybek et al., 2009; Baudrexel et al., 2010; Dalaker et al., 2009; Menke et al., 2009). In the present study we performed MRI imaging of brains of PD patients and age matched control brains to know the brain atrophy. Brain atrophy was calculated by measuring the thickness of the different brain regions, which include substantia nigra, hippocampus, cerebellum, caudate nucleus, midbrain, thalamus, frontal lobe and temporal lobe. Parkinson's disease was characterized by the neuronal loss in substantia nigra region of the brain (Gallagher and Schapira, 2009). A significant atrophy in the substantia nigra region of PD patients compared to control age matched control was observed. The atrophy in substantia nigra was due to the neuronal loss in that region in PD brain. A significant atrophy in the hippocampus, thalamus, and caudate nucleus regions of the PD brains was also observed. An earlier study showed significant DNA damage in terms of double strand breaks and single strand breaks in the hippocampus, thalamus and caudate nucleus regions of post mortem PD brains (Hegde et al., 2006). The present study supported DNA damage and neuronal loss by increased 8-OHdG levels and brain atrophy in these brain regions. Jokinen et al., (2009) also reported hippocampal brain atrophy and impaired memory in PD petients. It was observed atrophy in the frontal lobe, temporal lobe and midbrain regions but significant when compared to the atrophy observed in above brain regions. The atrophy changes indicated that substantia nigra, thalamus, hippocampus and caudate nucleus are the most vulnerable regions in PD brain.

In conclusion, the study provides clinical evaluation of probable biomarkers for the early diagnosis of the PD. We observed increased oxidative DNA damage biomarker 8-OHdG, increased serum total antioxidant capacity, decreased ceruloplasmin and ferritin levels, significant atrophy in the substantia nigra, thalamus, hippocampus and caudate nucleus regions. It can be proposed that above tests and analysis may provide a good diagnostic tool for the early diagnosis of the Parkinson's disease and the better management of the disease.

Chapter 3B

New evidence on increase of Iron and Copper and its correlation to DNA integrity in ageing human brain

3B.1. Introduction

Ageing is a multi-factorial process, which leads to irreversible damage to macromolecules (ie DNA, proteins and lipids), cells and organs. The rate of this process is attributable to individual genetic as well as to environmental factors. Several studies have addressed the relationships between DNA damage and ageing, and have suggested and age-dependent accumulation of DNA damage by demonstrating an age-response of cytogenetic and molecular genetic endpoints in human cells (Fenech and Morley 1985; Lindsey et al., 1991; Ganguly 1993; Wilson et al., 2008). The accumulation of DNA damage is due to an imbalance between two opposing mechanisms, the generation of DNA damage by endogenous metabolic or environmental processed and the eradication of this damage by the cell's repair machinery. Mutation rate appears to increase with age, indicating a decline in DNA repair efficiency with age (Bohr and Anson 1995, Walter et al., 1997) raise the question, if senescence per se leads to a higher susceptibility to DNA damage upon internal metal ion exposures. The major risk factors attributed for age related disorders are increase in oxidative stress and failure in antioxidant mechanisms (Ozcan et al., 2004; Kuloglu et al., 2002; Ranjekar et al., 2003; Frey et al., 2006; Frey et al., 2007; Benes et al., 2006). The oxidative stress by accumulation of paramagnetic trace metal ions like Cu and Fe leads to DNA instability and gene expression failure in normal ageing. Does the failure in DNA repair mechanism or accumulation of trace metal ions leads to ageing and age related disorders?. Further, DNA fragmentation and dysregulation in apoptotic mechanism (Margolis et al., 1994; Catts and Catts 2000; Evan and Littlewood 1998; Ansari et al., 1993; Benes et al., 2003; Buttner et al., 2007; Andreazza et al., 2007) have been well shown to be associated with age related neurodegenerative disorder like Alzheimer's disease (AD) and Parkinson's disease (PD) (Adamec, 1999; Alam et al., 1997; Tatton and Olanov 1999; Hegde et al., 2006). In the present study we corroborate these

findings by demonstrating an age-dependent increase in DNA strand breaks and accumulation of metal ions on the process of ageing.

The aim of this study was to assess the genomic integrity in terms of DNA fragmentation and its relation to the levels of redox active metals in frontal cortex and hippocampus brain regions of different age groups and to ascertain whether altered genome integrity play a role ageing and age-related disorders. To the best of our knowledge, this study is first of its kind in human brain subjects.

3B.2. Materials

Radiolabeled^{3} [H]-TTP (Sp.Act.40 Ci/nmol) was purchased from Amersham Radiochemicals, UK. Ribonuclease A (RNAse A), Proteinase K, Deoxyribonuclease I (DNAse I), dATP, dTTP, dCTP, dGTP, DNA polymerase I (from Escherichia coli), terminal deoxynucleotidyl transferase enzymes, 1kb and 100bp DNA ladders, and lamda DNA ladder were purchased from Genei, India. All other chemicals were of analytical grade and were purchased from Sisco Research Labs, Mumbai, India.

3B.3 Methodology

3B.3.1. Brain tissues

The demographic data of aged human subjects from where brains are collected is presented in Table 3B.1.

Number	Age (yr)	PMI (hr)	Tissue (pH)	Sex	Cause of Death
Group I <40 yrs					
N-1	25	4	6.76	F	Road traffic accident
N-2	38	5	6.61	F	Snake bite
N-3	21	4	6.71	F	Accidental burns
N-4	18	4	6.45	M	Road traffic accident
N-5	22	5	6.68	M	Road traffic accident
N-6	24	6	6.72	M	Road traffic accident
N-7	30	3	6.54	F	Accidental burns
N-8	37	8	6.45	M	Fall from height
Group II 41-60 yrs					
N-1	45	6	6.67	M	Road traffic accident
N-2	48	5	6.23	F	Road traffic accident

N-3	43	7	6.70	M	Road traffic accident
N-4	55	6	6.51	M	Road traffic accident
N-5	50	6	6.31	F	Road traffic accident
N-6	53	6	6.53	F	Road traffic accident
N-7	51	6	6.32	M	Road traffic accident
N-8	58	6	6.27	M	Road traffic accident
Group III >61 yrs					
N1	65	7	6.77	M	Natural death: collected under body donation to JSS
N2	71	6	6.39	M	Natural death: collected under body donation to JSS
N3	68	7	6.76	M	Natural death: collected under body donation to JSS
N4	77	6	6.57	F	Natural death: collected under body donation to JSS
N5	80	6	6.88	F	Natural death: collected under body donation to JSS
N6	63	6	6.35	F	Road traffic accident
N7	73	7	6.45	M	Road traffic accident
N8	77	6	6.55	M	Road traffic accident

Table 3B.1 Demographic data of Aged human subjects

Brains are grouped into three groups. Group I: below 40 years, Group II: between 41-60 years and Group III: above 60 years. The two regions namely hippocampus and frontal cortex of normal brains were separated and stored at -80^{o}C until further use. Eight brain samples from each group were included in the study. Human brain samples were collected from the Depression Brain Bank of JSS medical hospital and College, Mysore, India. Autopsies were performed on donors with written informed consent obtained direct next of kin. The control human brains were collected from accident victims, who had no history of long-term illness, psychiatric diseases, dementia, or neurological disease prior to death. We have excluded the subjects who had drug and alcohol abuse. The average postmortem interval between the time of death and collection of brain and freezing was ≤ 6h. Within one hour after death the body was kept in cool chamber maintained at 4˚C. The brain tissue was isolated and stored frozen at -80˚C till the analysis.

3B.3.2. Isolation of DNA from brain tissue

Genomic DNA was isolated from hippocampus and frontal cortex of frozen brain tissue by standard 'phenol-chloroform extraction' method after Sambrook et al (1989) with some modifications to prevent DNA fragmentation during isolation. Precautions were

taken to prevent in vitro DNA damage during phenol-chloroform genomic DNA extraction**.** The concentration of DNA was measured using UV/Visible spectrophotometer noting absorbance at 260 nm and purity checked by recording the ratio of absorbance at 260 nm/280 nm which should be ideally between 1.6 and 1.8.

3B.3.3. Nick translation assay

Single strand breaks: Single strand breaks (SSBs) are calculated through incorporation of ^{3}[H]-TMP into DNA samples when incubated with E. coli DNA polymerase I (Klenow Fragment) in a nick translation assay (Sutherland, 1983). DNA polymerase I adds nucleotides at the 3'-OH end of a SSB, generated by various means, using the other strand as template. When one of the deoxynucleotide triphosphates is labeled, then the incorporation of radioactivity into substrate DNA would be proportional to the number of SSBs present in the DNA sample. During the standardization of the essay conditions with the plasmid DNA(Cos T fragment of ג phage) having known number of SSBs, it was found that average of 1500 nucleotides are added at each of the 3'-OH group. From this, it is inferred that each picomole of TMP incorporated is equivalent to $1.6x10^{9}$ 3'-OH groups or SSBs. In a total reaction volume of 50 µl, the assay mixture consisted of: 40 mM Tris-HC1, pH 8.0, 1 mM β-mercaptoethanol, 7.5 mM $MgCl_2$, 4 mM ATP, 100µM each of dATP, dCTP, and dGTP and 25 µM of dTTP, 1 µCi of ^{3} [H]-TTP and 1µg of genomic DNA and 1 U of E. coli DNA polymerase I.

Double strand breaks: Terminal deoxynucleotidyl transferase catalyzes the addition of deoxynucleotides to the 3' termini of DNA and does not need direction from template strand. Here, 3'-ends of duplex DNA also serve as substrates. Similar conditions to incubate DNA with terminal transferase as in the case of E. coli polymerase I assay were used. The incorporation of the ^{3}[H]-dTTP into DNA would be proportional to the number of double strand breaks (DSBs) in the DNA. From the conditions and incubation (Sutherland, 1983; Bhaskar and Rao, 1994; Deng and Wu 1983) it is assumed that about 50 TMP residues are added at each of the 3'-ends of the duplex DNA. From this, it is calculated that each femtomole of TMP incorporation would be equivalent to 1.2×10^{7} 3' -ends or half of that number minus one DSBs. The assay mixture for terminal transferase

reaction consisted of a total volume of 50 µ1:100 mM sodium cacodylate buffer, pH 7.0, 1 mM $CoCl_2$, 0.2 mM DTT, 1 µ Ci of ^{3}[H]-dTTP, 1 µg DNA, and 1 U of the enzyme.

3B.3.4. Trace elemental analysis

Brain tissues were acid digested and preserved in dust free laminar air flow hood until further used. All the precautions were taken in accordance with NCCLS criteria (NCCLS standard approved guidelines to eliminate metal contamination while collecting and storing the samples). Trace elemental analysis were carried out using Inductively Coupled Plasma Atomic Emission Spectrometry (ICP-AES) model JOBIN YVON 38 sequential analyzer. The elements measured were Cu, Fe, and Zn. All dilutions were made with ultra pure milliQ water (18-mega ohms resistance) in a dust free environment. The optimization of ICPAES was carried out by line selection and detection limits for each element. The validation of the analysis were tested by analyzing matrix match multi element synthetic standard and certified standard reference material (Bovine liver 1577a) obtained from National Bureau of Standards, USA. The lines were selected for each element in such a way that interference from the other elements was minimal (Table 3B.2)

3B.3.5. Statistical analysis

All the data obtained in this study were statistically treated and the significance of differences among samples was calculated according to Student's *t* test. The statistical analysis was carried out using Microsoft Excel 2000 Soft-ware.

3B.4 Results

3B.4.1. Brain tissues

Brains were grouped into three groups. Group I: below 40 years, Group II: between 41-60 years and Group III: above 60 years. The control human brains were collected from accident victims, who had no history of long-term illness, psychiatric diseases, dementia, or neurological disease prior to death. We have excluded the subjects who had drug and alcohol abuse. The demographic details of the human brains collected from different age groups are depicted in Table 1.

3B.4.2. Concentration of DNA

The concentration of DNA was measured using UV/Visible spectrophotometer noting absorbance at 260 nm and purity checked by recording the ratio of absorbance at 260 nm/280 nm which were ideally between 1.6 and 1.8. The wavelength employed and the detection limit of the trace elements are summarized in Table 3B.2

Element	Wavelength nm)	Detection limit*	
		µg/ml	µmole/ml
Cu	224.7	0.002	0.00003
Zn	213.856	0.002	0.00003
Fe	259.94	0.005	0.00009

Table 3B.2 Wavelength for trace metal analysis and detection limit

3B.4.3. Trace elemental analysis

The levels of Fe and Cu were increased, while Zn levels were decreased from Group I to III. There is a significant increase in Cu and Fe in Group II and Group III in both frontal cortex and hippocampus region.

In frontal cortex, Cu and Fe are increased in all three Groups. The amount of Cu and Fe are significantly increased in Group II (p value > 0.05) and Group III (p value >0.001) (Fig 3B, A, B and C). A similar trend is observed in the hippocampus region, Cu and Fe are significantly elevated in Group II (p value > 0.05) and Group III (p value > 0.001) (Fig 3B, A, B and C). The significant increase in Cu and Fe and decrease in Zn is observed highly between Group II and III. This data indicates the accumulation of redox active metals are increased and the antioxidant metal are decreased on the process of ageing. The interesting observation accumulation of trace metals are more in frontal cortex compared to hippocampus.

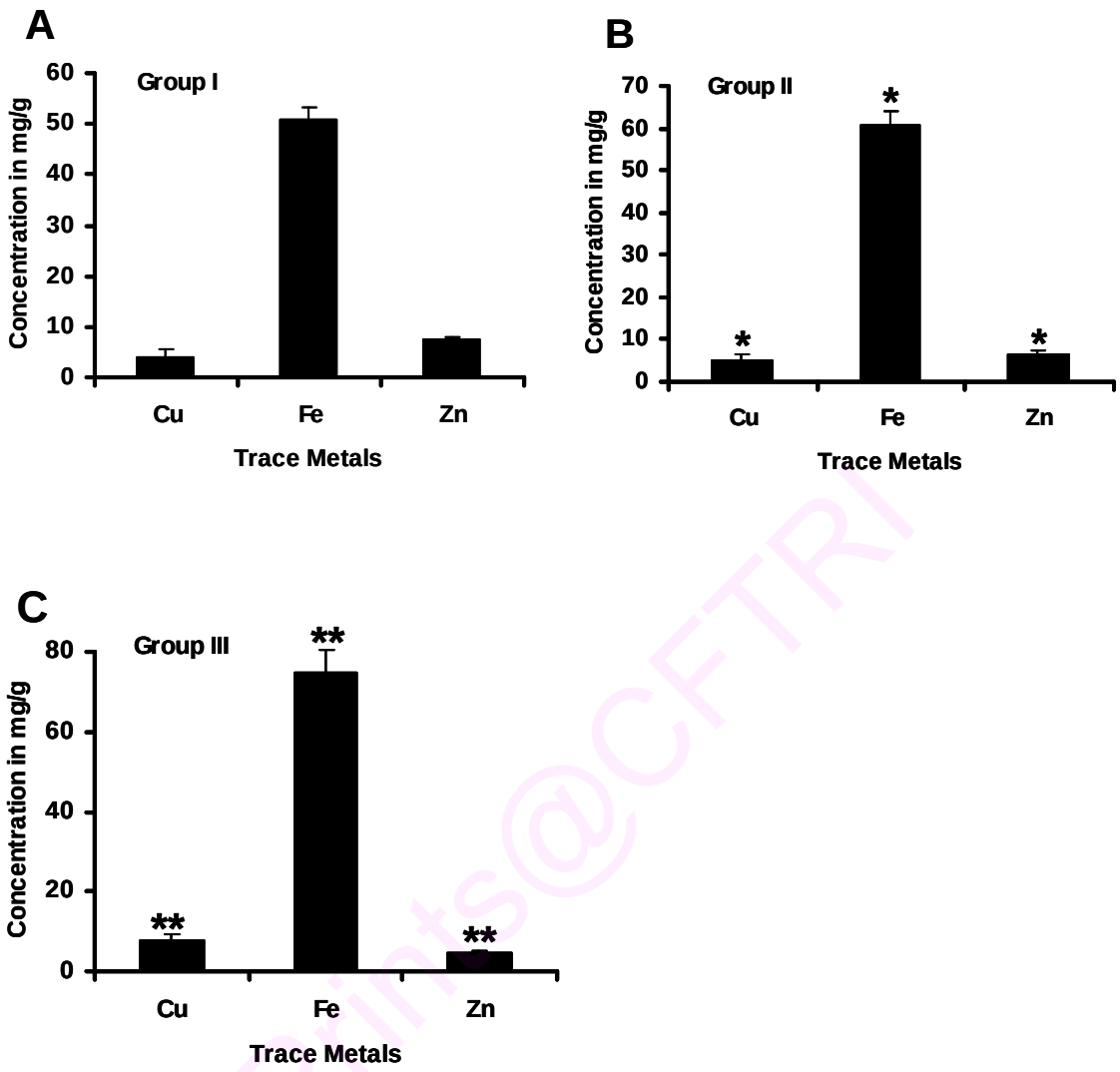

Figure 3B.1. Trace metals concentrations in frontal cortex regions of aged human brain subjects (concentration in mg/g of wet weight of tissue). Mean ± SD of 8 brains (n=8) in each group. **A,** Levels of Cu, Fe and Zn in Group I. **B,** Levels of Cu, Fe and Zn in Group II, *p> 0.05. **C,** Levels of Cu, Fe and Zn in Group III** p> 0.001.

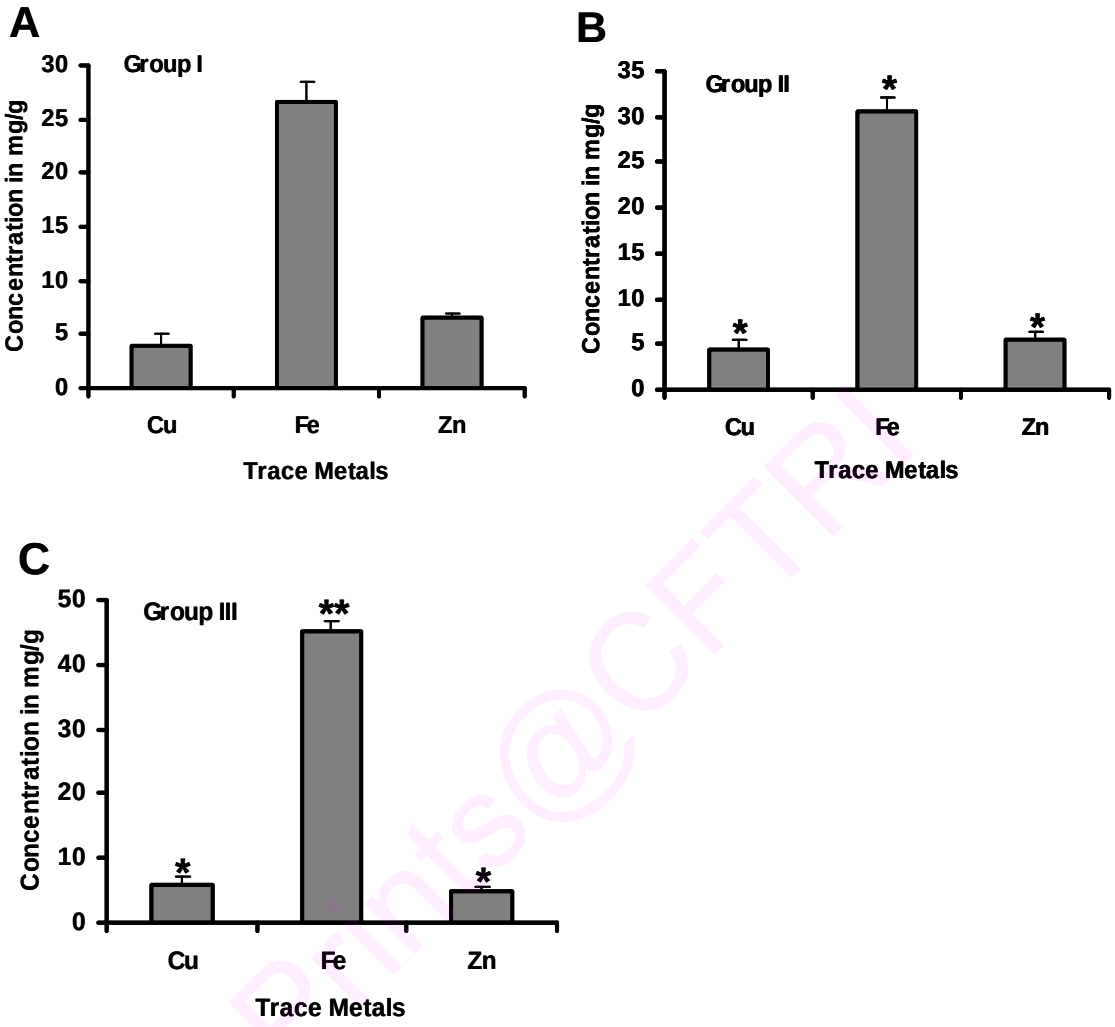

Figure 3B.2. Trace metals concentrations in hippocampus regions of aged human brain subjects (concentration in mg/g of wet weight of tissue). Mean ± SD of 8 brains (n=8) in each group. **A,** Levels of Cu, Fe and Zn in Group I. **B,** Levels of Cu, Fe and Zn in Group II, *p> 0.05. **C,** Levels of Cu, Fe and Zn in Group III** p> 0.001.

3B.4.4. Single Strand Breaks

The most prevalent type of DNA damage in mammalian cell is the SSBs. Single-stranded breakage is the end point of several types of structural insults inflicted on the genome by both endogenous and exogenous agents (Rao., 1993). Figure 3 showed numbers of SSBs per microgram of genomic DNA isolated from brain regions (Fig 3A, 3B and 3C). Accumulations of SSBs are more frequent in group III compared to Group II and I. The result showed that frontal cortex ($p>0.05$ and $p>0.001$) accumulated considerably higher number of SSBs compared to hippocampus. This could be due to the increased levels of Cu and Fe in frontal cortex and relatively lower amounts in hippocampus in Group III.

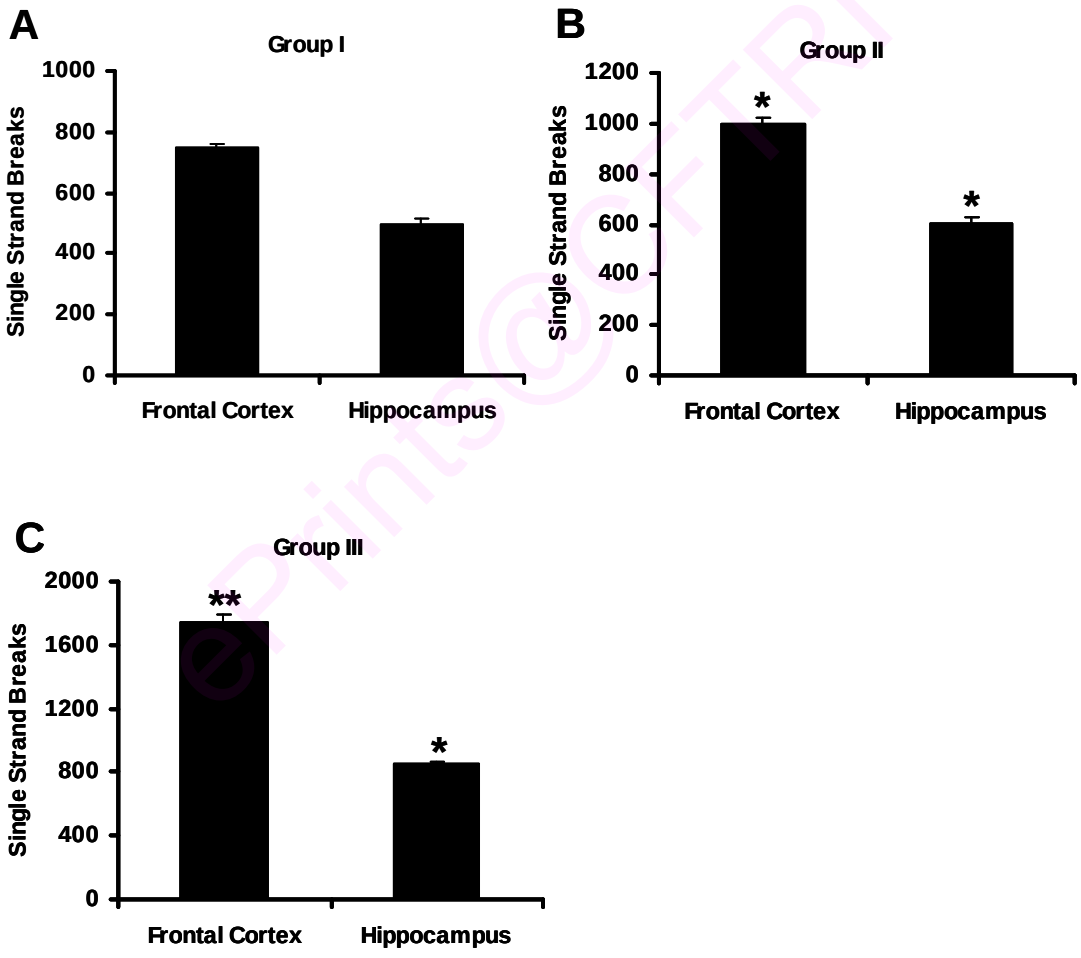

Figure 3B.3. Single strand breaks (SSBs (10^6)/µg DNA) frontal cortex and hippocampus regions of aged human brain subjects. **A,** SSBs of Group I. **B,** SSBs of Group II, *p> 0.05. **C,** SSBs of Group III** p> 0.001.

3B.4.5. Double Strand breaks

The DNA isolated from frontal cortex and hippocampus showed significantly higher number of DSBs ($p>0.05$ and $p>0.001$) in Fig 4A, 4B and 4C. Further, frontal cortex accumulated more DSBs than SSBs. The increase in DSBs was more in Group III compared to Group I and II. The present result showed that frontal cortex has more DSBs than SSBs whereas hippocampus had the presence of both DSBs and SSBs accumulated. A similar trend is observed in the accumulation of both SSBs and DSBs. The accumulation of SSBs and DSBs are directly proportional to the amount of redox active metals in frontal cortex and hippocampus region.

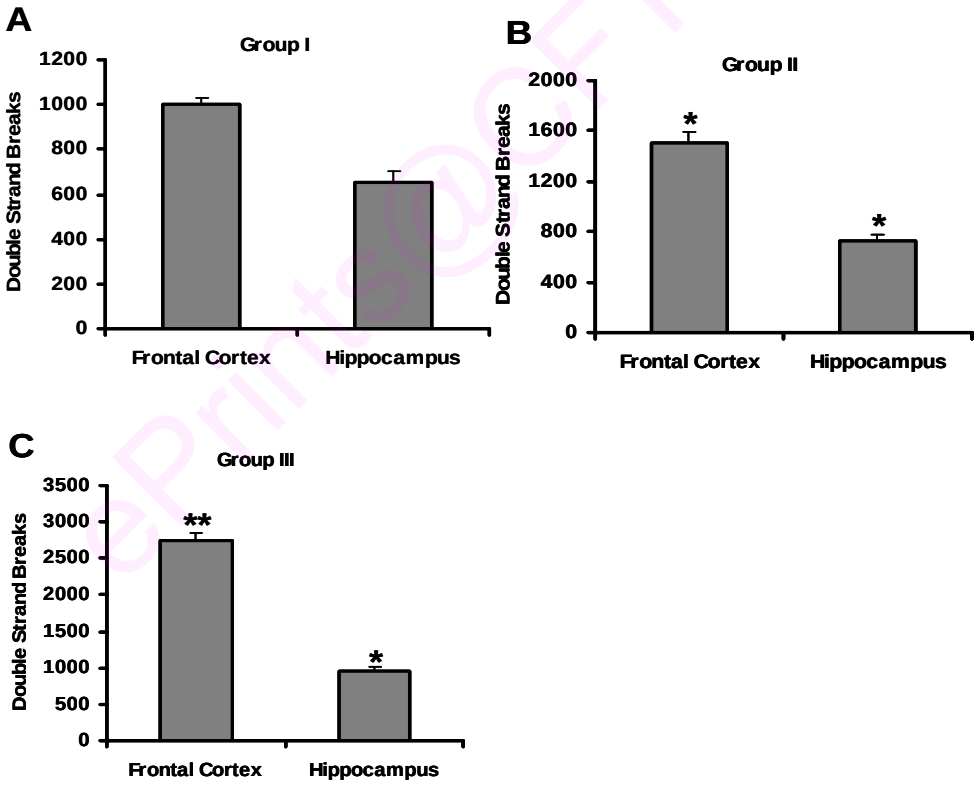

Figure 3B.4. Double strand breaks (DSBs x 10^6/μgDNA) frontal cortex and hippocampus regions of aged human brain subjects. **A,** DSBs of Group I. **B,** DSBs of Group II, *p> 0.05. **C,** DSBs of Group III** p> 0.001.

3B.5. Discussion

The present study was done to assess the genomic integrity in ageing human brain and a correlation between accumulations of redox active metal versus DNA strand breaks. The DNA integrity failure may lead to cell atrophy. Defective responses to DNA SSBs or DSBs can result in age related diseases, underscoring the critical importance of DNA repair for neural homeostasis (Simon et al., 2009; Adamec et al., 1999; Caldecott 2008). Human DNA repair-deficient syndromes are generally congenital, in which brain pathology reflects the consequences of developmentally incurred DNA damage (Caldecott, 2008). Although, it is unclear to what degree DNA strand-break repair defects in mature neural cells contributes to disease pathology. However, DNA single-strand breaks are a relatively common lesion which if not repaired can impact cells via interference with transcription (Sordet et al., 2010; Stilmann et al., 2009). Thus, this lesion, and probably to a lesser extent DNA double-strand breaks, may be particularly relevant to aging in the neural cell population. The consequences of defective DNA strand-break repair towards might lead to a connection between DNA strand breaks and aging in the brain.

The classical apoptotic DNA laddering pattern in ageing brain due to strand breaks has great pathophysiological significance. According to Didier et al. (1996) the DNA laddering on gel electrophoresis is a hallmark feature of end-stage apoptotic cell death and by this apoptosis can be distinguished from necrosis. Earlier studies showed that cell death can also be preceded by DNA fragmentation by Ca^{2+}, Mg^{2+} dependent DNAase into 180 and 200bp fragments with endonuclease activation occurring early in the process of cell death (Clarke, 1999; Wylie et al., 1980; Kerr et al., 1995; Kingsbury et al., 1998). The influence of perimortem conditions, anti-mortem hypoxia on DNA fragmentation in postmortem tissue are described in our previous study (Mushtak et al., 2008). However, we evaluated our results on DNA stability/damage and established that postmortem delay (<7) related DNA damage does not account for the changes in ageing brains. It was earlier shown that DNA fragmentation reduces the high activation energy barrier required to induce the conformational and topological changes in DNA (Hegde et al., 2006). In addition, the recent study showed that there is empiric link between late-life depression and

AD suggesting the defective responses to SSBs or DSBs can result in neurological diseases,

Our study is the first report to show that there is selective increase of single strand and double strand breaks in DNA of normal ageing human brain. The DNA fragmentation can potentially be triggered through many endogenous and exogenous factors such as trace metals, oxidative stress, mitochondrial dysfunction, apoptosis, decrease antioxidant enzymes, genetic factors etc., (Kuloglu et al., 2002; Frey et al., 2006; Frey et al., 2007; Benes et al., 2006). The first and most obvious possibilities are that neurons may be exposed to oxidative stress. The genes that play a central role in the clearance of free radicals generated by mitochondrial oxidation reactions such as glutathione synthase, catalase and SOD (Calabrese et al., 2010; Olinski et al., 2007; Cristiano et al., 1995). This suggests that the accumulation of ROS associated with the oxidative stress would tend to cause potential damage to DNA, proteins and lipids. However, the intact DNA from hippocampus may represent either an adaptive compensation to oxidative stress. To support, other finding suggested that GABAergic cells in hippocampus may be resistant to kainic acid - induced excitotoxicity (Devenport et al., 1990). Our earlier study have shown that metals like Fe, Al and Cu are accumulated more and these metals can bind and nicks DNA. Many of these insults potentially lead to single strand and double strand breaks in DNA leading to genomic instability (Hegde et al., 2006).

The longevity-enhancing mutations genomic rearrangements, which could be caused by misrepair of DSBs. These rearrangements are thought to contribute to transcriptional “noise,” which in turn could explain some age-related decline in tissue function. Paul Hasty (2008, 2004) has written two recent reviews, critically evaluating the role of DNA DSBs in the aging process. In the first (written with colleagues Han Li and James Mitchell), the authors argue from genetic evidence that DSB repair pathways are intimately connected with aging (Li et al., 2008; Hasty et al., 2003; Hasty 2005; Hasty and Vijg J 2004). There are many forms of DNA damage with double-strand breaks (DSBs) being the most toxic. DNA SSBs and DSBs are the potential causative factor for aging including factors that generate DNA strand breaks, faulty or failed repair, accumulation of

redox active metals may lead to age-dependent decline in fitness. Based on these comparisons we believe the basic mechanisms responsible for their aging phenotypes are fundamentally dependent on all the above factors, primarily the accumulation of trace metals leading to SSBs and DSBs.

Another plausible reason for accumulated DNA fragmentation in ageing brain could be due to decreased antioxidant enzymes such as glutathione synthase, catalase and SOD or decreased DNA repair capacity process (Calabrese et al., 2010; Olinski et al., 2007; Cristiano et al., 1995). Due to increased oxidative stress and genotoxic stress, the genomic DNA's structural integrity is under constant threat. Hence, any insufficiency in the machinery to counteract the damage lead to accumulation of DNA breaks (Caldecott 2008). A decline in DNA stability signifies the shift between DNA damage and repair. In conclusion, the present study has provided the first examination into the genome integrity in terms of DNA damage and its relation to redox metals levels in brain regions of ageing groups. Further this early and first study may provide initial insight to elucidate the correlation between the DNA damage and trace metals and its role in early or age related disorders.

Chapter 4A

New evidences on Tau–DNA interactions and relevance to neurodegeneration

4A.1 Introduction

Tau, a microtubule associated protein is mainly found in the neuronal cells (Weingarten et al., 1975). It is encoded by Tau gene on chromosome 17 and its alternate splicing results in six isoforms of Tau (Goedert et al., 1989). Tau is mainly involved in microtubule polymerization and their stabilization in the neurons (Drechsel et al., 1922; Wang and Liu, 2008). Deficiency of this protein in animal models display behavioral abnormalities, muscle weakness and reduced number of microtubules in the axon (Ikegami et al., 2000; Harada et al., 1994). Aggregation of Tau protein is observed in some neurological disease conditions which are collectively known as Tauopathies (Iqbal et al., 2009; Williams, 2006). Alzheimer's disease (AD) is a principal tauopathy where Tau is aggregated in the form of neurofibrillary tangles (NFTs) (Avila et al., 2004). The precise role of Tau in AD neurodeneration is not clearly understood (Delacourte, 2008; Brandt et al., 2005). In AD conditions, Tau looses its ability to organize microtubule assembly leading to axonal transport impairment (LaFerla and Oddo, 2005; Mandelkow et al., 2003). Further, Tau isolated from AD brain induced slower tubulin assembly than normal Tau (Lu and Wood, 1993; Alonso et al., 1996). It is not clear whether soluble or aggregated form of Tau is toxic? It has been shown that Tau transfection to PC12 cells results in toxicity associated with apoptosis, without Tau aggregation (Fath et al., 2002). Also study has shown that disaggregated Tau when exposed to neuronal cells showed increased cell death than the aggregated Tau (Gómez-Ramos et al., 2006). Further, Gomenz-Isla *et al*. (1997) showed that in AD brain neuronal loss exceeded several folds than the NFT bearing neurons (Gomenz-Isla et al., 1997). Also studies shown that neurodegeneration is not associated with NFT formation in drosophila models (Wittmann et al., 2001; Jackson et al., 2002). These observations suggest that Tau may induce toxicity in neurons other than classical aggregation pathway? Tau is mainly distributed in the cytoplasm and also localized in the nucleus of neuronal and non-neuronal cells. It has been reported that Tau is localized in the nuclei of neuroblastoma cell, PC12 cells and human macrophages (Loomis et al., 1990; Davis and Johnson, 1999; Haque et al., 1999). Tau is found to be associated with

ribosomes and nuclear organizer region (NOR) (Loomis et al., 1990). Studies also indicated that Tau might be associated with chromatin in the nucleus (Greenwood and Johnson, 1995). However, there is limited data on Tau interaction with DNA (Corces et al., 1980; Hua and He, 2003, 2003; Krylova et al., 2005) and its relevance to neurodegeneration is not yet understood. In the present communication, we present the mechanism of Tau binding to DNA and trying to answer following questions (i) Does Tau alter DNA conformation? (ii) Does Tau alter DNA integrity? (iii) Does Tau nick DNA like endonuclease? (iv) Can we propose a hypothesis on Tau-DNA complex role in neuronal cell dysfunction?

4A.2 Materials

Supercoiled pUC18 DNA (cesium chloride purified, 90% supercoiled structure, scDNA), was purchased from Banglore Genei, India. Tau protein was purchased from r-peptide (USA) and Partially phosphorylated Tau was purchased from Sigma (USA). Agarose, HEPES, Tris and EDTA were purchased from SISCO Research laboratories. Ethidium bromide, Copper grids, Aurinetricarboxylic acid (ATA) and $MgCl_2$ were from Sigma (USA) chemicals. Uranyl acetate was purchased from BDH chemicals.

4A.3. Methodology

4A.3.1 Purification of Tau protein: Tau protein was dissolved in cation-exchange buffer (20mM MES, 50mM NaC1, 1mM EDTA, 1mM $MgC1_2$, 2 mM DTT , 0.1mM PMSF , pH 6.8) and loaded on to cation-exchange chromatography column. The column was washed with 4 volumes of cation-exchange buffer. Protein was eluted with elution buffer (20mM MES, 1M NaC1, 1mM EDTA, 1mM $MgC1_2$, 2mM DTT , 0.1 mM PMSF , pH 6.8) with linear gradient and fractions were collected and OD of each fraction was measured at 280 nm (Barghorn et al., 2005). The protein fractions are pooled and lyophilized. Finally the protein is dissolved in triple distilled water and the concentration was determined using BCA method. Partially phosphorylated Tau was also purified by cation-exchange chromatography. The purity of the normal Tau protein and Partially phosphorylated Tau was analyzed on 10% SDS-PAGE.

4A.3.2 Tau-DNA interaction studies

r-Tau was incubated with either scDNA (2686bp) (DNA/Tau mass ratios 1 : 0.5 , 1 : 1, 1 : 2.5 and 1 : 5 in Tris-Cl (10 mM, pH 7.4) at 37°C for 12 hr. Bovine serum albumin (BSA) was taken as negative control, which did not bind to DNA. After the incubation time the samples were electrophoresed along with the control scDNA in 1% agarose gel at 50 V at room temperature. Gel was stained with ethidium bromide (EtBr) and scanned using gel documentation system. Similarly, scDNA was interacted with pp-Tau as mentioned above and analyzed by 1% agarose gel.

4A.3.3 Circular Dichroism (CD) studies

The secondary conformation of scDNA in the absence or presence of r-Tau (at DNA/Tau mass ratios 1 : 0.1, 1 : 0.5 , 1 : 0.75 and 1: 1) were recorded on JASCO J700 spectropolarimeter at 25°C, with 2mm cell length in the wavelength range between 200-320 nm in Tris-Cl buffer (5 mM, pH 7.4). The secondary conformation for the each spectrum was the average of four scans. Similarly, scDNA was incubated with pp-Tau and the secondary conformation of scDNA was analyzed by CD.

4A.3.4 Thermal denaturation studies: The integrity of scDNA upon r-Tau binding was studied using thermal denaturation studies. Changes in scDNA with r-Tau at DNA/Tau mass ratio 1:0.5, 1:1 and 1:5 for 12 hr. The melting temperature profiles of the incubated samples were recorded in HEPES buffer (10mM, pH 7.4) using Spectrophotometer equipped with a thermostat programmer and data processor (Amarsham Biosciences, HongKong). The melting profiles were recorded with increase of 1°C/min in the temperature range of 25-95°C. Similarly, scDNA was incubated with pp-Tau and the melting temperature profile of scDNA was analyzed by Spectrophotometer.

4A.3.5 Ethidium bromide (EtBr) binding studies

The changes in the integrity of scDNA upon r-Tau binding were studied by EtBr study. EtBr bound in moles per base pair of DNA was measured in Tris-Cl (10mM, pH 7.4) using HITACHI F-2000 Fluorescence Spectrofluorimeter. The fluorescence was measured using a constant amount of scDNA (0.5 μg) with increasing amounts of EtBr.

The fluorescence measurements were monitored with an excitation at 535 nm and emission at 600 nm using 10 mm path length.

The maximum amount of EtBr bound per base pair of DNA was calculated using Scatchard plots of 'r' vs 'r/Cf', in the DNA- EtBr reaction mixture at various titration intervals when increasing amount of EtBr was titrated to constant amount of DNA (Scatchard , 1949; Chatterjee and Rao, 1994). The concentration of bound EtBr in 1.0 mL dye-DNA mixture (Cb′) were calculated using the equation:

Cb´ = Co´[(*F*-*Fo*)/(*V*×*Fo*)]

Where,

Co = EtBr (pmoles) present in the dye-DNA mixture,

F = observed fluorescence at any point of dye-DNA mixture,

Fo = observed fluorescence of EtBr with no DNA,

V = experimentally derived value, ratio of bound EtBr/free EtBr at saturation point.

The concentration of free dye (Cf´) was then calculated by the relation

Cf´ = Co´- Cb´,

Where, Cf´, Co´, and Cb´ were expressed in pmoles. The amount of bound EtBr/base pair 'r' was calculated by

r = Cb´ (pmoles)/DNA concentration (pmoles of base pair).

A plot with r vs r/cf is plotted, point where the straight line intersects the X-axis is denoted as 'n'. 'n' is the maximum amount of dye bound per base pair (n), where Cf = Cf´ × 10^{15} M.

Similarly, EtBr binding to scDNA upon pp-Tau binding was calculated using scatchard plots.

4A.3.6 DNAse I Sensitivity assay

DNAse I digests the DNA and sensitivity of DNAse I digestion is a marker of DNA integrity changes. The integrity of DNA-r-Tau complex was studied by DNase I sensitivity assay. scDNA incubated with r-Tau in the mass ratio of 1:0.5 and 1:1 for 12 hr and treated with DNAse I for 1 hr. The reaction was stopped by adding EDTA and analyzed by 1% agarose gel electrophoresis.

4A.3.7 DNA nicking activity of Tau

scDNA was incubated with r-Tau at the DNA/Tau mass ratio 1: 0.5 in Tris-Hcl (10 mM, pH 7.4) at 37°C as a function of time (0.5, 1, 2, 6, 8, 12, 24 hr) both in the presence and absence of Mg (1 mM). The incubated samples were collected at corresponding time intervals and immediately frozen at -20°C. Samples were analyzed by 1% agarose gel.

4A.3.8 Tau-DNA interaction in the presence of Aurinetricarboxylic acid

scDNA was incubated with r-Tau in the presence of 1mM Magnesium, in the presence of endonuclease inhibitor Aurinetricarboxylic acid (ATA) as a function of time (12hr and 24hr). The samples after the respective incubated time intervals, analyzed by 1% agarose gel as described above.

4A.3.9 Transmission electron microscopy (TEM) studies

TEM studies were done to understand whether r-Tau used in the present study is in soluble or aggregated form. r-Tau protein alone and DNA-Tau complexes were scanned under Transmission electron microscope (TEM) for the aggregates if any? Tau alone (5µM) and Tau with scDNA was incubated for 48 h. The Tau samples (5µl) were placed on carbon coated copper grids of 300, mesh size and allowed to dry for 1 min. After blotting with filter paper, the remaining 5µl of the sample was placed and allowed to dry as above. The grid was negatively stained with a drop of 1% uranylacetate and blotted after 1 min. The samples were completely dried to avoid the moisture and examined under the microscope for the fibrils.

4A.4 Results

4A.4.1 Purity of Tau

Recombinant Tau (r-Tau, 441 aa) (rpeptide, USA,) showed a single band on 10% SDS-PAGE after indicating purity of Tau (Fig 4A.1A). The partially phosphorylated Tau (pp-Tau) purified from bovine serum (Sigma-Aldrich, USA) showed 5 bands on 10% SDS-PAGE which corresponds to 5 isoforms of Tau (Fig 4A.1B).

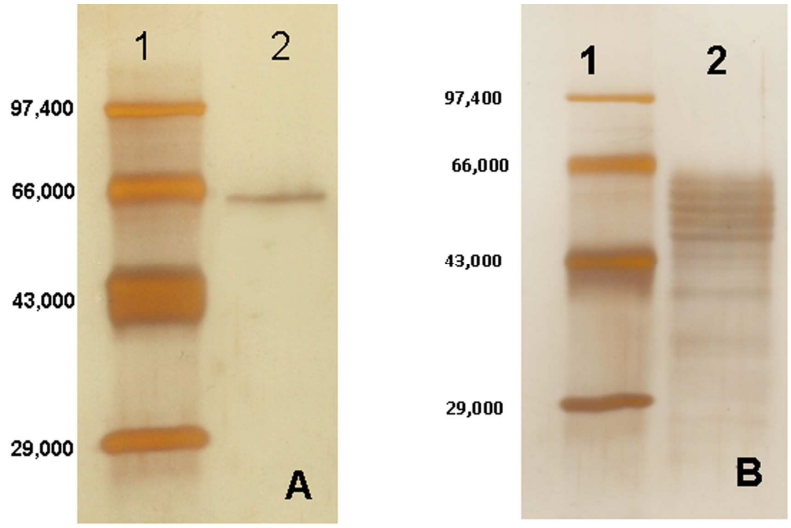

Figure 4A.1: Analysis of Purity of Tau protein: **A)** r-Tau protein analyzed on 10% SDS-PAGE after cation-exchange chromatography which showed single band. 1. Protein marker with range 29-97 kD. 2. Single band of r-Tau. **B)** pp-Tau analyzed on 10% SDS-PAGE after cation-exchange chromatography, shows 5 isomers of pp-Tau. 1. Protein marker with range 29-97 kD. 2. Five isomers of pp-Tau.

4A.4.2 Tau-DNA interaction studies

We have studied r-Tau and pp-Tau interaction with scDNA. scDNA gave two bands on 1% agrose gel, supercoiled DNA was found to be around 85% and open circular form was around 15% (Fig 4A.2) and a very faint band corresponding to dimmers. r-Tau at DNA/Tau mass ratio 1:0.5 and 1:1 converted scDNA into open circular form (Fig 4A.2). But r-Tau retarded the migration of both the supercoiled and open circular DNA forms at higher DNA/Tau mass ratio 1:2.5 and 1:5 (Fig 4A.2). At 1:5 ratio r-Tau converted total scDNA into open circular form and hence there is only one band. As BSA does not have DNA binding ability it was used as negative control. pp-Tau showed similar results with scDNA. pp-Tau at 1:1 mass ratio converted more scDNA into open circular form compared to unphosphorylated r-Tau (Fig 4A.3). This data indicated that both non-phosphorylated r-Tau and pp-Tau have DNA binding ability.

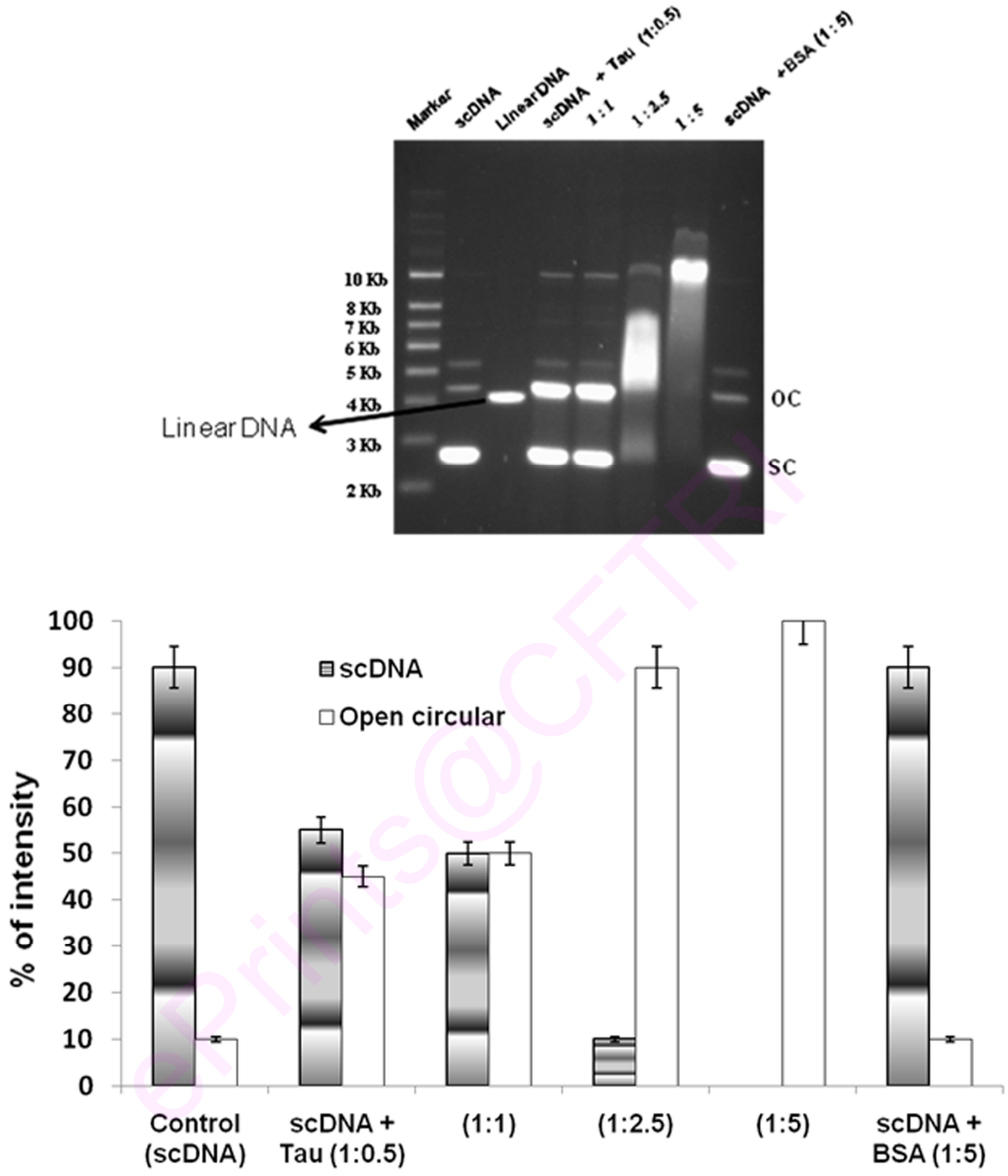

Figure 4A.2: Electrophoretic mobility shift assay: scDNA is interacted with r-Tau at DNA/Tau ratios, 1 : 0.5, 1 : 1, 1: 2.5, 1 : 5 for 12 hr and BSA is taken as negative control. The samples are analyzed by 1% agarose gel and the changes also expressed in bar diagram. SC- Supercoiled DNA, OC-Open circular DNA.

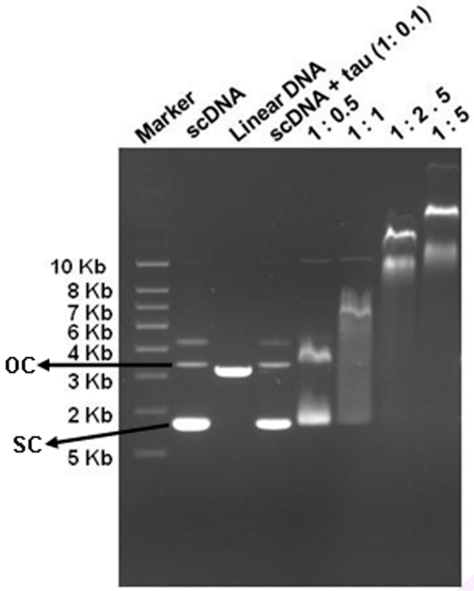

Figure 4A.3: Electrophoretic mobility shift assay : scDNA is incubated with pp-Tau DNA/Tau ratios, 1: 0.1, 1 : 0.5, 1 : 1, 1: 2.5, 1 : 5 and analyzed by 1% agarose gel. SC-Supercoiled DNA, OC-Opencircular DNA.

4A.4.3 Tau induced conformational change in scDNA

In CD spectrum, scDNA showed a characteristic of B-DNA conformation, having positive peak at 272 nm and a negative peak at 245nm (Fig 4A.4, a). r-Tau altered the scDNA CD spectrum in the near UV region at DNA/r-Tau mass ratios of 1: 0.75 and 1:1. r-Tau increased the 210 nm and 220 nm negative peak and also decreased the positive peak at 272 nm (Fig 4A.4, d and e). The spectra of scDNA-Tau complex is subtracted from the Tau spectra alone of same concentrations. Taken together, these changes indicate that r-Tau induces B-C-A mixed transition in scDNA (Gray et al., 1978). The pp-Tau also induced B-C-A mixed conformation in scDNA (data not shown).

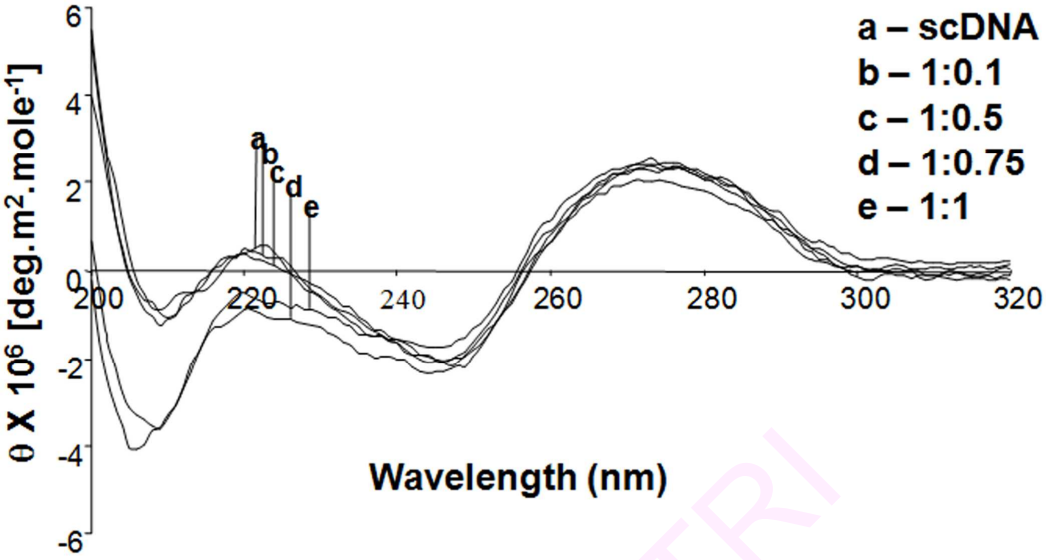

Figure 4A.4: CD spectroscopy of r-Tau-scDNA interaction. scDNA was titrated increasing concentrations of Tau at the mass ratios 1: 0 (a), 1: 0.1 (b), 1: 0.5 (c), 1: 0.75 (d), 1: 1 (e) and CD was recorded in the range of 200nm-320nm.

4A.4.4 Tau altered melting temperature profile of scDNA

The melting temperature (T_m) profile of scDNA showed the characteristic biphasic pattern. The first transition (T_{m1}) is being for the relaxation of supercoils in the scDNA and the second transition (T_{m2}) correspond to the opening of the double strands into single strands. The T_m values of scDNA are T_{m1} = 53°C and T_{m2} = 87°C. r-Tau interaction with scDNA changed the biphasic pattern to monophasic T_m at the mass ratios (DNA/Tau) 1:0.5, 1:1 and 1:5. The monophasic T_m values of scDNA are 80°C, 81°C and 85°C for mass ratios 1:0.5, 1:1 and 1:5 respectively (Table 4A.1). pp-Tau also converted biphasic T_m to monophasic at the mass ratios 1:0.5, 1:1 and 1:5 (Table 4A.1). This data indicates that both non-phosphorylated r-Tau and pp-Tau alter DNA integrity.

scDNA-Tau complex (Mass Ratio)	Melting Temperature (T_m)
scDNA	53 ± 1.14°C (T_{m1}), 87.5 ± 0.25°C (T_{m2}), Biphasic T_m
scDNA: r-Tau (1:0.5)	80.09 ± 0.4°C, Biphasic to Monophasic T_m
scDNA: r-Tau (1:1)	81.53 ± 0.25°C, Biphasic to Monophasic T_m
scDNA: r-Tau (1:5)	84.83 ± 0.3°C, Biphasic to Monophasic T_m
scDNA: pp-Tau (1:0.5)	81 ± 0.25°C, Biphasic to Monophasic T_m
scDNA: pp-Tau (1:1)	82.41 ± 1.09°C, Biphasic to Monophasic T_m
scDNA: pp-Tau (1:5)	84.32 ± 0.5°C, Biphasic to Monophasic T_m

Table 4A.1: Computation of alterations in T_m values for ScDNA in the presence of r-Tau and pp-Tau

4A.4.5 Ethidium Bromide binding studies

The integrity of scDNA is studied by indirectly measuring the number of EtBr molecules bound per base pair using Scatchard plot. The number of EtBr molecules bound per base pair of scDNA is 0.25. The number of EtBr molecules bound per base pair of DNA for DNA/r-Tau mass ratios 1:0.5, 1:1 and 1:5 are 0.33, 0.34 and 0.35, respectively (Fig 4A.5, Table 4A.2). The pp-Tau interaction with scDNA also increased the number of EtBr molecules bound per base pair of DNA. The data indicated that r-Tau and pp-Tau binding to scDNA increased the number of EtBr molecules bound per base pair of scDNA (Table 4A.2).

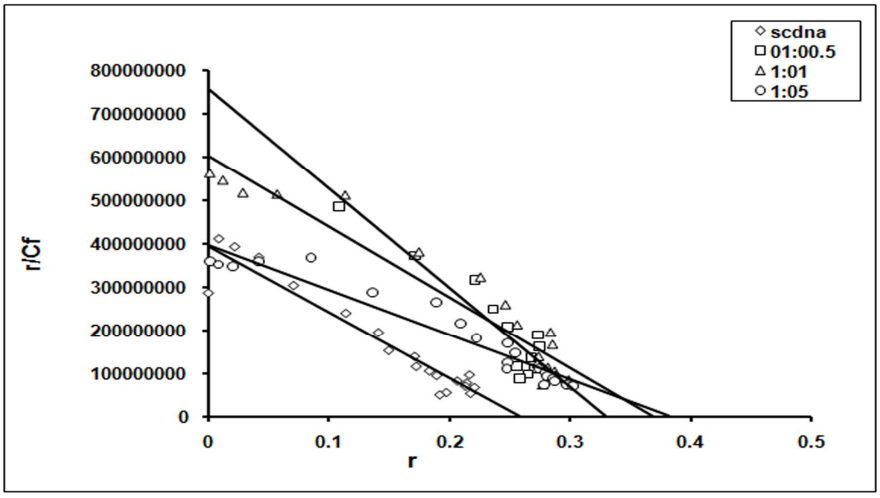

Figure 4A.5 : EtBr bindings studies: scDNA was incubated with r-Tau in the mass ratios of 1:0.5, 1:1 and 1:5 in 10mM Tris-Hcl (pH 7.4) at 37°C for 12 hr. Ethidium bromide binding pattern to incubated samples along with the control scDNA is investigated by titrating with increasing concentration of EtBr. Using scatchard plot EtBr molecules bound / base pair are calculated.

scDNA-Tau complex (Mass Ratio)	EtBr molecules bound per base pair
scDNA	0.24 ± 0.007
scDNA: r-Tau (1:0.5)	0.32 ± 0.005*
scDNA: r-Tau (1:1)	0.34 ± 0.002*
scDNA: r-Tau (1:5)	0.35 ± 0.005*
scDNA: pp-Tau (1:0.5)	0.31 ± 0.003*
scDNA: pp-Tau (1:1)	0.33 ± 0.005*
scDNA: pp-Tau (1:5)	0.35 ± 0.008*

Table 4A.2: Ethidium bromide molecules bound per base pair of DNA in tau-DNA interactions at *P<0.05 significance.

4A.4.6 Tau altered the supercoiled DNA integrity as revealed by DNAse I digestion studies

Agarose gel analysis showed that in DNAse I treated r-Tau-scDNA complex there is an increased conversion of supercoiled form to open circular and linear forms compared to scDNA alone treated with DNAse I (Fig 4A.6). The data indicates that Tau-scDNA complex is sensitive for DNAse I digestion and insights that r-Tau destabilizes DNA integrity.

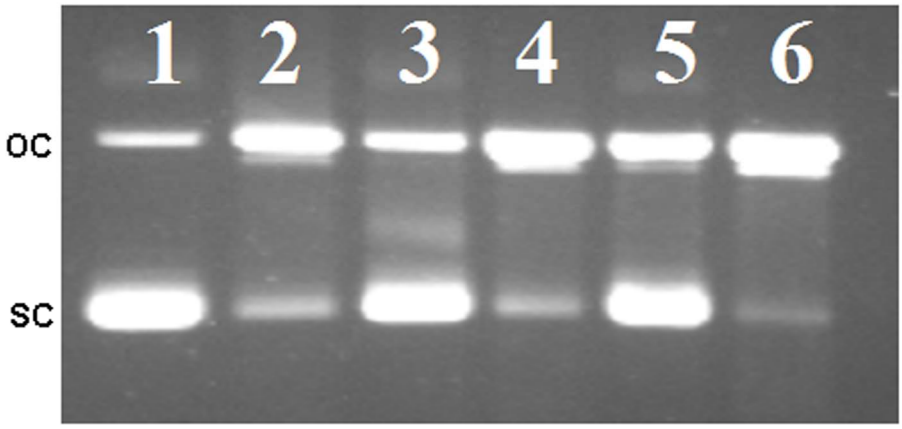

Figure 4A.6 : DNase I sensitivity of scDNA-Tau complex: scDNA-r-Tau complex digested with DNAse I. DNAse I treatment enhances the Tau effect of relaxing the supercoils of scDNA molecule. The scDNA-Tau complex and scDNA treated digested with DNAse I for 1 hr. 1.scDNA alone, 2. scDNA digested with DNAse I 3. scDNA +Tau (1 : 0.5), 4. scDNA +Tau (1 : 0.5) complex digested with DNAse I. 5. scDNA +Tau (1 : 1), 6. scDNA +Tau (1 : 1) complex digested with DNAse I. SC- Supercoiled DNA, OC-Open circular DNA.

4A.4.7 DNA nicking activity of Tau

Initially, we studied the role of r-Tau and pp-Tau in modulating scDNA integrity. r-Tau at mass ratio of 1:0.5 (DNA/Tau) relaxed the supercoils of scDNA in a time dependent manner. Initially r-Tau did not alter the scDNA integrity as a function of time of 0.5, 1, 2, 6, 8 hr both in the presence and absence of 1 mM MgCl (Fig 4A.7). We tried to understand whether DNA nicking activity of r-Tau resembles nuclease activity. The extended time function studies indicated that r-Tau converted scDNA into open circular form only in the absence Mg as a function of time, 12hr and 24hr (Fig 4A.8A and 8B, lane 3). But in the presence of Mg (1mM), Tau converted majority of scDNA into open circular and linear form at 24hr of incubation time (Fig 4A.8B, lane 5). We studied the Tau nicking in the presence of Mg as, Mg (1mM) is a co-factor for many endonucleases. We found that Mg enhanced r-Tau nicking resembling endonuclease behavior. To verify this, we examined the effect of Aurinetricarboxylic acid - A specific nuclease inhibitor on Tau-DNA interactions. ATA specifically inhibits DNA nicking of endonucleases typically by derivatizing the active site histidine residue of the enzyme. We investigated to understand whether ATA inhibits Tau nicking activity? It was found

that ATA (1mM) inhibited the DNA nicking activity of r-Tau (Fig 4A.8A and 8B, lane 4 and 6) indicating that Tau may be nicking DNA behaving endonuclease behavior.

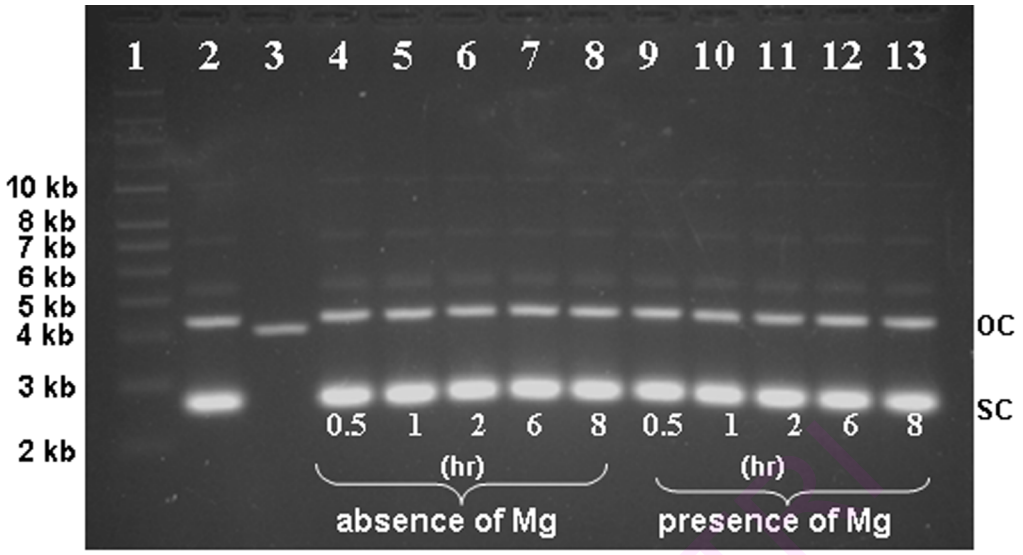

Figure 4A.7 : Evaluation of r-Tau, DNA nicking ability. scDNA incubated with r-Tau in the mass ratio of 1: 0.5 (DNA : Tau) with time periods 0.5 hr, 1 hr , 2 hr, 6 hr, 8 hr both in the presence and absence of 1 mM Mg. SC- Supercoiled DNA, OC-Open circular DNA.

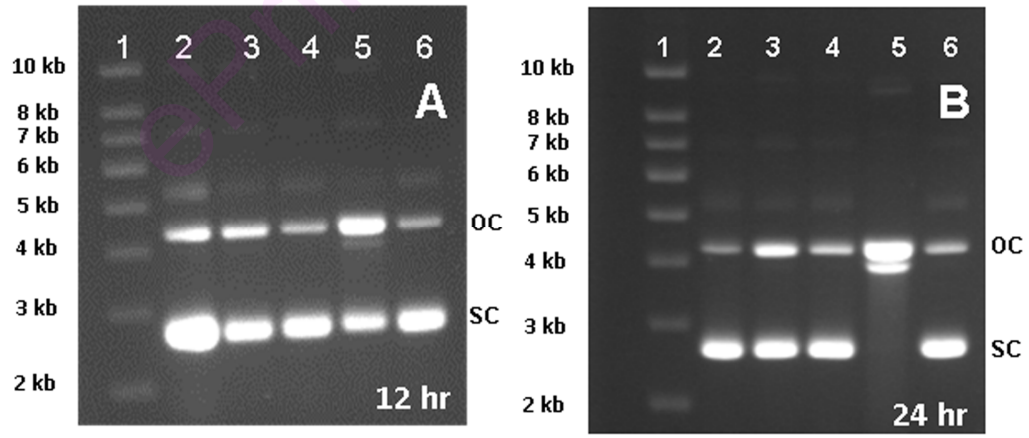

Figure 4A.8: Nicking activity of Tau : Inhibition of r-Tau, DNA nicking activity by ATA. scDNA is incubated with r-Tau in the presence of Mg (1mM) and ATA for 12 hr (Fig 9A) and 24 hr (Fig 9B). Lanes: 1. Marker, 2. scDNA , 3. scDNA + Tau, 4. scDNA

+ Tau +ATA, 5. scDNA + Tau + Mg^{2+} 6. scDNA + Tau + Mg^{2+} + ATA. SC-Supercoiled DNA, OC-Open circular DNA.

4A.4.8 Transmission Electron Microscopy studies

We investigated to study whether r-Tau is in soluble or aggregated form in the presence of scDNA? TEM studies showed that r-Tau did not aggregate at the concentration used for the scDNA-Tau interaction studies in TEM (Fig 4A.9B). These studies indicate that soluble form of Tau has DNA nicking activity. Native recombinant Tau is in random coil conformation (Fig 10). In scDNA-Tau complex, Tau exists in random coil conformation only (Fig 10). This indicates that Tau nicks DNA in monomeric random coil conformation.

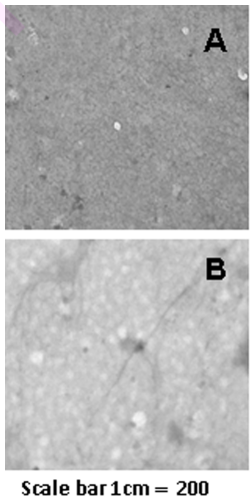

Figure 4A.9: Transmission Electron Microscopy: TEM images of r-Tau at 5 μM concentration after 48 hr incubation at 37°C. Tau did not formed into aggregates in Tau alone (A) and in the presence of scDNA (B)

4A.5 Discussion:

Tau protein belongs to the family of microtubule-associated proteins (MAPs) mainly expressed in the neurons. Tau is involved in the microtubule association and their stabilization in the neuron (Wang and Liu, 2008). Tau aggregation is the hallmark of all Tauopathies (Iqbal et al., 2009; Williams, 2006). AD is a principal Tauopathy, where Tau is associated with NFTs and PHFs in cytoplasm. The classical theory explains that Tau toxicity in all Tauopathies is due to aggregation of Tau (Mandelkow, 1999). It is still not clear whether Tau aggregation is the sole responsible factor of Tau toxicity (Brandt et al., 2005, Congdon et al., 2008).

Tau's main function is to promote microtubule assembly and stability in the cytoplasm. Several studies have shown that Tau is also distributed in the nucleus but its nuclear role is not yet defined? Greenwood *et al* (1995) showed that Tau protein is localized in the nucleus of neuroblastoma cells (Greenwood and Johnson, 1995). The reports also showed that Tau is associated with the chromatin fraction containing DNA and NOR in the nucleus (Loomis et al., 1990; Greenwood and Johnson, 1995). It is hypothesized that Tau might interact with rRNA genes and RNA of ribosomes (Sjöberg et al., 2006). The study has shown that Tau nuclear staining is extensive in undifferentiated SH-SY5Y cells and nuclear staining of Tau disappeared as SH-SY5Y cells differentiate into neurons. This suggested that Tau might play a role in cell cycle events in the nucleus (Uberti et al., 1997). It is further evidenced that Tau is localized in the nucleus in an autopsy sample with presenile dementia (Papasozomenos, 1995). Sheffield *et al*. (2006) studied the nucleoporins and nuclear pore complex associated proteins in AD (Sheffield et al., 2006). The authors have shown that there is a nuclear pore irregularity in the neurons and this is associated with the NFTs. Based on the literature, we hypothesize that the association of NFTs with nucleopore complex insights that Tau might be transported from cytoplasm to nucleus in the process of disease progression? It is shown that similar kind of translocation of α-Synuclein (protein abnormally aggregates in Parkinson's disease brain) into the nucleus in oxidatively stressed dopaminergic cells (Xu et al., 2006). Similar mechanism may be responsible for translocation of Tau into the nucleus in AD, as oxidative stress is an early event in AD as well? However this hypothesis is still open for discussion.

The key Question is, how does Tau bind with DNA? Corces *et al*. (1980) showed that Tau could bind to DNA. Hua *et al.,* (2003) showed that Tau stabilized the calfthymus DNA structure and protected the DNA from the reactive oxygen species. Krylova *et al.,* (2005) showed that Tau induced dissociation of double strands of DNA. Tau-λ DNA complex appears as beads on a coil under atomic fluorescence microscopy (AFM) showing the association of Tau with DNA (Qu et al., 2004). Sjöberg *et al.,* (2006) showed that Tau specifically binds to AT-rich satellite DNA sequences. All these studies indicate that Tau has DNA binding ability but the mechanism of Tau binding to DNA is still not clear.

We evidenced novel data on Tau altering the integrity of supercoils in scDNA. r-Tau retarded the migration of scDNA and also open circular form showing the Tau association with the DNA. The pp-Tau retarded the migration of both scDNA and open circular form. This indicates that unphosphorylated Tau and partially phoaphorylated Tau has the similar DNA binding ability. Hua Q *et al.,* also showed that Tau retarded the mobility of plasmid DNA in electrophoretic mobility shift assay experiments. But the authors incorrectly assigned the data showing that closed circular DNA as scDNA and vice versa and hence their interpretation varies (Hua et al., 2003). Our studies further showed that r-Tau altered the mobility of DSC and SSC DNA showing the DNA binding ability. Our results are in agreement with the study of krylova (2005) with reference to Tau binds to single stranded DNA sequences.

Our present study indicated that r-Tau induced B-C-A mixed conformation in scDNA and this is a new evidence. Similarly, pp-Tau also induced B-C-A mixed conformation in scDNA. Further, Qu *et al*. (2004) reported that Tau induces the bending in λ DNA. In the human genome, DNA is compactly arranged in the form of supercoiled pockets (Cook and Brazell, 1975). We have selected plasmid pUC18 scDNA as a model system in our study because of the observation that large amount of small scDNA pockets have been reported to be present in animal and human cells and these supercoiled pockets are known to be involved in gene expression. Further, the eukaryotic supercoiled pockets are proposed to be analogous to plasmid DNA supercoiling (Bauer et al., 1980). Hence we have used plasmid supercoiled DNA in our study. The results can be further correlated to human genomic DNA to get an insight in understanding the possible role of Tau in neurodegeneration with special emphasis to DNA topology. DNA conformation is an important aspect for the gene expression etc. our finding that Tau altering the scDNA conformation may have biological relevance?

We further evidenced that Tau alters DNA stability, however there are limited studies in this direction. The stability of scDNA is altered due to Tau binding as determined by alteration in T_m, EtBr binding and DNase I digestion sensitivity of Tau-scDNA complex. r-Tau favored the conversion of biphasic T_m to higher monophasic T_m. pp-Tau also converted biphasic T_m to monophasic T_m. Hua *et al.,* (2003) showed that Tau could stabilize calf thymus DNA as evidenced by an increase in T_m (Hua and He,

2003). EtBr binding studies showed that r-Tau and pp-Tau relax the supercoils in scDNA. The relaxation in supercoils is evidenced by an increase in the number of EtBr molecules bound per base pair. DNAse I digestion sensitivity studies showed that more scDNA is converted into open circular form thus showing sensitivity to DNAse I digestion. Wei *et al*., (2008) showed that Tau modulates the stability of DNA. The above data revealed that Tau alters the integrity of scDNA and our findings provide a mechanistic explanation to understand Tau induced DNA instability and conformational change.

Our novel results showed that Tau converted scDNA into open circular and linear forms suggesting that Tau may nick the DNA resembling endonuclease. Tau alone converts scDNA into open circular form, however the activity was significantly enhanced in the presence of Mg. Further we used endonuclease inhibitor, Aurintricarboxylic acid (ATA) to see whether it inhibits Tau nicking DNA. We found that ATA prevented Tau induced DNA nicking resembling endonuclease like activity. ATA preferentially interacts with histidine residues in endonuclease and cause inhibition (González et al., 1980). In Tau, there are 11 histidine molecules mainly present in the microtubule binding domain and also in proline rich domains. ATA may be inhibiting Tau DNA nicking activity through interaction with histidine molecules? Based on our contributions, we hypothesize a new role for Tau-DNA complex in neurodegeneration

Hypothesis on mechanism of Tau nicking DNA (Fig 4A.10) : Tau protein may bind to scDNA at minor grove and induce a B-C-A conformational change in the scDNA. B-C-A DNA is short and broad compared to B-form and minor grooves are broadened in B-C-A mixed conformation as discussed earlier. Tau after inducing the conformational change, may cleave the DNA by breaking phosphodiester bonds thus causing genomic instability. Insight conclusion: As reported earlier, Tau may translocates into the nucleus during stress (oxidative stress) conditions?. Still the mechanism is not clear. In the nucleus, Tau may alter the genomic functions by interacting with DNA. Tau may induces conformational change in the DNA from normal B-conformation to B-C-A mixed conformation. The conformational change induced by Tau may disturb the nucleosomal organization, which may lead to abnormal transcriptional regulation and

gene expression changes. It is hypothesized that conformational change and DNA instability in the presence of Tau may lead to neuronal cell dysfunction.

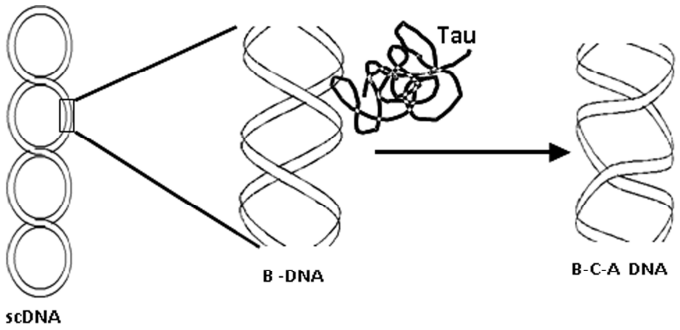

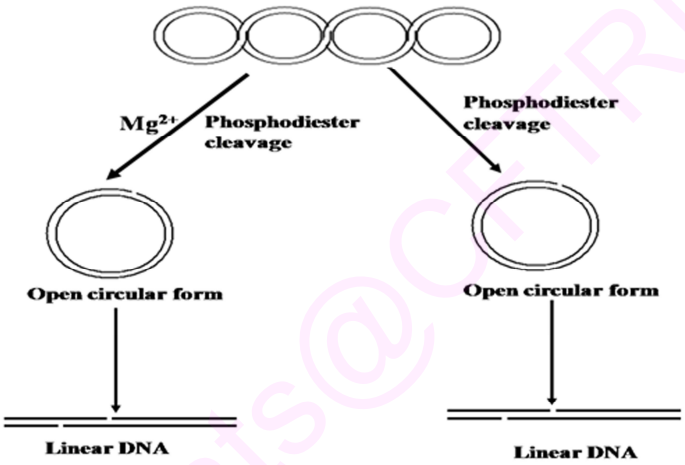

Chapter 4B

DNA binding properties of α-synuclein and AGE-α-synuclein (glycated α-synuclein)

4B.1 Introduction

Parkinson's disease (PD) is an age related neurodegenerative disease characterized by progressive neuronal loss in substantia nigra region of the brain. Multiple etiological factors are responsible for the development of the disease (Gallagher and Schapira, 2009). α-Synuclein is one of the important proteins, expressed in neurons and pathologically involved in Parkinson's disease (PD) (Bisaglia et al., 2009; Jellinger, 2009). α-Synuclein is localized both in synapse and nucleus (Maroteaux et al., 1988). The normal function of the α-synuclein is not understood yet, but studies showed that α-synuclein may be involved in synaptic development, vesicular binding etc (Hegde et al, 2010; Bayer et al., 1999; Kaplan et al., 2003; Di Rosa et al., 2003). The mechanism of α-synuclein in developing pathology is debatable (Waxman and Giasson, 2009). Studies have also shown that aggregation of α-synuclein is the pathological event in the development of Parkinson's disease (Uversky and Eliezer, 2009; Beyer and Ariza, 2009). α-Synuclein aggregates are found in the brain of PD patients and in the animal models of PD. α-Synuclein (140 aa) is natively in unfolded, random coil conformation. α-Synuclein localization in nucleus indicated possible role of the protein in the nucleus (Schneider et al., 2007; Mori et al., 2002; Specht et al., 2005; Yu et al., 2004). Kontopoulos et al. showed that α-synuclein targeting to nucleus induced neurodegeneration in flies (Kontopoulos et al., 2006). Several studies have shown that α-synuclein binds to DNA and histones (Hegde et al, 2003, 2006, 2007; Cherny et al., 2004; Goers et al., 2003).

Advanced Glycation End products (AGEs) are formed when reducing sugars like glucose, react with amino groups of proteins/lipids/nucleic acids through non-enzymatic glycation (Negre-Salvayre et al., 2009; Sensi et al, 1991). In aging process, by the continuous and constant exposure of α-synuclein to normal levels of glucose in circulation, formation of AGE-α-synuclein may get facilitated and may get aggravate

further due to various insults and exposures including oxidative stress (Sandyk, 1993). AGEs and α-synuclein are found in the brains of PD and are co-localised (Münchet al, 200). Under PD conditions α-synuclein may get glycated and glycated α-synuclein may induce cell death.

Hence, in the present work the we studied DNA binding properties of α-synuclein and glycated α-synuclein (AGE-synuclein) are studied and are discussed in relation to Parkinson's disease.

4B.2 Materials

α-Synuclein was purchased from r-peptide (USA). Supercoiled pUC18 DNA (cesium chloride purified, 90% supercoiled structure, scDNA) was purchased from Banglore Genei, India. Agarose, HEPES, Tris and EDTA were purchased from SISCO Research laboratories. Methy glyoxal, ethidium bromide, aurinetricarboxylic acid (ATA) and $MgCl_2$ were purchased from Sigma (USA).

4B.3 Methodology

4B.3.1 Preparation of AGE-α-synuclein

AGE-α-synuclein was prepared by incubating 60 μM of α-synuclein with 60 mM methylglyoxal (MGO) in 10 mM PBS buffer (pH 7.4) at 37°C for 144 h under sterile conditions. An aliquot (10 μl) from the incubation mixture was taken and made to 500 μl in PBS buffer pH 7.4 for the fluorescence analysis. The formation of AGE-α-synuclein was analyzed for every 24 h days monitoring its fluorescence at Ex 340 nm and Em: 360-500 nm using HITACHI spectrofluorometer.

4B.3.2 Circular dichroism of AGE-α-synuclein

The secondary conformation of α-synuclein and AGE-α-synuclein was recorded on JASCO J700 spectropolarimeter at 25°C with 2mm cell length in the wavelength range between 200-320 nm in Tris-Cl buffer (5 mM, pH 7.4). The sample that was incubated with MGO for 144 h was subjected to CD studies. The secondary conformation for each spectrum was the average of four scans.

4B.3.3 Intrinsic Tyrosine fluorescence

Tyrosine intrinsic fluorescence spectra were recorded on a HITACHI 2000 spectrofluorimeter in quartz with a 1 cm excitation light path. For tyrosine intrinsic fluorescence α-synuclein containing solution was excited at 275 nm and emission monitored in the range from 295 nm to 350 nm. The maximum emission was observed at 304 nm. The concentration of α-synuclein for the intrinsic tyrosine fluorescence was kept at 2 μM. In the present investigation, tyrosine intrinsic fluorescence was used to understand glycation induced folding in α-synuclein. The sample that was incubated with MGO for 144 h was subjected to intrinsic tyrosine fluorescence.

4B.3.4 Analysis of fructosamine in AGE-α-synuclein

The amount of glycated ketoamine in AGE-α-synuclein was estimated by fructosamine assay. The 144 h incubated sample (50 μl) was mixed with 1 ml of carbonate buffer (pH 10.8) containing 0.25 mM NBT (Nitroblue tetrazolium) and incubated for 10 min. Absorbance of the above reaction mixture was measured at 530 nm at 5^{th} and 10^{th} minute. Fructosamine formation was compared with the standard DMF (1-deoxy-1-morpholine-D-Fructose).

4B.3.5 Trypsin digestion

Proteolytic cleavage of proteins has been used as a probe of protein conformation and stability (Nadig et al., 1996; Fontana et al., 1997). We analyzed the proteolytic cleavage of AGE-α-synuclein with trypsin in comparision with native α-synuclein. Trypsin digestion of α-synuclein and AGE-α-synuclein were carried out according to the method described by Hegde et al. (2003) α-synuclein and AGE-α-synuclein were incubated with Trypsin (2 μg) in Tris-HCl buffer (pH 7.4) for 1 h and 2 h. After proteolytic clevage, the samples were immediately frozen at -20°C. The trypsin digestion pattern was analyzed on 12 % Tricine SDS-PAGE and stained with silver staining. Electrophoresis was carried out according to the method described by laemmli et al. (1970).

4B.3.6 Agarose gel studies

scDNA was incubated with α-synuclein at the DNA/α-synuclein mass ratio 1:4 in Tris-Hcl (10 mM, pH 7.4) at 37°C for 12 h. scDNA was also incubated with α-synuclein in the presence of magnesium Mg (co-factor for endonuclease) and Aurinetricarboxylic acid (ATA) (specific endonuclease inhibitor). The incubated samples were analyzed by 1% agarose gel. Similarly AGE-α-synuclein was incubated with scDNA and analysed on 1% agarose gel.

4B.3.7 Circular dichroism (CD) studies

The secondary conformation of scDNA in the presence of α-synuclein and AGE-α-synuclein (at DNA/α-synuclein mass ratios 1:4) was recorded on JASCO J700 spectropolarimeter at 25°C, with 2mm cell length in the wavelength range between 200-320 nm in Tris-Cl buffer (5 mM, pH 7.4). The secondary conformation for the each spectrum was the average of four scans.

4B.3.8 Thermal denaturation studies

The melting temperature (T_m) profiles of the α-synuclein and AGE α-synuclein binding to scDNA were recorded in HEPES buffer (10mM, pH 7.4) using spectrophotometer equipped with a thermostat programmer and data processor (Amarsham Biosciences, HongKong). The melting profiles were recorded with increase of 1°C/min in the temperature range of 25-95°C.

4B.3.9 Ethidium bromide (EtBr) binding studies

The changes in the integrity of scDNA upon α-synuclein and AGE α-synuclein binding were studied by EtBr study. EtBr bound in moles per base pair of DNA was measured in Tris-Cl (10mM, pH 7.4) using HITACHI F-2000 Fluorescence Spectrofluorimeter. The fluorescence was measured using a constant amount of scDNA (0.5 μg) with increasing amounts of EtBr. The fluorescence measurements were monitored with an Ex: 535 nm and Em: 600 nm using 10 mm path length. The maximum amount of EtBr bound per base pair of DNA was calculated using Scatchard plots of ‘r’ vs ‘r/Cf’, in the DNA- EtBr reaction mixture at various titration intervals when increasing amount of EtBr was titrated to constant amount of DNA (Scatchard, 1949; Chatterjee 1994). The

concentration of bound EtBr in 1.0 mL dye-DNA mixture (Cb′) were calculated using the equation:

Cb´ = Co´[(*F*-*Fo*)/(*V*×*Fo*)]

Where,

Co = EtBr (pmoles) present in the dye-DNA mixture,

F = observed fluorescence at any point of dye-DNA mixture,

Fo = observed fluorescence of EtBr with no DNA,

V = experimentally derived value, ratio of bound EtBr/free EtBr at saturation point.

The concentration of free dye (Cf´) was then calculated by the relation

Cf´ = Co´- Cb´,

Where, Cf´, Co´, and Cb´ were expressed in pmoles. The amount of bound EtBr/base pair 'r' was calculated by

r = Cb´ (pmoles)/DNA concentration (pmoles of base pair).

A plot with r vs r/cf is plotted, point where the straight line intersects the X-axis is denoted as 'n'. 'n' is the maximum amount of dye bound per base pair (n), where Cf = Cf´ × 10^{15} M.

4B.3.10 DNAse I Sensitivity assay

DNAse I digests the DNA and the sensitivity of DNAse I digestion is a marker of DNA integrity. scDNA incubated with α-synuclein and AGE-α-synuclein in the mass ratio of 1:2 for 12 hr and treated with DNAse I. The digestion of scDNA was monitored using spectrofluorimeter using ethidium bromide.

4B.3.11 Statistical analysis

Data are expressed as mean ± SEM of triplicates. Statistical analysis of data was performed using one-way analysis of variance (ANOVA) with a Tukey's multiple comparison post-test and significance at **P*<0.05, ***P*<0.01 and ****P*<0.001.

4B.4 Results

4B.4.1 Fluorescence detection of AGE-α-synuclein formation

To confirm the glycation of α-synuclein, fluroscence of modified α-synuclein was carried out. Fluorescence studies indicated an increase in the fluorescence of α-

synuclein at 380 nm, when it was incubated with methylglyoxal (MGO). While in case of α-synuclein incubated without MGO no such increase was observed (Fig.4B.1). There was gradual increase in the fluorescence upto 120 h and further incubation upto 144 h did not show further increase in fluorescence. The data confirms that α-synuclein modified to AGE-α-synuclein.

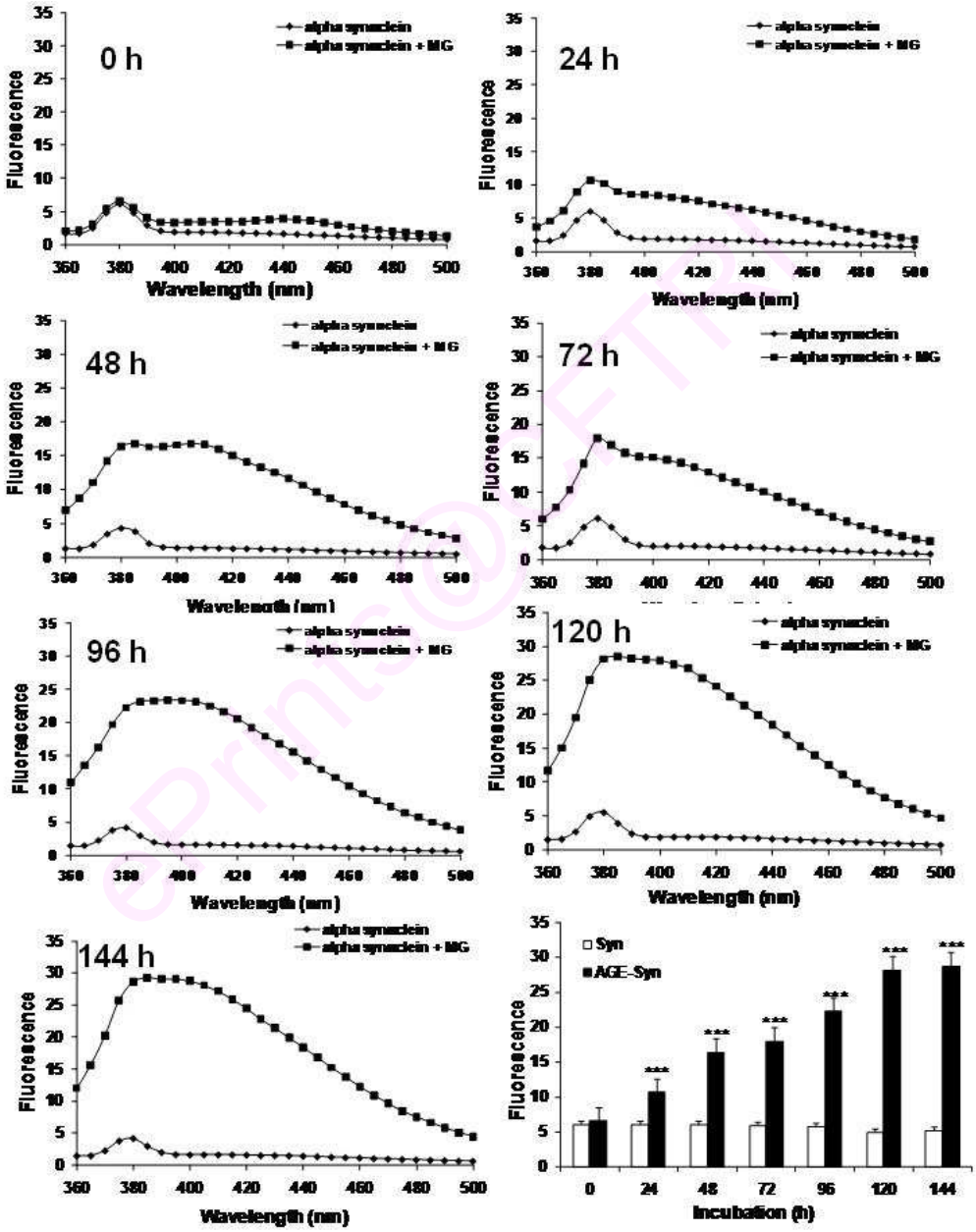

Figure 4B.1: Kinetics of α-synuclein glycation in the presence of methylglyoxal as a function time. Values are expressed as mean ± SEM of triplicates and significant at **P*<0.05, ***P*<0.01 and ****P*<0.001 in comparison to '0' h Synuclein control.

4B.4.2 Circular dichroism of AGE-α-synuclein

Circular dichroism of modified AGE-α-synuclein was carried out to know any conformational change induced by glycation. α-Synuclein normally exists in random coil conformation. The CD data showed that AGEs formation did not alter the secondary structure of α-synuclein. It was inferred that AGE-α-synuclein also exists in random coil conformation similar to native α-synuclein (Fig.4B.2).

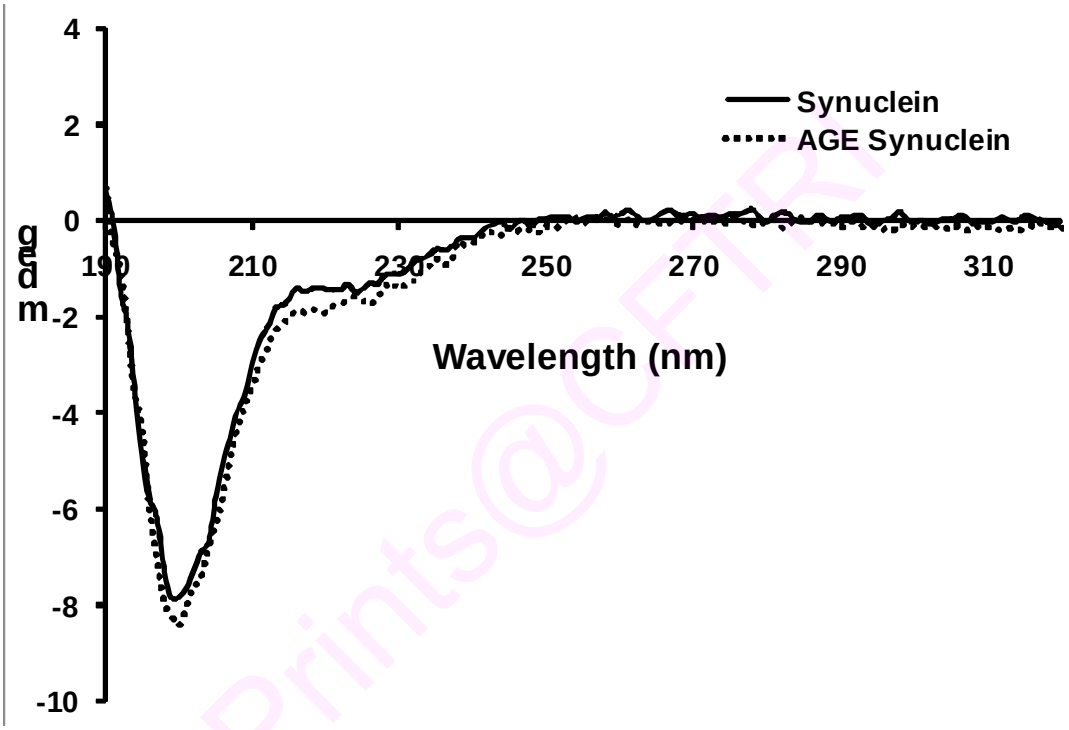

Figure 4B.2: CD spectra of α-Synuclein and AGE-α-Synuclein. α-Synuclein and AGE-α-Synuclein shows random coil conformation.

4B.4.3 Intrinsic tyrosine fluorescence of AGE-α-synuclein

α-Synuclein contains four tyrosine residues and there is no tryptophan. Hence, the tyrosine fluorescence was used to monitor folding of α-synuclein (Uversky et al., 2001). Glycation of α-syuclein decreased the intrinsic tyrosine fluorescence. Intrinsic tyrosine fluorescence indicated that some tyrosine molecules in α-synuclein might have

buried inside indicating folding of AGE-α-synuclein compared to native α-synuclein (Fig.4B.3).

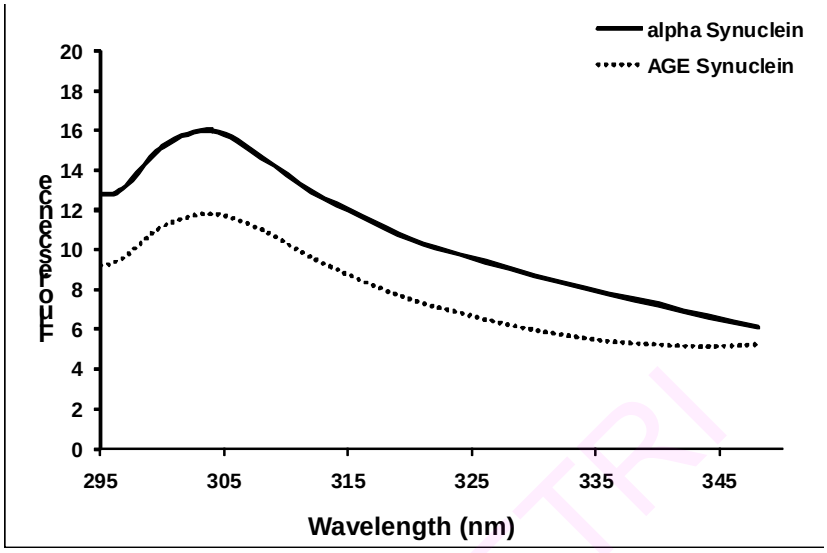

Figure 4B.3: Intrinsic tyrosine fluorescence of α-Synuclein and AGE-α-Synuclein. Glycation of α-syuclein decreased the intrinsic tyrosine fluorescence indicating folding of AGE-α-synuclein compared to native α-synuclein

4B.4.4 Analysis of fructosamine formation

Glycation involves formation fructosamine in the reaction between MGO and amino groups of protein. To characterize the glycation of α-synuclein fructosamine content in the AGE-α-synuclein was estimated. In native α-synuclein, fructosamine level was negligible, but in AGE-α-synuclein, fructosamine concentration was around 38.6 mmoles/50 ug of protein. The fructosamine formation confirms the glycation of α-synuclein (Fig.4B.4).

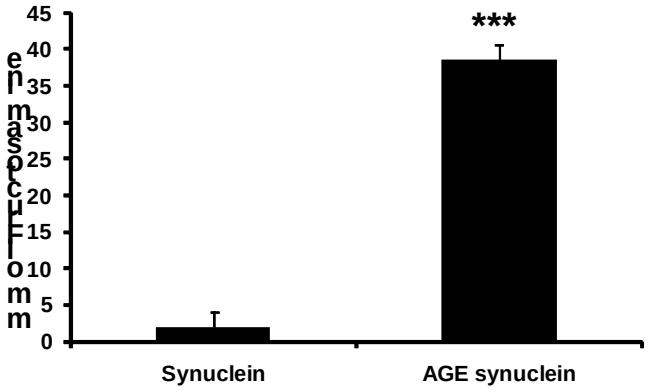

Figure 4B.4: Quantification of fructosamine in α-Synuclein and AGE-α-Synuclein. Values are expressed as mean ± SEM of triplicates and are significant at ***P<0.001.

4B.4.5 Trypsin digestion

Trypsin cleaves proteins into peptides at carboxyl ends of lysine and arginine. As fluorescence studies indicated change in the folding of glycated synuclein, cleavage of glycated synuclein by trypsin may be different. Fig.4B.5, indicates trypsin digestion pattern of α-synuclein, AGE-α-synuclein upon digestion with trypsin for 2 h and 4 h. At 2 h, the intensity of the band ~19 kD, which corresponds to α-synuclein, decreased markedly. While incubation for 4 h with trypsin the α-synuclein band completely disappeared. On the other hand, the AGE-α-synuclein band also disappeared by 4 h incubation with trypsin, but an intense tryptic peptide bands are seen between 3.5 and 14.3 kD region (Fig.4B.5 lane 5, 6). This indicates that α-synuclein and AGE-α-synuclein may have different folding.

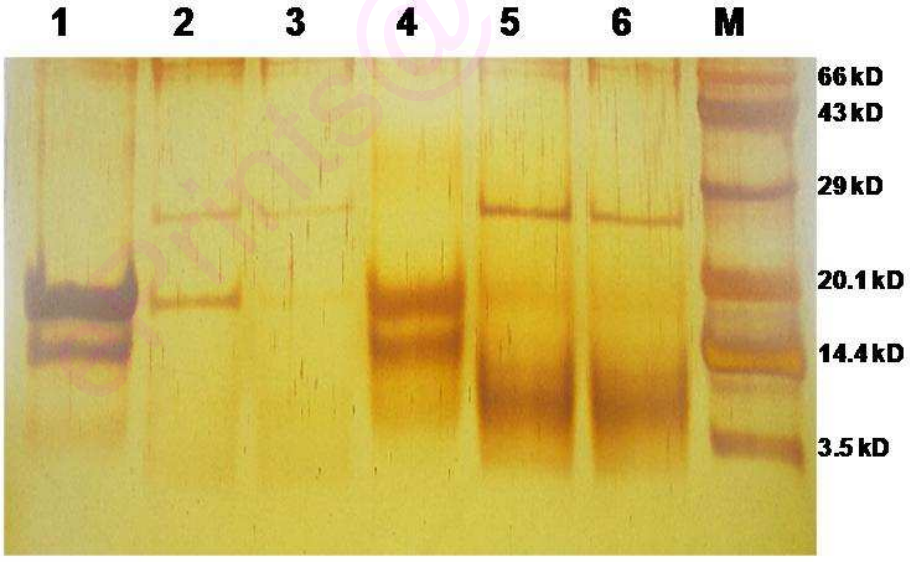

Figure 4B.5: α-Synuclein and AGE α-Synuclein digestion with Trypsin. 1) α-Synuclein alone 2) α-Synuclein digested with trypsin for 1 h. 3) α-Synuclein digested with trypsin for 2 h. 4) AGE α-Synuclein 5) AGE α-Synuclein digested with trypsin for 1 h 6) AGE α-Synuclein digested with trypsin for 2 h. Proteolytic cleavage of α-synuclein and AGE-α-synuclein with trypsin showed different digestion pattern indicating that glycation altered folding of α-synuclein

4B.4.6 Agarose gel studies

The interaction of α-synuclein to scDNA and scDNA integrity after interaction was analyzed by agarose gel studies. scDNA gives two bands on 1% agrose gel. The band SC indicates supercoiled form and was around 85%, OC indicates open circular band which was around 15% (Fig.4B.6, lane 1). L indicated the stranded linear DNA (E.co R I digest of scDNA). In the presence of α-synuclein, scDNA was converted to more opencircular form (lane 3) compared to control (lane 1) in the presence of α-synuclein indicating α-synuclein nicking (lane 3). Specific nuclease inhibitor ATA, inhibited the indicating α-synuclein nicking (lane 4). Further enhancement, in the nicking was observed when magnesium (co-factor for endonucleases) was added along with α-synuclein (lane 5). ATA also inhibited α-synuclein nicking in the presence magnesium, indicating the role α-synuclein as endonuclease (lane 6). AGE-α-synuclein also exhibited similar property, nicking scDNA (lane 7) and magnesium enhanced AGE-α-synuclein nicking (lane 9). ATA also prevented the AGE-α-synuclein nicking (lane 8 and lane 10). We found that both AGE-α-synuclein and α-synuclein nick the DNA.

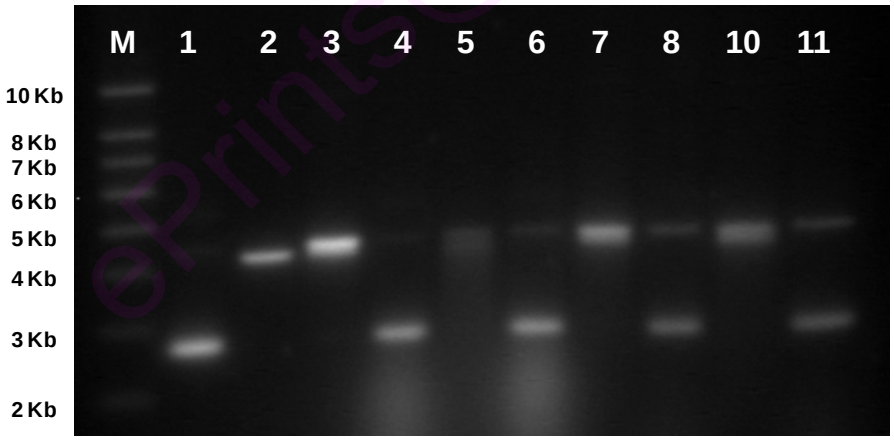

Figure 4B.6: DNA nicking activity of α-Synuclein and AGE Synuclein: Lanes: M) Marker, 1) scDNA , 2) Linear DNA, 3) scDNA + α-Synuclein, 4) scDNA + α-Synuclein + ATA, 5) scDNA + α-Synuclein + Mg^{2+}, 6) scDNA + α-Synuclein + Mg^{2+} + ATA, 7) scDNA + AGE- α-Synuclein, 8) scDNA + AGE-α-Synuclein + ATA, 9) scDNA + AGE-α-Synuclein + Mg^{2+}, 10) scDNA + AGE-α-Synuclein + Mg^{2+} + ATA.

4B.4.7 Circular dichroism (CD) studies

In CD spectrum, scDNA showed characteristic of B-DNA conformation, having positive peak at 272 nm and a negative peak at 245nm (Fig.4B.7). In the presence of α-synuclein scDNA CD spectrum was altered in the near UV region. α-Synuclein increased the 210 nm and 220 nm negative peak (Fig.9). The spectra of scDNA-α-synuclein complex is subtracted from the α-synuclein spectra alone of same concentrations. Taken together, these changes indicate that α-synuclein induces B-C-A mixed transition in scDNA (Gray et al., 1978). AGE-α-synuclein also induced B-C-A mixed conformation in scDNA similar to that of α-synuclein.

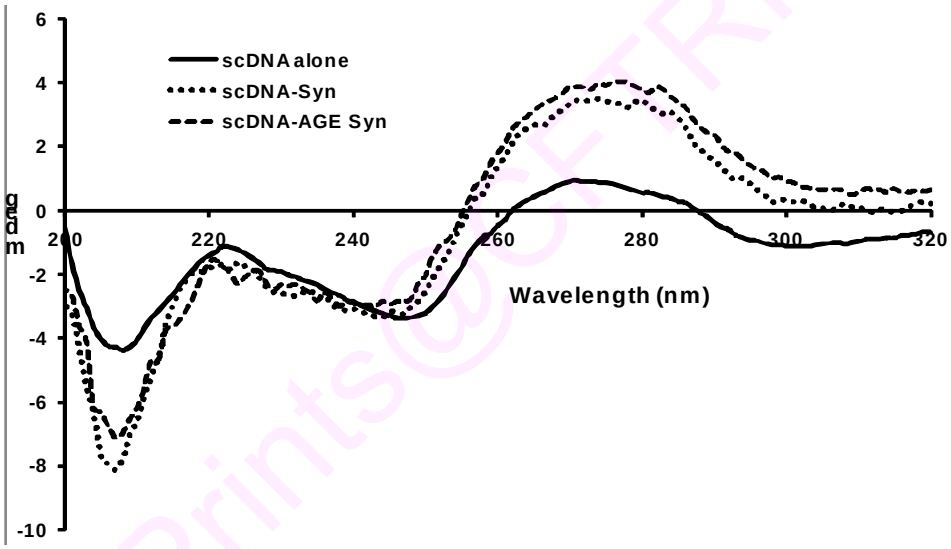

Figure 4B.7: CD spectra of α-Synuclein and AGE-α-Synuclein interaction with scDNA. scDNA is in B-form, α-Synuclein and AGE-α-Synuclein induced B-C-A mixed conformation in scDNA.

4B.4.8 Thermal denaturation studies

Thermal denaturation was preformed to know the integrity of scDNA upon AGE synuclein and synuclein binding to scDNA. The melting temperature (T_m) profile of scDNA showed characteristic biphasic pattern. The first transition (T_{m1}) was due to relaxation of supercoils in the scDNA and the second transition (T_{m2}) was due to opening of double strands into single strands. The T_m values of scDNA were T_{m1} =

54°C and T_{m2} = 86°C (Fig.4B.8). α-Synuclein and AGE α-synuclein interaction with scDNA changed the biphasic pattern to monophasic T_m . The monophasic T_m values of scDNA-α-synuclein and scDNA-AGE α-synuclein were 77°C and 79°C respectively. This data indicated that both scDNA-α-synuclein and scDNA-AGE α-synuclein altered DNA integrity.

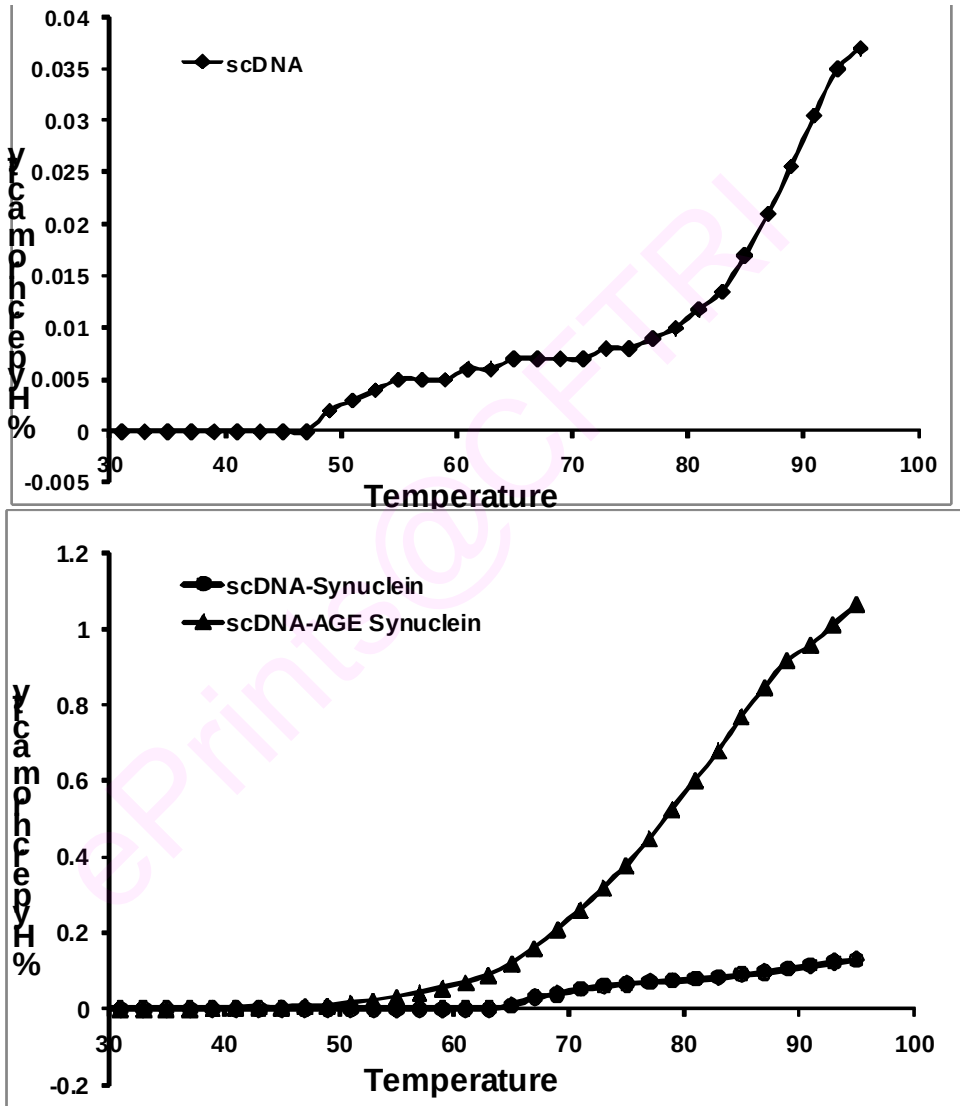

Figure 4B.8: Melting Temperature (T_m) profile of α-Synuclein and AGE α-Synuclein interaction with scDNA. T_m values of scDNA were T_{m1} = 54°C and T_{m2} = 86°C. Both α-Synuclein and AGE α-Synuclein converted biphsic Tm to monophasic Tm with 77°C and 79°C respectively.

4B.4.9 Ethidium bromide (EtBr) binding studies

The integrity of scDNA was studied by indirectly measuring the number of EtBr molecules bound per base pair using Scatchard plot. The number of EtBr molecules bound per base pair of scDNA was 0.28. The number of EtBr molecules bound per base pair of DNA for scDNA-α-synuclein and scDNA-AGE α-synuclein were 0.21 and 0.2 respectively (Fig.4B.9) The decrease in number of EtBr molecules bound per base pair indicated the binding of α-synuclein and AGE α-synuclein to scDNA.

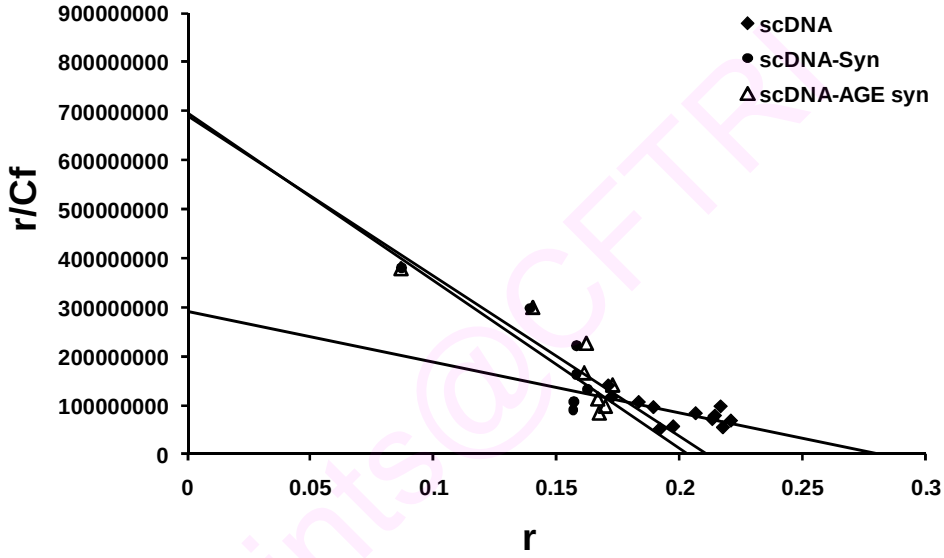

Figure 4B.9: scDNA was incubated with α-Synuclein and AGE α-Synuclein in the mass ratios of 1 : 4 in 10mM Tris-Hcl (pH 7.4) at 37°C for 12 hr. Ethidium bromide binding pattern to incubated samples along with the control scDNA is investigated by titrating with increasing concentration of EtBr. Using scatchard plot EtBr molecules bound / base pair are calculated. The number of EtBr molecules bound per base pair of scDNA, scDNA-α-synuclein and scDNA-AGE α-synuclein were 0.28, 0.21 and 0.2 respectively.

4B.4.10 DNAse I Sensitivity assay

The integrity of scDNA upon binding of α-synuclein and AGE-α-synuclein was studied by DNase I sensitivity assay. scDNA treated with DNase I showed increase in

the fluorescence indicating digestion of scDNA by DNAse I. scDNA-α-synuclein and scDNA-AGE-α-synuclein complexes treated with DNAse I showed static fluorescence intensity without much difference with time. Both scDNA-α-synuclein and scDNA-AGE-α-synuclein showed resistence to DNAse I (Fig.4B.10).

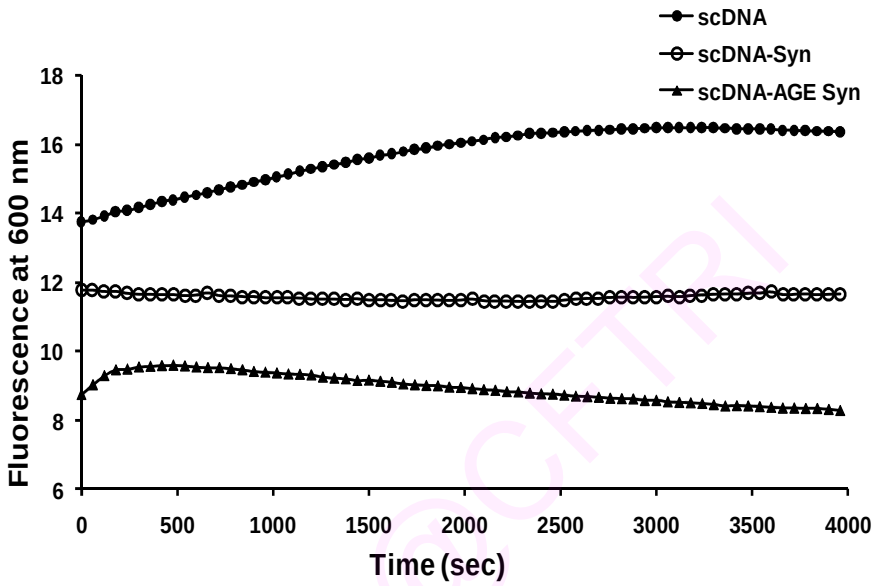

Figure 4B.10 DNase I sensitivity assay

Discussion

α-Synuclein is involved in the pathology of Parkinson's disease. α-Synuclein protein aggregates and forms LBs in the brains of Parkinson's disease (Spillantini et al., 1997). Recently, the role of α-synuclein in the nucleus has been focused. α-Synuclein was shown to interact with DNA and histone proteins in the nucleus altering the normal functions of DNA. It may also form advanced glycated α-synuclein under PD conditions. In this context, we analysed the effect of α-Synuclein and of AGE-α-Synuclein on DNA supercoiling taking pUC18 plasimd supercoiled DNA as our model system. Recent report by Choi and Lim showed that AGEs are formed in MPTP-intoxicated mouse model of Parkinson's disease (Choi and Lim, 2010). The AGEs formation was more in the substantia nigra region (region showing more neurodegeneration and Lewy bodies in PD brain) and showed more oligoformic form of α-synuclein. All the above studies indicated that α-synuclein may also get glycated

in the Parkinson's disease condition. In this context the role of glycation in the pathology of α-synuclein becomes important in PD.

α-Synuclein was glycated using methylglyoxal (MGO) as a glycating agent. MGO is formed as an intermediate of glucose during Maillard and Schiff's base formation in all tissues including brain and more so during high glucose conditions and oxidative stress. Oxidative stress was noticed in the early stages of Parkinson's disease. Glutathione (GSH) was involved in the detoxification of methylglyoxal and its levels are significantly decreased in the sunstantia nigra of PD patients (Sian et al., 1994). AGE-α-synuclein had similar random coil conformation as that of α-synuclein (Fig.4B.2) indicating that α-synuclein did not get aggregated during formation of AGE-α-synuclein.

Hegde et al. for the first time reported that α-synuclein bind to DNA and it is a novel property (Hegde et al., 2003). Other studies also reported the DNA binding ability of α-synuclein and DNA binding property of α-synuclein has been focused in the pathogenesis of PD and in normal cellular conditions. Hegde et al. showed that α-synuclein alters the DNA conformation from B-form to altered B-form and also uncoils the supercoiled DNA to open circular form (Hegde et al., 2003). As α-synuclein was co-localized with AGEs in PD brains, in the present study we analyzed the role of glycation on the DNA binding property of α-synuclein. It was shown that DNA binding alters the aggregation properties of α-synuclein but there are no reports showing the effect of glycation on DNA binding properties (Hegde et al., 2010; Cherny et al, 2004). Plasmid supercoiled DNA, pUC18 DNA was selected as model system for the DNA binding studies. Plasmid supercoiled DNA is analogous to eukaryotic small supercoiled DNA pockets and is known to be involved in the gene expression. AGE-α-synuclein also uncoiled the supercoiled DNA to open circular form similar to that of native α-synuclein. Magnesium (co-factor for endonucleases) enhanced both α-synuclein and AGE-α-synuclein nicking activity. ATA inhibited the α-synuclein nicking activity, but also prevented the AGE-α-synuclein nicking activity. AGE-α-synuclein induced conformational change in scDNA from B-form to B-C-A mixed conformation similar

to that of native α-synuclein. AGE-α-synuclein alters DNA integrity as evidenced by the melting temperature, ethidium bromide and DNAse I sensitivity studies. AGE-α-synuclein converted biphasic T_m to higher monophasic T_m similar to that of native α-synuclein. The T_m of AGE-α-synuclein-scDNA complex was more than that of α-synuclein-scDNA complex, indicating that AGE-α-synuclein stabilized the uncoiled scDNA compared to α-synuclein. AGE-α-synuclein and α-synuclein stabilizing the uncoiled scDNA was indicated by the decrease in the number of ethidum bromide binding molecules per base pair of DNA. DNAse I sensitive studies showed that both AGE-α-synuclein-scDNA and α-synuclein-scDNA were resistant to DNAse I digestion indicating their stabilizing effect on DNA.

In conclusion, our studies indicate AGE-α-synuclein binds to supercoiled DNA and relaxes the supercoils in the DNA molecule similar to α-synuclein. It also induces change in the secondary conformation of scDNA converting B-form of DNA into A-form of DNA. The association of AGE-α-synuclein with DNA and altering the secondary conformation suggests that AGE-α-synuclein may alter the chromatin structure in the nucleus. It may indicate that AGE-α-synuclein binds to DNA and stabilize DNA similar to that of native α-synuclein. Glycation of α-synuclein may results aggravation of pathological events occurring in parkinson's disease. Further *in vivo* studies in animal models are required to establish the pathological role of AGE-α-synuclein.

Chapter 4C

New evidence on neuromelanin from the substantia nigra of Parkinson's disease altering the DNA topology

4C.1 Introduction

Neuromelanin (NM) is an insoluble pigment found in neurons of specific brain regions of several animal species including humans. Neurons rich in NM are found especially in the substantia nigra (SN) and locus coeruleus (LC) (Nicolaus, 2005; Graham, 1979). The loss of neuromelanin containing cells within substantia nigra and the presence of large aggregates of neuromelanin suggest its role in Parkinson's disease (Hirsch et al., 1989). NM is formed by the oxidative polymerization of dopamine and noradrenaline with the involvement of cysteinyl derivatives (Fedorow et al, 2005). Neuromelanin is a multiplayer complex polymeric molecule consists of overlapped sheets of dihydroxyindole and benzothiazine rings (Odh et al., 1994). Neuromelanin molecule is composed of melanic, aliphatic, and peptide residues (Zecca et al., 2000; Zecca et al, 2001; Wakamatsu, 2003). The strong chelating ability of neuromelanin is due to dihydroxyindole groups present in the neuromelanin (Zecca et al., 1996). NM accumulates variety of metals, especially it accumulates large amount of iron in it (Zecca et al., 2003; Doubleet al., 2003). NM has high storage capacity for toxic metal and not reached to saturation point in SN of PD (Zecca et al., 1994; shima et al., 1997). NM is changed in the PD brain compared to the age matched controls (Fasano et al., 2006a; Fasano et al, 2006b). NM concentrations reduced up to 50% in PD compared to age matched controls (Zecca et al., 2002). NM can interact with peptides and lipids (Zecca et al., 2000).

It was hypothesized that NM may have ability to interact with DNA similar to amyloid β-peptides (Rao et al., 2006). However, there is no data to validate this hypothesis. The present work tries to answer, whether NM interacts with DNA like amyloid. The work focusses on the following aspects. a) Does NM binds to DNA? b) if it binds, does it alters the conformation of DNA? c) Does NM alters the stability of DNA? d) does NM damage DNA by itself, if so what is the mechanism? In the present study we have used three types of NM , 1) NM (PD-SN), isolated from the substantia nigra of PD brain. 2)

NM (N-SN), isolated from the substantia nigra of normal brain and 3) DAC, synthetic neuromelanin.

4C.2 Materials

Supercoiled pUC18 DNA (cesium chloride purified, 90% supercoiled structure, scDNA), was purchased from Banglore Genei, India. Agarose, HEPES, Tris and EDTA were purchased from SISCO Research laboratories. Ethidium bromide, ATA and $MgCl_2$ were from Sigma (USA) chemicals. NM (PD-SN), NM (N-SN) isolated from the human brains. DAC were gift from DR. Luggi Zecca from Italy.

4C.3 Methodology

4C.3.1 Agarose gel studies of neuromelanin-DNA interactions

scDNA (0.5 ug) was interacted with different concentrations of NM-SN (Neuromelanin isolated from substantia nigra of PD brain) and analyzed by agarose gel electrophoresis. scDNA was incubated with NM-SN with the increasing concentrations of neuromelanin 50 ng, 250 ng, 500 ng, 1.25 µg and 2.5 µg for 12 hr in 1 mM Tris-Hcl (pH 7.4) at 37°C. After incubation the samples were loaded on 1% agarose gel and electrophoresis was carried out at 50 V at room temperature for 5 hr along with the control scDNA, linear DNA and super coiled DNA marker. Gel was stained with ethidium bromide (EtBr) for 1 hr in cold condition (4°C) and scanned using gel documentation system. Similarly, scDNA was incubated with NM-C (Neuromelanin isolated fro the cortex of PD brain) with increasing concentrations of NM-C, 50 ng, 100 ng, 250 ng, 500 ng, 750 ng, 1 µg, 1.25 µg, and 2.5 µg for 12 hr in 1 mM Tris-Hcl (pH 7.4) at 37°C and analyzed by agarose gel electrophoresis. scDNA was incubated with DAC (synthetic neuromelanin) with the increasing concentrations of neuromelanin 50 ng, 250 ng, 500 ng, 1.25 µg and 2.5 µg for 12 hr in 1 mM Tris-HCl (pH 7.4) at 37°C and analyzed by agarose gel electrophoresis.

.

4C.3.2 Circular dichroism studies

The secondary conformation of native scDNA and scDNA in the presence of NM were recorded on JASCO J700 spectropolarimeter at 25°C, with 2mm cell length in the

wavelength range between 200-320 nm in Tris-Cl buffer (5 mM, pH 7.4). **(i)** CD spectra of scDNA was recorded in the presence of increasing concentrations of NM (PD-SN) in the mass ratio 1: 0.5, 1: 1, 1: 2.5 and 1: 5 of scDNA : NM-SN along with control scDNA. Each spectrum is the average of four scans. **(ii)** CD spectra of scDNA was recorded in the presence of increasing concentrations of NM-C in the mass ratio 1: 0.002, 1: 0.2, 1: 2, 1: 5, 1: 10 of scDNA : NM-C along with control scDNA. **(iii)** CD spectra of scDNA was recorded in the presence of increasing concentrations of DAC in the mass ratio 1: 0.1, 1: 1, 1: 2.5, 1: 5, 1 : 10 of scDNA : DAC along with control scDNA.

4C.3.3 Thermal denaturation studies: The integrity of scDNA in the presence of NM (PD-SN), NM (N-SN) and DAC were studied using thermal denaturation studies. scDNA was incubated with 0.5 μg, 1.25 μg and 2.5 μg of NM (PD-SN), NM (N-SN) and DAC in the mass ratio 1:5 for 12 hr in 10 mM HEPES buffer (pH 7.4). The melting temperature profiles of the incubated samples were recorded in HEPES buffer (10mM, pH 7.4) using spectrophotometer equipped with a thermostat programmer and data processor (Amarsham Biosciences, HongKong). The melting profiles were recorded with increase of 1°C/min in the temperature range of 25-95°C.

4C.3.4 Ethidium bromide binding studies: The effect of neuromelanin binding on the integrity of scDNA was studied by ethidium bromide binding study. Ethidium bromide (EtBr) bound in moles per base pair of scDNA was measured in Tris-Cl (10mM, pH 7.4) using HITACHI F-2000 Fluorescence Spectrofluorimeter. The fluorescence was measured using a constant amount of scDNA (0.5 μg) with increasing EtBr. The fluorescence measurements were monitored with an excitation at 535 nm and emission at 600 nm with 10 mm path length.

The maximum amount of EtBr bound per base pair of DNA was calculated using Scatchard plots of 'r' vs 'r/Cf', in the DNA- EtBr reaction mixture at various titration intervals when increasing amount of EtBr was titrated to constant amount of DNA (Scatchard, 1949; Chatterjee and Rao, 1994). The concentration of bound EtBr in 1.0 mL dye-DNA mixture (Cb′) were calculated using the equation:

$Cb' = Co'[(F-Fo)/(V \times Fo)]$

Where,

Co = EtBr (pmoles) present in the dye-DNA mixture,

F = observed fluorescence at any point of dye-DNA mixture,

Fo = observed fluorescence of EtBr with no DNA,

V = experimentally derived value, ratio of bound EtBr/free EtBr at saturation point.

The concentration of free dye (Cf´) was then calculated by the relation

Cf´ = Co´- Cb´,

Where, Cf´, Co´, and Cb´ were expressed in pmoles. The amount of bound EtBr/base pair 'r' was calculated by

r = Cb´ (pmoles)/DNA concentration (pmoles of base pair).

A plot with r vs r/cf is plotted, point where the straight line intersects the X-axis is denoted as 'n'. 'n' is the maximum amount of dye bound per base pair (n), where Cf = Cf´ × 10^{15} M.

4C.3.6 Characterization of DNA nicking property of NM-SN

Time kinetics: scDNA was incubated with NM (SN) at the concentration of 5 μg, for the time intervals of 12hr, 24hr, 36hr and 48hr.

Effect of Mg^{2+} : scDNA interacted with NM (SN) in the presence of 1 mM Mg^{2+} for the time intervals of 12hr, 24hr, 36hr and 48hr. Mg^{2+} at 1 mM acts as co-factor for endonuclease.

Effect of ATA on DNA nicking activity of NM (SN) : scDNA interacted with NM SN, and MM-SN + 1 mM Mg^{2+} in the presence of a specific nuclease inhibitor Aurinetricarboxylic acid (ATA) (1 mM) for the time intervals of 12hr, 24hr, 36hr and 48hr. The samples after the incubated time intervals analyzed on 1% agarose gel.

4C.4 Results

4C.4.1 NM-scDNA interaction studies

scDNA gives two bands on 1% agrose gel, The band SC indicates supercoiled form and is around 85%, OC indicates open circular band (OC) which is around 15% (Fig 4C.1A

, lane a). L, indicated the stranded linear DNA (E.co R I digest of scDNA). **(i)** NM-SN converted scDNA into open cirular form at the concentration of 2.5 μg (lane 7). At lower concentrations of NM-SN (50 ng. 250 ng, 500 ng and 1.25 μg) NM-SN does not converted scDNA into open cirular form (Fig4C. 1A). **(ii)** NM-C did not affect the integrity of scDNA as evident by similar agarose gel electrophoresis pattern as compared to control (Fig 4C.1B). **(iii)** DAC did not alter the scDNA and open cirular DNA mobility in agarose electrophoresis (Fig 4C.1C).

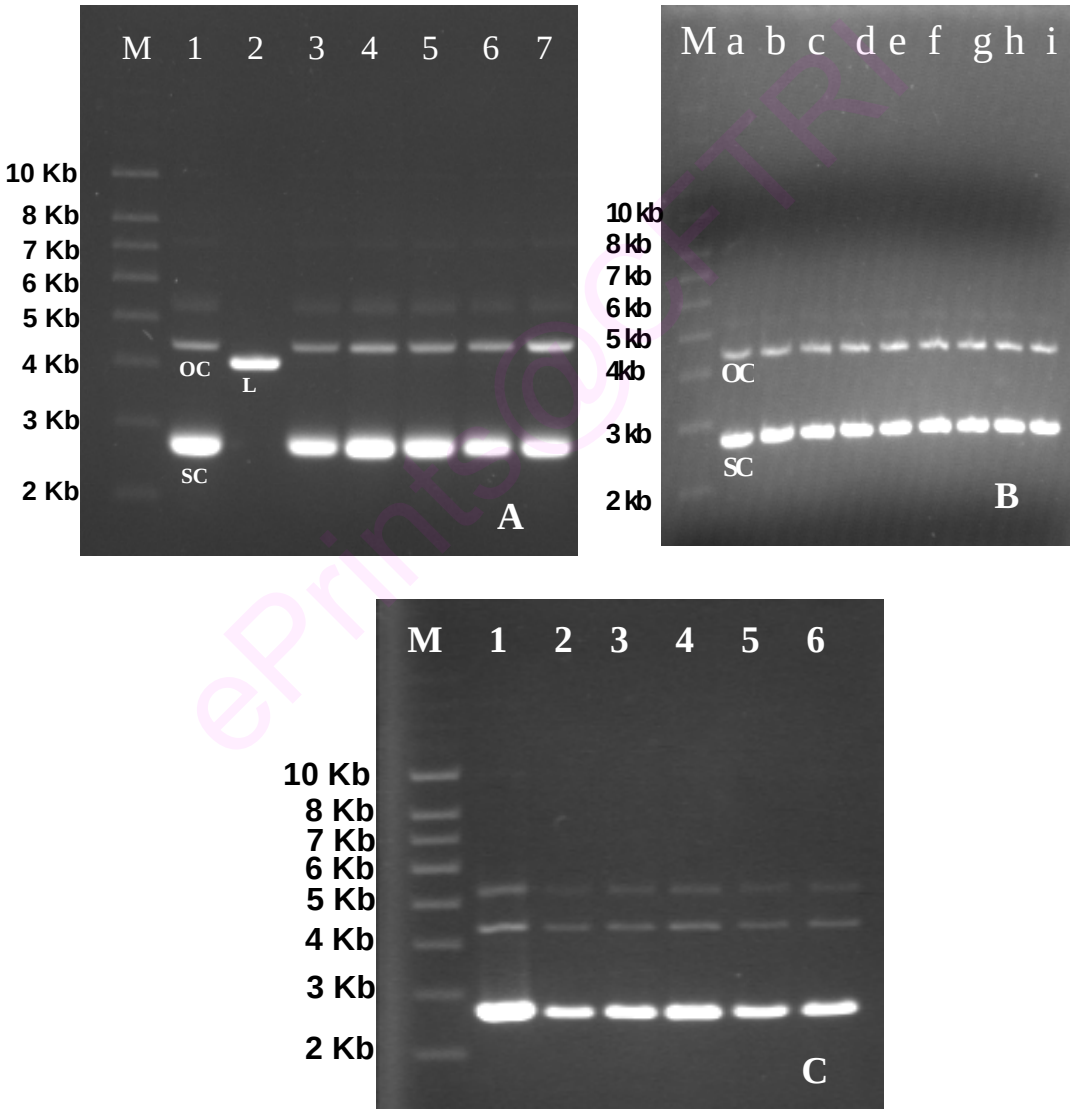

Figure 4C.1: Electrophoretic mobility shift assay : **(A)** scDNA was incubated with NM-SN with the increasing concentrations of neuromelanin 50 ng (3), 250 ng (4), 500

ng (5), 1.25 μg (6) and 2.5 μg (7) for 12 hr in 1 mM Tris-Hcl (pH 7.4) at 37°C and analyzed on 1% agarose gel along with marker (M), scDNA alone (1) and Linear DNA (2). (B) scDNA was incubated with NM-C with 50 ng (b), 100 ng (c), 250 ng (d), 500 ng (e), 750 ng (f), 1 μg (g), 1.25 μg (h) and 2.5 μg (i) **(D)** scDNA was incubated with synthetic neuromelanin DAC7with 50 ng (2), 250 ng (3), 500 ng (4), 1.25 μg (5) and 2.5 μg (6) for 12 hr in 1 mM Tris-Hcl (pH 7.4) at 37°C and analyzed on 1% agarose gel along with marker (M) and scDNA alone (1).

4C.4.2 Neuromelanin induced conformational change in scDNA

(i) In CD spectrum, scDNA showed a characteristic of B-DNA having the positive peak at 272 nm and a negative peak at 245nm (Fig 4C.2a). In the presence of NM-SN, scDNA conformation is altered. NM-SN caused a decrease in the 275 positive peak with no significant change at 245nm. Also there is a decrease in negative peak at 220 nm and 210 nm in the presence of NM (PD-SN). This kind of change is associated with B-C-A form of the DNA (Fig 4C.2). **(ii)** In the presence of NM-C, scDNA conformation altered. NM caused a decrease in the 275nm positive peak and increase in the 245 negative peak of the CD signal. The alteration in the intensity of peaks increased as the concentration of the NM increased (Fig 4C.3). This kind of change is associated with altered B-form of the DNA. **(iii)** In the presence of DAC, scDNA conformation altered. DAC caused an increase in the 245 negative peak of the CD signal (Fig 4C.4). This kind of change is associated with altered B-form of the DNA.

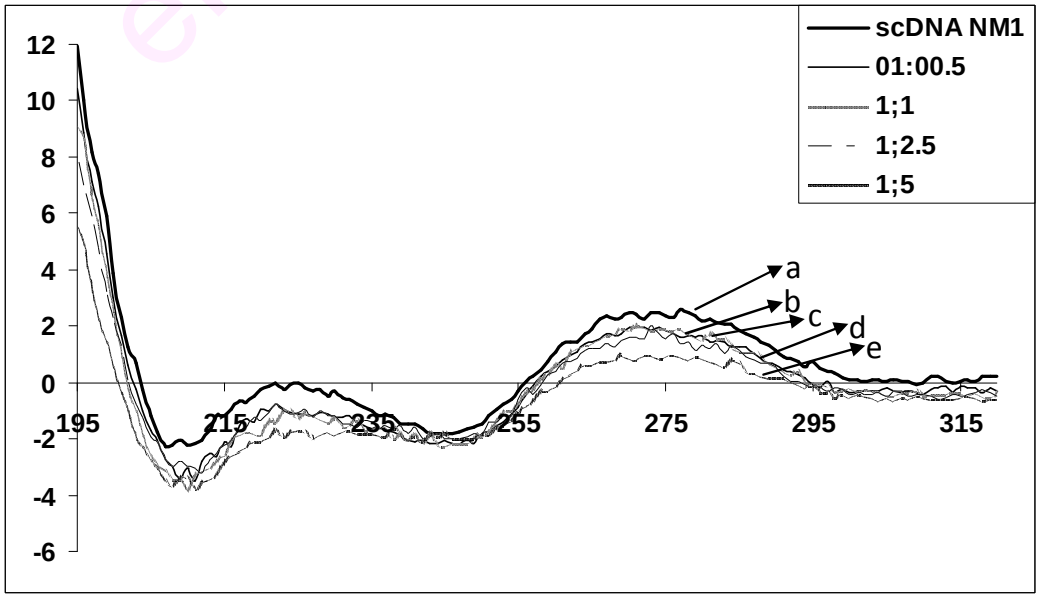

Figure 4C.2: CD spectroscopy of scDNA-NM-SN interaction. scDNA was titrated against increasing concentrations of NM-SN in the mass ratios 1: 0.5 (b), 1: 1 (c), 1: 2.5 (d) and 1: 5 (e) of scDNA : NM-SN along with control scDNA. Each spectrum is the average of four scans.

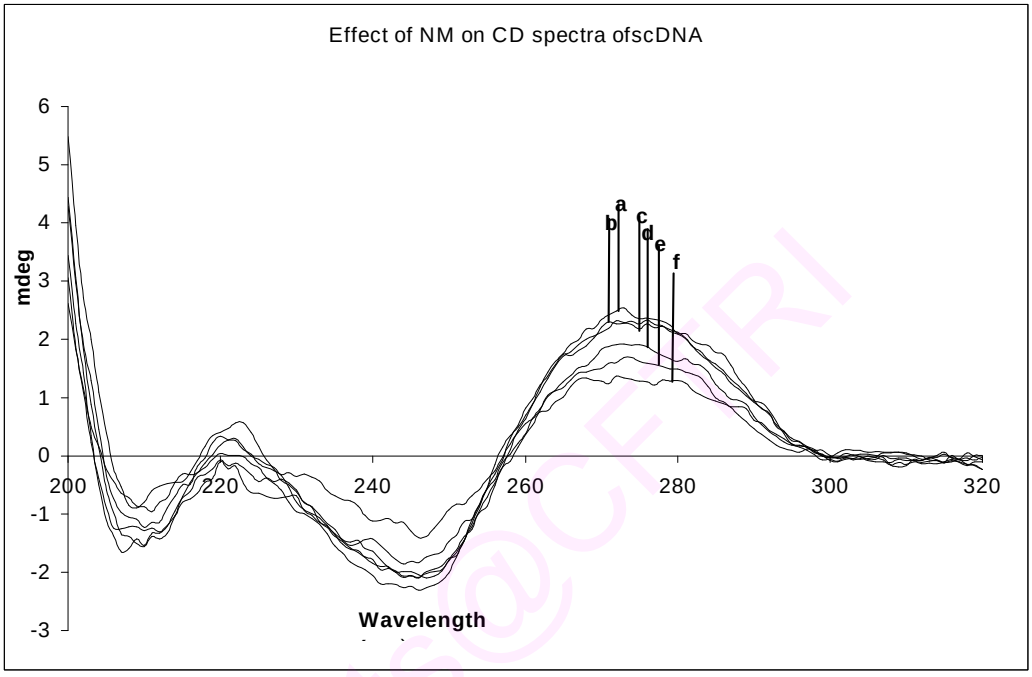

Figure 4C.3: CD Spectra of scDNA was recorded in the presence of increasing concentrations of NM-C in the mass ratio 1: 0.002 (b), 1: 0.2 (c), 1: 2 (d), 1: 5 (e), 1: 10 (f) .

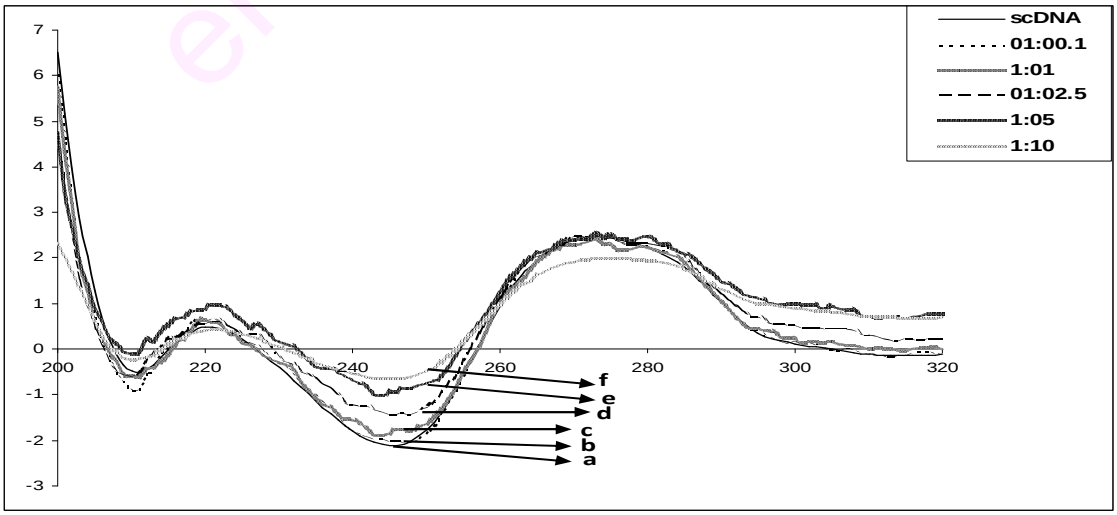

Figure 4C.4: CD Spectra of scDNA was recorded in the presence of increasing concentrations of DAC in the mass ratio 1: 0.1 (b), 1: 1 (c), 1: 2.5 (d), 1: 5 (e), 1;10 (f)

4C.4.3 Thermal denaturation studies

The melting temperature (T_m) profile of scDNA shows the characteristic biphasic pattern. The first transition (T_{m1}) is being the relaxation of supercoils in the scDNA and the second transition (T_{m2}) correspond to the opening of the double strands into single strands. The T_m values of scDNA are T_{m1} = 47°C and T_{m2} = 89°C. In the presence of NM-SN, characteristic biphasic pattern scDNA changed to monophasic. The melting temperature of scDNA in the presence of 1µg and 2.5 µg of NM-SN are T_m = 89°C and T_m = 89°C respectively. **(2)** The T_m values of scDNA are T_{m1} = 47°C and T_{m2} = 87°C. In the presence of 2.5 ug of NM-C, characteristic biphasic pattern scDNA did not alter. Both T_m values increased in the presence of 2.5 µg of NM-C, having T_{m1}=48°C and T_{m2} = 88°C. **(3)** The T_m values of scDNA are T_{m1} = 47°C and T_{m2} = 87°C. In the presence of 2.5 ug of DAC, characteristic biphasic pattern scDNA did not alter. Both T_m values increased in the presence of 2.5 µg of DAC, having T_{m1}=48°C and T_{m2} = 88°C.

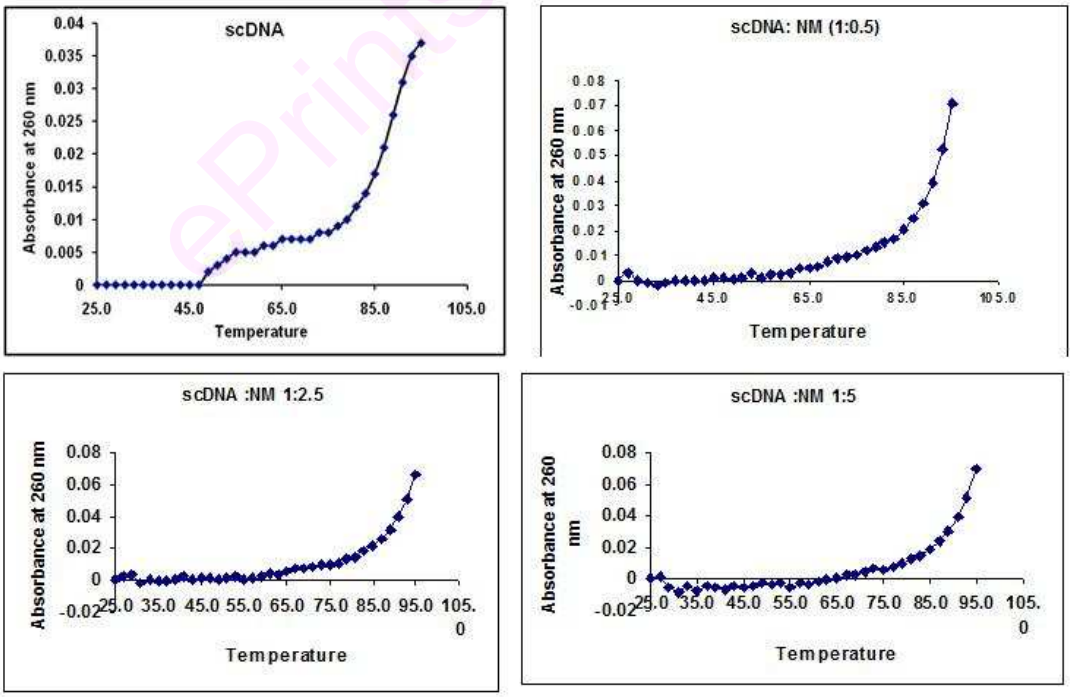

Figure 4C.5: scDNA was incubated with 0.5 µg, 1.25 µg and 2.5 µg of NM-SN in the mass ratio 1:1, 1:2.5, and 1:5 for 12 hr in 10 mM HEPES buffer (pH 7.4). The melting temperature profiles of the incubated samples were recorded in HEPES buffer (10mM, pH 7.4) using spectrophotometer equipped with a thermostat programmer and data processor (Amarsham Biosciences, HongKong).

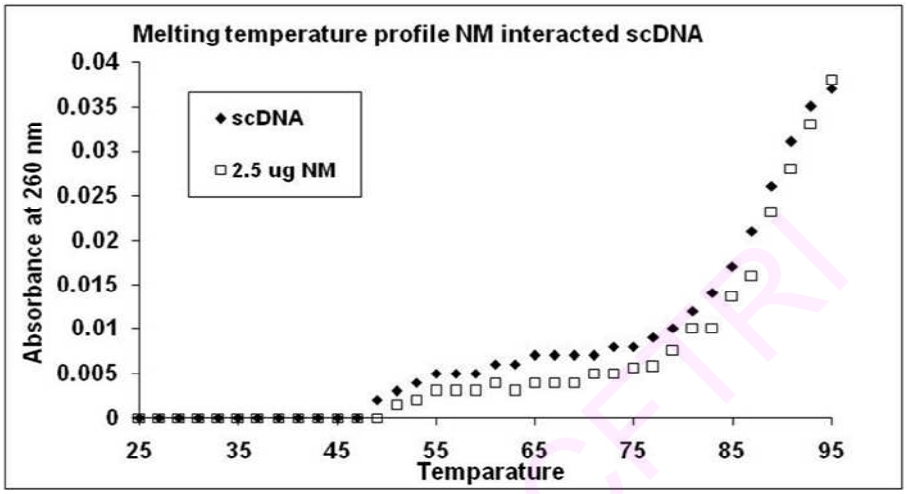

Figure 4C.6: scDNA was incubated with 2.5 µg of NM-C in the mass ratio 1:5 for 12 hr in 10 mM HEPES buffer (pH 7.4). The melting temperature profiles of the incubated samples were recorded in HEPES buffer (10mM, pH 7.4) using spectrophotometer equipped with a thermostat programmer and data processor (Amarsham Biosciences, HongKong).

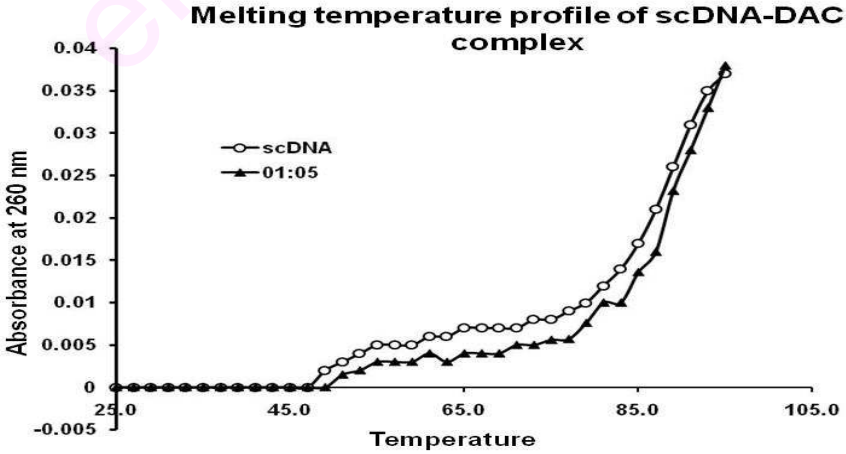

Figure 4C.7: scDNA was incubated with 2.5 µg of DAC in the mass ratio 1:5 for 12 hr in 10 mM HEPES buffer (pH 7.4). The melting temperature profiles of the incubated samples were recorded in HEPES buffer (10mM, pH 7.4) using spectrophotometer equipped with a thermostat programmer and data processor (Amarsham Biosciences, HongKong).

4C.4.4 Ethidium bromide binding studies

The integrity of scDNA is studied by indirectly measuring the number of EtBr molecules bound per base pair using Scatchard plot. The number of EtBr molecules bound per base pair of scDNA was 0.26. In the presence of NM-SN the number of EtBr molecules bound /bp of are 0.28 (1:1) and 0.34 (1:5) respectively (Fig 4C.8). **(2)** The number of EtBr molecules bound per base pair of scDNA was 0.22. In the presence of NM-C the number of EtBr molecules bound / bp of are 0.25 (1:5) (Fig 4C.9) **(3)** The number of EtBr molecules bound per base pair of scDNA was 0.17. In the presence of DAC the number of EtBr molecules bound /bp of are 0.182 (1: 5) (Fig 4C.10).

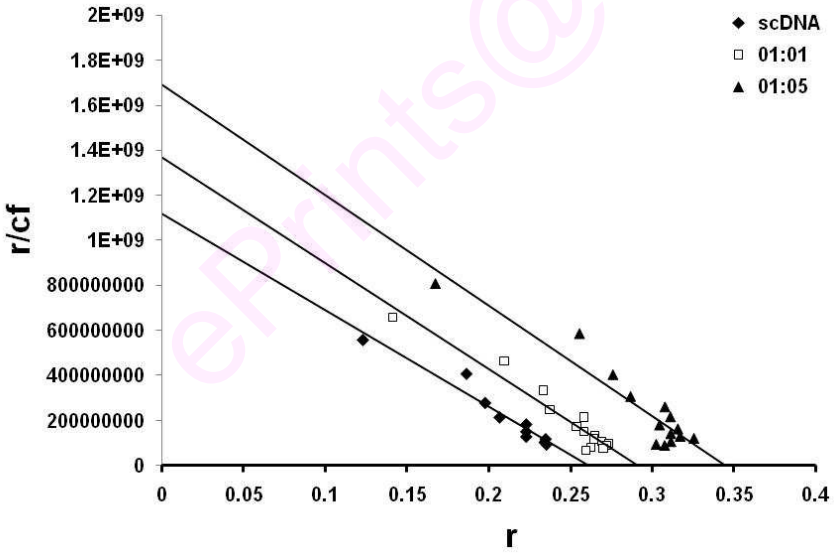

Figure 4C.8: scDNA was incubated with NM (PD-SN) in the mass ratio 1:1 and 1:5 for 12 hr in 1 mM Tris-Hcl (pH 7.4) at 37°C. Ethidium bromide binding pattern to incubated samples along with the control scDNA are investigated by titrating with increasing concentration of EtBr. Using scatchard plot EtBr molecules bound / base pair are calculated. The number of EtBr molecules bound / base pair for the mass ratios are 0.26 (1:1) and 0.34 (1:5) respectively.

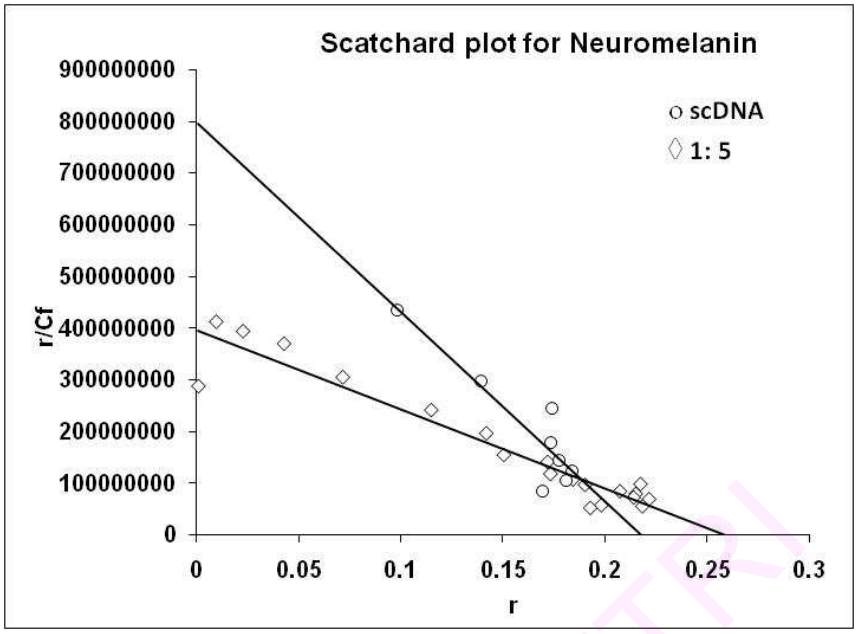

Figure 4C.9: scDNA was incubated with NM (N-SN) in the mass ratio 1:5 for 12 hr in 1 mM Tris-Hcl (pH 7.4) at 37°C. Ethidium bromide binding pattern to incubated samples along with the control scDNA are investigated by titrating with increasing concentration of EtBr. Using scatchard plot EtBr molecules bound / base pair are calculated. The number of EtBr molecules bound / base pair for the mass ratios are 0.25 (1:5).

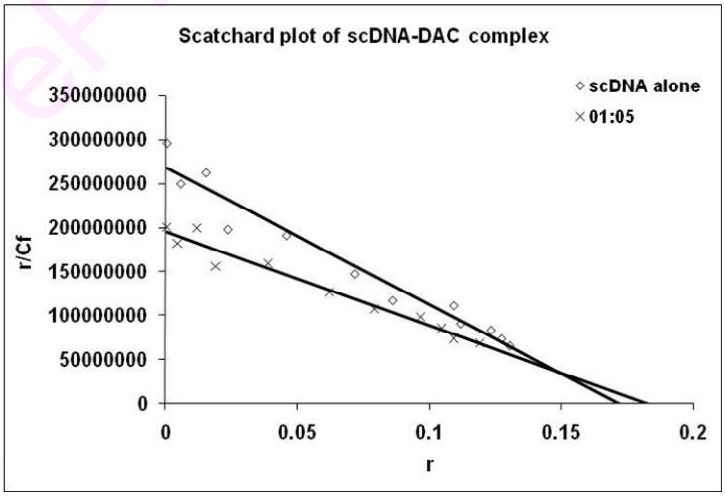

Figure 4C.10: scDNA was incubated with DAC in the mass ratio 1:5 for 12 hr in 1 mM Tris-Hcl (pH 7.4) at 37°C. Ethidium bromide binding pattern to incubated samples along with the control scDNA are investigated by titrating with increasing concentration of EtBr. Using scatchard plot EtBr molecules bound / base pair are calculated. The number of EtBr molecules bound / base pair for the mass ratios are 0.182 (1: 5).

4C.4.5 NM-SN nicking activity as a function of time and inhibition by specific nuclease inhibitor

Time kinetics: NM-SN converted scDNA into open circular form and linear form at different time intervals of 12 hr, 24hr, 36hr and 48hr (Fig 4C.11 lane 2 of A, B, C, D). The nicking activity of NM-SN increased with incubation time. At 12 hr of incubation there is no linear form formation. But at 24, 36 and 48 hr incubation time NM-SN induced linear form formation. The data suggested that NM-SN able to convert SC to OC and linear forms by nicking.

Effect of Mg^{2+} : NM-SN in the presence of Mg^{2+} ions (1mM), converted all scDNA into open circular and linear form at 12hr and 24 hr of incubation times (Fig 4C.11 lane 4 of A and B). NM-SN totally damaged the scDNA in the presence of Mg^{2+} ions (1mM) at 36 hr and 48 hr (lane 4 of C and D). Mg^{2+} (1mM) is a co-factor for endonuclease. NM-SN may be nicking the DNA like endonuclease.

Effect of ATA on DNA nicking activity of NM-SN : A specific nuclease inhibitor ATA at 1 mM prevented the conversion of SC form to OC form and linear forms indicating that ATA inhibited nicking ability of NM-SN, but not totally (Fig 4C: lane 3 and 5 of A,B,C,D). ATA inhibited the nicking activity of NM-SN on scDNA about 50 % as seen by the intensity of the bands formed. The data indicated that NM-SN might be nicking the DNA like endonuclease.

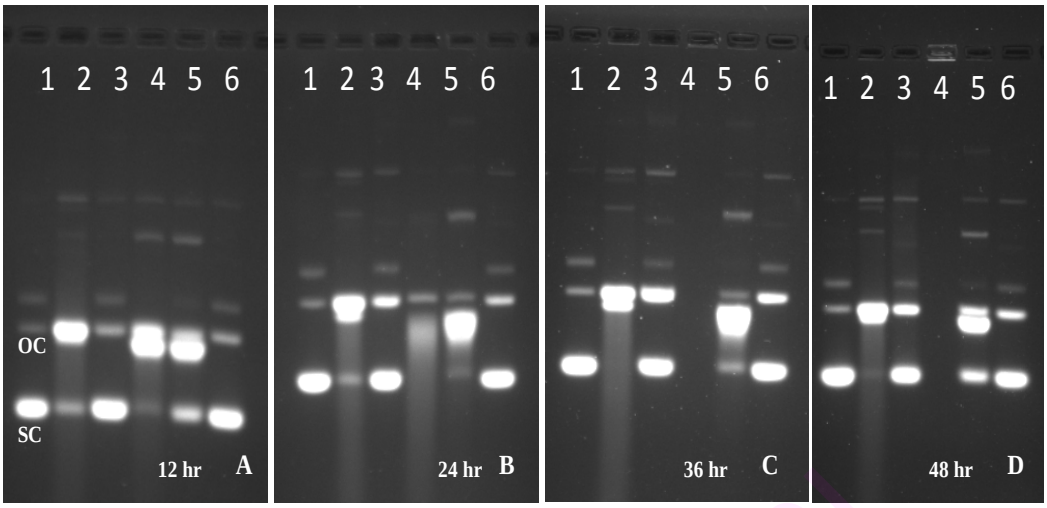

Figure 4C.11: Nuclease activity of NM-SN. NM-SN is incubated with scDNA in the presence of Mg^{2+} and ATA for 12 hr (Fig 9a), 24 hr (Fig 9b), 36 hr (Fig 9c) and 48 hr (Fig 9d). Lanes: 1. scDNA , 2. scDNA + NM-SN, 3. scDNA + NM-SN +ATA, 4. scDNA + NM-SN + Mg^{2+} 5. scDNA + Tau + Mg^{2+} + ATA. 6. scDNA+ATA.

Table 4C.1: Comparison of NM-SN, NM-C and DAC interaction with scDNA

S.N0	Experiment	NM(SN) (Neuromelanin isolated from substantia nigra of PD brain)	NM-C (Neuromelanin isolated from other brain region)	DAC7 (Synthetic neuromelanin)
1	Conformation (CD)	B-C-A mixed conformation	Altered B	Altered B
2	Gel studies	Able to convert SC to OC	No change	No change
3	Thermal denaturation	Biphasic T_m to Monophasic T_m	No change in Biphasic T_m	No change in Biphasic T_m
4	EtBr binding studies	EtBr molecules bound per base pair	EtBr molecules bound per base	No significant change in EtBr

		increased	**pair increased**	**molecules bound per base pair**
5	**Mg^{2+} 1 mM**	**Enhanced DNA nicking**	**-----**	**------**
6	**ATA (specific nuclease inhibitor)**	**Inhibited DNA nicking** **Partially inhibited NM nicking in the presence of Mg**	**--------**	**-------**

4C.5 Discussion

Neuromelanin is found in the form of large granules in the substantia nigra of PD brain. NM is believed to be involved in the pathogenesis of PD. It was hypothesized that NM can interact with DNA like Aβ peptides. In the present study, interaction of three different neuromelanins (NM-SN, NM-C and DAC) with scDNA as model system was analyzed. Three different neuromelanins are , NM-SN isolated from the substantia nigra of PD brain, NM-C isolated from the cortex of the PD brain and DAC a synthetic neuromelanin.

Agarosegel electrophoresis has shown that NM-SN isolated from the substantia nigra of PD brain, able to convert scDNA to open circular form (Fig4C.1, lane 7) indicating that NM-SN can bind to DNA. While, NM-C and DAC did not show any ability to convert scDNA into open circular form indicating these two compounds may or may not bind to DNA. NM-SN nicking activity enhanced with time (Fig 4C.11, lane 2 of A, B, C, D)

NM-SN induced B-C-A mixed conformation in scDNA, where as NM-C and DAC induced altered B-conformation in scDNA. Conformation studies indicated that NM-SN, NM-C and DAC bind to DNA.

scDNA has biphasic melting temperature profile having two melting temperatures T_{m1} and T_{m2} . NM-SN changed the biphasic T_m to monophasic $T_{m.}$ NM-C isolated from the

normal brain retained biphasic $T_{m.}$ Synthetic neuromelanin DAC also retained biphasic T_m. Both NM-SN and NM-C increased the number of EtBr molecules bound per base pair of DNA. Whereas DAC did not show significant change in the EtBr molecules bound per base pair of DNA. The above data indicated that all neuromelanin molecules NM-SN, NM-C and DAC altered the stability of DNA and NM-SN had high potential in altering DNA stability.

NM-SN converted scDNA into open circular form, where NM-C and DAC could not convert scDNA into open circular. This indicated that NM isolated from the substantia nigra of PD brain could damage the DNA by nicking. To investigate by which mechanism NM-SN could induce DNA nicking, it was analyzed DNA nicking in the presence of Mg^{2+} and ATA. Mg^{2+} at 1 mM acts as co-factor for the endonuclease. Mg^{2+} enhanced the DNA nicking of NM-SN. ATA is a specific nuclease inhibitor inhibited the DNA nicking activity of NM (PD-SN) only. ATA partially inhibited the DNA nicking activity of NM-SN in the presence of Mg^{2+}. The above data indicated that NM-SN might damage the DNA by inducing nicks in DNA like endonuclease.

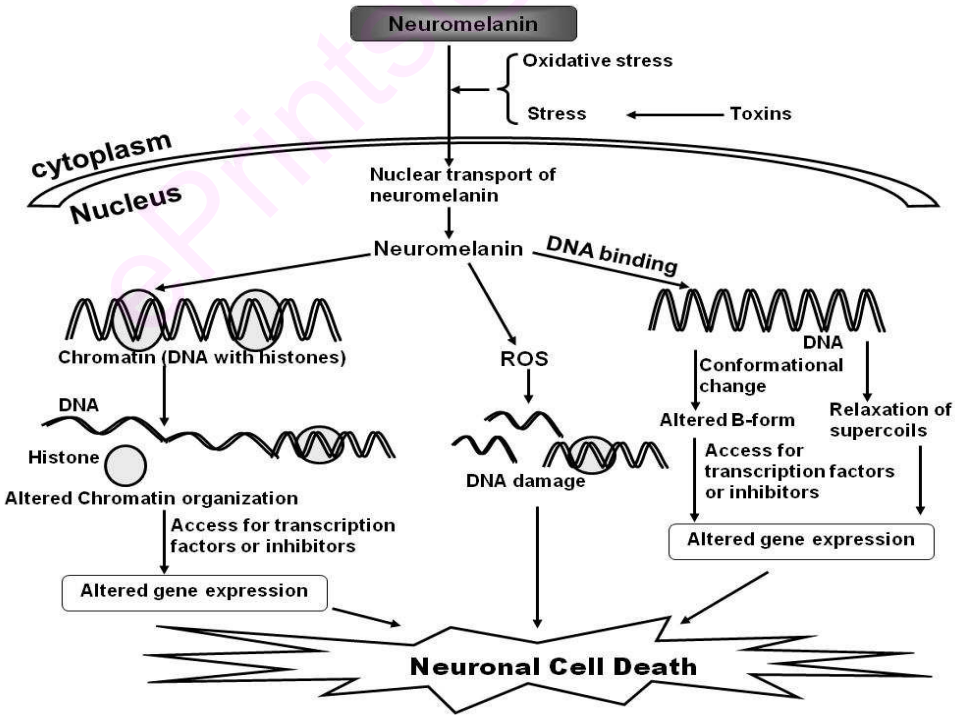

Figure 4C.12 : Hypothesis on neuromelanin induced neuronal cell death

Chapter 4D

New evidence on α-Synuclein and Tau binding to conformation and sequence specific GC* rich DNA: relevance to neurological disorders

4D.1 Introduction

The DNA conformation and stability are very important for the normal cell functions. DNA is polymorphic in nature and adopts different conformations in the cell in different physiological conditions (Rich, 1993). The altered conformation in DNA results in the altered gene expression (Bacolla and Wells, 2009). The role of DNA dynamics in neurodegeneration is not clearly understood (Hegde et al, 2010; Vasudevaraju et al, 2008). Earlier studies from our lab have shown that genomic integrity is altered in Parkinson's disease (PD) and Alzheimer's Disease (AD) (Hegde et al, 2006; Suram et al, 2002). The genomic DNA in PD is altered from B-form to altered B conformation (Hegde et al, 2006), while in AD, genomic DNA is altered from B-form to Z-form (Suram et al, 2002). The biological factors responsible for DNA dynamics change are not clear. We hypothesize that neuroproteins like α-Synuclein and Tau may be involved in the conformational and stability transitions in DNA (Vasudevaraju et al, 2008; Hegde et al, 2003). Further in support of our hypothesis, we have evidences on the nuclear localization of α-Synuclein and Tau (Loomis et al, 1990; Maroteaux, 1988), but the studies related to DNA binding abilities are limitted (Hegde et al, 2003; Hegde et al, 2007). α-Synuclein (144 aa) is involved in the pathogenesis of Parkinson's Disease (PD) (Bisaglia et al, 2009). α-Synuclein is highly conserved; natively unfolded protein exists in random coil conformation (Maroteaux et al, 1988; Broersen et al., 2006; Surguchov, 2008). The normal functions of α-Synuclein in the neuron is not clear (Surguchov, 2008; Waxman and Giasson, 2009). Also the mechanism of α-Synuclein toxicity in PD is not yet clearly understood (Waxman and Giasson, 2009). However, the localization of α-Synuclein in the nucleus suggests that it may interact with chromatin (Goers et al, 2003; Lin et al., 2004; Zhang et al., 2008). Unlike α-Synuclein, Tau normal functions are established. Tau main function is to polymerize and stabilize the microtubules in the neuron (Weingarten et al.,

1975). Tau is responsible for the neurofibrillary tangles (NFTs) formation in AD (Brunden et al., 2009; Spires-Jones et al, 2009). Tau protein is normally present in the cytoplasm (Weingarten et al., 1975). Tau is also found to be localized in the nuclear region and has ability to bind to DNA (Loomis et al, 1990; Davis and Johnson, 1999; Haque et al, 1999). But the mechanism of both α-Synuclein and Tau binding to DNA is not clear. In the present investigation, we propose to understand whether α-Synuclein and Tau bind to DNA in a conformation and sequence specific manner. We have selected oligonucleotide CGCGCGCG as a model DNA which natively exists in B conformation and in the presence of 4M NaCl, the oligo goes to Z conformation (Wang et al, 1987; 23). This sequence is present in the promoter region of human genome and hence has biological relevance (Antequera, 2003).

4D.2 Materials

α-Synuclein and Tau were purchased from rPeptide, USA. CGCGCGCG oligonucleotide was custom synthesized from Sigma Aldrich, USA. Tris and HEPES were purchased from Sisco Research Lab, India. The CGCGCGCG oligonucleotide, which was custom synthesized were in single standed structures. The single stranded CGCGCGCG oligonucleotide dissolved in triple distilled water and incubated in boiling water bath for 5 min and then cooled at room temperature. The oligonucleotides annealed to double stranded duplexes (Trewick and Dearden, 1994).

4D.3 Methodology

4D.3.1 Circular Dichroism (CD) studies

The Secondary conformation of oligonucleotide $(CGCGCGCG)_2$ was analyzed using Circular Dichroism (CD) spectroscopy. The $(CGCGCGCG)_2$ oligonucleotide was dissolved in Tris-Cl buffer (5 mM, pH 7.4) and CD spectrum was recorded using JASCO J700 spectropolarimeter at 25°C, with 2mm cell length in the wavelength range between 200-320 nm. Each spectrum was the average of four scans. The $(CGCGCGCG)_2$ oligonucleotide was converted from B-DNA to Z-DNA in the presence of 4M NaCl (incubated for 12 hr at 37°C). The Z-form of the oligonucleotide was confirmed by CD.

The B-form of the oligonucleotide was incubated with α-Synuclein and Tau in the mass ration of 1:2 (oligo/protein) in 10 mM Tris-HCl (pH 7.4) buffer for 12 hr at 37°C. The oligonucleotide alone (control) was also incubated in the 10 mM Tris-HCl (pH 7.4) buffer for 12 hr at 37°C. The CD spectra of the B-DNA-α-Synuclein and B-DNA-Tau complexes were recorded. Similarly, the Z-form of the oligonucleotide was incubated with α-Synuclein and Tau in the mass ratio of 1:2 (oligo/protein) in 10 mM Tris-HCl (pH 7.4) buffer for 12 hr at 37°C. The CD spectra of Z-DNA-α-Synuclein and Z-DNA-Tau complexes were recorded. The background correction was done by deducting the spectral contribution from α-Synuclein and Tau alone at the concentrations used. The DNA conformations were assigned using the standard references (Gray et al., 1995)

4D.3.2 Thermal Denaturation studies

The stability of B-DNA and Z-DNA forms of oligonucleotide and the oligo-protein complexes was studied using thermal denaturation studies and ethidium bromide binding studies. Thermal denaturation of oligonucleotide was carried out using UV-Visible Spectrophotometer equipped with thermostat control (Amarsham Bioscience, Hong Kong). The 2 μg of B-DNA and Z-DNA forms of $(CGCGCGCG)_2$ was dissolved in 10 mM HEPES buffer (pH 7.4) and melting temperature (Tm) profile was recorded with 1°C raise of temperature per minute in the temperature range of 25°C-95°C. Both, B-form and Z-form of the oligonucleotide were incubated with α-Synuclein and Tau proteins in the mass ratio of 1:2 (oligo/protein) in 10 mM HEPES (pH 7.4) buffer at 12 hr at 37°C. The T_m was calculated using the graph plotted between temperature vs absorbance, which is called as melting curve. The temperature at which the absorbance is 50% between the minimum and maximum absorbance is called as melting temperature (T_m).

4D.3.3 Ethidium Bromide (EtBr) binding studies

For the above samples as mentioned in Tm studies, the EtBr bound in moles per base pair of DNA was measured in Tris-Cl (10mM, pH 7.4) using HITACHI F-2000 Fluorescence Spectrofluorimeter. The fluorescence was measured using a constant amount of scDNA

(0.5 μg) with increasing amounts of EtBr. The fluorescence measurements were monitored with an excitation at 535 nm and emission at 600 nm using 10 mm path length.

The maximum amount of EtBr bound per base pair of DNA was calculated using Scatchard plots of 'r' vs 'r/Cf' [Chatterjee and Rao, 1994; Scatchard 1949). The concentration of bound EtBr in 1.0 mL dye-DNA mixture (Cb′) was calculated using the equation:

Cb´ = Co´[(*F*-*Fo*)/(*V*×*Fo*)]

Where,

Co = EtBr (pmoles) present in the dye-DNA mixture,

F = observed fluorescence at any point of dye-DNA mixture,

Fo = observed fluorescence of EtBr with no DNA,

V = experimentally derived value, ratio of bound EtBr/free EtBr at saturation point.

The concentration of free dye (Cf´) was then calculated by the relation

Cf´ = Co´- Cb´,

Where, Cf´, Co´, and Cb´ were expressed in pmoles. The amount of bound EtBr/base pair 'r' was calculated by

r = Cb´ (pmoles)/DNA concentration (pmoles of base pair).

A plot with r vs r/cf is plotted, point where the straight line intersects the X-axis was denoted as 'n'. 'n' was the maximum amount of dye bound per base pair (n), where Cf = Cf´ × 10^{15} M.

The number of EtBr molecules bound per base pair DNA was calculated for B-DNA and Z-DNA in the presence and absence of synuclein and Tau. The data was analyzed using Scatchard plots.

4D.4 Results

4D.4.1 Circular Dichroism (CD) studies

The CD spectra of native $(CGCGCGCG)_2$ showed a characteristic B-DNA conformation having 280 nm positive peak and 255 nm negative peak. Further, the CD spectrum of $(CGCGCGCG)_2$ oligonucleotide in the presence of 4M NaCl showed Z-DNA formation

with characteristic 295, 208 nm negative peak showing the conversion of B-form to Z-form (Fig 4D.1a). The CD spectrum of B-form of oligonucleotide in the presence of α-Synuclein complex showed a shift in the positive peak from 280 nm to 275 nm and a decrease in the intensity of the negative peaks at 235 nm and 210 nm compared to B-form alone (Fig 4D.1b). These changes were characteristic of altered B-DNA conformation (Gray et al., 1995). Further, CD spectrum of B-DNA in the presence of Tau also showed similar changes (Fig 4D.1d). Thus it was inferred that both α-Synuclein and Tau induced altered B-DNA conformation from B-DNA. The CD spectra of Z-DNA in the presence of α-Synuclein and Tau did not alter any spectral changes of Z-form (Fig 4D.1 c and e). Both the complexes showed characteristic 290 nm negative peaks indicating that oligonucleotide in the complexes also exist in Z-DNA conformation only.

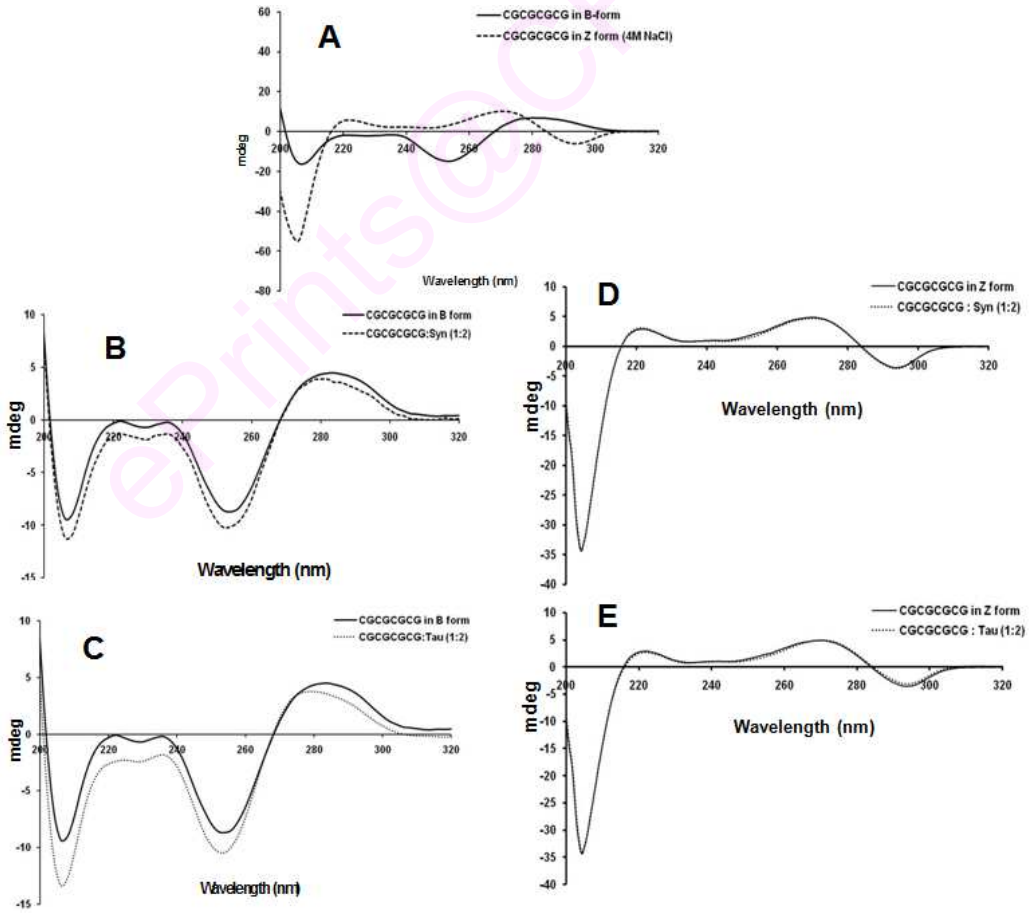

Figure 4D.1: Circular Dichroism spectroscopy of $(CGCGCGCG)_2$ oligonucleotide complexes. A. $(CGCGCGCG)_2$ oligonucleotide in B-DNA conformation and Z-DNA conformation. B. α-Synuclein induced altered B-conformation in B-DNA of $(CGCGCGCG)_2$. C. Tau induced altered B-conformation in B-DNA of $(CGCGCGCG)_2$. D. α-Synuclein - Z-DNA of $(CGCGCGCG)_2$ complex in Z-DNA conformation. E. Tau - Z-DNA of $(CGCGCGCG)_2$ complex in Z-DNA conformation.

4D.4.2 Thermal Denaturation studies

The melting temperature (T_m) of the B-form and Z-form of the oligonucleotide was 71°C and 81°C respectively. The T_m of the Z-form of the oligonucleotide was greater than the B-form, indicating that Z-form was more stable than B-form. The T_m of B-DNA in the presence of α-Synuclein and Tau was found to be similar, 77°C. The data indicated that both α-Synuclein and Tau had stabilized B-DNA as evidenced by higher Tm. The T_m of Z-DNA in the presence of α-Synuclein and Tau was 83°C. The data indicates that both α-Synuclein and Tau further stabilized the Z-conformation of the oligonucleotide (Table 4D.1).

Ethidium Bromide (EtBr) binding studies

The number EtBr molecules bound per base pair DNA for B-form and Z-form of the oligonucleotide were 0.0022 and 0.0031 respectively. This indicates that Z-DNA has more EtBr binding ability. The B-DNA were titrated against EtBr in the presence of α-Synuclein and Tau and the number EtBr molecules bound per base pair DNA were 0.0013 and 0.0021 respectively. The date indicated that the number EtBr molecules bound per base pair for complexes were less than the corresponding native B-form of oligonucleotide confirming the formation of altered B-DNA conformation in the presence of α-Synuclein and Tau. The number EtBr molecules bound per base pair DNA for Z-DNA in the presence of α-Synuclein and Tau was similar 0.0032 and this value is more that native Z-DNA (Table 4D.1).

Melting Temperature (Tm) profile		EtBr molecules bound per base pair of DNA	
Native B-DNA	**71° ± 0.42**	**Native B-DNA**	**0.0022 ± 0.00003**
Native Z-DNA	**81° ± 1.1**	**Native Z-DNA**	**0.0031 ± 0.00007**
B-DNA-α-Synuclein (1:2)	**77° ± 0.64**	**B-DNA-α-Synuclein (1:2)**	**0.00135 ± 0.00003**
B-DNA-Tau (1:2)	**77° ± 0.25**	**B-DNA-Tau (1:2)**	**0.0021 ± 0.00002**
Z-DNA-α-Synuclein (1:2)	**83° ± 0.87**	**Z-DNA-α-Synuclein (1:2)**	**0.0032 ± 0.00006**
B-DNA-Tau (1:2)	**83° ± 0.88**	**B-DNA-Tau (1:2)**	**0.0032 ± 0.00005**

Table 4D.1: The data on Melting temperature (T_m) and Ethidium bromide binding to $(CGCGCGCG)_2$- α-Synuclein and $(CGCGCGCG)_2$- Tau complexes both in B-form and Z-form. The values in parenthesis represents mass ratio. The data is average of triplicate

Discussion:

DNA was polymorphic in nature having different conformations in cells under physiological conditions (Rich, 1993). The B-DNA conformation was the normal conformation of DNA in cells having biological functions (Watson and crick, 1953). The DNA also exists in other conformations like Z, A, C under experimental conditions (Ghosh and Bansal, 2003). These alternate conformations of DNA will have altered major and minor groove patterns (Ghosh and Bansal, 2003) and this may alter gene expressions. Many transcription factors were minor grove binders (Hinoi et al, 2002). If minor grove patterns were altered in these alternative DNA conformations, then the binding abilities of proteins will change. However, the biology of alternate DNA conformations in the regulation of functions of DNA is still not clear (Bacolla and Wells, 2009). The conformation and physics of Z-DNA was widely studied but the biological implications like transcription regulation, chromatin remodeling and nucleosomal positioning were still not clear (Liu et al, 2006; Oh et al, 2002; Wang et al, 1979; Wong et al, 2007). The Z-DNA formation occurs in the stretches of alternative purine-pyrimidine residues (Li et al,

2009). And alternative purine-pyrimidine residues were widely distributed in the promoter regions of several genes (Antequera, 2003). Recent study showed that Z-DNA conformation was present in the promoter region of selected genes in the human genome (Dröge and Pohl, 1991). Also the study indicated that these alternative structures could be stabilized by some specific proteins which results in the altered gene expression (Oh et al, 2002). Another study had shown the similar kind of altered function was observed in transcription activity by T7 RNA polymerase in relevance to Z-DNA (Oh et al, 2005). This suggests that alternate DNA conformations and their specific binding molecules might affect the normal genomic functions. We presume that the similar mechanisms may be operating in neurons in neurodegeneration?. One of the examples is the Vesicular Inhibitory Amino Acid Transporter (viaat) transports GABA or glycine neurotransmitters into synaptic vesicles. This promoter activity was dependent on GC rich region which was adjacent to the SP and EGR transcription factor binding sites and any modulation in GC rich region may alter the neurobiology of GABA. In the present study, we investigated the binding ability of neuroproteins like α-Synuclein and Tau to sequence and conformation specific oligonucleotide $(CGCGCGCG)_2$. These sequences were involved in gene expression and the major component of promoter regions (Antequera, 2003; Oh et al, 2005). The present study had insighted a significant answer for the question, whether α-Synuclein and Tau bind to DNA in a conformation specific manner?. This study has great relevance in understanding the genomic biology of neurodegeneration. The earlier studies from our lab have reported the presence of altered B-DNA and Z-DNA in PD and AD brains respectively (Hegde et al, 2006; Suram et al, 2002). The normal brain has B-DNA conformation. In moderately affected AD brain, DNA is in B-Z intermediate form, while in severely affected AD brain, DNA was in Z-form (Hegde et al, 2006; Suram et al, 2002). We hypothesized whether proteins like amyloid, synuclein, Tau have any role in binding to DNA and modulating DNA topology (Vasudevaraju et al, 2008). Hegde et al., (2003) has shown that Aβ is localized in the nuclear region of AD brain and proposed a possible mechanism for Aβ playing a role in DNA conformational change. Suram et al (2002) reported a conformational change in genomic DNA from normal B-DNA to B-Z intermediate in moderate AD and B-DNA to Z-DNA in severe AD. These observations

indicate that Aβ proteins may alter the DNA integrity leading to altered gene expression in AD.

However these studies could not answer whether these proteins binds to sequence and conformation specific DNA. The present study answered the above crucial questions indicating that α-Synuclein and Tau bind to B and Z-forms and favored the conformational transition. Both Tau and α-Synuclein interacted with sequence specific DNA and caused conformational transition from B to altered B-DNA. Also both the proteins stabilize Z-DNA conformation. These have altered minor and major groove patterns and thus may have significant biological implications in relevance to gene expression pattern in neurodegeneration? We hypothesized the implication of α-Synuclein/Tau binding to DNA and stabilizing the altered conformations of DNA in neuronal cell dysfunction (Fig 4D.2). Both α-Synuclein/Tau may bind to CG rich region in the promoter region of the gene and alter the conformation from B-DNA to altered B-DNA. Altered conformation in the promoter region may allow the binding of transcription factors and alter the gene expression. The altered regulation of the gene expression may result in neuronal cell dysfunction and finally lead to neuronal cell death. The negative supercoils generated during transcription, may induce the formation of Z-DNA in CG rich regions. Normally, after transcription the negative supercoils are relaxed and the Z-DNA is again converted to B-DNA. Both α-Synuclein/Tau may bind to Z-DNA conformation that is already formed due to transcriptional stress and further these proteins stabilize the Z-DNA conformation. The Z-DNA stabilization may result in the inhibition of transcription factors binding or may stop the movement of RNA polymerase. This may lead to the suppression of genes and finally to neuronal cell dysfunction. Both α-Synuclein and Tau may probably induce alternate DNA conformations in neurodegeneration and also may stabilize these conformations in the process of disease progression? Further work is in progress in this direction.

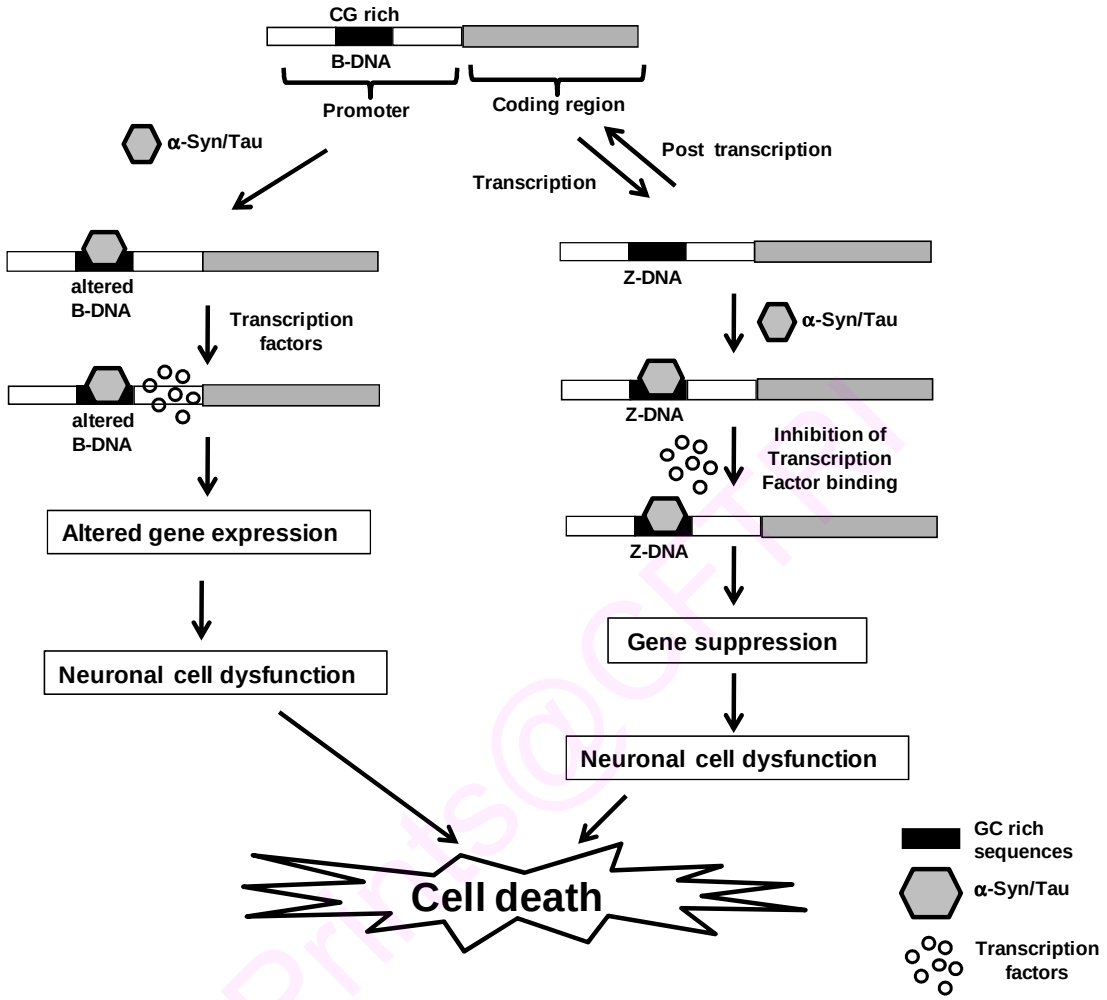

Figure 4D.2: A hypothesis on the implication of sequence specific binding of α-Synuclein/Tau in neuronal cell death. Both α-Synuclein/Tau may bind to CG rich region in the promoter region of the gene and alter the conformation from B-DNA to altered B-DNA. The altered conformation in the promoter region may allow the binding of transcription factors and alter the gene expression. The altered regulation of the gene expression may result in neuronal cell dysfunction and finally lead to neuronal cell death. The negative supercoils generated during transcription may induce the formation of Z-DNA in CG rich regions. Normally, after transcription the negative supercoils are relaxed

and the Z-DNA is again converted to B-DNA. Both α-Synuclein/Tau may bind to Z-DNA conformation formed due to transcriptional stress and stabilize the Z-DNA conformation. Z-DNA stabilization may result in the inhibition of transcription factors binding or may stop the movement of RNA polymerase. This may lead to the suppression of genes and finally to neuronal cell dysfunction.

Chapter 4E

Studies on actinomycin D induced changes in supercoiled DNA integrity

4E.1 Introduction

Actinomycin D (AMD) is an anticancer drug and used as a chemotherapeutic drug to cure brain tumors etc. AMD is used in Wilm's tumor (Green, 1997), Chiasmatic or hypothalamic gliomas of childhood (Packer et al, 1988) and central nervous system (CNS) tumors (Rustin et al, 1989). AMD also used along with the other anticancer drugs like Vinblastine, Bleomycin, Cyclophosphamide etc., in the treatment of brain tumors (Allen et al, 1985). AMD contains phenoxazone chromophore combined with two identical pentapeptide lactone rings (Lackner, 1975; Chen et al, 2002). AMD inhibits the transcription by occupying the RNA polymerase binding site on DNA (Phillips and Crothers, 1986). AMD binds to duplex DNA by intercalating with the chromophore and the pentapeptides are placed in the minor groove (Yoo and Rill, 2001). AMD shows sequence specific binding to GpC sites (Kamitori and Takusagawa, 1992). GpC forms strong hydrogen bonds in the minor groove region with pentapeptide rings of AMD. The hydrogen bonds are formed between carbonyl oxygen, amide groups of threonine residues of each pentapeptide to N-2 amino group, N-3 ring nitrogen of guanine residues (Kamitori and Takusagawa, 1992; Chen, 1988, 1992). AMD also binds to the single stranded DNA (ssDNA) with similar affinity as that of duplex DNA (Wadkins, 1998). Chen et al (chen et al, 1993) reported that AMD binds to ssDNA in the hairpin stem formed with in the ssDNA at GpC site. The mode of binding is similar to that of duplex DNA at the hairpin stem. Based on this property, Brown et al (1994) proposed that AMD might inhibit the transcription by stabilizing the cruciform structure of DNA at the transcription site. In the present study, we have studied the effect of AMD on supercoiling nature of DNA molecule. DNA is compactly arranged in the nucleus in the form of superhelical turns and in higher order of condensation. This superhelical turns are proposed to be involved in gene expression (Cook and Brazell, 1975; Bauer et al, 1980; Wang and Lynch, 1993; Fisher, 1984). Hence, we have employed pUC18 plasmid supercoiled DNA as our model

system, as superhelical regions in human DNA are analogous to the plasmid DNA superhelical turns (Serban et al, 2002).

4E.2 Materials

Supercoiled pUC18 plasmid DNA (scDNA, cesium chloride purified, 90% supercoiled structure), M13 single stranded circular DNA (SSC) and M13 double stranded circular DNA (DSC) were purchased from Banglore Genei, India. Actinomycin D-mannitol and ethidium bromide were from Sigma (USA) chemicals. Agarose, HEPES, Tris and EDTA were purchased from SISCO Research laboratories.

4E.3 Methodology

4E.3.1 Circular Dichroism (CD) Studies

The secondary conformations of scDNA were recorded on a JASCO J 700 Spectropolarimeter at 25°C, with 2 mm cell length in the range of 200-320 nm. Each spectrum was the average of four scans. The CD spectra of scDNA : AMD complexes the mole ratio of 1:1, 1:5, 1:50, 1:100, 1:500, 1:1000 are recorded in HEPES buffer (0.1 mM, pH 7.4). The spectra of AMD alone were subtracted from AMD-scDNA complex.

4E.3.2 Agarose Gel Studies

pUC18 scDNA (0.5 μg) was incubated with increasing concentrations (5-600 μM) of AMD in Tris-Cl (1mM, pH 7.4) at 37°C for 12 h. The incubated samples, control scDNA and supercoiled DNA ladder (2-10 kb) were loaded on 1% agarose gel and electrophoresed at 50 V at room temperature. SSC and DSC were incubated with AMD at concentrations 10 μM and 100 μM (concentrations at which CD, ethidium bromide, Tm studies showed changes) and electrophoresced. The samples are stained with ethidium bromide and viewed under UV light using with gel documentation system.

4E.3.3 Melting Temperature (T_m) Studies

The melting profile (T_m) curves for scDNA and scDNA with the 10, 100, 150, 300 μM actinomycin D were recorded in HEPES buffer (0.1 mM, pH 7.4) using Spectrophotometer

equipped with a thermostat programmer and data processor (Amersham Biosciences, Hong Kong). The melting profiles were recorded with increase of 1°C/ min in the temperature range of 25-95°C. 3 μg of scDNA used for each experiment. The temperature at which there was a 50% hyperchromic shift is considered as the melting temperature.

4E.3.4 Ethidium bromide binding studies

Ethidium bromide (EtBr) bound in moles per base pair of scDNA were measured in HEPES (0.1 mM, pH 7.4) using HITACHI F-2000 Fluorescence Spectrofluorimeter. The fluorescence was measured using a constant amount of scDNA (0.5 μg) with increasing EtBr. The fluorescence measurements were monitored with an excitation at 535 nm and emission at 600 nm with 10 mm path length.

The maximum amount of EtBr bound per base pair of DNA was calculated using Scatchard plots of 'r' vs 'r/Cf', in the DNA- EtBr reaction mixture at various titration intervals when increasing amount of EtBr was titrated to constant amount of DNA. The concentration of bound EtBr in 1.0 mL dye-DNA mixture (Cb′) were calculated using the equation:

$Cb' = Co'[(F-Fo)/(V \times Fo)]$

Where,

Co = EtBr (pmoles) present in the dye-DNA mixture,

F = observed fluorescence at any point of dye-DNA mixture,

Fo = observed fluorescence of EtBr with no DNA,

V = experimentally derived value, ratio of bound EtBr/free EtBr at saturation point.

The concentration of free dye (Cf′) was then calculated by the relation

$Cf' = Co' - Cb'$,

Where, Cf′, Co′, and Cb′ were expressed in pmoles. The amount of bound EtBr/base pair 'r' was calculated by

R = Cb′ (pmoles)/DNA concentration (pmoles of base pair).

A plot with r vs r/cf is plotted, point where the straight line intersects the X-axis is denoted as 'n'. 'n' is the maximum amount of dye bound per base pair (n), where Cf = Cf´ $\times 10^{15}$ M.

4E.3.5 Deoxyribonuclease I digestion of scDNA treated with AMD

The integrity of scDNA in the presence of AMD was studied by DNase I sensitivity test. A saturated reaction mixture of scDNA and EtBr in the ratio of 1 : 1 ratio (W/W, 0.5 µg scDNA + 0.5 µg EtBr) was treated with DNAse I (0.5 µg/mL) for the control. EtBr fluorescence was monitored for 45 min at excitation 535 nm and emission at 600 nm. The effect of AMD on DNase I sensitivity was studied by addition of 100 µM AMD with ScDNA and then treated with the DNAse I, EtBr fluorescence was recorded for 45 min.

4E.3.6 Desktop Molecular Modeling (DTMM)

Computer modeling showed the specific bonding pattern of pentapeptide binding to GC and AT base pair (Fig 4E.6)

4E.4 Results

4E.4.1 CD studies

Far UV CD spectra of scDNA (Fig 4E.1,a) showed a positive peak at 272 nm which is a characteristic feature of B-DNA conformation and negative peak at 245 nm. Addition of increasing concentrations of AMD in the mole ratios of 5, 50, 100, 500 and 1000 to scDNA, produced a red shift of peak at 270 nm (Fig 4E.1). The positive peak of 1 : 5 (b), 1 : 50 (c), 1 : 100 (d), 1 : 500 (e) and 1 : 1000 (f) molar ratios of scDNA : AMD are 273.6, 276.8, 280, 280 and 280 respectively. The negative peak at 245 nm is decreased slightly when compared to control scDNA. The above CD spectra indicate that AMD induced B-A transition in the scDNA as demonstrated by a red shift in the red shift in CD spectra.

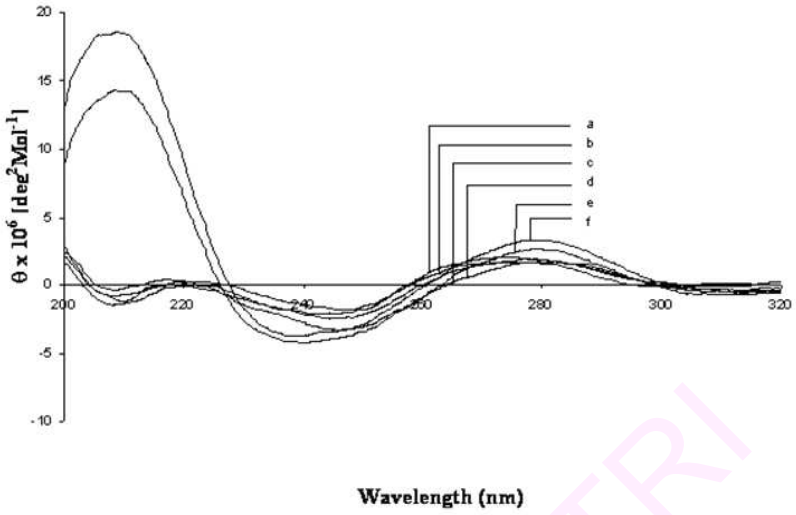

Figure 4E.1: CD spectra of scDNA in the presence of AMD in mole ratio. (a) scDNA, (b) 1 : 5, (c) 1 : 50, (d) 1 : 100, (e) 1 : 500, (f) 1 : 1000 mole ratios of scDNA : AMD. At mole ratios higher than 1 : 100 the normal positive peak at 272 nm of scDNA shifted to 280 nm.

4E.4.2 Agarose gel studies

ScDNA alone on an agarose gel showed 2 bands, one is supercoiled and other one is open circular forms of DNA (Fig 4E.2A, lane A). When scDNA is titrated with increasing concentrations of AMD (5-600 μM), AMD retards the migration of supercoiled band, but do not alter the open circular DNA mobility (Fig 4E.2A, lanes B-I). Further studies on the interaction of AMD with single stranded (SSC) or double stranded circular (DSC) DNA, (Fig 4E.2B, lane d), showed that AMD has no effect on SSC (Fig 4E.2B, lane e-f). But AMD retarded the mobility of DSC (Fig 4E.2B, lane h-i). The studies reveal that AMD binds to scDNA, DSC and not to SSC.

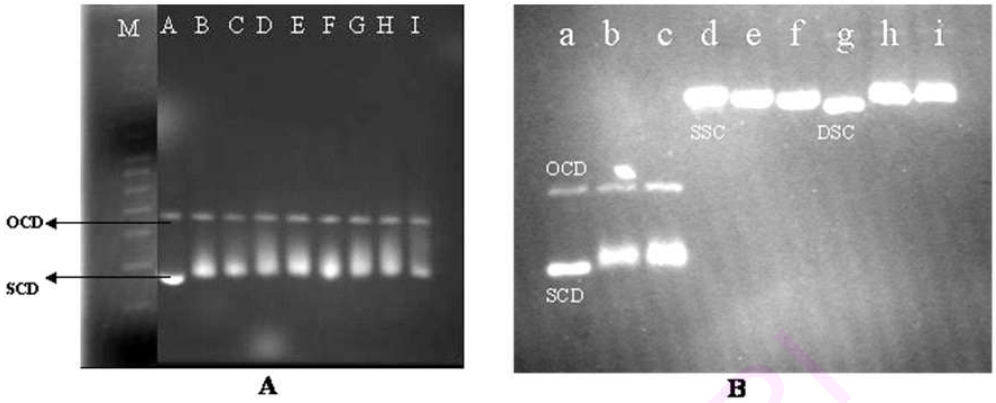

Figure 4E.2: A: **AMD interaction with supercoiled DNA :** 0.5 µg of pUC18 scDNA was interacted with 5 µM(lane B), 10 µM (lane C), 50 µM (lane D), 100 µM (lane E), 150 µM (lane F), 300 µM (lane G), 450 µM (lane H), 600 µM (lane I) Actinomycin D (AMD). The scDNA (lane A) and supercoiled DNA Ladder marker (lane M) **B**: **AMD interaction with SSC and DSC :** (a) scDNA, (b) scDNA with 10 µM AMD, (c) scDNA with 100 µM AMD, (d) SSC DNA, (e) SSC with 10 µM AMD, (f) SSC DNA, with 100 µM AMD, (g) DSC DNA, (h) DSC with 10 µM AMD, (i) DSC with 100 µM AMD.

4E.4.3 Melting temperature studies

Melting temperature studies are carried out to understand the effect of AMD on the stability of scDNA (Fig 4E.3). ScDNA melting profile showed a characteristic biphasic pattern having two melting temperatures T_{m1}= 52°C and T_{m2} = 87°C. T_{m1} signifies the uncoiling of the supercoiled DNA and Tm_2 indicates the opening of the double strand of DNA. At 10 µM concentration of AMD, both T_{m1} and T_{m2} scDNA increased to 63°C and 89°C respectively. But at 100 µM and 150 µM of AMD, only T_{m1} values are decreased to 47°C and 45°C with no significant change in T_{m2} (Table 4E.1). At 300 µM of AMD, there is a steep decrease in the absorbance at 260 nm indicating aggregation of DNA. The significant changes in T_{m1} indicate that AMD preferentially binds to scDNA only.

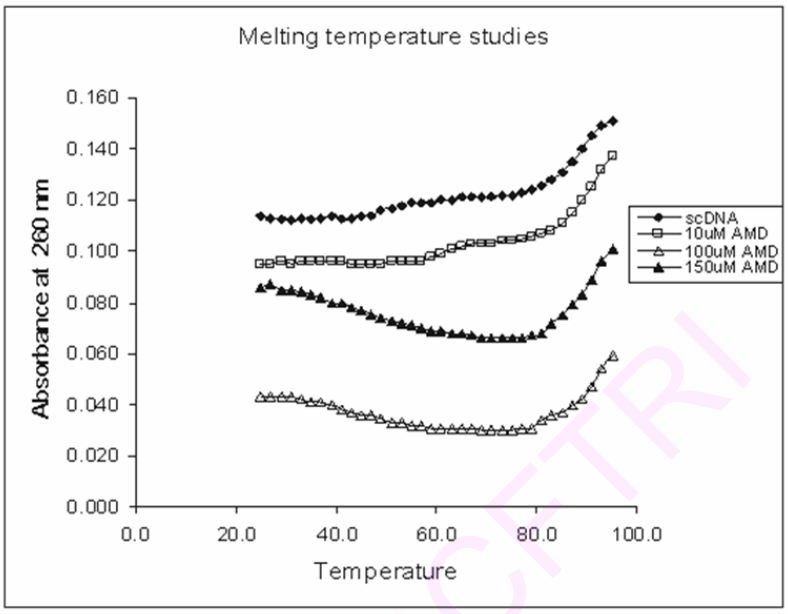

Figure 4E.3: The melting profile (T_m) curves for scDNA and scDNA samples incubated with the 10, 100, 150, and 300 μM AMD.

	Tm_1	Tm_2
scDNA	52°C	87°C
scDNA+10uM AMD	63°C	89°C
scDNA+100uM AMD	47°C	90°C
scDNA+150uM AMD	45°C	88°C

Table 4E.1: Melting temperature (T_m) values of scDNA in the absence and presence of AMD.

4E.4.4 Ethidium Bromide (EtBr) binding studies

The alteration in the integrity of scDNA induced by AMD is studied by computing the changes in the EtBr molecules binding to scDNA. Number of EtBr molecules bound per base pair of DNA is calculated using scatchard plots in the presence and absence of AMD (Fig 4E.4). The number of EtBr molecules bound per base pair in scDNA alone is 0.26. In the presence of lower concentration of AMD (10 μM), the number of EtBr molecules bound per base pair is decreases to 0.14. But in the presence of higher (100 μM-300 μM) AMD concentration, EtBr molecules / bp is similar to control (around to 0.25). The results indicate that lower AMD concentrations alter the EtBr binding profile DNA.

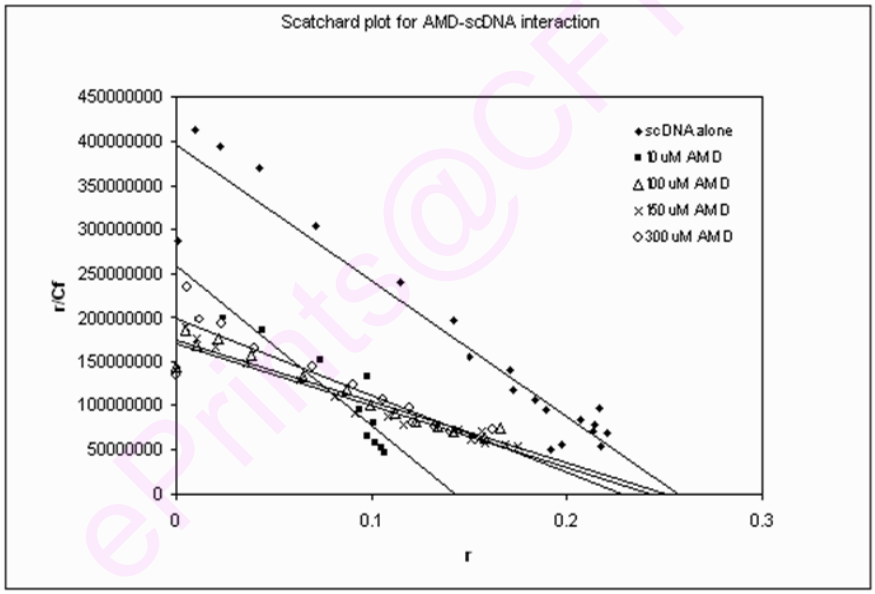

Figure 4E.4: Scatchard plot of ethidium bromide binding pattern to scDNA in the absence and presence of AMD. The number of EtBr molecules bound per base pair are computed.

4E.4.5 DNAse I sensitivity study for scDNA-AMD complex

Actinomycin D treatment made scDNA stable against DNAse I digestion. The pattern of EtBr fluorescence for AMD+scDNA complex exposed to DNASe1, is similar to scDNA

alone without DNAse digestion (Fig 4E.5, D and B). DNAse I digestion of scDNA increases the EtBr fluorescence (Fig 4E.5, C).

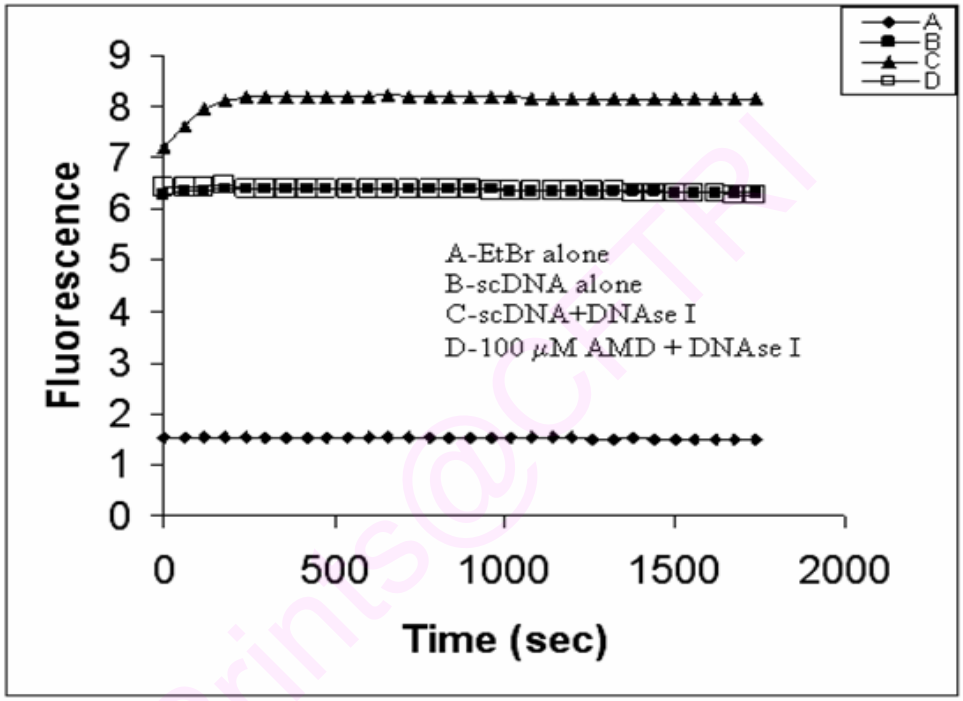

Figure 4E.5: Effect of AMD on DNAse I sensitivity to scDNA. A saturated reaction mixture of scDNA and EtBr in the ratio of 1 : 1 ratio (W/W, 0.5 μg scDNA + 0.5μ g EtBr) is treated with DNAse I (0.5 μg/mL) in the presence and absence of AMD.

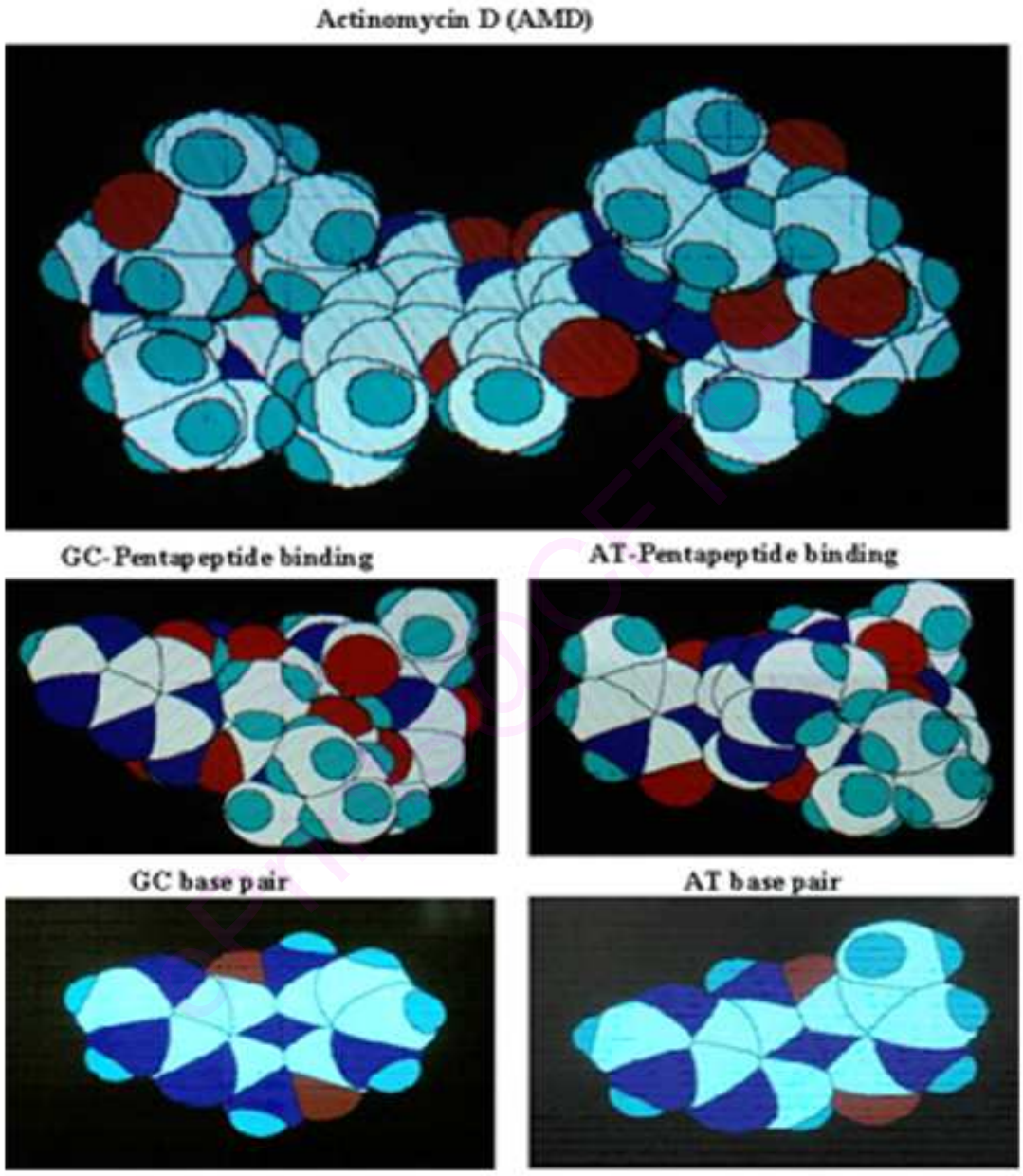

Fig. 4E.6 : Desktop Molecular Modeling (DTMM) of pentapeptide of AMD binding to GC and AT base pairs.

Discussion

Actinomycin D (AMD) is an anticancer drug used in the treatment of brain tumors (Green , 1997; Packer, 1988). AMD exerts its anti-tumorogenic activity by inactivating the transcription process in tumor cells (Aivasashvilli and Beabealashvilli, 1983). The mode of action of AMD is by intercalating the duplex DNA and two cyclic pentapeptide rings are positioned in the minor groove of the DNA (Yoo and Rill, 2001; Kamitori and Takusagawa, 1992; Muller and Crothers, 1968; Sobell and Jain, 1972). AMD has affinity to GpC sites. AMD also binds to single stranded DNA (ssDNA) and favor hairpin conformation (Chen et al, 1993). The overall mechanism of action of AMD is proposed to be through intercalation with DNA and inhibition of DNA transcription, blocks RNA and protein synthesis (Guo et al, 1998; Kawamata and Imanishi, 1960; Wassermann, 1990). AMD not only affect the tumor cells, but also alter the cellular processes of normal cells (Kawanishi and Hiraku, 2004). AMD is also reported to induce the apoptotic cell death in normal cells like hepatocytes (Li et al, 2006). At the concentration 1ug /ml, AMD induces typical apoptotic cell death (Shim et al, 2004; Fraschini et al, 2005). AMD also showed the toxic effects on lymphoblastoid cell lines (Sawada et al, 2005). AMD inhibits the DNA repair activities (Barret et al, 1997). AMD incubation with cell nuclei showed progressive denaturation of nucleosomal structure and stabilization of supercoiled DNA (Almagor and Cole, 1989). Our studies are focused in understanding the effect of AMD on scDNA topology and integrity by using pUC18 as model system. Plasmid supercoiled DNA is analogous to the small supercoiled DNA packets observed in human genome (Fisher, 1984). Small supercoiled DNA packets are found in the human genome and are involved in gene expression (Cook and Brazell, 1975; Bauer et al, 1980; Wang and Lynch, 1993). The rate of supercoil generation, propagation and elimination (supercoiling dynamics) are important in the gene regulation process (Crut et al, 2007). From the results obtained, we conclude that actinomycin D alters the topology and stability of the scDNA. AMD induces the B-A DNA conformational transition as evidenced by red shift in 272 nm positive peak and this observation is in agreement with the findings of Hou et al (Hou et al, 2002). There are few studies showing the effect of AMD on scDNA (Simpkins and Pearlman, 1984;

Leoni et al, 1989). Our study and literature evidences indicated that actinomycin D effecting supercoiling nature of DNA. Actinomycin D binding to supercoiled DNA may inhibit the transcription by blocking the RNA polymerase but also possibly alters the supercoiling nature in the domain. Further work is in progress in order to understand this phenomenon.

Actinomycin D affects the integrity of supercoiled DNA in terms of its topology and stability. Actinomycin D induces B-A conformational transition in scDNA. Actinomycin D may alter the gene expression by affecting the supercoiling of DNA apart from blocking the RNA polymerase.

Summary and conclusions

The progressive loss of structure and function of neurons is the final consequence of the all neurodegenerative diseases. Several pathways are involved in the process of neurodegeneration in different neurodegentive diseases and often the pathways overlap. Risk factors like aggregation of modified proteins, disturbance in trace metal homeostasis, protein and DNA conformation, oxidative stress are implicated in age related neurodegeneration in diseases like Parkinson's and Alzheimer's disease. Aging is a multi-factorial process, which leads to irreversible damage to macromolecules (DNA, proteins and lipids), cells and organs and also in age related neurodegenerative disorders. DNA in eukaryotic cell is arranged in the form of compactly condensed state known as chromatin. Chromatin organization is a dynamic process occurring in the living cells by continuously opening and reorganizing according to cellular needs. Chromatin organization plays an important role in regulation of the gene expression. The regulation at chromatin level depends on modifications of DNA (especially methylation at cytosine residues), incorporations of histone varients, post-translational histone modifications and other molecules which can interact with nucleosome core particles. Environmental factors may induce epigenetic modifications leading to the neurodegeneration

α-synuclein protein is involved in etiopathogenesis of the Parkinson's disease. α-synuclein proteins aggregates in PD conditions and neuronal cell death observed in PD brain. In a study, α-synuclein targeting to nucleus induced neurodegeneration and histone deacetylase inhibitor administration prevented the neurotoxicity indicating role of α-synuclein in chromatin regulation in PD. MPP(+) induced misfolded α-synuclein aggregates are degraded by ubiquitin-binding histone deacetylase-6 (HDAC-6) indicating the role of chromatin modifying enzymes in PD. Single stranded breaks (SSB) and double stranded breaks (DSB) are accumulated in the DNA of PD brain samples indicating the DNA damage in PD. Increased 8OHdG levels are observed in the substantia nigra of Parkinson's disease patients. Tau (microtubule associated

protein) involved in microtubule polymerization and their stabilization in the neurons. Tau is involved in the pathogenesis of Parkinson's disease and Alzheimer's disease. Tau protein is also localized in the nucleus and has shown chromatin and DNA binding properties. Neuromelanin (NM) is an insoluble pigment and loss of neuromelanin containing cells within substantia nigra suggest its role in Parkinson's disease. Curcumin is a hydrophobic polyphenol derived from the rhizome (turmeric) of the herb Curcuma longa. Curcumin is also used widely as pharmacological active compound because of its wide spectrum of biological activities. Curcumin has been reported to have the antioxidant, antimicrobial, anti-inflamatory and anti-carcinogeneic activities. Curcumin treatment prevented the α-synuclein induced toxicity through its antioxidant properties. Curcumin is also shown to have epigenetic regulating properties in gene expression.

Chapter 1: General introduction

The genral introduction covers the different pathways in neurodegeneration and in parkinson's disease. The introduction focuded on the role of chromatin organization, Tau protein, α-synuclein, neuromelanin and biomarker in Parkinson's disease. The introduction also focuses on thereupetic potential of commonly used dietary curcumin and its role in chromatin organization.

1. Neuronal cell death is the common hallmark of all age related neurodegenerative diseases like Parkinson's disease (PD) with overlapping pathways.

2. Mitochondrial dysfunction is the common mechanism leading to neuronal cell death in neurodegeneration in PD. Programmed cell death (apoptosis) was observed in the neurons of the PD brains

3. Oxidative stress and oxidative DNA damage interims of oxidatively modified bases, single and double strand breaks in DNA was observed in PD.

4. α-synuclein, tau, neuromelanin are involved in the pathogenesis of PD. α-Synuclein aggregates are found in the brain of PD patients and in the animal models of PD. Tau

aggregation is also observed in PD brains. Neuromelanin is found in the form of large granules in the substantia nigra of PD brain

5. α-synuclein, tau, neuromelanin are localized in the nuclear region. α-synuclein and tau was shown to bind to DNA and histone proteins.

6. α-synuclein targeting to the nucleus induced neurotoxicity and histone deacetylase inhibitors rescued the neurotoxicity indicating its role in chromatin organization.

7. Methylation in *SNCA* intron 1 of alpha synuclein is found reduced in the PD brain samples. Hypomethylation of DNA in Tumor necrosis factor (TNFα) promoter region is observed in the promoter regions in PD patients

8. Pesticide dieldrin treatment induced neuronal cell death by the hyperacetylation of histone molecules indicating the role of pesticides in chromatin alteration. Pesticides are known as the risk factors for the parkinson's disease.

9. There is no established biomarker for the parkinson's disease. Development of reliable biomarker for PD helps in early detection and prevention of further neurodegeneration.

10. Curcumin is a hydrophobic polyphenol derived from the rhizome (turmeric) of the herb Curcuma longa. Curcumin showed neuroprotection against 1-methyl-4-phenyl-1,2,3,6-tetrahydropyridine (MPTP) induced toxicity in PD model.

The introduction engulfed with objectives at the end.

Chapter 2: Studies on the chromatin organization in Parkinson's disease and the role of curcumin on chromatin organization, tau-DNA interactions and α-synuclein-DNA interactions.

Chapter 2A: Chromatin organization in Parkinson's disease.

1. Five normal and five PD-affected human brain samples were obtained from the National Institute of Mental Health and Neurosciences (NIMHANS), India.

2. Nuclei and DNA were isolated from 20 control and 20 PD brain regions. Chromatin and histone proteins were prepared from the nuclei.

3. Chromatin organization is studied by thermal denaturation, circular dichroism, micrococcal nuclease digestion, methylation analysis of genomic DNA and histone acetylation.

4. Thermal denaturation analysis of the chromatin samples showed decrease in the melting transition temperature in PD chromatin compared to that of age matched control brains.

5. CD studies with chromatin samples showed differences between the PD chromatin and control chromatin. CD spectral changes observed in PD hippocampal region may be due to differences in their histone acetylation status.

6. Histone H3 acetylation in all the PD chromatin samples was observed, with only 50% of control brains showed histone acetylation.

7. Micrococcal nuclease digestion revealed that PD chromatin is more sensitive to digestion compared to that of control. This showed that more loose chromatin loops are present in PD chromatin compared to control.

8. Restriction digestion analysis with methylation specific Msp I and HpaII endonuclease revealed the differences in the methylation status of the DNA between PD and normal subjects.

The above results clearly indicated that chromatin organization is altered in PD brain

Chapter 2B: Role of curcumin on chromatin organization, tau-DNA interactions and α-synuclein-DNA interactions.

1. Curcumin is purified from turmeric and terahydrocurcumin (THC) was prepared. Curcumin and THC purity is analyzed by TLC, HPLC and NMR.

2. Curcumin and THC binds to chromatin as indicated by the altered absorbance and fluorescence spectrum, ethidium bromide binding of curcumin-chromatin and THC-chromatin complex.

3. Curcumin altered the chromatin organization by altering its integrity as evidenced by decreased thermal transition of curcumin-chromatin complex.

4. Curcumin did not alter the secondary conformation of chromatin components, but binding of curcumin to chromatin evidenced by the small changes in the CD spectrum.

5. Curcumin binds to scDNA as indicated by the absorption, fluorescence and EtBr binding. Curcumin altered integrity of scDNA observed by the thermal denaturation studies.

6. Curcumin and THC also binds to tau, α-synuclein proteins involved in neurodegeneration. Curcumin and THC could not able to prevent the tau, α-synuclein induced DNA nicking.

7. NMR studies showed that curcumin could not able to bind nucleosides indicating that requisite of secondary conformation of DNA for the interaction.

8. Further, in vivo studies are needed to establish curcumin ability of altering chromatin organization and tau-DNA, α-synuclein-DNA interaction are either protective or toxic.

Chapter 3: Biomarker study on Parkinson's disease and increase of Iron and Copper and its correlation to DNA integrity in ageing human brain

Chapter 3A: Biomarker study on Parkinson's disease

1. The patients from JSS Medical Hospital were clinically identified for PD by the neurologist and the patients who met the commonly accepted diagnostic criteria for PD were selected.

2. Venous blood (10 ml) was collected from each PD and control patient and serum separated by centrifugation. The serum was frozen at -20°C and protected from exposure to light until analysis.

3. Serum 8-OHdG levels were found to be higher in the Parkinson's disease patients compared with that of the age matched control samples.

4. The increase in the total antioxidant capacity in serum samples of PD compared to control indicated that oxidative stress is more in PD patients compared to control.

5. Serum ceruloplasmin and ferritin levels are decreased in PD patients compared to age matched controls.

6. MRI imaging of brains of PD and control subjects is carried out at Vikram Hospital under the supervision of chief radiologist. The average thickness of the all the regions were calculated and compared with that of control brain thickness.

7. Atrophy is observed in terms of reduction in the thickness of the brain regions in caudate nucleus, thalamus, hippocampus and substantia nigra regions in PD brain compared to control brain regions significant at $p<0.05$.

8. Reduction in the in the frontal lobe, temporal lobe and midbrain regions, was observed.

The results clearly indicated that serum parameters coupled with MRI changes act as biomarkers for PD

Chapter 3B: New evidence on increase of iron and copper and its correlation to DNA integrity in ageing human brain

1. Human brain samples are collected from the Depression Brain Bank of JSS Medical Hospital and College, Mysore, India

2. Genomic DNA is isolated from hippocampus and frontal cortex of frozen brain tissue by standard 'phenol-chloroform extraction' method.

3. The levels of Fe and Cu are increased, while Zn levels were decreased from Group I to III. There is a significant increase in Cu and Fe in Group II and Group III in both frontal cortex and hippocampus region.

4. Accumulations of SSBs are more frequent in group III compared to Group II and I. The result showed that frontal cortex ($p>0.05$ and $p >0.001$) accumulated considerably higher number of SSBs compared to hippocampus. This could be due to the increased levels of Cu and Fe in frontal cortex and relatively lower amounts in hippocampus in Group III.

The present result showed that frontal cortex has more DSBs than SSBs whereas hippocampus had the presence of both DSBs and SSBs accumulated

Chapter 4: DNA binding properties of neuropeptides, curcumin and actinomycin D

Chapter 4A: New evidences on Tau–DNA interactions and relevance to neurodegeneration

1. Both non-phosphorylated r-Tau (recombinant tau) and pp-Tau (partially phosphorylated tau) have DNA binding ability

2. r-Tau induces B-C-A mixed transition in scDNA and pp-Tau also induced B-C-A mixed conformation in scDNA

3. Both non-phosphorylated r-Tau and pp-Tau alter DNA integrity. Both converted biphasic melting profile to monophasic melting profile.

4. The r-Tau and pp-Tau binding to scDNA increased the number of EtBr molecules bound per base pair of scDNA indicating altered DNA integrity.

5. Tau-scDNA complex was sensitive for DNAse I digestion and insights that r-Tau destabilizes DNA integrity.

6. Tau converted scDNA into open circular and linear forms suggesting that Tau may nick the DNA resembling endonuclease.

The data clearly showed that Tau binds to DNA and alter its stability.

Chapter 4B: DNA binding properties of α-synuclein and AGE-α-synuclein (glycated α-synuclein).

1. α-synuclein and AGE-α-synuclein nick the scDNA like endonuclease. Magnesium enhanced α-synuclein and AGE-α-synuclein nicking. Specific nuclease inhibitor aurinetricarboxylic acid inhibited the α-synuclein and AGE-α-synuclein nicking.

2. α-synuclein and AGE-α-synuclein induced B-C-A mixed conformation in scDNA similar to that of α-synuclein

3. Both α-synuclein and AGE α-synuclein altered DNA integrity as evidenced by the transition of biphasic melting profile to monophasic melting profile and decreased ethidium bromide binding.

4. Both scDNA-α-synuclein and scDNA-AGE-α-synuclein showed resistence to DNAse I.

Chapter 4C: New evidence on Neuromelanin from the substantia nigra of Parkinson's disease altering the DNA topology

1. Neuromelanin is found in the form of large granules in the substantia nigra of PD brain and involved in PD pathogenesis. NM (PD-SN) was isolated from the substantia nigra of PD brain, NM (N-SN) was isolated from the other region of the brain and DAC a synthetic neuromelanin.

2. NM (PD-SN) converted scDNA into open circular form, where as NM (N-SN) and DAC could not convert scDNA into open circular.

3. NM (PD-SN) induced B-C-A mixed conformation in scDNA, where as NM (N-SN) and DAC induced altered B-conformation in scDNA.

4. NM (PD-SN), NM (N-SN) and DAC altered the stability of DNA. NM (PD-SN) had high potential in altering DNA stability.

Chapter 4D: New evidence on α-Synuclein and Tau binding to conformation and sequence specific GC* rich DNA

1. Double stranded oligonucleotide $(CGCGCGCG)_2$ exists in B-DNA conformation and is converted to Z-DNA in the presence of high sodium concentration (4 M NaCl).

2. The circular dichroism studies indicated that both α-Synuclein and Tau bind to B-DNA conformation of (CGCGCGCG)2 and induce altered B-form.

3. The melting temperature (T_m) of the B-form and Z-form of the oligonucleotide was 71°C and 81°C, respectively. The T_m of the Z-form of the oligonucleotide was greater than the B-form, indicating that Z-form is more stable than B-form.

4. α-Synuclein and Tau proteins increased the melting temperature and decreased the number of EtBr molecules bound per base pair of DNA of B-form indicating that DNA stability is favored to altered B-DNA conformation.

Both α-Synuclein and Tau bind to Z-DNA conformation of $(CGCGCGCG)_2$ and further stabilized the Z-conformation

Chapter 4E: Studies on actionomycin D induced changes in supercoiled DNA integrity

1. Actinomycin D (AMD) is used as a model compound to understand supercoiled DNA topology and stability.

2. AMD induced B to A conformational change in scDNA as demonstrated by a red shift in the CD spectra at 272 nm.

3. AMD also altered the stability of scDNA as evidenced by the alterations in melting temperature and also in ethidium bromide binding pattern to DNA.

All these results clearly showed that Chromatin instability and DNA/protein interactions have significant role in PD neurodegeneration. Some of these findings are significantly new in PD research and published in impact journals.

Bibliography

REFERENCES

Abe T, Tohgi H, Isobe C, Murata T, Sato C. Remarkable increase in the concentration of 8-hydroxyguanosine in cerebrospinal fluid from patients with Alzheimer's disease. J Neurosci Res. 2002 ; 70 : 447-450.

Abel T, Zukin RS. Epigenetic targets of HDAC inhibition in neurodegenerative and psychiatric disorders. Curr Opin Pharmacol. 2008; 8 : 57-64.

Adamec E, Vonsattel JP, Nixon RA. DNA strand breaks in Alzheimer's disease. Brain Res. 1999 ; 849 : 67-77.

Aivasashvilli VA, Beabealashvilli RS. Sequence-specific inhibition of RNA elongation by actinomycin D. FEBS Lett. 1983; 160 : 124-128.

Alam ZI, Jenner A, Daniel SE, Lees AJ, Cairns N, Marsden CD, Jenner P, Halliwell B. Oxidative DNA damage in the parkinsonian brain: an apparent selective increase in 8-hydroxyguanine levels in substantia nigra. J Neurochem. 1997; 69 : 1196-203.

Allen JC, Bosl G, Walker R. Chemotherapy trials in recurrent primary intracranial germ cell tumors. J Neurooncol. 1985; 3 : 147-152.

Almagor M, Cole RD. Differential scanning calorimetry of nuclei as a test for the effects of anticancer drugs on human chromatin. Cancer Res. 1989; 49 : 5561-5566.

Almeida S, Cunha-Oliveira T, Laço M, Oliveira CR, Rego AC. Dysregulation of CREB activation and histone acetylation in 3-nitropropionic acid-treated cortical neurons: prevention by BDNF and NGF. Neurotox Res. 2010; 17 : 399-405.

Alonso AC, Grundke-Iqbal I, Iqbal K. Alzheimer's disease hyperphosphorylated tau sequesters normal tau into tangles of filaments and disassembles microtubules. Nat Med. 1996; 2 : 783-787.

Alvira D, Ferrer I, Gutierrez-Cuesta J, Garcia-Castro B, Pallàs M, Camins A. Activation of the calpain/cdk5/p25 pathway in the girus cinguli in Parkinson's disease. Parkinsonism Relat Disord. 2008;14: 309-13.

Anand P, Thomas SG, Kunnumakkara AB, Sundaram C, Harikumar KB, Sung B, Tharakan ST, Misra K, Priyadarsini IK, Rajasekharan KN, Aggarwal BB. Biological activities of curcumin and its analogues (Congeners) made by man and Mother Nature. Biochem Pharmacol. 2008; 76 : 1590-611.

Andreazza AC, Frey BN, Erdtmann B, Salvador M, Rombaldi F, Santin A, Goncalves CA, Kapczinski F. DNA damage in bipolar disorder. Psychiatry Res. 2007 ; 153 : 27-32.

Ansari B, Coates PJ, Greenstein BD, Hall PA. In situ end-labeling detects DNA strand breaks in apoptosis and other physiological and pathological states. J Pathol. 1993 ; 170 : 1-8.

Antequera F. Structure, function and evolution of CpG island promoters. Cell Mol Life Sci. 2003; 60 : 1647-1658.

Archer HA, Edison P, Brooks DJ, Barnes J, Frost C, Yeatman T, Fox NC, Rossor MN. Amyloid load and cerebral atrophy in Alzheimer's disease: An C-11-PIB positron emission tomography study. Ann Neurol. 2006; 60,145-147.

Avila J, Lucas JJ, Perez M, Hernandez F, Role of tau protein in both physiological and pathological conditions. Physiol Rev. 2004 : 84 361-384.

Aybek S, Lazeyras F, Gronchi-Perrin A, Burkhard PR, Villemure JG, Vingerhoets FJ. Hippocampal atrophy predicts conversion to dementia after STN-DBS in Parkinson's disease. Parkinsonism Relat Disord. 2009 ; 15 : 521-524.

Baba M, Nakajo S, Tu PH, Tomita T, Nakaya K, Lee VM, Trojanowski JQ, Iwatsubo T. Aggregation of alpha-synuclein in Lewy bodies of sporadic Parkinson's disease and dementia with Lewy bodies. Am J Pathol. 1998; 152 : 879-84.

Bacolla A and Wells RD. Non-B DNA conformations as determinants of mutagenesis and human disease. Mol Carcinog. 2009; 48 : 273-285.

Bai L, Morozov AV. Gene regulation by nucleosome positioning. Trends Genet. 2010; 26: 476-483.

Balasubramanyam K, Varier RA, Altaf M, Swaminathan V, Siddappa NB, Ranga U, Kundu TK. Curcumin, a novel p300/CREB-binding protein-specific inhibitor of acetyltransferase, represses the acetylation of histone/nonhistone proteins and histone acetyltransferase-dependent chromatin transcription. J Biol Chem. 2004 ; 279 : 51163-51171.

Bandyopadhyaya G, Sinha S, Chattopadhyay BD, Chakraborty A. Protective role of curcumin against nicotine-induced genotoxicity on rat liver under restricted dietary protein. Eur J Pharmacol. 2008; 588 : 151-157.

Baptista MJ, O'Farrell C, Daya S, Ahmad R, Miller DW, Hardy J, Farrer MJ, Cookson MR. Co-ordinate transcriptional regulation of dopamine synthesis genes by alpha-synuclein in human neuroblastoma cell lines. J Neurochem. 2003; 85 : 957-68.

Barghorn S, Biernat J, Mandelkow E. Purification of recombinant tau protein and preparation of Alzheimer-paired helical filaments in vitro. Methods Mol Biol. 2005; 299: 35-51.

Barnes J, Scahill RI, Boyes RG, Frost C, Lewis EB, Rossor CL, Rossor MN, Fox NC. Differentiating AD from aging using semi-automated measurement of hippocampal atrophy rates. Neuroimage. 2004; 23, 574-581.

Barret JM, Salles B, Provot C, Hill BT. Evaluation of DNA repair inhibition by antitumor or antibiotic drugs using a chemiluminescence microplate assay. Carcinogenesis. 1997 ; 18 : 2441-2445.

Barrett RM, Wood MA. Beyond transcription factors: the role of chromatin modifying enzymes in regulating transcription required for memory. Learn Mem. 2008; 15 : 460-467.

Bartzokis G, Tishler TA, Lu PH, Villablanca P, Altshuler LL, Carter M, Huang D, Edwards N, Mintz J. Brain ferritin iron may influence age- and gender-related risks of neurodegeneration. Neurobiol Aging. 2007 ; 28 : 414-423.

Baudrexel S, Nürnberger L, Rüb U, Seifried C, Klein JC, Deller T, Steinmetz H, Deichmann R, Hilker R. Quantitative mapping of T1 and T2* discloses nigral and brainstem pathology in early Parkinson's disease. Neuroimage. 2010 ; 51 : 512-520.

Bauer WR, Crick FH, White JH. Supercoiled DNA. Sci Am. 1980; 243 : 100-113.

Bayer TA, Jäkälä P, Hartmann T, Egensperger R, Buslei R, Falkai P, Beyreuther K. Neural expression profile of alpha-synuclein in developing human cortex, Neuroreport. 1999; 10 : 2799-2803.

Benes FM, Matzilevich D, Burke RE, Walsh J. The expression of proapoptosis genes is increased in bipolar disorder, but not in schizophrenia. Mol Psychiat. 2006 ; 11 : 241-251.

Benes FM, Walsh J, Bhattacharyya S, Sheth A, Berretta S. DNA fragmentation decreased in schizophrenia but not bipolar disorder. Arch Gen Psychiatry. 2003 ; 60 : 359-364.

Ben-Shachar D, Riederer P, Youdim MB. Iron-melanin interaction and lipid peroxidation: implications for Parkinson's disease. J Neurochem. 1991; 57: 1609-1614.

Beyer K, Ariza A. Protein aggregation mechanisms in synucleinopathies: commonalities and differences, J Neuropathol Exp Neurol. 2007; 66 : 965-974.

Bharucha KJ, Friedman JK, Vincent AS, Ross ED. Lower serum ceruloplasmin levels correlate with younger age of onset in Parkinson's disease. J Neurol. 2008 ; 255 : 1957-1962.

Bhaskar, MS, Rao KS. Altered conformation and increased strand breaks in neuronal and astroglial DNA of ageing rat brain. Biochem Mol Biol Int. 1994 ; 33 : 377-384.

Binder LI, Frankfurter A, Rebhun, LI. The distribution of tau in the mammalian central nervous system. J Cell Biol. 1985; 101 : 1371-1378.

Bisaglia M, Mammi S, Bubacco L. Structural insights on physiological functions and pathological effects of alpha-synuclein, FASEB J. 2009; 23 : 329-340.

Bohr VA, Anson RM. DNA damage, mutation and fine structure DNA repair in aging. Mutat Res. 1995; 338 : 25-34.

Boll MC, Sotelo J, Otero E, Alcaraz-Zubeldia M, Rios C. Reduced ferroxidase activity in the cerebrospinal fluid from patients with Parkinson's disease. Neurosci Lett. 1999 23 ; 265 : 155-158.

Brandt R, Hundelt M, Shahani N. Tau alteration and neuronal degeneration in tauopathies: mechanisms and models. Biochim Biophys Acta. 2005; 1739 : 331-354.

Broersen K, van den Brink D, Fraser G, Goedert M and Davletov B. Alpha-synuclein adopts an alpha-helical conformation in the presence of polyunsaturated fatty acids to hinder micelle formation. Biochemistry. 2006; 45 : 15610-15616.

Brown DR, Kurz M, Kearns DR, Hsu VL. Formation of multiple complexes between actinomycin D and a DNA hairpin: structural characterization by multinuclear NMR. Biochemistry. 1994; 33 : 651-664.

Brunden KR, Trojanowski JQ and Lee VM. Advances in tau-focused drug discovery for Alzheimer's disease and related tauopathies. Nat Rev Drug Discov. 2009; 8 : 783-793.

Buckley NJ, Johnson R, Zuccato C, Bithell A, Cattaneo E. The role of REST in transcriptional and epigenetic dysregulation in Huntington's disease. Neurobiol Dis. 2010 ; 39 : 28-39.

Bussell R Jr, Eliezer D. A structural and functional role for 11-mer repeats in alpha-synuclein and other exchangeable lipid binding proteins. J Mol Biol. 2003; 329 : 763-78.

Buttner N, Bhattacharyya S, Walsh J, Benes FM. DNA fragmentation is increased in non-GABAergic neurons in bipolar disorder but not in schizophrenia. Schizophr Res. 2007 ; 93 : 33-41.

Calabrese V, Cornelius C, Mancuso C, Lentile R, Stella AM, Butterfield DA. Redox homeostasis and cellular stress response in aging and neurodegeneration. Methods Mol Biol. 2010 ; 610 : 285-308.

Caldecott KW. Single-strand break repair and genetic disease. Nat Rev Genet. 2008 ; 9 : 619-631.

Calne S, Schoenberg B, Martin W, Uitti RJ, Spencer P, Calne DB. Familial Parkinson's disease: possible role of environmental factors. Can J Neurol Sci. 1987; 14 : 303-5.

Catts VS, Catts SV. Apoptosis and schizophrenia: is the tumour suppressor gene, p53, a candidate susceptibility gene? Schizophr Res. 2000; 41: 405-415.

Chandra S, Chen X, Rizo J, Jahn R, Südhof TC. A broken alpha -helix in folded alpha -Synuclein. J Biol Chem. 2003; 278 : 15313-8.

Chatterjee B, Rao GRK Superhelical density of goat mitochondrial DNA: Fluorescent studies. Indian J Biochem Biophys 1994; 31, 77-79.

Chen FM, Jones CM, Johnson QL. Dissociation kinetics of actinomycin D from oligonucleotides with hairpin motifs. Biochemistry. 1993; 32 : 5554-5559.

Chen FM, Sha F. Actinomycin D binds to d(TGTCATG) with 2:1 drug to duplex stoichiometry. Biochemistry. 2002; 41 : 5043-5049.

Chen FM. Binding specificities of actinomycin D to non-self-complementary -XGCY-tetranucleotide sequences. Biochemistry. 1992; 31 : 6223-6228.

Chen FM. Binding specificities of actinomycin D to self-complementary tetranucleotide sequences -XGCY-. Biochemistry. 1988; 27 : 6393-6397.

Chen KL, Wang SS, Yang YY, Yuan RY, Chen RM, Hu CJ. The epigenetic effects of amyloid-beta(1-40) on global DNA and neprilysin genes in murine cerebral endothelial cells. Biochem Biophys Res Commun. 2009; 378 : 57-61.

Chen P, Li G. Dynamics of the higher-order structure of chromatin. Protein Cell. 2010; 1 : 967-971.

Chen Y, Shu W, Chen W, Wu Q, Liu H, Cui G. Curcumin, both histone deacetylase and p300/CBP-specific inhibitor, represses the activity of nuclear factor kappa B and Notch 1 in Raji cells. Basic Clin Pharmacol Toxicol. 2007; 101 : 427-433.

Cherny D, Hoyer W, Subramaniam V, Jovin TM. Double-stranded DNA stimulates the fibrillation of alpha-synuclein in vitro and is associated with the mature fibrils: an electron microscopy study, J Mol Biol. 2004 : 344, 929-938.

Chesselet MF. In vivo alpha-synuclein overexpression in rodents: a useful model of Parkinson's disease? Exp Neurol. 2008; 209 : 22-7.

Choi YG, Lim S. N(ε)-(carboxymethyl)lysine linkage to α-synuclein and involvement of advanced glycation end products in α-synuclein deposits in an MPTP-intoxicated mouse model, Biochimie 2010; 92 : 1379-1386.

Chung S, Yao H, Caito S, Hwang JW, Arunachalam G, Rahman I. Regulation of SIRT1 in cellular functions: role of polyphenols. Arch Biochem Biophys. 2010; 501 : 79-90.

Clarke PGH. Apoptosis versus necrosis: How valid a dichotomy for neurons? In: Koliatsos VE, Ratan RR, editors. Cell death and Disease of Nervous system, New York: Humana Press; 1999; p. 3-28.

Cole NB, Murphy DD. The cell biology of alpha-synuclein: a sticky problem? Neuromolecular Med 2002; 1: 95-109.

Cole NB, Murphy DD, Grider T, Rueter S, Brasaemle D, Nussbaum RL. Lipid droplet binding and oligomerization properties of the Parkinson's disease protein alpha-synuclein. J Biol Chem. 2002; 277 : 6344-52.

Congdon EE, Duff KE. Is tau aggregation toxic or protective? J Alzheimers Dis. 2008; 14 : 453-457.

Connor JR, Snyder BS, Arosio P, Loeffler DA, LeWitt P. A quantitative analysis of isoferritins in select regions of aged, parkinsonian, and Alzheimer's diseased brains. J Neurochem. 1995 ; 65 : 717-724.

Conway KA, Harper JD, Lansbury PT Jr. Fibrils formed in vitro from alpha-synuclein and two mutant forms linked to Parkinson's disease are typical amyloid. Biochemistry. 2000 ; 39 : 2552-63.

Cook PR, Brazell IA. Supercoils in human DNA. J Cell Sci. 1975; 19 : 261-279.

Corces VG, Manso R, De La Torre J, Avila J, Nasr A, Wiche G. Effects of DNA on microtubule assembly. Eur J Biochem. 1980; 105 : 7-16.

Cristiano F, de Haan JB, Iannello RC, Kola I. Changes in the levels of enzymes which modulate the antioxidant balance occur during aging and correlate with cellular damage. Mech Ageing Dev. 1995; 80 : 93-105.

Crut A, Koster DA, Seidel R, Wiggins CH, Dekker NH. Fast dynamics of supercoiled DNA revealed by single-molecule experiments. Proc Natl Acad Sci U S A. 2007; 104 : 11957-11962.

Crutchley JL, Wang XQ, Ferraiuolo MA, Dostie J. Chromatin conformation signatures: ideal human disease biomarkers? Biomark Med. 2010; 4 : 611-629.

Dalaker TO, Larsen JP, Bergsland N, Beyer MK, Alves G, Dwyer MG, Tysnes OB, Benedict RH, Kelemen A, Bronnick K, Zivadinov R. Brain atrophy and white matter hyperintensities in early Parkinson's disease(a). Mov Disord. 2009 ; 24 : 2233-2241.

Davis PK and Johnson GV. The microtubule binding of Tau and high molecular weight Tau in apoptotic PC12 cells is impaired because of altered phosphorylation. J Biol Chem. 1999; 274 : 35686-35692.

Davydov V, Hansen LA, Shackelford DA. Is DNA repair compromised in Alzheimer’s disease? Neurobiol Ageing. 2003; 24 : 953-968.

Delacourte A, Tau pathology and neurodegeneration: an obvious but misunderstood link. J Alzheimers Dis. 2008; 14 : 437-440.

Deng G, Wu R. Terminal transferase: use of the tailing of DNA and for in vitro mutagenesis. Methods Enzymol. 1983; 100 : 96 -116.

Dev KK, van der Putten H, Sommer B, Rovelli G. Part I: parkin-associated proteins and Parkinson's disease. Neuropharmacology. 2003; 45 : 1-13.

Devenport CJ, Brown WJ, Babb TL. GABAergic neurons are spared after intrahippocampal kainate in the rat. Epilepsy Res. 1990; 5 : 28-42.

Dexter DT, Carayon A, Vidailhet M, Ruberg M, Agid F, Agid Y, Lees AJ, Wells FR, Jenner P, Marsden CD. Decreased ferritin levels in brain in Parkinson's disease. J Neurochem. 1990 ; 55 : 16-20.

Dexter DT, Wells FR, Lees AJ, Agid F, Agid Y, Jenner P, Marsden CD. Increased nigral iron content and alterations in other metal ions occurring in brain in Parkinson's disease. J Neurochem. 1989; 52 :1 830-836.

Di Rosa G, Puzzo D, Sant'Angelo A, Trinchese F, Arancio O. Alpha-synuclein: between synaptic function and dysfunction, Histol Histopathol. 2003; 18 : 1257-1266.

Didier M, Bursztajn S, Adamec E, Passani L, Nixon RA, Coyle JT, Wei JY, Berman SA, DNA strand breaks induced by sustained glutamate excitotoxicity in primary neuronal cultures. J Neurosci. 1996; 16 : 2238- 2250.

Double KL, Gerlach M, Schünemann V, Trautwein AX, Zecca L, Gallorini M, Youdim MB, Riederer P, Ben-Shachar D. Iron-binding characteristics of neuromelanin of the human substantia nigra. Biochem Pharmacol. 2003; 66 : 489-494.

Drechsel DN, Hyman AA, Cobb MH, Kirschner MW. Modulation of the dynamic instability of tubulin assembly by the microtubule-associated protein tau. Mol Biol Cell. 1992 : 3 : 1141-1154.

Dröge P and Pohl FM. The influence of an alternate template conformation on elongating phage T7 RNA polymerase. Nucleic Acids Res. 1991; 19 : 5301-5306.

Duce JA, Smith DP, Blake RE, Crouch PJ, Li QX, Masters CL, Trounce IA. Linker histone H1 binds to disease associated amyloid-like fibrils. J Mol Biol. 2006 ; 361 :493-505.

Eliezer D, Kutluay E, Bussell R Jr, Browne G. Conformational properties of alpha-synuclein in its free and lipid-associated states. J Mol Biol. 2001; 307 : 1061-73.

Epstein J, Sanderson IR, Macdonald TT. Curcumin as a therapeutic agent: the evidence from in vitro, animal and human studies. Br J Nutr. 2010; 103 : 1545-1557.

Evan G, Littlewood T. A matter of life and cell death. Science. 1998; 281 : 1317-1322.

Fasano M, Bergamasco B, Lopiano L. Is neuromelanin changed in Parkinson's disease? Investigations by magnetic spectroscopies. J Neural Transm. 2006 ;113 : 769-774.

Fasano M, Bergamasco B, Lopiano L. Modifications of the iron-neuromelanin system in Parkinson's disease. J Neurochem. 2006 ; 96 : 909-916.

Fath T, Eidenmüller J, Brandt R. Tau-mediated cytotoxicity in a pseudohyperphosphorylation model of Alzheimer's disease. J Neurosci. 2002; 22 : 9733-9741.

Faucheux BA, Martin ME, Beaumont C, Hunot S, Hauw JJ, Agid Y, Hirsch EC. Lack of up-regulation of ferritin is associated with sustained iron regulatory protein-1 binding activity in the substantia nigra of patients with Parkinson's disease. J Neurochem. 2002 ; 83 : 320-330.

Feany MB, Bender WW. A Drosophila model of Parkinson's disease. Nature. 2000 ; 404 : 394-8.

Fedorow H, Tribl F, Halliday G, Gerlach M, Riederer P, Double KL. Neuromelanin in human dopamine neurons: comparison with peripheral melanins and relevance to Parkinson's disease. Prog Neurobiol. 2005; 75 : 109-124.

Fenech M, Morley AA. The effect of donor age on spontaneous and induced micronuclei. Mutat Res. 1985; 148 : 99-105.

Fernández-Checa JC, Fernández A, Morales A, Marí M, García-Ruiz C, Colell A. Oxidative stress and altered mitochondrial function in neurodegenerative diseases: lessons from mouse models. CNS Neurol Disord Drug Targets. 2010;9 : 439-54.

Fisher LM. DNA supercoiling and gene expression. Nature. 1984; 307 : 686-687.

Fontana A, Zambonin M, Polverino de Laureto P, De Filippis V, Clementi A, Scaramella E. Probing the conformational state of apomyoglobin by limited proteolysis, J Mol Biol. 1997; 266 : 223-230.

Fontán-Lozano A, Romero-Granados R, Troncoso J, Múnera A, Delgado-García JM, Carrión AM. Histone deacetylase inhibitors improve learning consolidation in young and in KA-induced-neurodegeneration and SAMP-8-mutant mice. Mol Cell Neurosci. 2008 ; 39: 193-201.

Fraschini A, Bottone MG, Scovassi AI, Denegri M, Risueño MC, Testillano PS, Martin TE, Biggiogera M, Pellicciari C. Changes in extranucleolar transcription during actinomycin D-induced apoptosis. Histol Histopathol. 2005; 20 : 107-117.

Frey BN, Andreazza AC, Kunz M, Gomes KM, Quevedo J, Salvador M, Goncalves CA, Kapczinski F. Increased oxidative stress and DNA damage in bipolar disorder: A twin-case report. Prog Neuropsychopharmacol Biol Psychiatry. 2007; 31 : 283-285.

Frey BN, Valvassori SS, Gomes KM, Martins MR, Pizzol DF, Kapczinski F, Quevedo J. Increased oxidative stress in submitochondrial particles after chronic amphetamine exposure. Brain Res. 2006; 1097 : 224-229.

Fu S, Kurzrock R. Development of curcumin as an epigenetic agent. Cancer. 2010 ; 116 : 4670-4676.

Fukuda H, Sano N, Muto S, Horikoshi M. Simple histone acetylation plays a complex role in the regulation of gene expression. Brief Funct Genomic Proteomic. 2006; 5 : 190-208.

Fuso A, Nicolia V, Cavallaro RA, Scarpa S. DNA methylase and demethylase activities are modulated by one-carbon metabolism in Alzheimer's disease models. J Nutr Biochem. 2010. Jun 21. [Epub ahead of print]

Gabus C, Auxilien S, Péchoux C, Dormont D, Swietnicki W, Morillas M, Surewicz W, Nandi P, Darlix JL. The prion protein has DNA strand transfer properties similar to retroviral nucleocapsid protein. J Mol Biol. 2001; 307 : 1011-21.

Gallagher DA, Schapira AH. Etiopathogenesis and treatment of Parkinson's disease, Curr Top Med Chem. 2009; 9 : 860-868.

Galpern WR, Lang AE. Interface between tauopathies and synucleinopathies: a tale of two proteins. Ann Neurol. 2006; 59 : 449-58.

Galvin JE, Schuck TM, Lee VM, Trojanowski JQ. Differential expression and distribution of alpha-, beta-, and gamma-synuclein in the developing human substantia nigra. Exp Neurol. 2001; 168 : 347-55.

Ganguly BB. Cell division, chromosomal damage and micronucleus formation in peripheral lymphocytes of healthy donors: related to donor's age. Mutat Res. 1993; 295 : 135-148.

Garcia-Alloza M, Borrelli LA, Rozkalne A, Hyman BT, Bacskai BJ. Curcumin labels amyloid pathology in vivo, disrupts existing plaques, and partially restores distorted neurites in an Alzheimer mouse model. J Neurochem. 2007; 102 : 1095-1104.

Gavrieli Y, Sherman Y, Ben-Sasson SA. Identification of programmed cell death in situ via specific labeling of nuclear DNA fragmentation. J Cell Biol. 1992; 119 : 493-501.

George JM, Jin H, Woods WS, Clayton DF. Characterization of a novel protein regulated during the critical period for song learning in the zebra finch. Neuron. 1995; 15 : 361-72.

George JM. The synucleins. Genome Biol. 2002; 3 : REVIEWS3002.

Ghosh A and Bansal M A. Glossary of DNA structures from A to Z. Acta Cryst. 2003; D59 : 620–626.

Giasson BI, Uryu K, Trojanowski JQ, Lee VM. Mutant and wild type human alpha-synucleins assemble into elongated filaments with distinct morphologies in vitro. J Biol Chem. 1999; 274 : 7619-22.

Gmitterová K, Heinemann U, Gawinecka J, Varges D, Ciesielczyk B, Valkovic P, Benetin J, Zerr I. 8-OHdG in cerebrospinal fluid as a marker of oxidative stress in various neurodegenerative diseases. Neurodegener Dis. 2009; 6 : 263-269.

Goedert M, Spillantini MG, Jakes R, Rutherford D, Crowther RA. Multiple isoforms of human microtubule-associated protein tau: sequences and localization in neurofibrillary tangles of Alzheimer's disease. Neuron. 1989; 3 : 519-526.

Goel A, Kunnumakkara AB, Aggarwal BB. Curcumin as "Curecumin": from kitchen to clinic. Biochem Pharmacol. 2008; 75 : 787-809.

Goers J, Manning-Bog AB, McCormack AL, Millett IS, Doniach S, Di Monte DA, Uversky VN, Fink AL. Nuclear localization of alpha-synuclein and its interaction with histones, Biochemistry. 2003; 42 : 8465-8471.

Gold R, Schmied M, Giegerich G, Breitschopf H, Hartung HP, Toyka KV, Lassmann H. Differentiation between cellular apoptosis and necrosis by the combined use of in situ tailing and nick translation techniques. Lab Invest. 1994; 71 : 219-25.

Gómez-Isla T, Hollister R, West H, Mui S, Growdon JH, Petersen RC, Parisi JE, Hyman BT. Neuronal loss correlates with but exceeds neurofibrillary tangles in Alzheimer's disease. Ann Neurol. 1997; 41 : 17-24.

Gómez-Ramos A, Díaz-Hernández M, Cuadros R, Hernández F, Avila J. Extracellular tau is toxic to neuronal cells. FEBS Lett. 2006; 580 : 4842-4850.

González RG, Haxo RS, Schleich T. Mechanism of action of polymeric aurintricarboxylic acid, a potent inhibitor of protein--nucleic acid interactions. Biochemistry. 1980; 19 : 4299-4303.

Gorell JM, Johnson CC, Rybicki BA, Peterson EL, Kortsha GX, Brown GG, Richardson RJ. Occupational exposure to manganese, copper, lead, iron, mercury and zinc and the risk of Parkinson's disease. Neurotoxicology. 1999; 20 : 239-47.

Goris A, Williams-Gray CH, Clark GR, Foltynie T, Lewis SJ, Brown J, Ban M, Spillantini MG, Compston A, Burn DJ, Chinnery PF, Barker RA, Sawcer SJ. Tau and alpha-synuclein in susceptibility to, and dementia in, Parkinson's disease. Ann Neurol. 2007; 62 : 145-53.

Götz ME, Double K, Gerlach M, Youdim MB, Riederer P. The relevance of iron in the pathogenesis of Parkinson's disease. Ann N Y Acad Sci. 2004; 1012 : 193-208.

Grabenauer M, Bernstein SL, Lee JC, Wyttenbach T, Dupuis NF, Gray HB, Winkler JR, Bowers MT. Spermine binding to Parkinson's protein alpha-synuclein and its disease-related A30P and A53T mutants. J Phys Chem B. 2008; 112 : 11147-54.

Graham DG. On the origin and significance of neuromelanin. Arch Pathol Lab Med. 1979; 103 : 359-362.

Graham DG. Oxidative pathways for catecholamines in the genesis of neuromelanin and cytotoxic quinones. Mol Pharmacol. 1978; 14 : 633-643.

Gray DM, Hung SH and Johnson KH. Absorption and circular dichroism spectroscopy of nucleic acid duplexes and triplexes. Methods Enzymol. 1995; 246 : 19-34.

Gray DM, Taylor TN, Lang D. Dehydrated circular DNA: circular dichroism of molecules in ethanolic solutions. Biopolymers. 1978; 17 : 145-157.

Green DM. Wilms' tumour. Eur J Cancer. 1997; 33 : 409-418

Greenwood JA, Johnson GV. Localization and in situ phosphorylation state of nuclear tau. Exp Cell Res. 1995; 220 : 332-337.

Grimes SR Jr, Smart PG. Changes in the structural organization of chromatin during spermatogenesis in the rat. Biochim Biophys Acta. 1985; 824 : 128-139.

Grünblatt E, Zehetmayer S, Jacob CP, Müller T, Jost WH, Riederer P. Pilot study: peripheral biomarkers for diagnosing sporadic Parkinson's disease. J Neural Transm. 2010 ; 117 : 1387-1393.

Guo J, Wu T, Bess J, Henderson LE, Levin JG. Actinomycin D inhibits human immunodeficiency virus type 1 minus-strand transfer in in vitro and endogenous reverse transcriptase assays. J Virol. 1998; 72 : 6716-6724.

Gupta VB, Anitha S, Hegde ML, Zecca L, Garruto RM, Ravid R, Shankar SK, Stein R, Shanmugavelu P, Jagannatha Rao KS. Aluminium in Alzheimer's disease: are we still at a crossroad? Cell Mol Life Sci. 2005; 62 : 143-58.

Gupta VB, Hegde ML, Rao KS. Role of protein conformational dynamics and DNA integrity in relevance to neuronal cell death in neurodegeneration. Curr Alzheimer Res. 2006 ; 3 : 297-309.

Halperin I, Morelli M, Korczyn AD, Youdim MB, Mandel SA. Biomarkers for evaluation of clinical efficacy of multipotential neuroprotective drugs for Alzheimer's and Parkinson's diseases. Neurotherapeutics. 2009 ; 6 : 128-140.

Haque N, Tanaka T, Iqbal K and Grundke-Iqbal I. Regulation of expression, phosphorylation and biological activity of tau during differentiation in SY5Y cells. Brain Res. 1999; 838, 69-77.

Haque N, Tanaka T, Iqbal K, Grundke-Iqbal I. Regulation of expression, phosphorylation and biological activity of tau during differentiation in SY5Y cells. Brain Res. 1999; 838 : 69-77.

Harada A, Oguchi K, Okabe S, Kuno J, Terada S, Ohshima T, Sato-Yoshitake R, Takei, Y, Noda T, Hirokawa N. Altered microtubule organization in small-calibre axons of mice lacking tau protein. Nature. 1994; 369 : 488-491.

Harish G, Venkateshappa C, Mythri RB, Dubey SK, Mishra K, Singh N, Vali S, Bharath MM. Bioconjugates of curcumin display improved protection against glutathione depletion mediated oxidative stress in a dopaminergic neuronal cell line: Implications for Parkinson's disease. Bioorg Med Chem. 2010 ; 18: 2631-8.

Hasegawa T, Matsuzaki M, Takeda A, Kikuchi A, Akita H, Perry G, Smith MA, Itoyama Y. Accelerated alpha-synuclein aggregation after differentiation of SH-SY5Y neuroblastoma cells. Brain Res. 2004; 1013 : 51-9.

Hashimoto M, Hsu LJ, Rockenstein E, Takenouchi T, Mallory M, Masliah E. alpha-Synuclein protects against oxidative stress via inactivation of the c-Jun N-terminal kinase stress-signaling pathway in neuronal cells. J Biol Chem. 2002; 277 : 11465-72.

Hasty P, Campisi J, Hoeijmakers J, van Steeg H, Vijg J. Aging and genome maintenance: lessons from the mouse? Science. 2003; 299 : 1355-1359.

Hasty P, Vijg J. Accelerating aging by mouse reverse genetics: a rational approach to understanding longevity. Aging Cell. 2004; 3 : 55-65.

Hasty P. The impact of DNA damage, genetic mutation and cellular responses on cancer prevention, longevity and aging: observations in humans and mice. Mech Ageing Dev. 2005; 126 : 71-77.

Healy J, Tipton K. Ceruloplasmin and what it might do. J Neural Transm. 2007; 114 : 777-781.

Hegde ML and Jagannatha Rao KS. Challenges and complexities of alpha-synuclein toxicity: new postulates in unfolding the mystery associated with Parkinson's disease. Arch Biochem Biophys. 2003; 418 : 169-178.

Hegde ML and Rao KS. DNA induces folding in alpha-synuclein: understanding the mechanism using chaperone property of osmolytes. Arch Biochem Biophys. 2007; 464 : 57-69.

Hegde ML, Anitha S, Latha KS, Mustak MS, Stein R, Ravid R, Rao KS. First evidence for helical transitions in supercoiled DNA by amyloid Beta Peptide (1-42) and aluminum: a new insight in understanding Alzheimer's disease. J Mol Neurosci. 2004; 22 : 19-31.

Hegde ML, Bharathi P, Suram A, Venugopal C, Jagannathan R, Poddar P, Srinivas P, Sambamurti K, Rao KJ, Scancar J, Messori L, Zecca L, Zatta P. Challenges associated with metal chelation therapy in Alzheimer's disease. J Alzheimers Dis. 2009; 17 : 457-68.

Hegde ML, Gupta VB, Anitha M, Harikrishna T, Shankar SK, Muthane U, Subba Rao K, Jagannatha Rao KS. Studies on genomic DNA topology and stability in brain regions of Parkinson's disease. Arch Biochem Biophys. 2006 ; 449 : 143-156.

Hegde ML, Hegde PM, Holthauzen LM, Hazra TK, Rao KS, Mitra S. Specific Inhibition of NEIL-initiated repair of oxidized base damage in human genome by copper and iron: potential etiological linkage to neurodegenerative diseases. J Biol Chem. 2010; 285 : 28812-28825.

Hegde ML, Shanmugavelu P, Vengamma B, Rao TS, Menon RB, Rao RV, Rao KS. Serum trace element levels and the complexity of inter-element relations in patients with Parkinson's disease. J Trace Elem Med Biol. 2004 ; 18 : 163-171.

Hegde ML, Vasudevaraju P, Rao KJ. DNA induced folding/fibrillation of alpha-synuclein: new insights in Parkinson's disease, Front Biosci. 2010; 15 : 418-436.

Heintz NH. Phosphorylation of proteins that regulate the cell cycle and cancer: an international perspective. Jpn J Clin Oncol. 1997; 27 : 288.

Herceg Z, Wang ZQ. Functions of poly(ADP-ribose) polymerase (PARP) in DNA repair, genomic integrity and cell death. Mutat Res. 2001; 477 : 97-110.

Hinoi E, Balcar VJ, Kuramoto N, Nakamichi N and Yoneda Y. Nuclear transcription factors in the hippocampus. Prog Neurobiol. 2002; 68 : 145-165.

Hirsch EC, Graybiel AM, Agid Y. Selective vulnerability of pigmented dopaminergic neurons in Parkinson's disease. Acta Neurol Scand Suppl. 1989; 126 : 19-22.

Hofer A, Gasser T. New aspects of genetic contributions to Parkinson's disease. J Mol Neurosci. 2004; 24 : 417-24.

Höglinger GU, Breunig JJ, Depboylu C, Rouaux C, Michel PP, Alvarez-Fischer D, Boutillier AL, Degregori J, Oertel WH, Rakic P, Hirsch EC, Hunot S. The pRb/E2F cell-cycle pathway mediates cell death in Parkinson's disease. Proc Natl Acad Sci. 2007; 104 : 3585-90.

Hou MH, Robinson H, Gao YG, Wang AH. Crystal structure of actinomycin D bound to the CTG triplet repeat sequences linked to neurological diseases. Nucleic Acids Res. 2002; 30 : 4910-4917.

Hua Q, He RQ, Haque N, Qu MH, del Carmen Alonso A, Grundke-Iqbal I, Iqbal K. Microtubule associated protein tau binds to double-stranded but not single-stranded DNA. Cell Mol Life Sci 2003; 60 : 413-421.

Hua Q, He RQ. Tau could protect DNA double helix structure. Biochim Biophys Acta. 2003; 1645: 205-211.

Hua Q, He RQ. Effect of phosphorylation and aggregation on tau binding to DNA. Protein Pept Lett. 2002; 9 : 349-357.

Huang J, Plass C, Gerhäuser C. Cancer Chemoprevention by Targeting the Epigenome. Curr Drug Targets. 2010 Dec 15. [Epub ahead of print]

Ikegami S, Harada A, Hirokawa N. Muscle weakness, hyperactivity, and impairment in fear conditioning in tau-deficient mice. Neurosci Lett. 2000; 279 : 129-132.

Ikezu T, Okamoto T, Komatsuzaki K, Matsui T, Martyn JA, Nishimoto I. Negative transactivation of cAMP response element by familial Alzheimer's mutants of APP. EMBO J. 1996; 15 : 2468-75.

Iqbal K, Liu F, Gong CX, Alonso Adel C, Grundke-Iqbal I, Mechanisms of tau-induced neurodegeneration . Acta Neuropathol. 2009; 118 : 53-69.

Ishrat T, Hoda MN, Khan MB, Yousuf S, Ahmad M, Khan MM, Ahmad A, Islam F. Amelioration of cognitive deficits and neurodegeneration by curcumin in rat model of sporadic dementia of Alzheimer's type (SDAT). Eur Neuropsychopharmacol. 2009 ;19 : 636-647.

Jack CR Jr , Shiung MM, Weigand SD, Obrien PC, GunterJL, Boeve BF, Knopman DS, Smith GE, Ivnik RJ, Tangallos EG, Petersen RC. Brain trophy rates predict subsequent clinical conversion in normal elderly and amnestic MCI. Neurology 2005; 65, 1227-1231.

Jackson GR, Wiedau-Pazos M, Sang TK, Wagle N, Brown CA, Massachi S, Geschwind DH. Human wild-type tau interacts with wingless pathway components and produces neurofibrillary pathology in Drosophila. Neuron. 2002; 34 : 509-519.

Jang JH, Surh YJ. beta-Amyloid induces oxidative DNA damage and cell death through activation of c-Jun N terminal kinase. Ann N Y Acad Sci. 2002; 973 : 228-36.

Jasencakova Z, Groth A. Restoring chromatin after replication: how new and old histone marks come together. Semin Cell Dev Biol. 2010; 21 : 231-237.

Jellinger KA. A critical evaluation of current staging of alpha-synuclein pathology in Lewy body disorders, Biochim Biophys Acta. 2009; 1792 : 730-740.

Jenco JM, Rawlingson A, Daniels B, Morris AJ. Regulation of phospholipase D2: selective inhibition of mammalian phospholipase D isoenzymes by alpha- and beta-synucleins. Biochemistry. 1998; 37 : 4901-9.

Jenner P Oxidative stress in Parkinson's disease, Ann Neurol. 2003; 53 : Suppl 3, S26-36; discussion S36-8.

Jenner P. Oxidative mechanisms in nigral cell death in Parkinson's disease. Mov Disord. 1998; 13 Suppl 1: 24-34.

Jo E, McLaurin J, Yip CM, St George-Hyslop P, Fraser PE. alpha-Synuclein membrane interactions and lipid specificity. J Biol Chem. 2000; 275 : 34328-34.

Joe B, Vijaykumar M, Lokesh BR. Biological properties of curcumin-cellular and molecular mechanisms of action. Crit Rev Food Sci Nutr. 2004; 44 : 97-111.

Joffe B, Leonhardt H, Solovei I. Differentiation and large scale spatial organization of the genome. Curr Opin Genet Dev. 2010; 20 : 562-569.

Johnson GV, Stoothoff WH. Tau phosphorylation in neuronal cell function and dysfunction. J Cell Sci. 2004: 117 : 5721-5729.

Jokinen P, Brück A, Aalto S, Forsback S, Parkkola R, Rinne JO. Impaired cognitive performance in Parkinson's disease is related to caudate dopaminergic hypofunction and hippocampal atrophy. Parkinsonism Relat Disord. 2009; 15 : 88-93.

Jowaed A, Schmitt I, Kaut O, Wüllner U. Methylation regulates alpha-synuclein expression and is decreased in Parkinson's disease patients' brains. J Neurosci. 2010; 30 : 6355-6359.

Kalra S, Bergeron C, Lang AE. Lewy body disease and dementia. A review. Arch Intern Med. 1996; 156 : 487-93.

Kamitori S, Takusagawa F. Crystal structure of the 2:1 complex between d(GAAGCTTC) and the anticancer drug actinomycin D. J Mol Biol. 1992; 225 : 445-456.

Kaplan B, Ratner V, Haas E. Alpha-synuclein: its biological function and role in neurodegenerative diseases, J Mol Neurosci. 2003; 20 : 83-92.

Kawamata J, Imanishi M. Interaction of actinomycin with deoxyribonucleic acid. Nature. 1960; 187 :1112-1113.

Kawanishi S, Hiraku Y. Amplification of anticancer drug-induced DNA damage and apoptosis by DNA-binding compounds. Curr Med Chem Anticancer Agents. 2004; 4 : 415-419.

Kerr JFR, Gobe GC, Winterford CM, Harmon BV. Anatomical Methods in cell death. In: Schwartz LM, Osborne BA, editors. Methods in Cell biology: Cell Death, New York: Academic press; 1995; p.1-27.

Khanna S, Park HA, Sen CK, Golakoti T, Sengupta K, Venkateswarlu S, Roy S. Neuroprotective and antiinflammatory properties of a novel demethylated curcuminoid. Antioxid Redox Signal. 2009; 11 : 449-468.

Kim D, Frank CL, Dobbin MM, Tsunemoto RK, Tu W, Peng PL, Guan JS, Lee BH, Moy LY, Giusti P, Broodie N, Mazitschek R, Delalle I, Haggarty SJ, Neve RL, Lu Y, Tsai LH. Deregulation of HDAC1 by p25/Cdk5 in neurotoxicity. Neuron. 2008 ; 60 : 803-817.

Kim D, Tsai LH. Linking cell cycle reentry and DNA damage in neurodegeneration. Ann N Y Acad Sci. 2009 ; 1170 : 674-679.

Kingsbury AE, Marsden CD, Foster OJ. DNA fragmentation in human substantia nigra: apoptosis or perimortem effect? Mov. Disord. 1998; 13: 877-884.

Knovich MA, Storey JA, Coffman LG, Torti SV, Torti FM. Ferritin for the clinician. Blood Rev. 2009 ; 23 : 95-104.

Kontopoulos E, Parvin JD, Feany MB. Alpha-synuclein acts in the nucleus to inhibit histone acetylation and promote neurotoxicity. Hum Mol Genet. 2006; 15 : 3012-23

Kornberg RD, LaPointe JW, Lorch Y. Preparation of nucleosomes and chromatin. Methods Enzymol. 1989;170:3-14.

Kornberg RD. Structure of chromatin. Annu Rev Biochem. 1977; 46 : 931-54.

Koutsilieri E, Scheller C, Grünblatt E, Nara K, Li J, Riederer P Free radicals in Parkinson's disease, J Neurol. 2002; 249 : Suppl 2, II 1-5.

Kouzarides T. Chromatin modifications and their function. Cell. 2007; 128 : 693-705.

Krüger R, Kuhn W, Müller T, Woitalla D, Graeber M, Kösel S, Przuntek H, Epplen JT, Schöls L, Riess O. Ala30Pro mutation in the gene encoding alpha-synuclein in Parkinson's disease. Nat Genet. 1998; 18 : 106-8.

Krylova SM, Musheev M, Nutiu R, Li Y, Lee G, Krylov SN, Tau protein binds single-stranded DNA sequence specifically--the proof obtained in vitro with non-equilibrium capillary electrophoresis of equilibrium mixtures. FEBS Lett. 2005; 579 : 1371-1375.

Kuloglu M, Ustundag B, Atmaca M, Canatan H, Tezcan AE, Clinkilinc N. Lipid peroxidation and antioxidant enzyme levels in patients with schizophrenia and bipolar disorder. Cell Biochem Funct. 2002; 20 : 171-175.

Kunwar A, Simon E, Singh U, Chittela RK, Sharma D, Sandur SK, Priyadarsini IK. Interaction of a Curcumin Analogue Dimethoxycurcumin with DNA. Chem Biol Drug Des. 2011 Jan 18. doi: 10.1111/j.1747-0285.2011.01083.x. [Epub ahead of print]

Lackner H. Three-dimensional structure of the actinomycins. Angew Chem Int Ed Engl. 1975; 14 : 375-386.

Laemmli UK. Cleavage of structural proteins during the assembly of the head of bacteriophage T4, Nature. 1970; 227 : 680-685.

LaFerla FM, Oddo S. Alzheimer's disease: Abeta, tau and synaptic dysfunction. Trends Mol Med. 2005; 11 : 170-176.

Lavedan C. The synuclein family. Genome Res. 1998; 8, 871-880.

Le Couteur DG, McLean AJ, Taylor MC, Woodham BL, Board PG. Pesticides and Parkinson's disease. Biomed Pharmacother. 1999; 53 : 122-30.

Lee HG, Zhu X, Takeda A, Perry G, Smith MA. Emerging evidence for the neuroprotective role of alpha-synuclein. Exp Neurol. 2006; 200 : 1-7.

Leng Y, Chase TN, Bennett MC. Muscarinic receptor stimulation induces translocation of an alpha-synuclein oligomer from plasma membrane to a light vesicle fraction in cytoplasm. J Biol Chem. 2001; 276 : 28212-8.

Leoni L, Morosetti S, Palermo C, Sampaolese B, Savino M. Specific interactions between DNA left-handed supercoils and actinomycin D. Biophys Chem. 1989; 33 : 11-17.

Lerch JP, Evans AC. Cortical thickness analysis examined through power analysis and a population simulation. Neuroimage. 2005; 24, 163-73.

Lewy F, Lewandowski N, Abelsdorff G. In handbuch der neurologie. Springer Verlag Berlin 1912; 3 : 920-923.

Li H, Mitchell JR, Hasty P. DNA double-strand breaks: a potential causative factor for mammalian aging? Mech Ageing Dev. 2008; 129 : 416-424.

Li H, Xiao J, Li J, Lu L, Feng S and Dröge P. Human genomic Z-DNA segments probed by the Z alpha domain of ADAR1. Nucleic Acids Res. 2009; 37 : 2737-2746.

Li W, Cai S, Cai L, Li X. Anti-apoptotic effect of hepatocyte growth factor from actinomycin D in hepatocyte-derived HL7702 cells is associated with activation of PI3K/Akt signaling. Toxicol Lett. 2006; 165 : 142-148.

Li X, Romero P, Rani M, Dunker AK, Obradovic Z. Predicting Protein Disorder for N-, C-, and Internal Regions. Genome Inform Ser Workshop Genome Inform. 1999; 10 : 30-40.

Lin WL, DeLucia MW, Dickson DW. Alpha-synuclein immunoreactivity in neuronal nuclear inclusions and neurites in multiple system atrophy. Neurosci Lett. 2004; 354 : 99-102.

Lindsey J, McGill NI, Lindsey LA, Green DK, Cooke HJ. In vivo loss of telomeric repeats with age in humans. Mutat Res. 1991; 256 : 45-48.

Lowry OH, Rosebrough NJ, Farr AL and Randall RJ. Protein measurement with the Folin phenol reagent. J Biol Chem. 1951; 193 : 265-275.

Liu H, Mulholland N, Fu H and Zhao K. Cooperative activity of BRG1 and Z-DNA formation in chromatin remodeling. Mol Cell Biol. 2006; 26 : 2550–2559.

Liu HL, Chen Y, Cui GH, Zhou JF. Curcumin, a potent anti-tumor reagent, is a novel histone deacetylase inhibitor regulating B-NHL cell line Raji proliferation. Acta Pharmacol Sin. 2005; 26 : 603-609.

Liu Z, Xie Z, Jones W, Pavlovicz RE, Liu S, Yu J, Li PK, Lin J, Fuchs JR, Marcucci G, Li C, Chan KK. Curcumin is a potent DNA hypomethylation agent. Bioorg Med Chem Lett. 2009; 19 : 706-709.

Liu Z, Yu Y, Li X, Ross CA, Smith WW. Curcumin protects against A53T alpha-synuclein-induced toxicity in a PC12 inducible cell model for Parkinsonism. Pharmacol Res. 2011 Jan 12. [Epub ahead of print]

Loeffler DA, LeWitt PA, Juneau PL, Sima AA, Nguyen HU, DeMaggio AJ, Brickman CM, Brewer GJ, Dick RD, Troyer MD, Kanaley L. Increased regional brain concentrations of ceruloplasmin in neurodegenerative disorders. Brain Res. 1996 ; 738 : 265-274.

Longoni G, Agosta F, Kostić VS, Stojković T, Pagani E, Stošić-Opinćal T, Filippi M. MRI measurements of brainstem structures in patients with Richardson's syndrome, progressive supranuclear palsy-parkinsonism, and Parkinson's disease. Mov Disord. 2010 Dec 15. [Epub ahead of print]

Loomis PA, Howard TH, Castleberry RP and Binder LI. Identification of nuclear tau isoforms in human neuroblastoma cells. Proc Natl Acad Sci U S A. 1990; 87 : 8422-8426.

Lu Q, Wood JG. Functional studies of Alzheimer’s disease tau protein. J Neurosci. 1993; 13 : 508-515.

Maher P, Akaishi T, Schubert D, Abe K.A pyrazole derivative of curcumin enhances memory. Neurobiol Aging. 2010; 31 : 706-9.

Maher P, Akaishi T, Schubert D, Abe K.A pyrazole derivative of curcumin enhances memory. Neurobiol Aging. 2010; 31 : 706-9.

Mandelkow E. Alzheimer's disease. The tangled tale of tau. Nature. 1999; 402 : 588-589.

Mandelkow EM, Stamer K, Vogel R, Thies E, Mandelkow E. Clogging of axons by tau, inhibition of axonal traffic and starvation of synapses. Neurobiol Aging. 2003; 24 : 1079-1085.

Manjunatha H, Srinivasan K. Hypolipidemic and antioxidant effects of dietary curcumin and capsaicin in induced hypercholesterolemic rats. Lipids. 2007 ; 42 : 1133-1142.

Manjunatha H, Srinivasan K. Protective effect of dietary curcumin and capsaicin on induced oxidation of low-density lipoprotein, iron-induced hepatotoxicity and carrageenan-induced inflammation in experimental rats. FEBS J. 2006; 273 : 4528-4537.

Manning-Bog AB, McCormack AL, Purisai MG, Bolin LM, Di Monte DA. Alpha-synuclein overexpression protects against paraquat-induced neurodegeneration. J Neurosci. 2003 ; 23 : 3095-9.

Margolis RL, Chuang DM, Post RM. Programmed cell death: implications for neuropsychiatric disorders. Biol Psychiatry. 1994; 35 : 946-956.

Maroteaux L, Campanelli JT, Scheller RH. Synuclein: a neuron-specific protein localized to the nucleus and presynaptic nerve terminal. J Neurosci. 1988; 8 : 2804-2815.

Marques SC, Oliveira CR, Pereira CM, Outeiro TF. Epigenetics in neurodegeneration: A new layer of complexity. Prog Neuropsychopharmacol Biol Psychiatry. 2010 Aug 22. [Epub ahead of print]

Martin FL, Williamson SJ, Paleologou KE, Hewitt R, El-Agnaf OM, Allsop D. Fe(II)-induced DNA damage in alpha-synuclein-transfected human dopaminergic BE(2)-M17 neuroblastoma cells: detection by the Comet assay. J Neurochem. 2003; 87 : 620-30.

Matsuoka Y, Vila M, Lincoln S, McCormack A, Picciano M, LaFrancois J, Yu X, Dickson D, Langston WJ, McGowan E, Farrer M, Hardy J, Duff K, Przedborski S, Di Monte DA. Lack of nigral pathology in transgenic mice expressing human alpha-synuclein driven by the tyrosine hydroxylase promoter. Neurobiol Dis. 2001; 8 : 535-9.

Matsuzaki M, Hasegawa T, Takeda A, Kikuchi A, Furukawa K, Kato Y, Itoyama Y. Histochemical features of stress-induced aggregates in alpha-synuclein overexpressing cells. Brain Res. 2004; 1004 : 83-90.

Mazloom AR, Basu K, Mandal SS, Das SK. Chromatin remodeling in silico: a stochastic model for SWI/SNF. Biosystems. 2010; 99 : 179-91.

McGeer EG, Klegeris A, McGeer PL. Inflammation, the complement system and the diseases of aging. Neurobiol Aging. 2005; 26 Suppl 1: 94-7.

Menke RA, Jbabdi S, Miller KL, Matthews PM, Zarei M. Connectivity-based segmentation of the substantia nigra in human and its implications in Parkinson's disease. Neuroimage. 2010; 52 : 1175-1180.

Menke RA, Scholz J, Miller KL, Deoni S, Jbabdi S, Matthews PM, Zarei M. MRI characteristics of the substantia nigra in Parkinson's disease: a combined quantitative T1 and DTI study. Neuroimage. 2009 ; 47 : 435-441.

Misteli T. Higher-order genome organization in human disease. Cold Spring Harb Perspect Biol. 2010; 2 : a000794.

Mohorko N, Repovs G, Popović M, Kovacs GG, Bresjanac M. Curcumin labeling of neuronal fibrillar tau inclusions in human brain samples. J Neuropathol Exp Neurol. 2010; 69 : 405-14.

Moreira PI, Zhu X, Wang X, Lee HG, Nunomura A, Petersen RB, Perry G, Smith MA. Mitochondria: a therapeutic target in neurodegeneration. Biochim Biophys Acta. 2010; 1802 : 212-20.

Mori F, Tanji K, Yoshimoto M, Takahashi H, Wakabayashi K. Immunohistochemical comparison of alpha- and beta-synuclein in adult rat central nervous system, Brain Res. 2002; 941 : 118-126.

Müller W, Crothers DM. Studies of the binding of actinomycin and related compounds to DNA. J Mol Biol. 1968; 35 : 251-290.

Münch G, Lüth HJ, Wong A, Arendt T, Hirsch E, Ravid R, Riederer P. Crosslinking of alpha-synuclein by advanced glycation endproducts--an early pathophysiological step in Lewy body formation? J Chem Neuroanat. 2000; 20 : 253-257.

Murphy DD, Rueter SM, Trojanowski JQ, Lee VM. Synucleins are developmentally expressed, and alpha-synuclein regulates the size of the presynaptic vesicular pool in primary hippocampal neurons. J Neurosci. 2000; 20 : 3214-20.

Mustak MS, Rao TS, Shanmugavelu P, Sunder NM, Menon RB, Rao RV, Rao KS. Assessment of serum macro and trace element homeostasis and the complexity of inter-element relations in bipolar mood disorders. Clin Chim Acta. 2008; 394 : 47-53.

Mzhel'skaya TI. Biological functions of ceruloplasmin and their deficiency caused by mutation in genes regulating copper and iron metabolism. Bull Exp Biol Med. 2000 ; 130 : 719-727.

Nadig G, Ratnaparkhi GS, Varadarajan R, Vishveshwara S. Dynamics of ribonuclease A and ribonuclease S: computational and experimental studies, Protein Sci. 1996; 5 : 2104-2114.

Nafisi S, Adelzadeh M, Norouzi Z, Sarbolouki MN. Curcumin binding to DNA and RNA. DNA Cell Biol. 2009; 28 : 201-208.

Nandi PK, Leclerc E, Nicole JC, Takahashi M. DNA-induced partial unfolding of prion protein leads to its polymerisation to amyloid. J Mol Biol. 2002; 322 : 153-161.

Nandi PK. Polymerization of human prion peptide HuPrP 106-126 to amyloid in nucleic acid solution. Arch Virol. 1998;143 : 1251-1263.

Negre-Salvayre A, Salvayre R, Augé N, Pamplona R, Portero-Otín M. Hyperglycemia and glycation in diabetic complications, Antioxid Redox Signal. 2009; 11, 3071-3109.

Nicholas AP, Lubin FD, Hallett PJ, Vattem P, Ravenscroft P, Bezard E, Zhou S, Fox SH, Brotchie JM, Sweatt JD, Standaert DG. Striatal histone modifications in models of levodopa-induced dyskinesia. J Neurochem. 2008; 106 : 486-494.

Nicolaus BJ. A critical review of the function of neuromelanin and an attempt to provide a unified theory. Med Hypotheses. 2005; 65 : 791-796.

Nunomura A, Chiba S, Kosaka K, Takeda A, Castellani RJ, Smith MA, Perry G. Neuronal RNA oxidation is a prominent feature of dementia with Lewy bodies. Neuroreport. 2002 ; 13 : 2035-9.

Odh G, Carstam R, Paulson J, Wittbjer A, Rosengren E, Rorsman H. Neuromelanin of the human substantia nigra: a mixed-type melanin. J Neurochem. 1994; 62 : 2030-2036.

Oh DB, Kim YG and Rich A. Z-DNA-binding proteins can act as potent effectors of gene expression in vivo. Proc. Natl Acad. Sci. USA. 2002: 99 : 16666–16671.

Oh WJ, Noggle SA, Maddox DM and Condie BG. The mouse vesicular inhibitory amino acid transporter gene: expression during embryogenesis, analysis of its core promoter in neural stem cells and a reconsideration of its alternate splicing. Gene 2005; 351 : 39-49.

Olanow CW. The pathogenesis of cell death in Parkinson's disease - 2007. Mov Disord. 2007; 22 : S335-S342.

Olinski R, Siomek A, Rozalski R, Gackowski D, Foksinski M, Guz J, Dziaman T, Szpila A, Tudek B. Oxidative damage to DNA and antioxidant status in aging and age-related diseases. Acta Biochim Pol. 2007 ; 54 : 11-26.

Ono K, Hirohata M, Yamada M. Alpha-synuclein assembly as a therapeutic target of Parkinson's disease and related disorders. Curr Pharm Des. 2008;14 : 3247-3266.

Ortiz-Ortiz MA, Morán JM, Ruiz-Mesa LM, Niso-Santano M, Bravo-SanPedro JM, Gómez-Sánchez R, González-Polo RA, Fuentes JM. Curcumin exposure induces expression of the Parkinson's disease-associated leucine-rich repeat kinase 2 (LRRK2) in rat mesencephalic cells. Neurosci Lett. 2010 ; 468 :120-4.

Ostrerova N, Petrucelli L, Farrer M, Mehta N, Choi P, Hardy J, Wolozin B. alpha-Synuclein shares physical and functional homology with 14-3-3 proteins. J Neurosci. 1999 ; 19 : 5782-91.

Outeiro TF, Kontopoulos E, Altmann SM, Kufareva I, Strathearn KE, Amore AM, Volk CB, Maxwell MM, Rochet JC, McLean PJ, Young AB, Abagyan R, Feany MB, Hyman BT, Kazantsev AG. Sirtuin 2 inhibitors rescue alpha-synuclein-mediated toxicity in models of Parkinson's disease. Science. 2007; 317 : 516-9.

Ozcan ME, Gulec M, Ozerol E, Polat R, Akyol O. Antioxidant enzyme activities and oxidative stress in affective disorders. Int Clinpsychopharmacol. 2004; 19 : 89-95.

Packer RJ, Sutton LN, Bilaniuk LT, Radcliffe J, Rosenstock JG, Siegel KR, Bunin GR, Savino PJ, Bruce DA, Schut L. Treatment of chiasmatic/hypothalamic gliomas of childhood with chemotherapy: an update. Ann Neurol. 1988 ; 23 : 79-85.

Pallos J, Bodai L, Lukacsovich T, Purcell JM, Steffan JS, Thompson LM, Marsh JL. Inhibition of specific HDACs and sirtuins suppresses pathogenesis in a Drosophila model of Huntington's disease. Hum Mol Genet. 2008; 17 : 3767-75.

Pan R, Qiu S, Lu DX, Dong J. Curcumin improves learning and memory ability and its neuroprotective mechanism in mice. Chin Med J (Engl). 2008 ; 121 : 832-9.

Pande MB, Nagabhushan P, Hegde ML, Rao TS, Rao KS. An algorithmic approach to understand trace elemental homeostasis in serum samples of Parkinson disease. Comput Biol Med. 2005 ; 35 : 475-493.

Pandey N, Strider J, Nolan WC, Yan SX, Galvin JE. Curcumin inhibits aggregation of alpha-synuclein. Acta Neuropathol. 2008; 115 : 479-89.

Papasozomenos SC. Nuclear tau immunoreactivity in presenile dementia with motor neuron disease: a case report. Clin Neuropathol. 1995; 14 : 100-104.

Parkinson J. An essay on the Shaking Palsy (Sherwood, Neely and Jones) London (1817).

Patel BN, Dunn RJ, Jeong SY, Zhu Q, Julien JP, David S. Ceruloplasmin regulates iron levels in the CNS and prevents free radical injury. J Neurosci. 2002 ; 22 : 6578-6586.

Perrin RJ, Woods WS, Clayton DF, George JM. Exposure to long chain polyunsaturated fatty acids triggers rapid multimerization of synucleins. J Biol Chem. 2001; 276 : 41958-41962.

Perrin RJ, Woods WS, Clayton DF, George JM. Interaction of human alpha-Synuclein and Parkinson's disease variants with phospholipids. Structural analysis using site-directed mutagenesis. J Biol Chem. 2000; 275 : 34393-34398.

Petersen K, Olesen OF, Mikkelsen JD. Developmental expression of alpha-synuclein in rat hippocampus and cerebral cortex. Neuroscience. 1999; 91 : 651-9.

Petri S, Kiaei M, Kipiani K, Chen J, Calingasan NY, Crow JP, Beal MF. Additive neuroprotective effects of a histone deacetylase inhibitor and a catalytic antioxidant in a transgenic mouse model of amyotrophic lateral sclerosis. Neurobiol Dis. 2006; 22 : 40-9.

Petruzzi MJ, Green DM. Wilms' tumor. Pediatr Clin North Am. 1997;44 : 939-952.

Phillips DR, Crothers DM. Kinetics and sequence specificity of drug-DNA interactions: an in vitro transcription assay. Biochemistry. 1986; 25 : 7355-7362.

Pieper HC, Evert BO, Kaut O, Riederer PF, Waha A, Wüllner U. Different methylation of the TNF-alpha promoter in cortex and substantia nigra: Implications for selective neuronal vulnerability. Neurobiol Dis. 2008; 32 : 521-7.

Pletnikova O, West N, Lee MK, Rudow GL, Skolasky RL, Dawson TM, Marsh L, Troncoso JC. Abeta deposition is associated with enhanced cortical alpha-synuclein lesions in Lewy body diseases. Neurobiol Aging. 2005; 26 : 1183-92.

Polo SE, Almouzni G. DNA damage leaves its mark on chromatin. Cell Cycle. 2007; 6 : 2355-9.

Polymeropoulos MH, Lavedan C, Leroy E, Ide SE, Dehejia A, Dutra A, Pike B, Root H, Rubenstein J, Boyer R, Stenroos ES, Chandrasekharappa S, Athanassiadou A, Papapetropoulos T, Johnson WG, Lazzarini AM, Duvoisin RC, Di Iorio G, Golbe LI, Nussbaum RL. Mutation in the alpha-synuclein gene identified in families with Parkinson's disease. Science. 1997; 276 : 2045-7.

Postberg J, Lipps HJ, Cremer T. Evolutionary origin of the cell nucleus and its functional architecture. Essays Biochem. 2010; 48 : 1-24.

Prakash KM, Tan EK. Development of Parkinson's disease biomarkers. Expert Rev Neurother. 2010 ; 10 : 1811-1825.

Qu MH, Li H, Tian R, Nie CL, Liu Y, Han BS, He RQ, Neuronal tau induces DNA conformational changes observed by atomic force microscopy. Neuroreport. 2004; 15: 2723-2727.

Rahman I. Dietary polyphenols mediated regulation of oxidative stress and chromatin remodeling in inflammation. Nutr Rev. 2008; 66 Suppl 1: S42-5.

Rajeswari A, Sabesan M. Inhibition of monoamine oxidase-B by the polyphenolic compound, curcumin and its metabolite tetrahydrocurcumin, in a model of Parkinson's disease induced by MPTP neurodegeneration in mice. Inflammopharmacology. 2008 ; 16 : 96-99.

Rajput AH, Birdi S. Epidemiology of Parkinson's disease. Parkinsonism Relat Disord. 1997; 3 : 175-86.

Ranjekar PK, Hinge A, Hegde MV, Ghate M, Kale A, Sitasawad S, Wagh UV, Debsikdar VB, Mahadik SP. Decreased antioxidant enzymes and membrane essential polyunsaturated fatty acids in schizophrenic and bipolar mood disorder patients. Psychiatry Res. 2003; 121 : 109-122.

Rao BJ, Brahmachari SK, Rao MR. Structural organization of the meiotic prophase chromatin in the rat testis. J Biol Chem. 1983; 258 : 13478-13485.

Rao KS, Hegde ML, Anitha S, Musicco M, Zucca FA, Turro NJ, Zecca L. Amyloid beta and neuromelanin--toxic or protective molecules? The cellular context makes the difference. Prog Neurobiol. 2006; 78 : 364-73.

Rao KS. Free radical induced oxidative damage to DNA: relation to brain aging and neurological disorders. Indian J Biochem Biophys. 2009 ; 46 : 9-15.

Rao KS. Genomic damage and its repair in young and ageing brain. Mol Neurobiol. 1993; 7 : 23- 48.

Rathke-Hartlieb S, Kahle PJ, Neumann M, Ozmen L, Haid S, Okochi M, Haass C, Schulz JB. Sensitivity to MPTP is not increased in Parkinson's disease-associated mutant alpha-synuclein transgenic mice.J Neurochem. 2001; 77 : 1181-4.

Ravikumar B, Rubinsztein DC. Can autophagy protect against neurodegeneration caused by aggregate-prone proteins? Neuroreport. 2004; 15 : 2443-5.

Rich A. DNA comes in many forms. Gene. 1993; 135 : 99–109.

Riehm MR, Harrington RE. Protein-dependent conformational behavior of DNA in chromatin. Biochemistry. 1987; 26 : 2878-2886.

Rippe K. Dynamic organization of the cell nucleus. Curr Opin Genet Dev. 2007 ; 17 : 373-380.

Rolig RL, McKinnon PJ. Linking DNA damage and neurodegeneration. Trends Neurosci. 2000 ; 23: 417-24.

Roselli F, Pisciotta NM, Pennelli M, Aniello MS, Gigante A, De Caro MF, Ferrannini E, Tartaglione B, Niccoli-Asabella A, Defazio G, Livrea P, Rubini G. Midbrain SERT in degenerative parkinsonisms: a 123I-FP-CIT SPECT study. Mov Disord. 2010 ; 25 : 1853-1859.

Rossi G, Dalprà L, Crosti F, Lissoni S, Sciacca FL, Catania M, Di Fede G, Mangieri M, Giaccone G, Croci D, Tagliavini F. A new function of microtubule-associated protein tau: involvement in chromosome stability. Cell Cycle. 2008; 7 : 1788-1794.

Roth TL, Roth ED, Sweatt JD. Epigenetic regulation of genes in learning and memory. Essays Biochem. 2010; 48 : 263-274.

Rouaux C, Jokic N, Mbebi C, Boutillier S, Loeffler JP, Boutillier AL. Critical loss of CBP/p300 histone acetylase activity by caspase-6 during neurodegeneration. EMBO J. 2003; 22 : 6537-49.

Rouaux C, Loeffler JP, Boutillier AL. Targeting CREB-binding protein (CBP) loss of function as a therapeutic strategy in neurological disorders. Biochem Pharmacol. 2004 ; 68 : 1157-64.

Rustin GJ, Newlands ES, Begent RH, Dent J, Bagshawe KD. Weekly alternating etoposide, methotrexate, and actinomycin/vincristine and cyclophosphamide chemotherapy for the treatment of CNS metastases of choriocarcinoma. J Clin Oncol. 1989; 7: 900-903.

Saha RN, Pahan K. HATs and HDACs in neurodegeneration: a tale of disconcerted acetylation homeostasis. Cell Death Differ. 2006; 13 : 539-50.

Sambrook J, Fritsch EF, Maniatis T. Molecular Cloning-A Laboratory Manual. 2nd ed. Cold Spring Harbor Lab: New York; 1989.

Sandyk R. The relationship between diabetes mellitus and Parkinson's disease, Int J Neurosci. 1993; 69 : 125-130.

Sangchot P, Sharma S, Chetsawang B, Porter J, Govitrapong P, Ebadi M. Deferoxamine attenuates iron-induced oxidative stress and prevents mitochondrial aggregation and alpha-synuclein translocation in SK-N-SH cells in culture. Dev Neurosci. 2002;24 : 143-53.

Sawada K, Noda K, Nakajima H, Shimbara N, Furuichi Y, Sugimoto M. Differential cytotoxicity of anticancer agents in pre- and post-immortal lymphoblastoid cell lines. Biol Pharm Bull. 2005; 28 : 1202-1207.

Sayre LM, Perry G, Smith MA. Oxidative stress and neurotoxicity. Chem Res Toxicol. 2008 ; 21 : 172-188.

Scarpa S, Fuso A, D'Anselmi F, Cavallaro RA. Presenilin 1 gene silencing by S-adenosylmethionine: a treatment for Alzheimer disease? FEBS Lett. 2003 ; 541: 145-148.

Scatchard G The attraction of proteins for small molecules and ions. Ann N Y Acad Sci. (USA) 1949; 51: 660-672.

Scherzer CR. Chipping away at diagnostics for neurodegenerative diseases. Neurobiol Dis. 2009 ; 35: 148-56.

Scherzer CR. Chipping away at diagnostics for neurodegenerative diseases. Neurobiol Dis. 2009 ; 35 : 148-156.

Schneider BL, Seehus CR, Capowski EE, Aebischer P, Zhang SC, Svendsen CN. Over-expression of alpha-synuclein in human neural progenitors leads to specific changes in fate and differentiation, Hum Mol Genet. 2007; 16 : 651-666.

Segrest JP, Jones MK, De Loof H, Brouillette CG, Venkatachalapathi YV, Anantharamaiah GM. The amphipathic helix in the exchangeable apolipoproteins: a review of secondary structure and function. J Lipid Res. 1992; 33 : 141-66.

Sensi M, Pricci F, Andreani D, Di Mario U. Advanced nonenzymatic glycation endproducts (AGE): their relevance to aging and the pathogenesis of late diabetic complications. Diabetes Res. 1991; 16 : 1-9.

Serban D, Benevides JM, Thomas GJ Jr. DNA secondary structure and Raman markers of supercoiling in Escherichia coli plasmid pUC19. Biochemistry. 2002; 41 : 847-853.

Sheffield LG, Miskiewicz HB, Tannenbaum LB, Mirra SS. Nuclear pore complex proteins in Alzheimer disease. J. Neuropathol. Exp. Neurol. 2006; 65 : 45-54.

Shim D, Kang HY, Jeon BW, Kang SS, Chang SI, Kim HY. Protein kinase B inhibits apoptosis induced by actinomycin D in ECV304 cells through phosphorylation of caspase 8. Arch Biochem Biophys. 2004; 425 : 214-220.

Shima T, Sarna T, Swartz HM, Stroppolo A, Gerbasi R, Zecca L. Binding of iron to neuromelanin of human substantia nigra and synthetic melanin: an electron paramagnetic resonance spectroscopy study. Free Radic Biol Med. 1997; 23 : 110-119.

Sian J, Dexter DT, Lees AJ, Daniel S, Agid Y, Javoy-Agid F, Jenner P, Marsden CD. Alterations in glutathione levels in Parkinson's disease and other neurodegenerative disorders affecting basal ganglia, Ann Neurol, 1994; 36 : 348-355.

Siino JS, Yau PM, Imai BS, Gatewood JM, Bradbury EM. Effect of DNA length and H4 acetylation on the thermal stability of reconstituted nucleosome particles. Biochem Biophys Res Commun. 2003; 302 : 885-891.

Simon K, Mukundan A, Dewundara S, Van Remmen H, Dombkowski AA, Cabelof DC. Transcriptional profiling of the age-related response to genotoxic stress points to differential DNA damage response with age. Mech Ageing Dev. 2009; 130 : 637-647.

Simpkins H, Pearlman LF. The binding of actinomycin D and Adriamycin to supercoiled DNA, single-stranded DNA and polynucleotides. Biochim Biophys Acta. 1984; 783 : 293-300.

Sjoberg MK, Shestakova E, Mansuroglu Z, Maccioni RB, Bonnefoy E. Tau protein binds to pericentromeric DNA: a putative role for nuclear tau in nucleolar organization. J Cell Sci. 2006; 119: 2025-2034.

Smeyne RJ, Jackson-Lewis V. The MPTP model of Parkinson's disease. Brain Res Mol Brain Res. 2005; 134 : 57-66.

Sobell HM, Jain SC. Stereochemistry of actinomycin binding to DNA. II. Detailed molecular model of actinomycin-DNA complex and its implications. J Mol Biol. 1972; 68 : 21-34.

Song C, Kanthasamy A, Anantharam V, Sun F, Kanthasamy AG. Environmental neurotoxic pesticide increases histone acetylation to promote apoptosis in dopaminergic neuronal cells: relevance to epigenetic mechanisms of neurodegeneration. Mol Pharmacol. 2010; 77 : 621-632.

Sordet O, Nakamura AJ, Redon CE, Pommier Y. DNA double-strand breaks and ATM activation by transcription-blocking DNA lesions. Cell Cycle. 2010; 9 : 274-278.

Specht CG, Tigaret CM, Rast GF, Thalhammer A, Rudhard Y, Schoepfer R. Subcellular localisation of recombinant alpha- and gamma-synuclein. Mol Cell Neurosci. 2005 ; 28 : 326-334.

Spillantini MG, Schmidt ML, Lee VM, Trojanowski JQ, Jakes R, Goedert M. Alpha-synuclein in Lewy bodies, Nature. 1997; 388 : 839-840.

Spires-Jones TL, Stoothoff WH, de Calignon A, Jones PB and Hyman BT. Tau pathophysiology in neurodegeneration: a tangled issue. Trends Neurosci. 2009; 32 : 150-159.

Stefanis L, Kholodilov N, Rideout HJ, Burke RE, Greene LA. Synuclein-1 is selectively up-regulated in response to nerve growth factor treatment in PC12 cells. J Neurochem. 2001; 76 : 1165-1176.

Stilmann M, Hinz M, Arslan SC, Zimmer A, Schreiber V, Scheidereit C. A nuclear poly (ADP-ribose)-dependent signalosome confers DNA damage-induced IkappaB kinase activation. Mol Cell. 2009; 36 : 365-378.

Straface E, Matarrese P, Gambardella L, Vona R, Sgadari A, Silveri MC, Malorni W. Oxidative imbalance and cathepsin D changes as peripheral blood biomarkers of Alzheimer disease: a pilot study. FEBS Lett. 2005 ; 579 : 2759-2766.

Su M, Shi JJ, Yang YP, Li J, Zhang YL, Chen J, Hu LF, Liu CF. HDAC6 regulates aggresome-autophagy degradation pathway of alpha-synuclein in response to MPP(+) -induced stress. J Neurochem. 2011 Jan 14. doi: 10.1111/j.1471-4159.2011.07180.x. [Epub ahead of print].

Subramanian M, Sreejayan, Rao MN, Devasagayam TP, Singh BB. Diminution of singlet oxygen-induced DNA damage by curcumin and related antioxidants. Mutat Res. 1994 ; 311 : 249-55.

Sun H, Yang X, Zhu J, Lv T, Chen Y, Chen G, Zhong L, Li Y, Huang X, Huang G, Tian J. Inhibition of p300-HAT results in a reduced histone acetylation and down-regulation of gene expression in cardiac myocytes. Life Sci. 2010; 87 : 707-714.

Suram A, Hegde ML, Rao KS. A new evidence for DNA nicking property of amyloid beta-peptide (1-42): relevance to Alzheimer's disease. Arch Biochem Biophys. 2007; 463 : 245-52.

Suram A, Rao KS, Latha KS and Viswamitra MA. First evidence to show the topological change of DNA from B-DNA to Z-DNA conformation in the hippocampus of Alzheimer's brain. Neuromolecular Med, 2002; 2 : 289-297.

Surguchov A. Molecular and cellular biology of synucleins. Int Rev Cell Mol Biol. 2008; 270, 225-317.

Sutherland BM. Titration of pyrimidine dimer contents of nonradioactive deoxyribonucleic acid by electrophoresis in alkaline agarose gels. Biochemistry. 1983; 22 : 745-749.

Tabner BJ, Turnbull S, El-Agnaf OM, Allsop D. Formation of hydrogen peroxide and hydroxyl radicals from A(beta) and alpha-synuclein as a possible mechanism of cell death in Alzheimer's disease and Parkinson's disease. Free Radic Biol Med. 2002; 32 : 1076-83.

Tatton WG, Chalmers-Redman R, Brown D, Tatton N. Apoptosis in Parkinson's disease: signals for neuronal degradation. Ann Neurol. 2003; Suppl 3:S61-70.

Tatton WG, Olanov CW. Apoptosis in neurodegenerative diseases: the role of mitochondria. Biochem Biophys Acta. 1999; 1410 : 195-213.

Thurston VC, Pena P, Pestell R, Binder LI. Nucleolar localization of the microtubule-associated protein tau in neuroblastomas using sense and anti-sense transfection strategies. Cell Motil Cytoskeleton. 1997; 38: 100-110.

Tikoo K, Hamid QA, Ali Z. Structure of active chromatin: higher-order folding of transcriptionally active chromatin in control and hypothyroid rat liver. Biochem J. 1997 ; 322 : 289-96.

Tórsdóttir G, Kristinsson J, Sveinbjörnsdóttir S, Snaedal J, Jóhannesson T. Copper, ceruloplasmin, superoxide dismutase and iron parameters in Parkinson's disease. Pharmacol Toxicol. 1999 ; 85 : 239-243.

Tórsdóttir G, Sveinbjörnsdóttir S, Kristinsson J, Snaedal J, Jóhannesson T. Ceruloplasmin and superoxide dismutase (SOD1) in Parkinson's disease: a follow-up study. J Neurol Sci. 2006; 241 : 53-58.

Trewick SA and Dearden P. A rapid protocol for DNA extraction and primer annealing for PCR sequencing. Biotechniques. 1994; 17 : 842-844.

Trojanowski JQ, Lee VM. Parkinson's disease and related neurodegenerative synucleinopathies linked to progressive accumulations of synuclein aggregates in brain. Parkinsonism Relat Disord. 2001; 7 : 247-251.

Tsuboi Y, Uchikado H, Dickson DW. Neuropathology of Parkinson's disease dementia and dementia with Lewy bodies with reference to striatal pathology. Parkinsonism Relat Disord. 2007; 13 Suppl 3:S221-4.

Uberti D, Rizzini C, Spano PF, Memo M, Characterization of tau proteins in human neuroblastoma SH-SY5Y cell line. Neurosci Lett. 1997; 235 : 149-153.

Uversky VN, Eliezer D. Biophysics of Parkinson's disease: structure and aggregation of alpha-synuclein, Curr Protein Pept Sci, 2009; 10 : 483-499.

Uversky VN, Gillespie JR, Fink AL. Why are "natively unfolded" proteins unstructured under physiologic conditions? Proteins. 2000 Nov 15;41(3):415-427.

Uversky VN, Li J, Fink AL. Metal-triggered structural transformations, aggregation, and fibrillation of human alpha-synuclein. A possible molecular NK between Parkinson's disease and heavy metal exposure, J Biol Chem. 2001; 276 : 44284-44296.

Uversky VN, Li J, Fink AL. Trimethylamine-N-oxide-induced folding of alpha-synuclein. FEBS Lett. 2001; 509 : 31-35.

Uversky VN. Natively unfolded proteins: a point where biology waits for physics. Protein Sci. 2002; 11 : 739-756.

Valavanidis A, Vlachogianni T, Fiotakis C. 8-hydroxy-2' -deoxyguanosine (8-OHdG): A critical biomarker of oxidative stress and carcinogenesis. J Environ Sci Health C Environ Carcinog Ecotoxicol Rev. 2009 ; 27 : 120-139.

Vasudevaraju P, Bharathi, Garruto RM, Sambamurti K and Rao KS. Role of DNA dynamics in Alzheimer's disease. Brain Res Rev. 2008; 58 : 136-148.

Vila M, Vukosavic S, Jackson-Lewis V, Neystat M, Jakowec M, Przedborski S. Alpha-synuclein up-regulation in substantia nigra dopaminergic neurons following administration of the parkinsonian toxin MPTP. J Neurochem. 2000; 74 : 721-729.

Wadkins RM, Vladu B, Tung CS. Actinomycin D binds to metastable hairpins in single-stranded DNA. Biochemistry. 1998; 37 : 11915-11923.

Wakamatsu K, Fujikawa K, Zucca FA, Zecca L, Ito S. The structure of neuromelanin as studied by chemical degradative methods. J Neurochem. 2003; 86 : 1015-1023.

Wallace RB, Sargent TD, Murphy RF, Bonner J. Physical properties of chemically acetylated rat liver chromatin. Proc Natl Acad Sci U S A. 1977; 74 : 3244-8.

Walter CA, Grabowski DT, Street KA, Conrad CC, Richardson A. Analysis and modulation of DNA repair in aging. Mech Ageing Dev. 1997; 98 : 203-222.

Wang AH, Quigley GJ, Kolpak FJ, Crawford JL, van Boom JH, van der Marel G and Rich A. Molecular structure of a left-handed double helical DNA fragment at atomic resolution. Nature. 1979; 282 : 680-686.

Wang F, Yang J, Wu X, Wang F, Ding H. Investigation of the interaction between curcumin and nucleic acids in the presence of CTAB. Spectrochim Acta A Mol Biomol Spectrosc. 2007; 67 : 385-390.

Wang JC, Lynch AS. Transcription and DNA supercoiling. Curr Opin Genet Dev. 1993; 3 : 764-768.

Wang JZ, Liu F. Microtubule-associated protein tau in development, degeneration and protection of neurons. Prog Neurobiol. 2008; 85 : 148-175.

Wang MS, Boddapati S, Emadi S, Sierks MR. Curcumin reduces alpha-synuclein induced cytotoxicity in Parkinson's disease cell model. BMC Neurosci. 2010 ; 11 : 57.

Wang Y, Thomas GA, Peticolas WL. Sequence dependent conformations of oligomeric DNA's in aqueous solutions and in crystals. J Biomol Struct Dyn. 1987; 5 : 249-274.

Waragai M, Sekiyama K, Sekigawa A, Takamatsu Y, Fujita M, Hashimoto M. α-Synuclein and DJ-1 as Potential Biological Fluid Biomarkers for Parkinson's Disease. Int J Mol Sci. 2010 ; 11 : 4257-4266.

Wassermann K, Markovits J, Jaxel C, Capranico G, Kohn KW, Pommier Y. Effects of morpholinyl doxorubicins, doxorubicin, and actinomycin D on mammalian DNA topoisomerases I and II. Mol Pharmacol. 1990; 38 : 38-45.

Watson JD and Crick FH. Molecular structure of nucleic acids; a structure for deoxyribose nucleic acid. Nature. 1953; 171 : 737–738.

Waxman EA, Giasson BI. Molecular mechanisms of alpha-synuclein neurodegeneration, Biochim Biophys Acta. 2009; 1792 : 616-624.

Wei Y, Qu MH, Wang XS, Chen L, Wang DL, Liu Y, Hua Q, He RQ. Binding to the minor groove of the double-strand, tau protein prevents DNA from damage by peroxidation. PLoS ONE 2008; 3 : e2600.

Weingarten MD, Lockwood AH, Hwo SY, Kirschner MW. A protein factor essential for microtubule assembly. Proc.Natl Acad Sci U S A. 1975; 72 : 1858-1862.

Williams DR. Tauopathies: classification and clinical update on neurodegenerative diseases associated with microtubule-associated protein tau. Intern Med J. 2006; 36 : 652-660.

Wilson DM 3rd, Bohr VA, McKinnon PJ. DNA damage, DNA repair, ageing and age-related disease. Mech Ageing Dev. 2008; 129 : 349-352.

Wittmann CW, Wszolek MF, Shulman JM, Salvaterra PM, Lewis J, Hutton M, Feany MB. Tauopathy in Drosophila: neurodegeneration without neurofibrillary tangles. Science. 2001; 293 : 711-714.

Wong B, Chen S, Kwon JA and Rich A. Characterization of Z-DNA as a nucleosome-boundary element in yeast Saccharomyces cerevisiae. Proc Natl Acad Sci U S A. 2007; 104 : 2229-2234.

Wu Y, Le W, Jankovic J. Preclinical biomarkers of Parkinson disease. Arch Neurol. 2011; 68 : 22-30.

Wyllie AH, Kerr JF, Currie AR. Cell death: the significance of apoptosis. Int Rev Cytol. 1980; 68 : 251-306.

Xu S, Zhou M, Yu S, Cai Y, Zhang A, Uéda K. Chan P. Oxidative stress induces nuclear translocation of C-terminus of alpha-synuclein in dopaminergic cells. Biochem Biophys Res Commun. 2006; 342 : 330-335.

Yamada M, Iwatsubo T, Mizuno Y, Mochizuki H. Overexpression of alpha-synuclein in rat substantia nigra results in loss of dopaminergic neurons, phosphorylation of alpha-synuclein and activation of caspase-9: resemblance to pathogenetic changes in Parkinson's disease. J Neurochem. 2004; 91 : 451-461.

Yang F, Lim GP, Begum AN, Ubeda OJ, Simmons MR, Ambegaokar SS, Chen PP, Kayed R, Glabe CG, Frautschy SA, Cole GM. Curcumin inhibits formation of amyloid beta oligomers and fibrils, binds plaques, and reduces amyloid in vivo. J Biol Chem. 2005; 280 : 5892-5901.

Yang S, Zhang D, Yang Z, Hu X, Qian S, Liu J, Wilson B, Block M, Hong JS. Curcumin protects dopaminergic neuron against LPS induced neurotoxicity in primary rat neuron/glia culture. Neurochem Res. 2008; 33: 2044-2053.

Yoo H, Rill RL. Actinomycin D binding to unstructured, single-stranded DNA. J Mol Recognit. 2001; 14 : 145-150.

Yu S, Li X, Liu G, Han J, Zhang C, Li Y, Xu S, Liu C, Gao Y, Yang H, Uéda K, Chan P. Extensive nuclear localization of alpha-synuclein in normal rat brain neurons revealed by a novel monoclonal antibody. Neuroscience. 2007; 145 : 539-555.

Yu S, Zuo X, Li Y, Zhang C, Zhou M, Zhang YA, Uéda K, Chan P. Inhibition of tyrosine hydroxylase expression in alpha-synuclein-transfected dopaminergic neuronal cells. Neurosci Lett. 2004; 367 : 34-39.

Yun JM, Jialal I, Devaraj S. Epigenetic regulation of high glucose-induced proinflammatory cytokine production in monocytes by curcumin. J Nutr Biochem. 2010 Jul 21.

Zarranz JJ, Alegre J, Gómez-Esteban JC, Lezcano E, Ros R, Ampuero I, Vidal L, Hoenicka J, Rodriguez O, Atarés B, Llorens V, Gomez Tortosa E, del Ser T, Muñoz DG, de Yebenes JG. The new mutation, E46K, of alpha-synuclein causes Parkinson and Lewy body dementia. Ann Neurol. 2004; 55 : 164-73.

Zecca L, Costi P, Mecacci C, Ito S, Terreni M, Sonnino S. Interaction of human substantia nigra neuromelanin with lipids and peptides. J Neurochem. 2000; 74 : 1758-1765.

Zecca L, Fariello R, Riederer P, Sulzer D, Gatti A, Tampellini D. The absolute concentration of nigral neuromelanin, assayed by a new sensitive method, increases

throughout the life and is dramatically decreased in Parkinson's disease. FEBS Lett. 2002; 510 : 216-220.

Zecca L, Pietra R, Goj C, Mecacci C, Radice D, Sabbioni E. Iron and other metals in neuromelanin, substantia nigra, and putamen of human brain. J Neurochem. 1994 ; 62 : 1097-1101.

Zecca L, Shima T, Stroppolo A, Goj C, Battiston GA, Gerbasi R, Sarna T, Swartz HM. Interaction of neuromelanin and iron in substantia nigra and other areas of human brain. Neuroscience. 1996 ; 73 : 407-415.

Zecca L, Stroppolo A, Gatti A, Tampellini D, Toscani M, Gallorini M, Giaveri G, Arosio P, Santambrogio P, Fariello RG, Karatekin E, Kleinman MH, Turro N, Hornykiewicz O, Zucca FA. The role of iron and copper molecules in the neuronal vulnerability of locus coeruleus and substantia nigra during aging. Proc Natl Acad Sci U S A. 2004; 101 : 9843-9848.

Zecca L, Tampellini D, Gerlach M, Riederer P, Fariello RG, Sulzer D. Substantia nigra neuromelanin: structure, synthesis, and molecular behaviour. Mol Pathol. 2001; 54 : 414-418.

Zecca L, Youdim MB, Riederer P, Connor JR, Crichton RR. Iron, brain ageing and neurodegenerative disorders. Nat Rev Neurosci. 2004; 5 : 863-73.

Zecca L, Zucca FA, Wilms H, Sulzer D. Neuromelanin of the substantia nigra: a neuronal black hole with protective and toxic characteristics. Trends Neurosci. 2003 ; 26 : 578-580.

Zhang L, Zhang C, Zhu Y, Cai Q, Chan P, Uéda K, Yu S and Yang H. Semi-quantitative analysis of alpha-synuclein in subcellular pools of rat brain neurons: an immunogold electron microscopic study using a C-terminal specific monoclonal antibody. Brain Res. 2008; 1244 : 40-52.

Zhang L, Zhang C, Zhu Y, Cai Q, Chan P, Uéda K, Yu S, Yang H. Semi-quantitative analysis of alpha-synuclein in subcellular pools of rat brain neurons: an immunogold electron microscopic study using a C-terminal specific monoclonal antibody. Brain Res. 2008 ; 1244 : 40-52.

Ziv I, Melamed E. Role of apoptosis in the pathogenesis of Parkinson's disease: A novel therapeutic opportunity? Mov Disord 1998; 13: 865-70.

Ziv Y, Bielopolski D, Galanty Y, Lukas C, Taya Y, Schultz DC, Lukas J, Bekker-Jensen S, Bartek J, Shiloh Y. Chromatin relaxation in response to DNA double-strand breaks is modulated by a novel ATM- and KAP-1 dependent pathway. Nat Cell Biol. 2006 ; 8 : 870-876.

Zsila F, Bikadi Z, Simonyi M. Circular dichroism spectroscopic studies reveal pH dependent binding of curcumin in the minor groove of natural and synthetic nucleic acids. Org Biomol Chem. 2004; 2 : 2902-2910.

Publications

PAPERS IN SCIENTIFIC JOURNALS

- **Vasudevaraju P**, Bharathia, Garruto R.M., Sambamurti K., Rao K.S.J. (2008), Role of DNA dynamics in Alzheimer's disease. Brain Research reviews, 58, 136-148.

- **Vasudevaraju P,** Rao K.S.J (2008) Studies on actinomycin D induced changes in supercoiled DNA integrity. Current Trends in Biotechnology and Pharmacy, 2, 433-441.

- Bharathi, **Vasudevaraju P**, Rao KSJ, (2008) Molecular Studies on Neurotoxicitiy of Aluminium. Indian Journal of Medical Research, 128, 184-196

- Hegde ML, **Vasudevaraju P**, Rao KJ. (2010) DNA induced folding/fibrillation of alpha-synuclein: new insights in Parkinson's disease: Landmark review. Frontiers in Bioscience 15, 418-36.

- Sathyanarayana Rao TS, Asha MR, Jagannatha Rao KS, **Vasudevaraju P**. (2009) The biochemistry of belief. Indian Journal of Psychiatry. 51, 239-241.

- Sathynarayana Rao TS, Ramesh BN, **Vasudevaraju P**, Rao KSJ. (2010) Molecular Biology Research in Neuropsychiatry: India's contribution. Indian Journal of Psychiatry (In press)

- **Vasudevaraju P,** Indi SS and Rao KSJ . (2010) New evidences on Tau–DNA interactions and relevance to neurodegeneration. Neurochemistry international 57, 51–57.

- **Vasudevaraju P**, Bharathi , T Jyothsna, NM Shamasundar, Subba K Rao, BM Balaraj, KSJ Rao, TS Sathyanarayana Rao. (2010) New evidence on iron, copper accumulation and zinc depletion and its correlation with DNA integrity in aging human brain regions. Indian Journal of Psychiatry, 52 (2) 140-144.

PROCEEDINGS OF CONFERENCE / BOOK CHAPTERS

- **P.Vasudevaraju**, Vali G and Rao KSJ . (Poster) "Molecular studies on Tau altering the integriety of DNA and its relevance to neurodegeneration". SFN annual meerting, November 15-19, 2008, Washington DC, USA. Awarded IBRO-SFN travel award for attending the meeting.

- **P.Vasudevaraju** (2009) New evidence on Neuromelanin from the substantia nigra of Parkinson's disease altering the DNA topology. 'Young Scientist Award' presentation under Medical Sciences section in Indian Science Congress for 97th Indian Science Congress held at Tiruvanathapuram, January 3-7, 2010.